MANTS

Carsten Rott

Sungkyunkwan University, Korea

rott@skku.edu

Jan 27, 2017

Indirect Search for Dark Matter

Evidence for Dark Matter

The Dark Matter Mystery

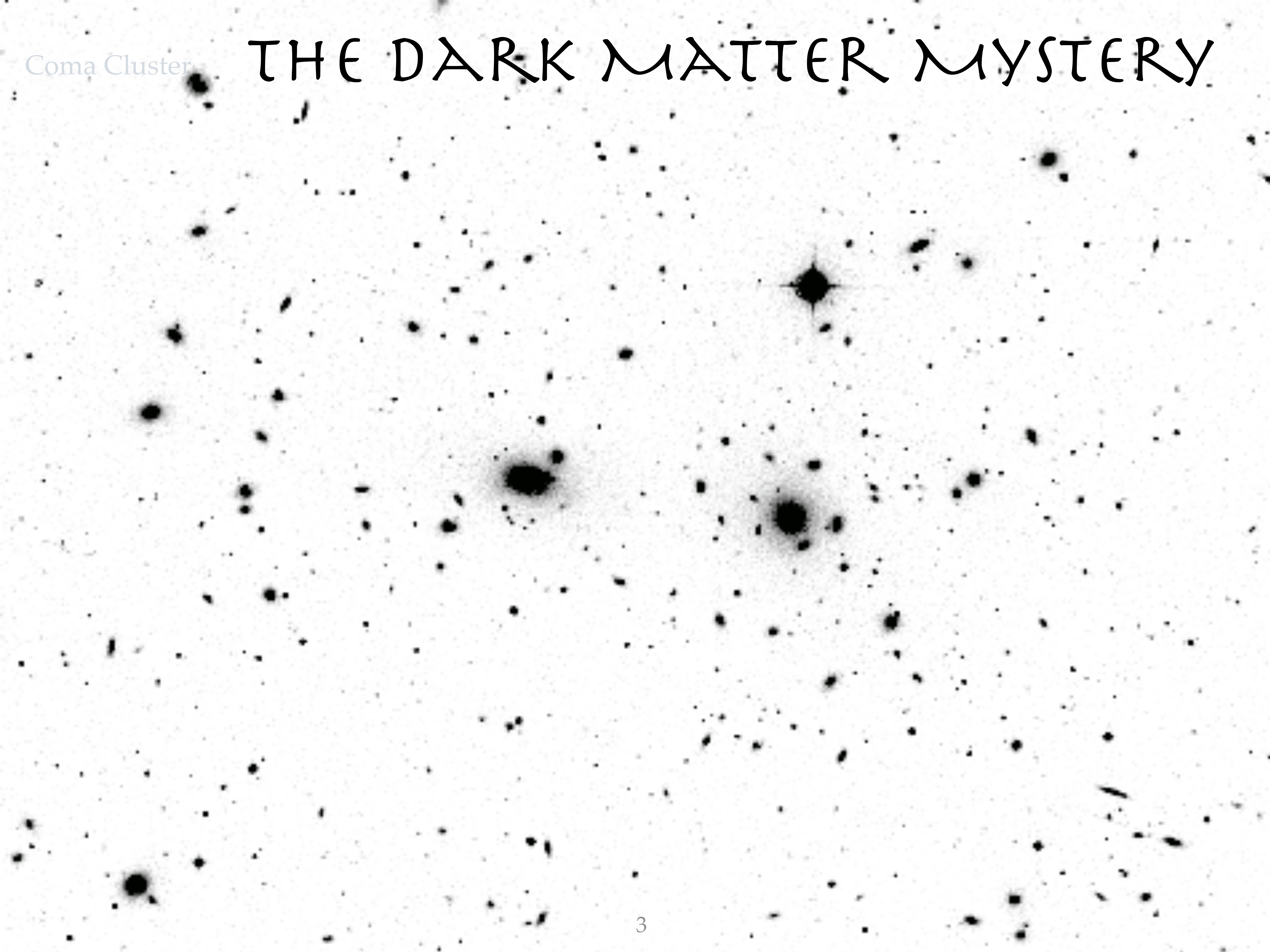

The Dark Matter Mystery

Coma Cluster

Virial Theorem: The time average total kinetic energy relates to the total potential energy in a stable system bound by a potential

$$\langle T \rangle_\tau = -\frac{1}{2} \langle V_{\mathrm{TOT}} \rangle_\tau$$

- Since Zwicky observed the Coma cluster evidence has hardened
  - Structure formations - Cosmological simulations
  - Gravitational lensing
  - Rotation curves
  - Cosmic microwave background
  - ...

- Dark Matter already gravitationally “observed”, but ...
  - What is it ?
  - What are it’s properties ?

Galactic rotation curves

Galactic Rotation Curves

- Some of the first measurements of rotation curves of Galaxies were performed by Vera Rubin and her team in the 70s and 80s
  - Result: Rotation curves stay flat as far out as can be measured

Vera Cooper Rubin (July 23, 1928 – December 25, 2016)

Galactic Rotation Curves

Vera Rubin measuring galaxy rotation curves (~1970)

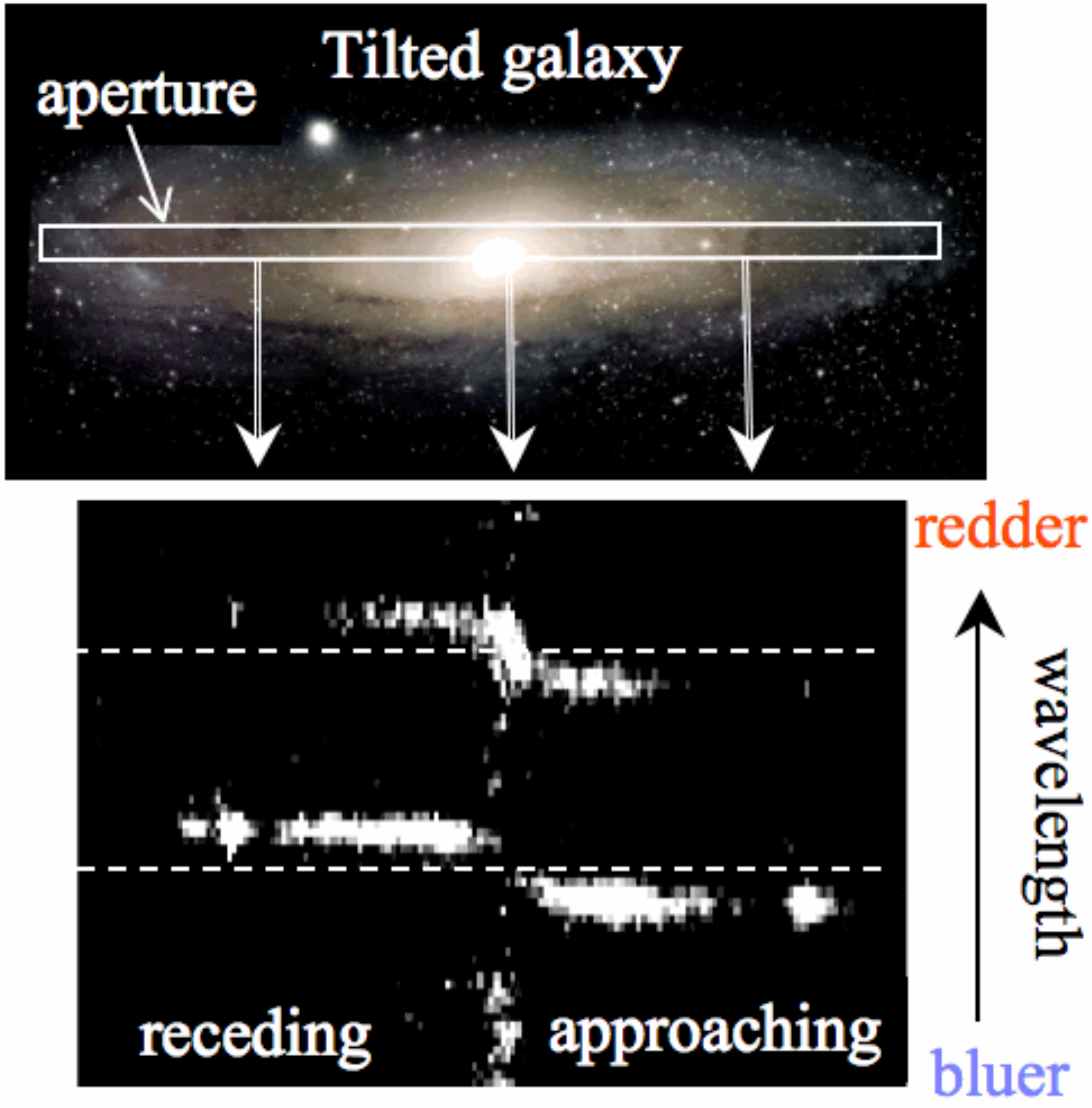

Resulting spectrum of light within aperture

Galactic Rotation Curves

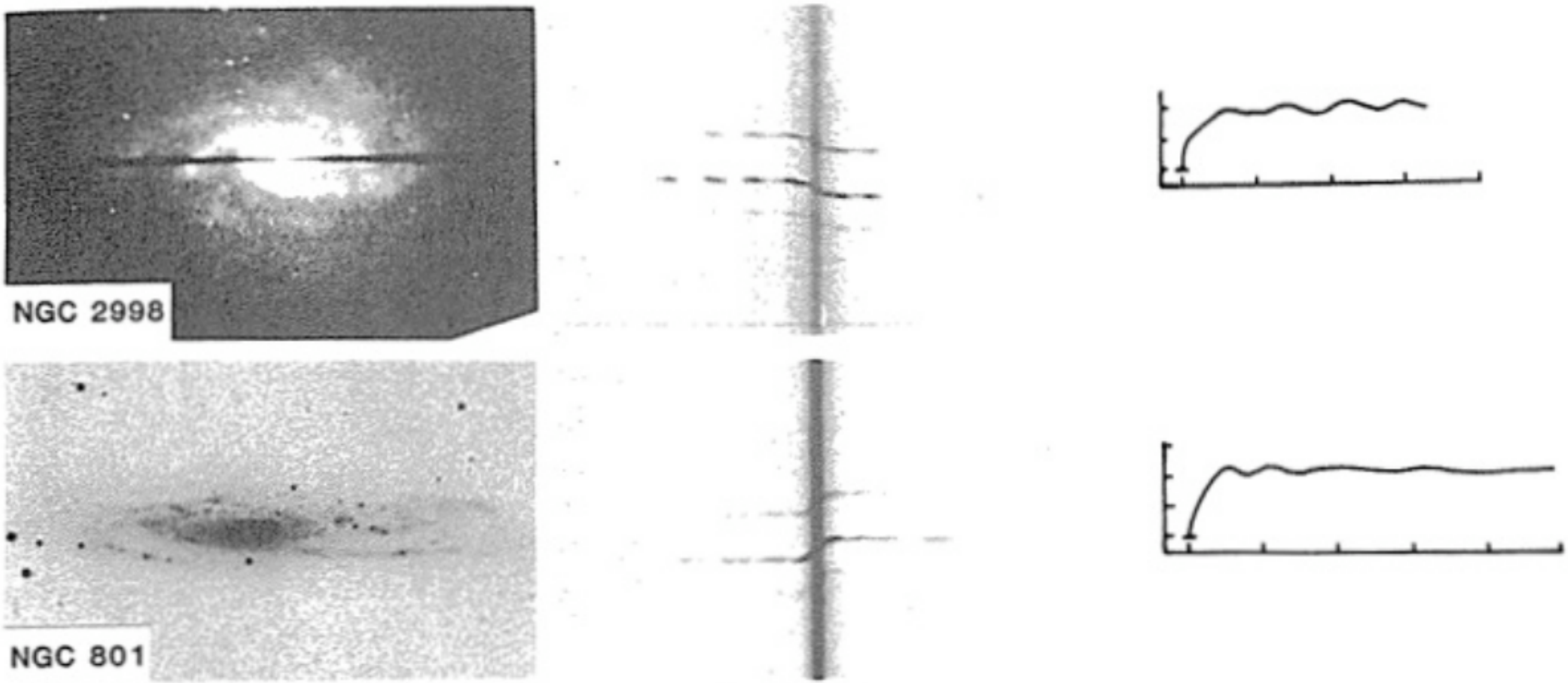

H-alpha 656.281nm trace of ionised hydrogen

Galactic Rotation Curves

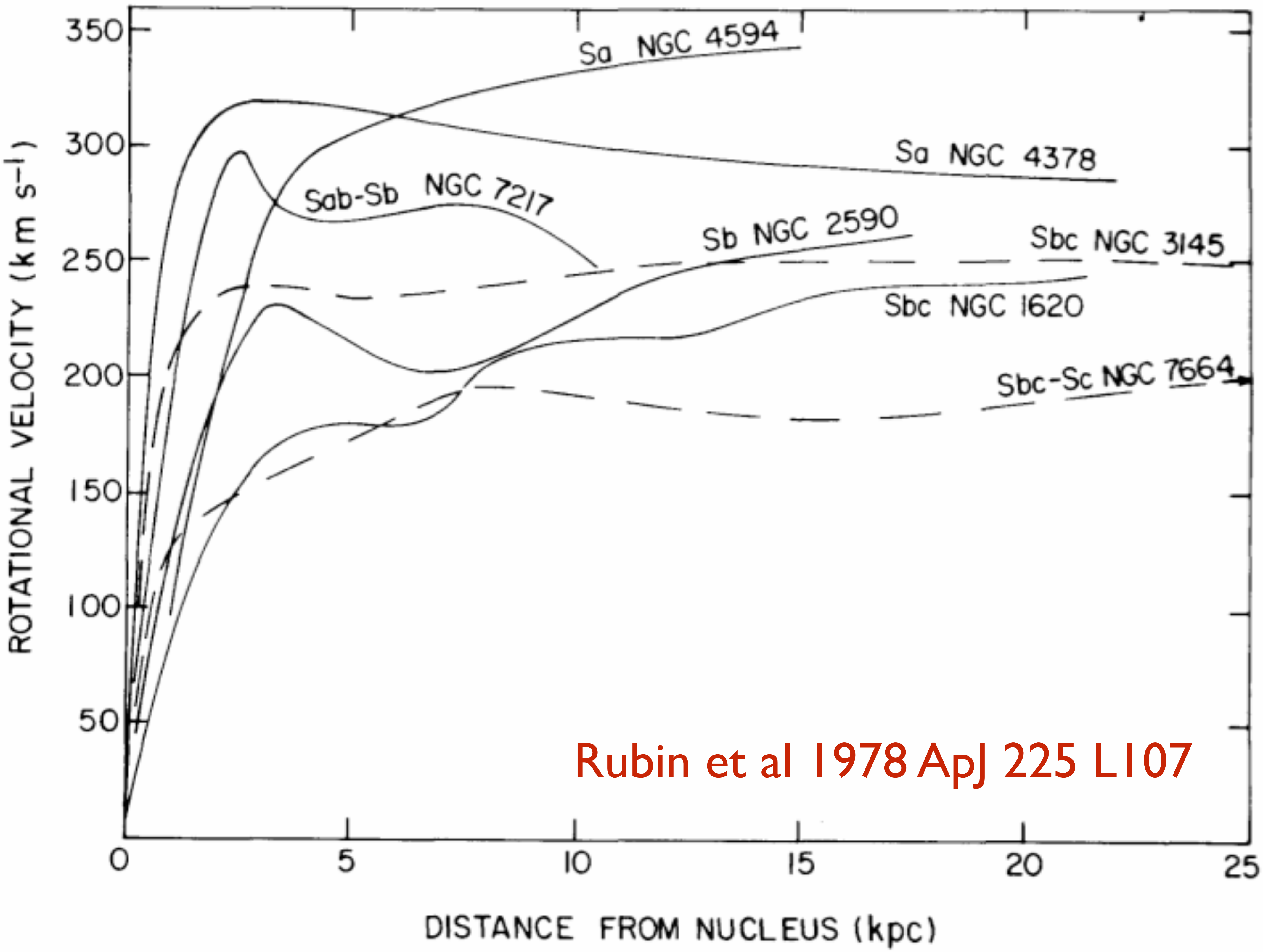

Rubin et al 1978 ApJ 225 L107

Galactic Rotation Curves

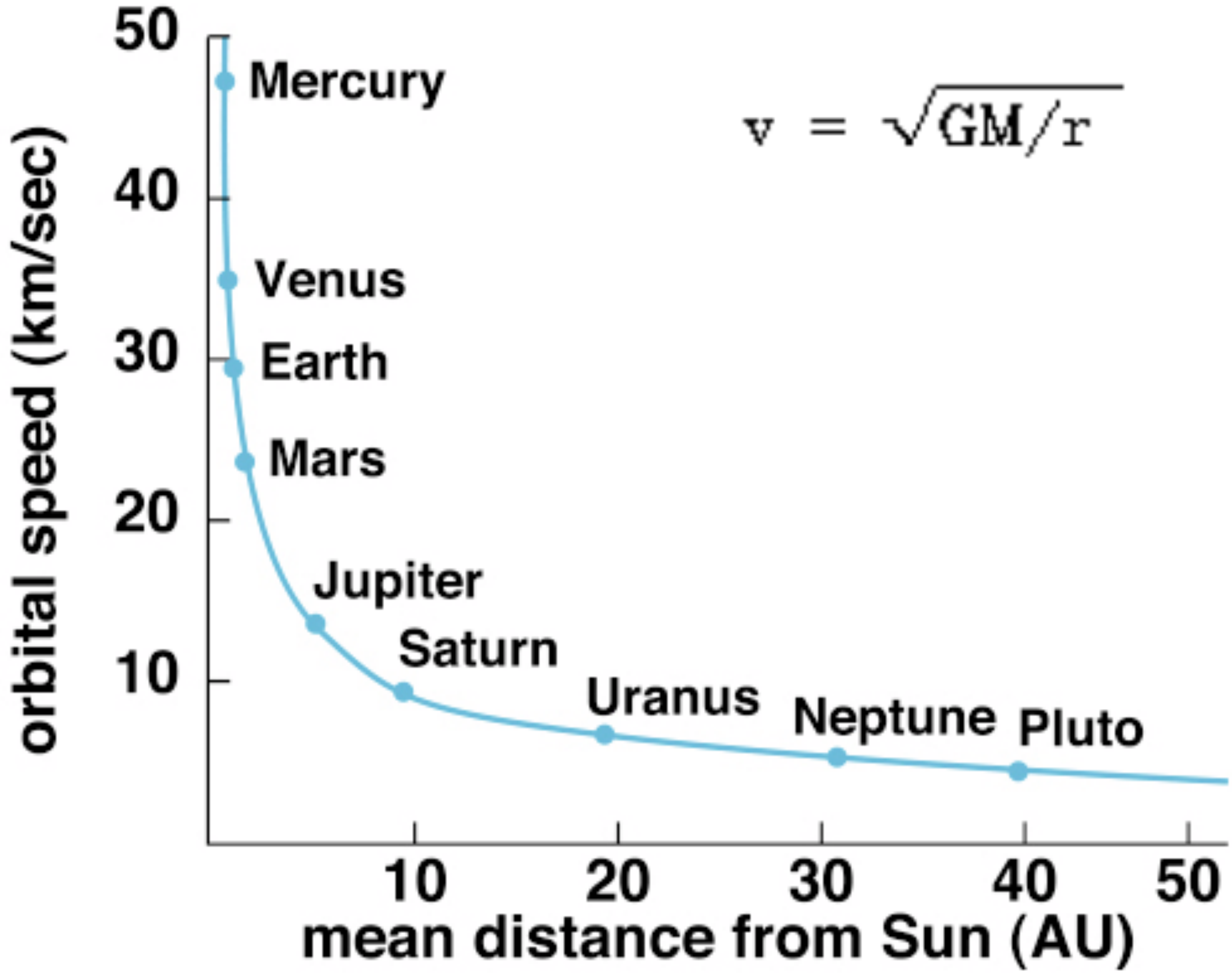

- Density profile can be derived from rotation curve

$$v^2(r) = \frac{GM(r)}{r}$$

- Based on luminous matter rotation curve can be predicted

$$v_{lum}^2(r) = \frac{GM_{lum}(r)}{r}$$

- Mass to light ratio is the ratio of matter over visible matter
    - M/L

Milky Way fits to observed rotation curve

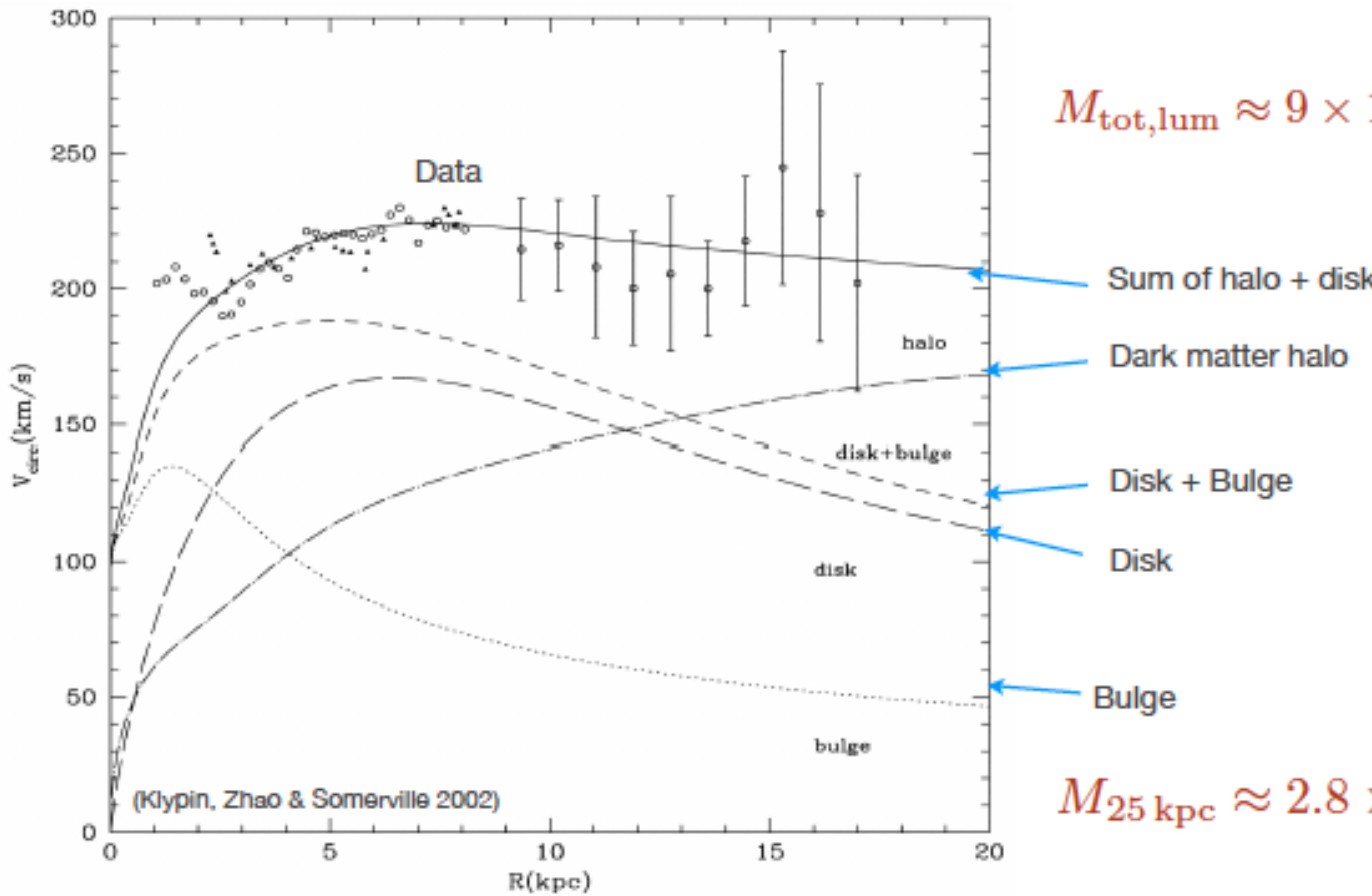

$M_{\mathrm{tot,lum}} \approx 9 \times 10^{10} M_{\odot}$

$M_{25\,\mathrm{kpc}} \approx 2.8 \times 10^{11} M_{\odot}$

$M_{230\,\mathrm{kpc}} \approx 1.3 \times 10^{12} M_{\odot}$

In reality one models each contribution (disk, bulge) separately

Galactic Rotation Curves

- Recent compilation of all existing data in Nature Physics paper, February 9, 2015

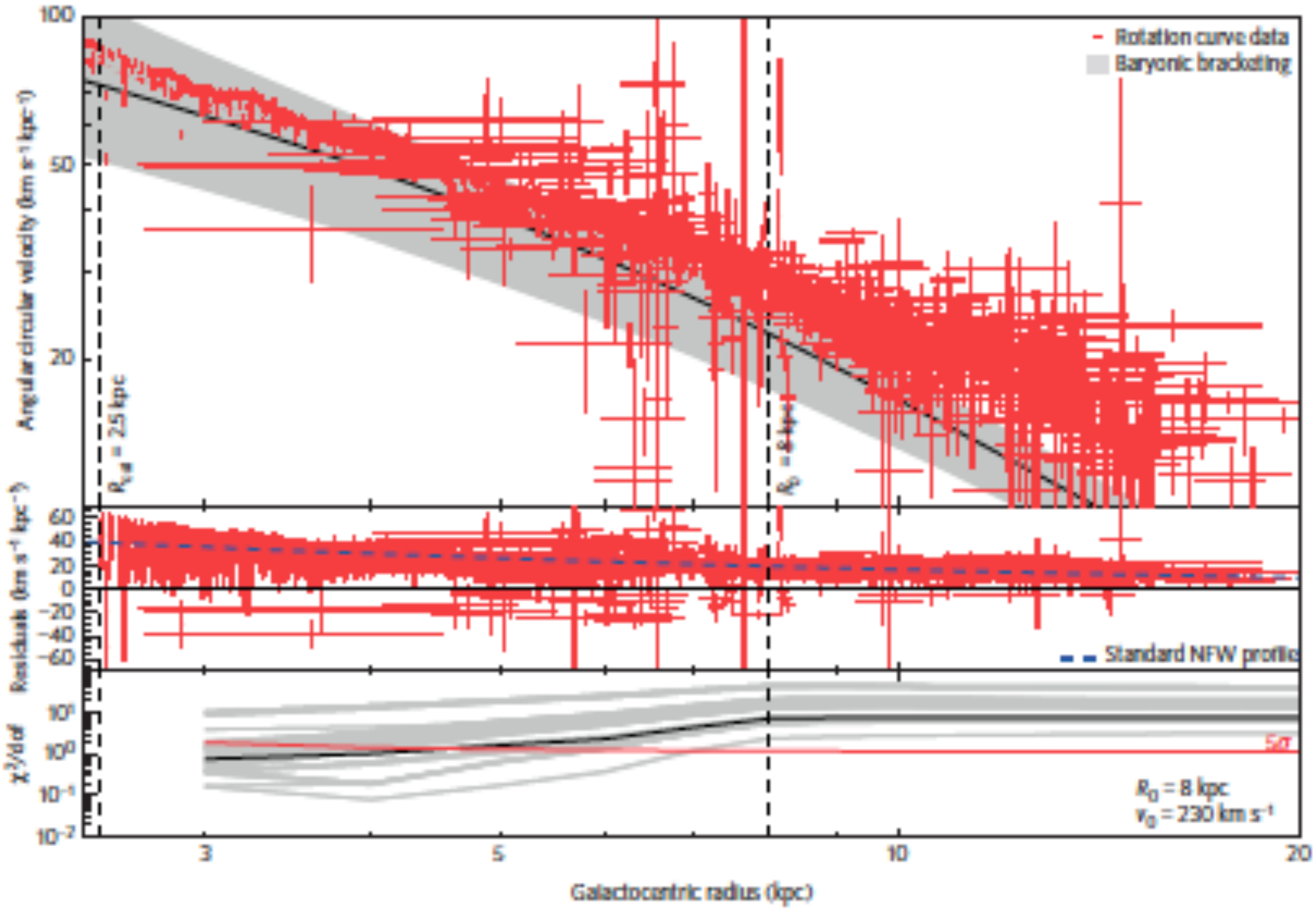

Angular velocity measurements (red) together with the contribution of all baryonic models (grey band); errors are 1-sigma uncertainties

Residuals between observed and predicted angular velocities for the fiducial baryonic model

F. Iocco, M. Pato, G. Bertone, Nature Physics, DOI 10.1038

Gravitational Lensing

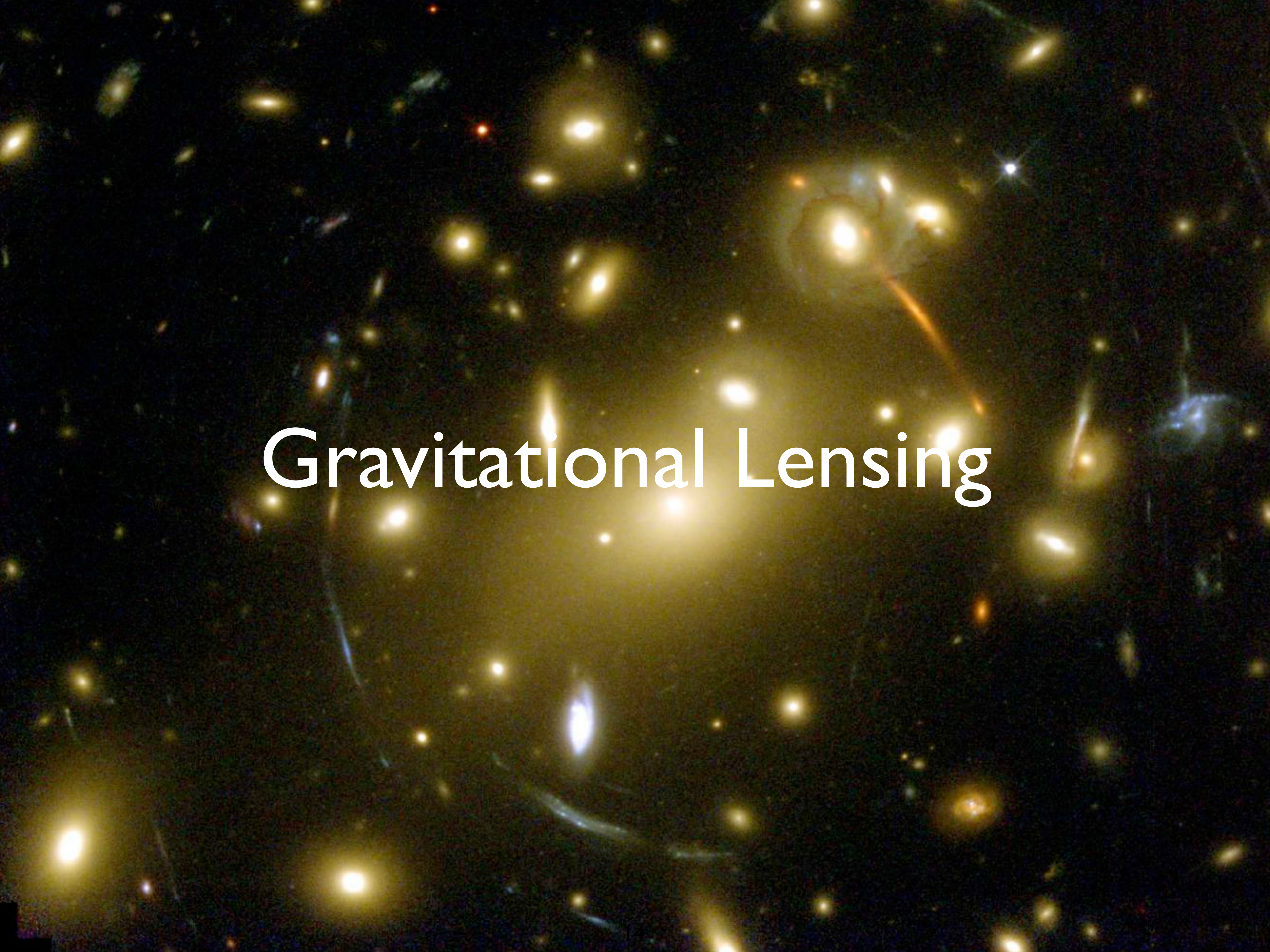

Gravitational lensing

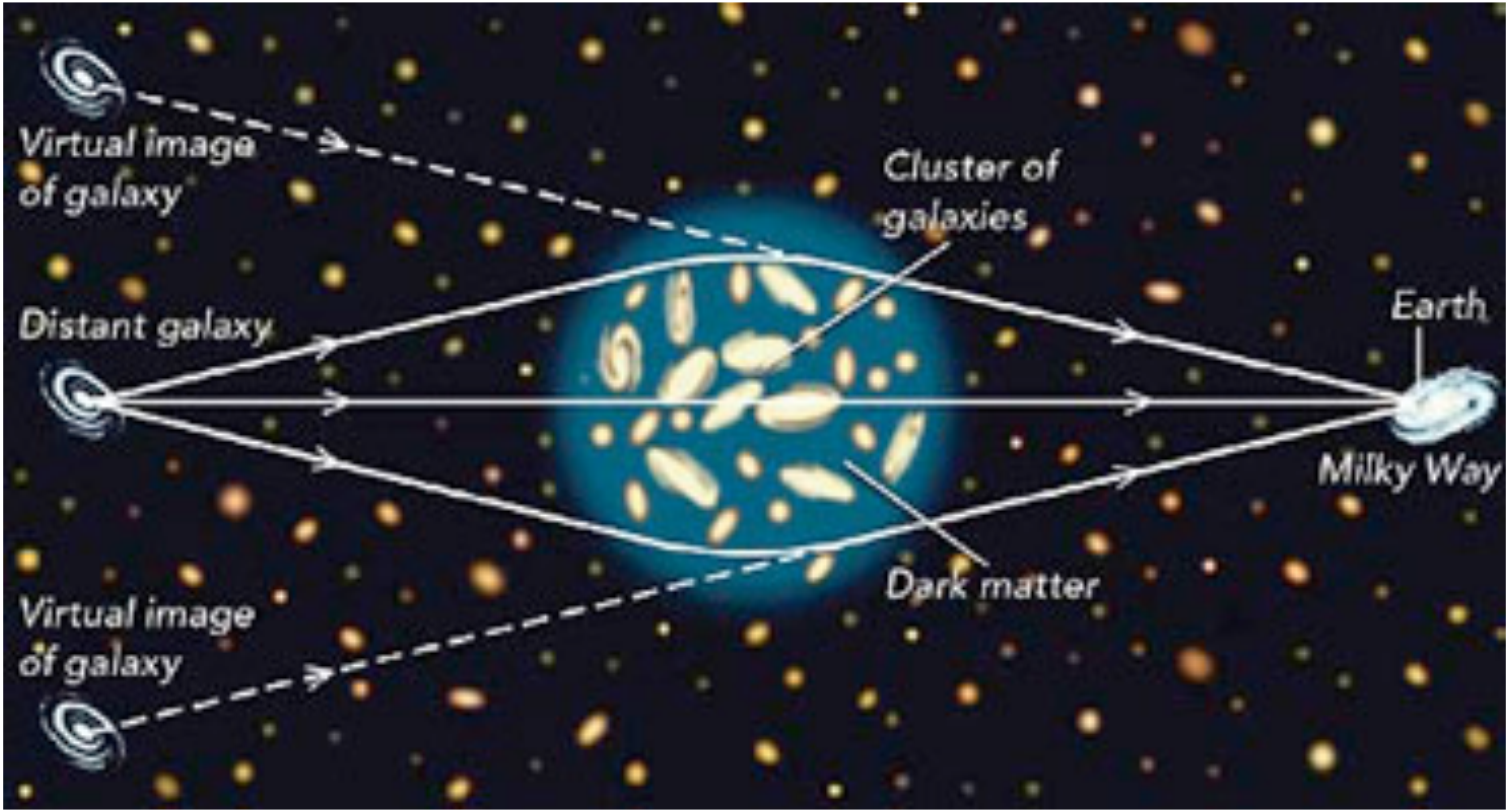

Bullet cluster

Cosmic Microwave Background (CMB)

What is CMB

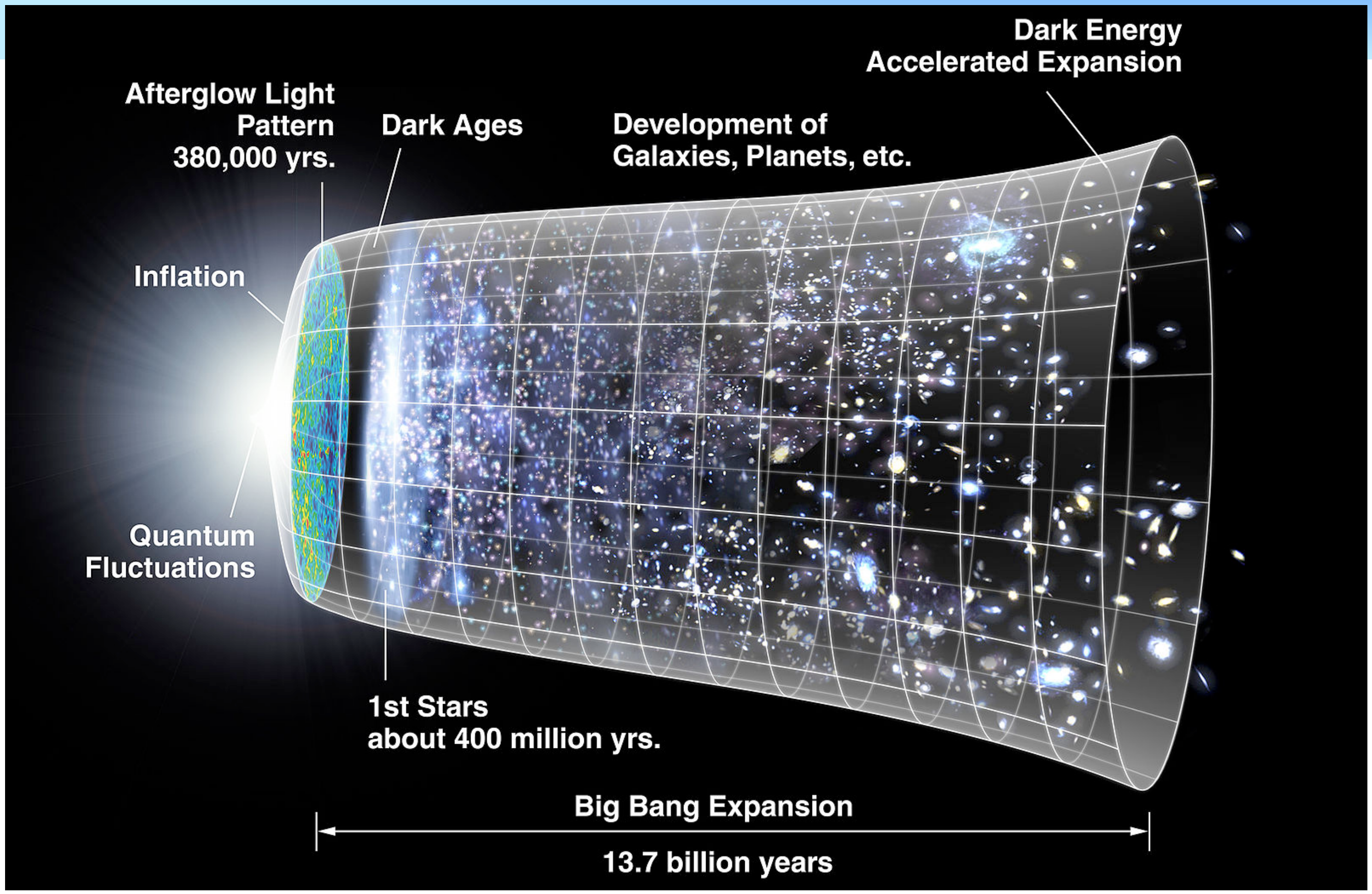

Accidental discovery of cosmic microwave background (CMB) radiation in 1964 by Arno Allan Penzias and Robert Woodrow Wilson with the Holmdel Horn Antenna. Nobel Prize 1978

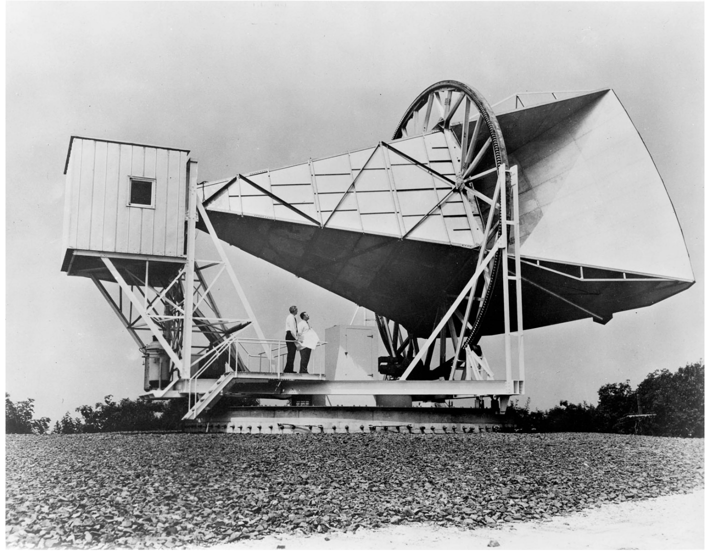

- The entire Universe is filled with radiation in the form of a 2.7K black-body.
- This radiation is a relic of the hot, dense, early phase of the Universe (big bang).
- The light travels to us from a “surface of last scattering” at z~1100 (when the Universe was 10-3 times smaller than today and only 380,000yr old).
  - At this z the Universe was finally cold enough for protons to capture electrons to form neutral Hydrogen.
  - Optical depth to photon scattering quickly drops from $\tau \gg 1$ to $\tau \ll 1$.
- The radiation has almost the same intensity in all directions, however contains tiny fluctuations in intensity (or temperature) at the level of 10-4: CMB anisotropy.

PLANCK

Looking back to the dawn of time

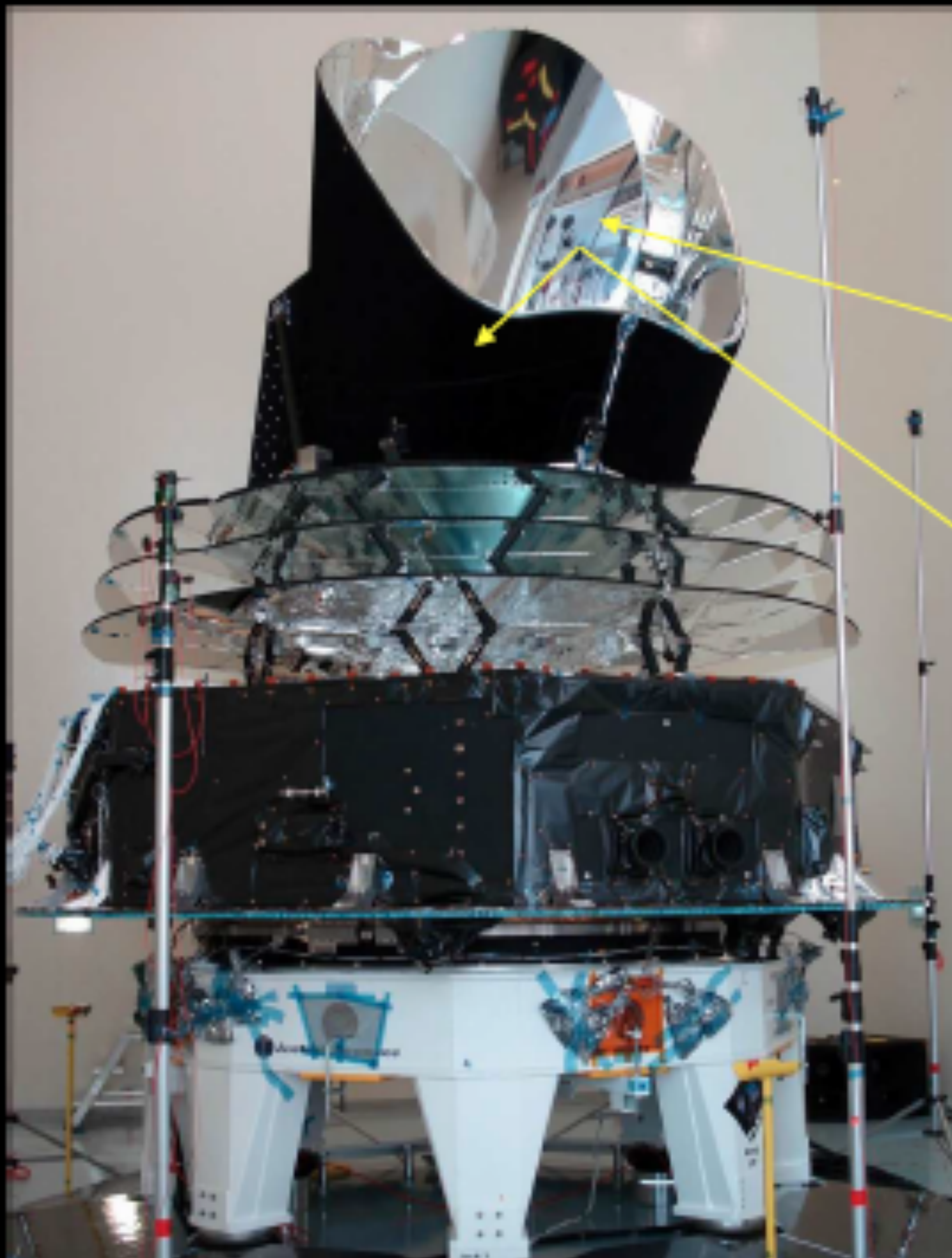

Planck Telescope
1.5x1.9m off-axis
Gregorian
T = 50 K

LFI Radiometers
30-70 GHz, T = 20 K

HFI Bolometers
100-857 GHz, T = 0.1 K

Planck vs WMAP

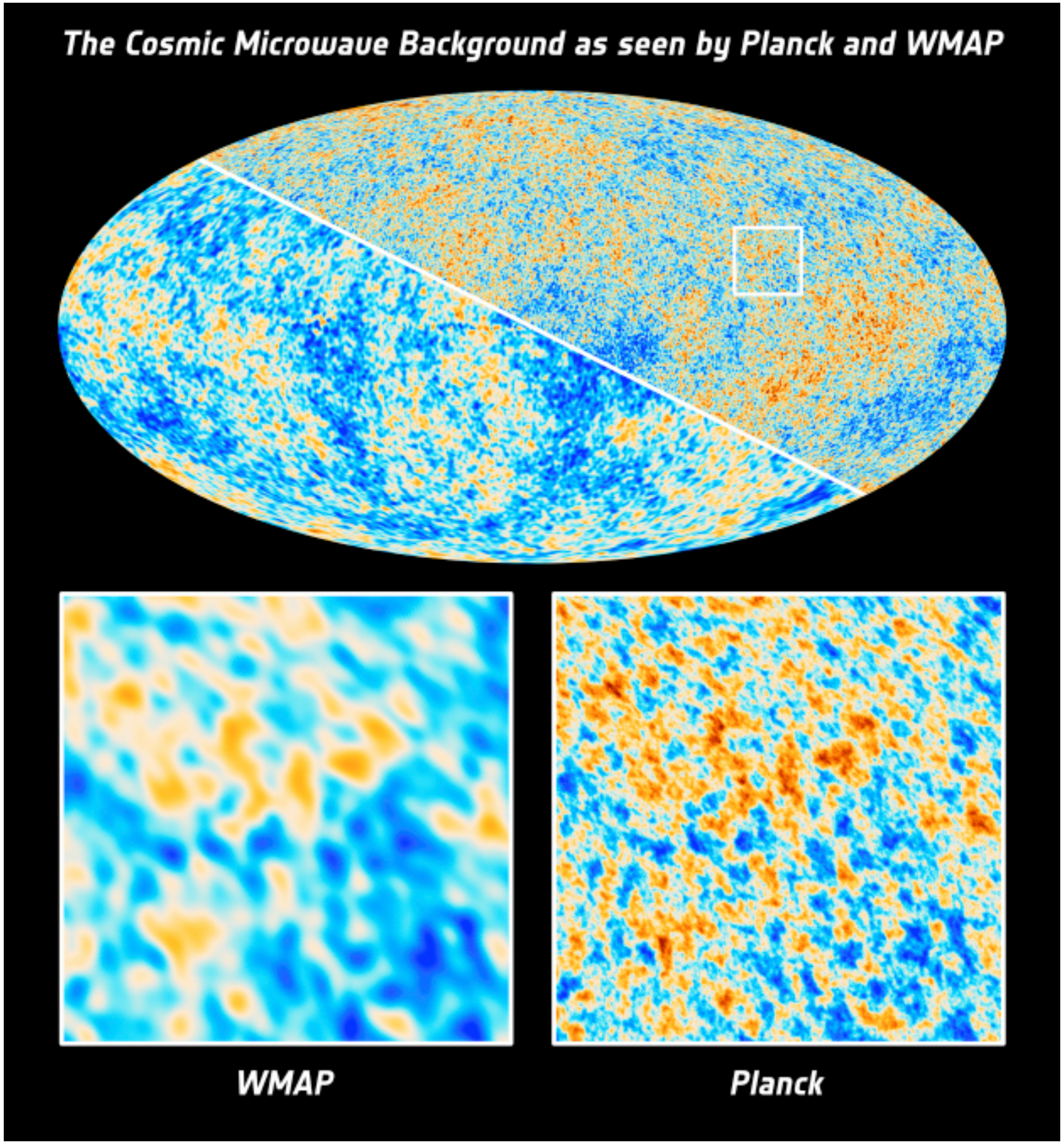

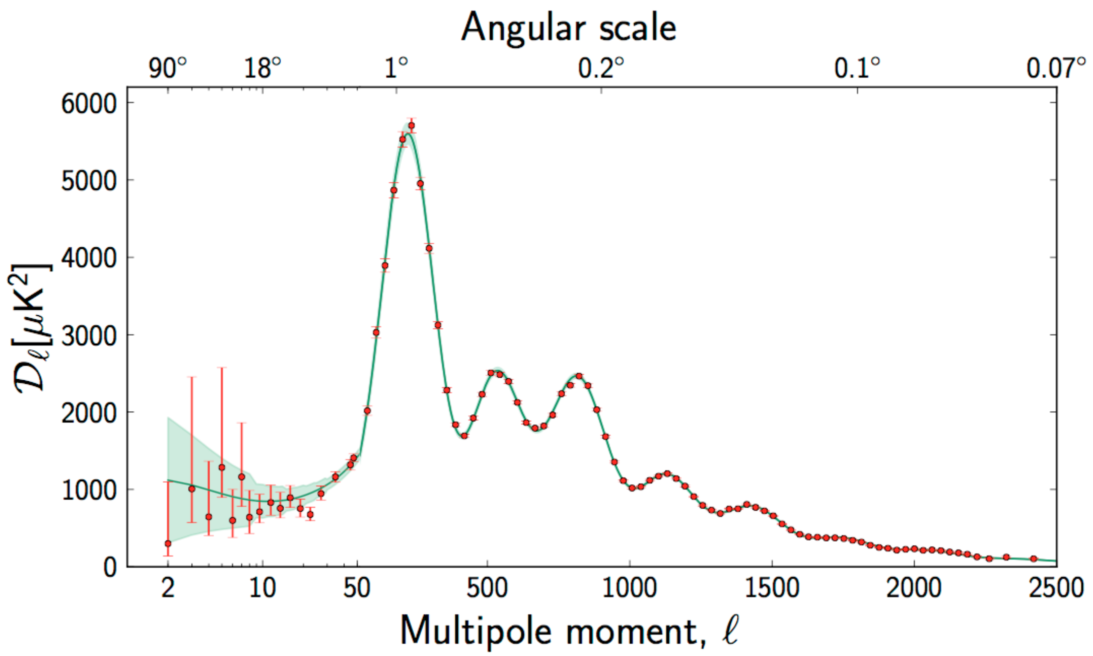

Date: 20 March 2013
Satellite: Planck
Depicts: Cosmic Microwave Background
Copyright: ESA and the Planck Collaboration; NASA / WMAP Science Team

This image shows temperature fluctuations in the Cosmic Microwave Background as seen by ESA's Planck satellite (upper right half) and by its predecessor, NASA's Wilkinson Microwave Anisotropy Probe (WMAP; lower left half).

Planck

http://www.esa.int/Planck

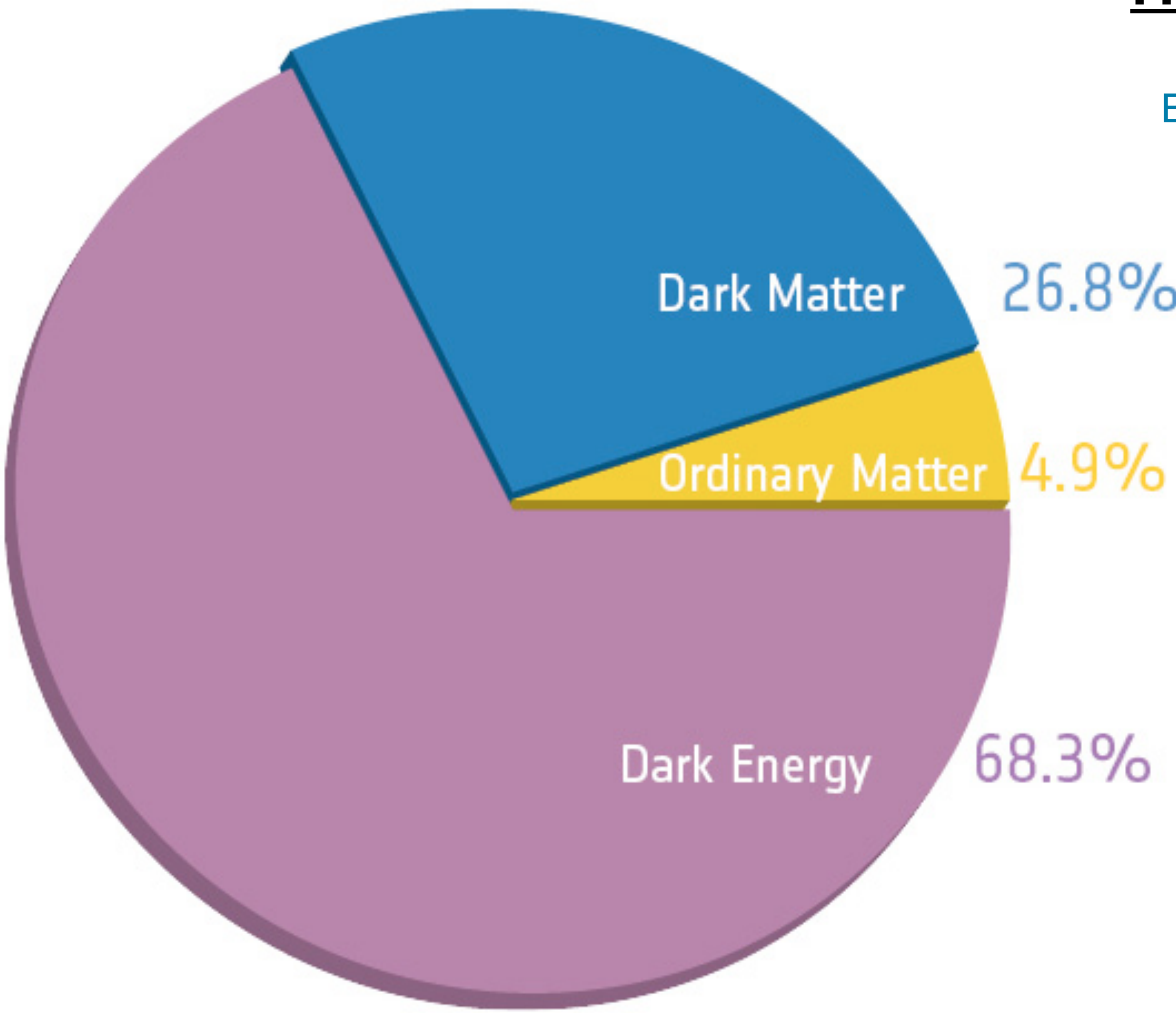

Based on Planck data:

- Universe contains
  - ~ 5% baryonic matter, the building blocks of stars and planets.
  - ~27% is dark matter, which does not emit or absorb light. Detected indirectly through its gravity.
  - ~68% dark energy, which acts as a sort of an anti-gravity and responsible for the present-day acceleration of the universal expansion.

https://arxiv.org/abs/1502.01589

https://lambda.gsfc.nasa.gov/education/cmb_plotter/

Structure formation

Structure formation

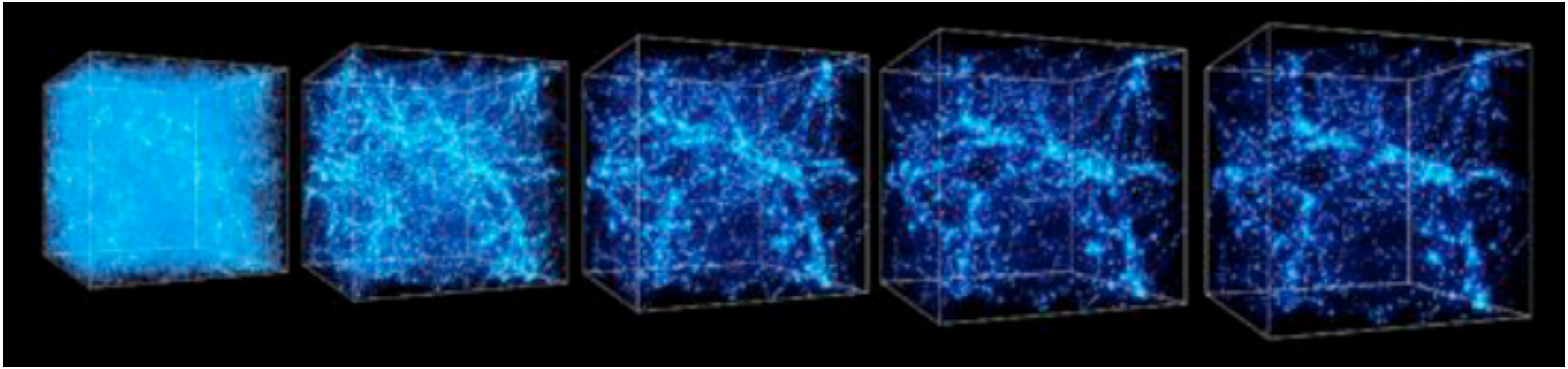

over densities grow to large structures, observed today

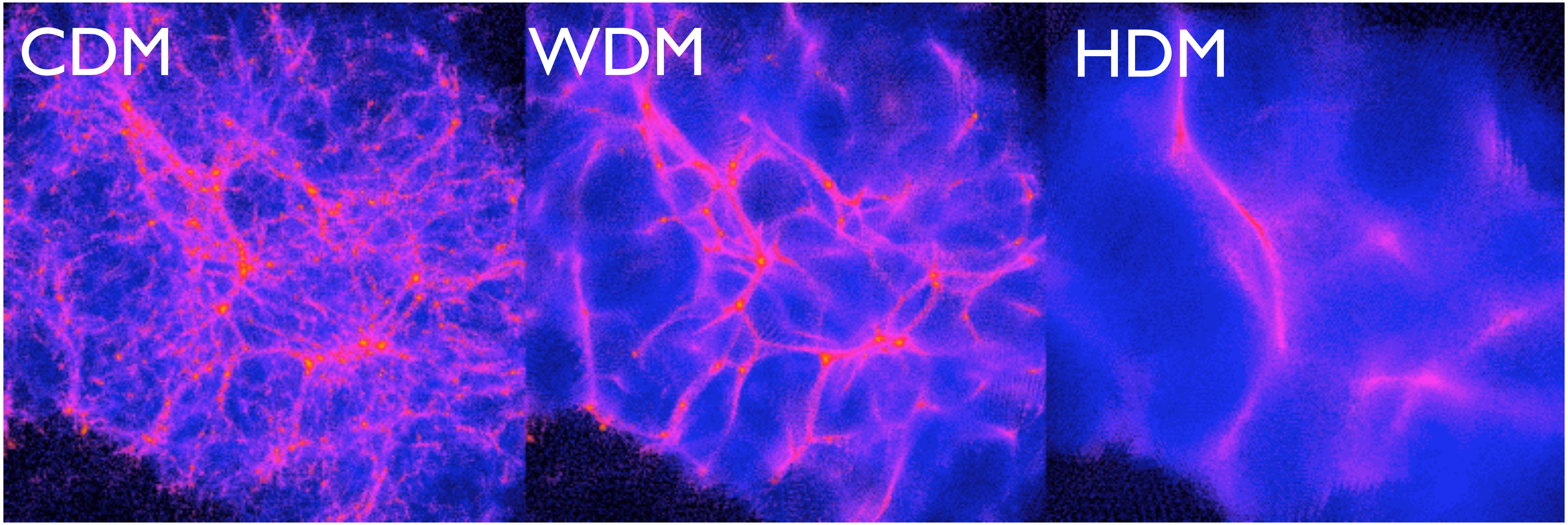

Cold, Warm, and Hot dark matter simulations, credit ITP, University of Zurich.

SDSS

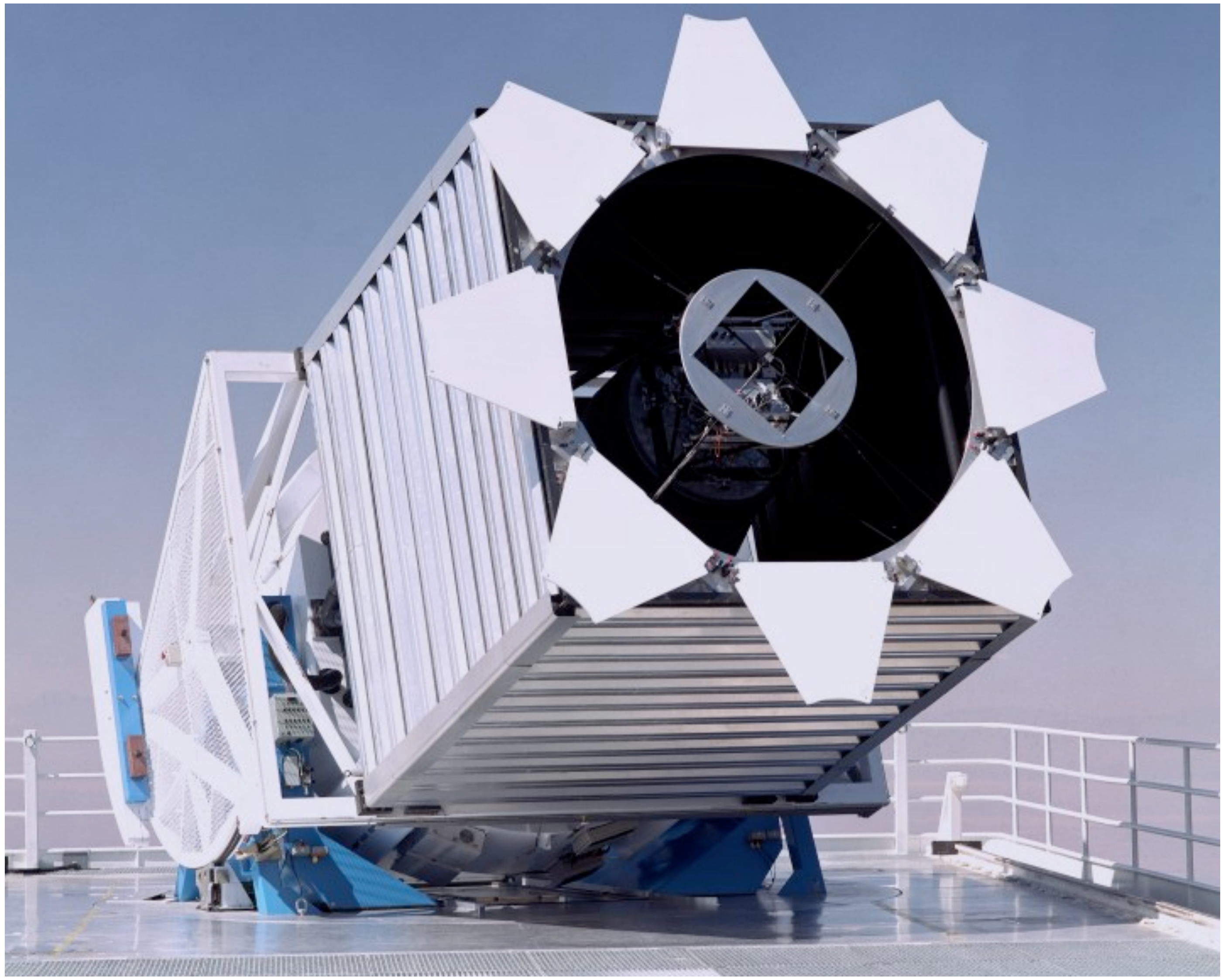

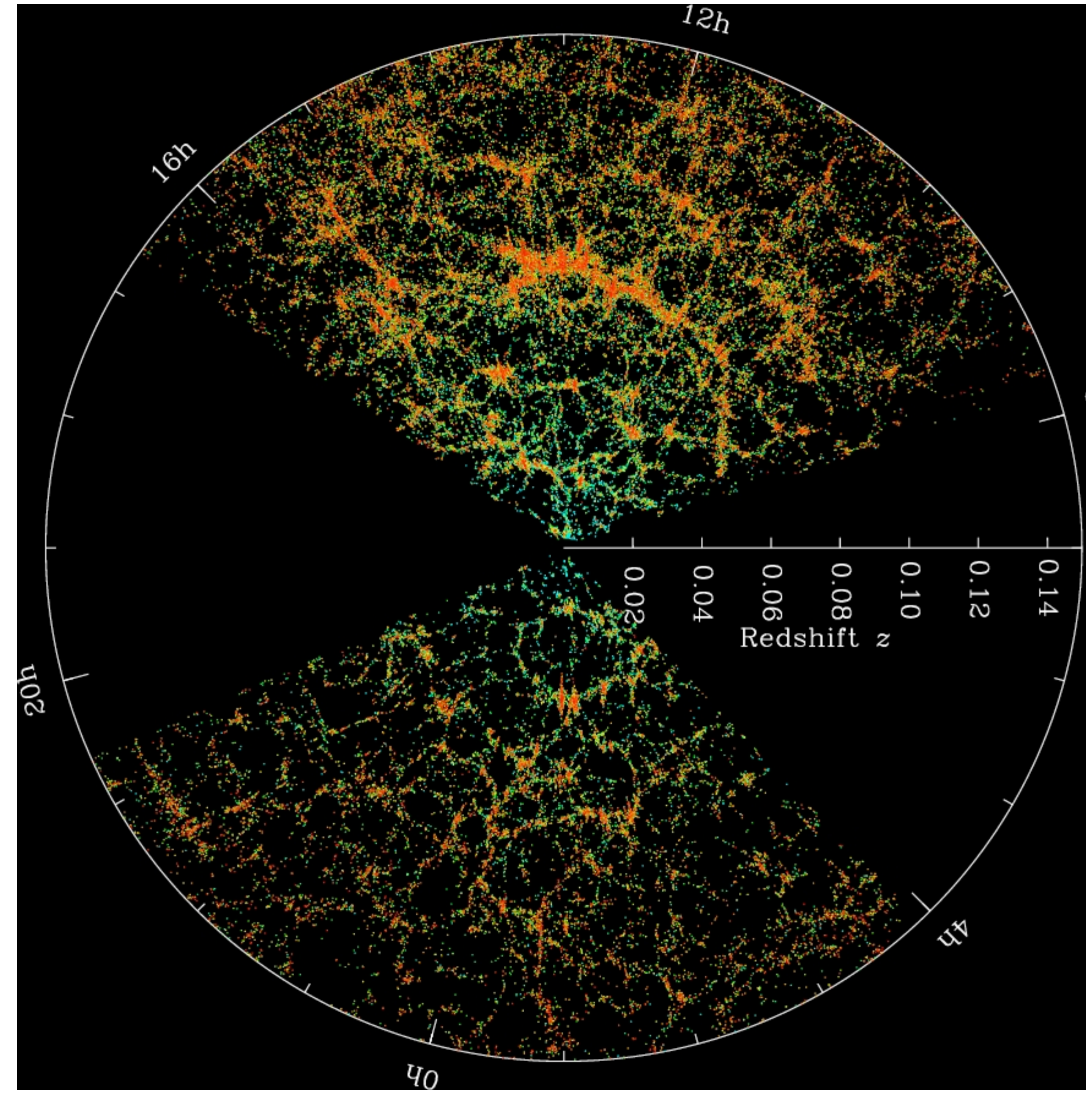

Alfred P. Sloan Foundation

2.5m du Pont Telescope at Las Campanas

2.5m Telescope at Apache Point Observatory

SDSS

Sloan Digital Sky Survey III

January 15, 2002

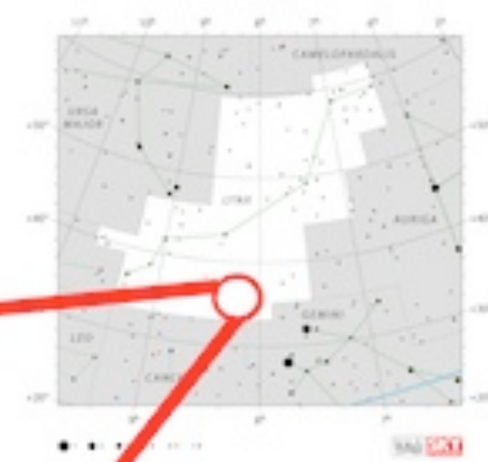

This aluminum plate was used by the Sloan Digital Sky Survey (SDSS) to make a 3D map of the universe. The images above and left show the sky area where this plate was used; the red circle shows the area observed by the plate. Each hole matches a star, galaxy, or quasar.

Using this plate, the SDSS can measure the distance and chemical makeup of 640 stars and galaxies at once.

Structure Formation Conclusions

- Dark Matter cannot be hot (relativistic)
  - Neutrinos are not a good dark matter candidate
- Dark Matter should be cold (v<<c)
  - Dark Matter might still be warm

What is dark matter ?

General Observational Evidence

- Dark matter should be
  - non-relativistic velocities (Cold)
  - not electro-magnetically interacting (Neutral)
  - not strongly interacting with itself or with baryonic matter (Non-baryonic)
  - has not decayed (Stable)

So what is dark matter ?

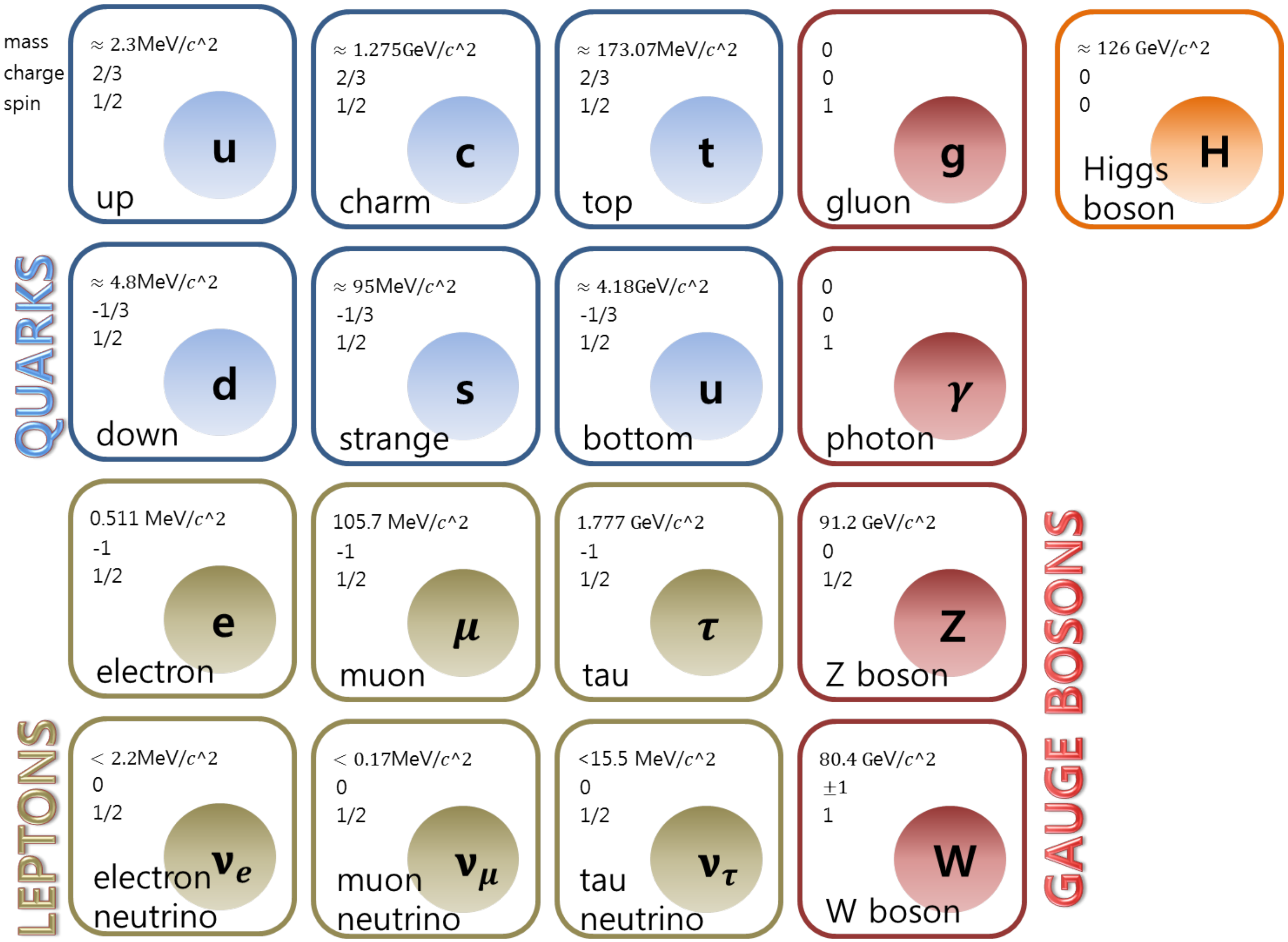

Structure Formation Conclusions

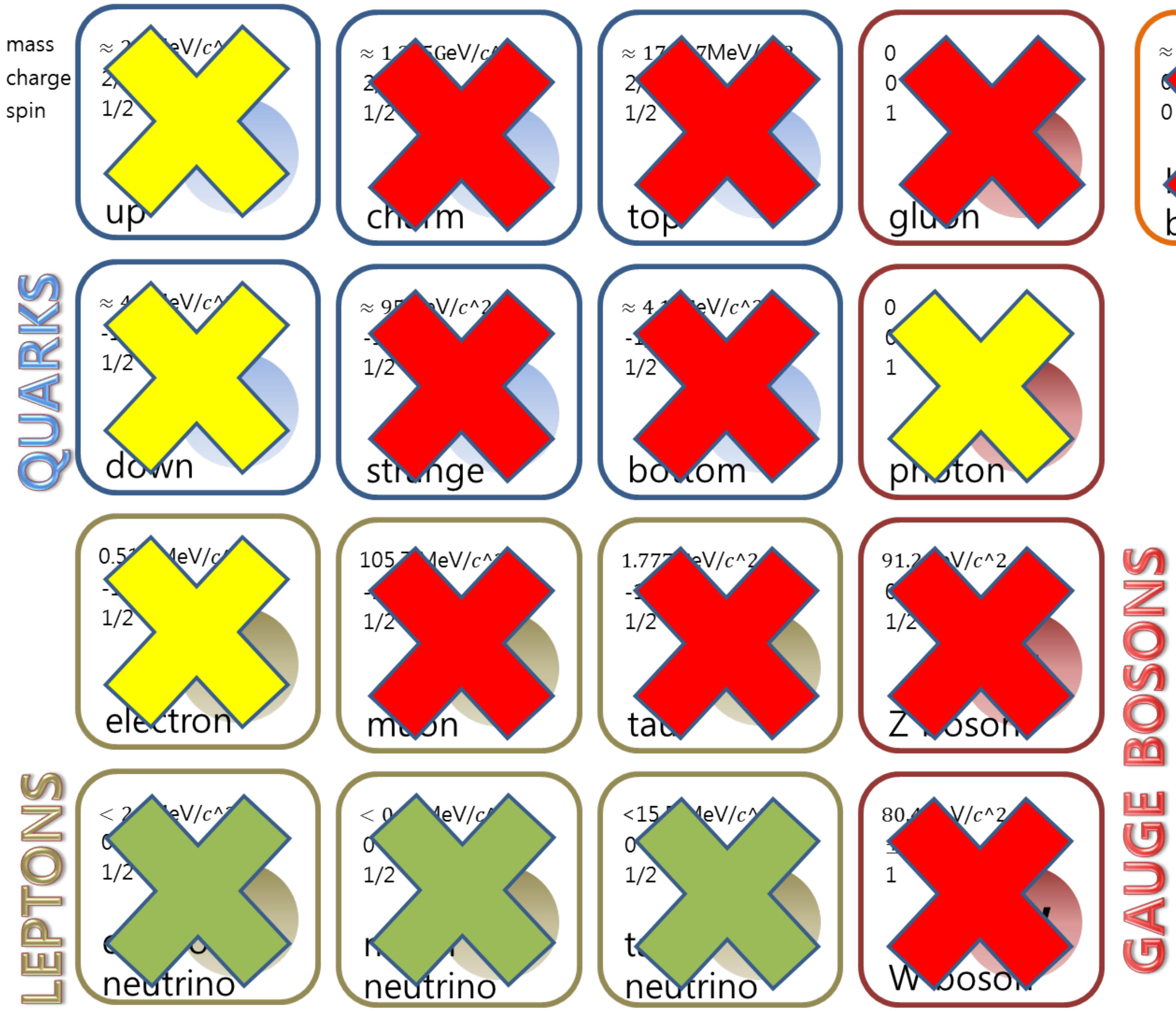

- not stable
- Electromagnetic interaction
- hot dark matter

Weakly Interacting Massive Particle (χ)

- **Observational Evidence for Dark Matter points to**
  - Non-baryonic
  - Cold massive
  - Not strongly interacting
  - Stable (long lived)

WIMP

- **WIMPs often arise naturally in extensions to the Standard Model of Particle Physics: Supersymmetry, ...**

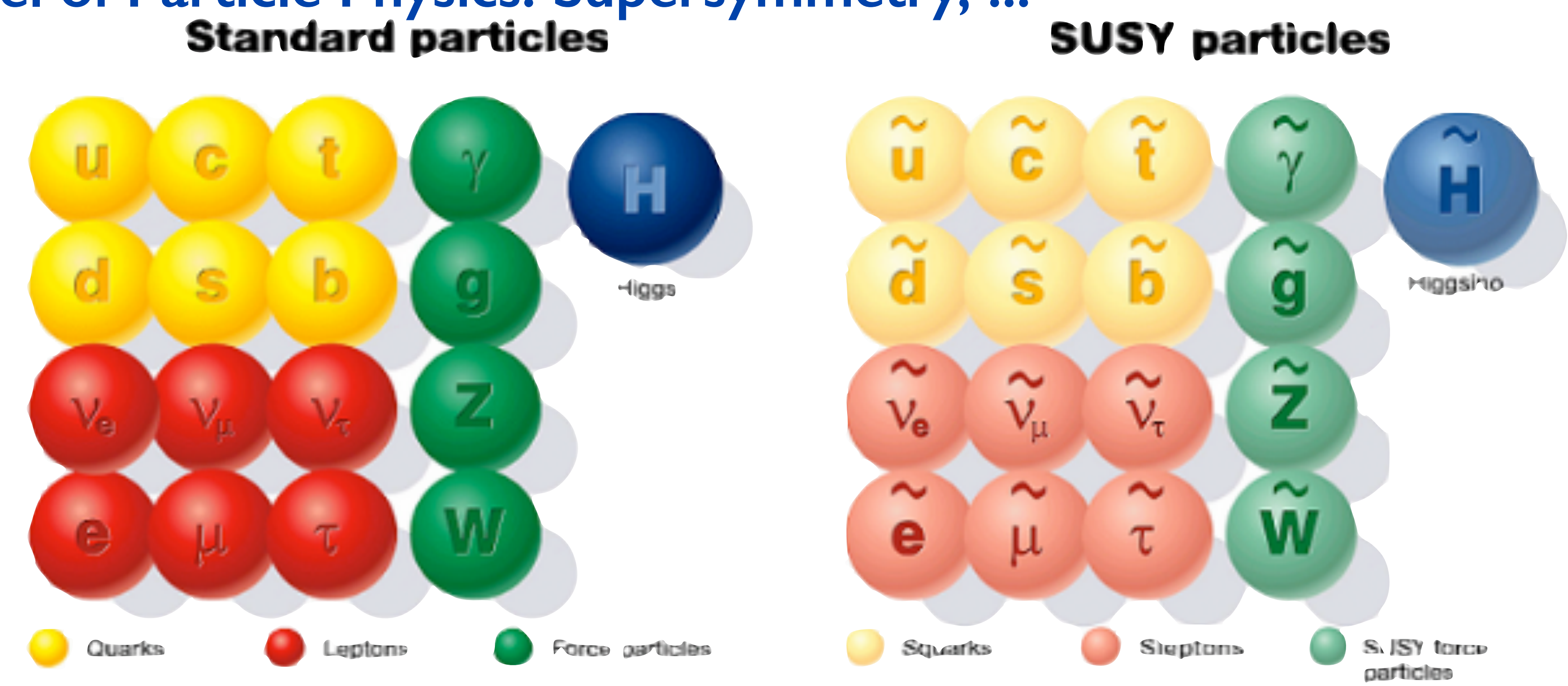

Indirect Dark Matter Searches

Searches for WIMPs

Production	Scattering	Annihilation

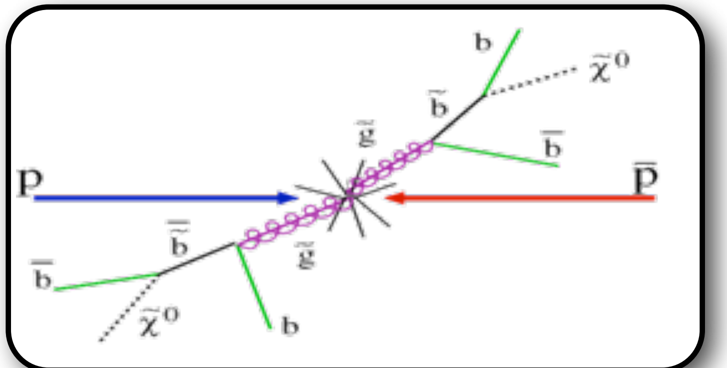

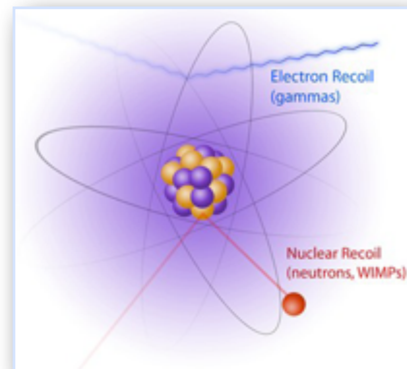

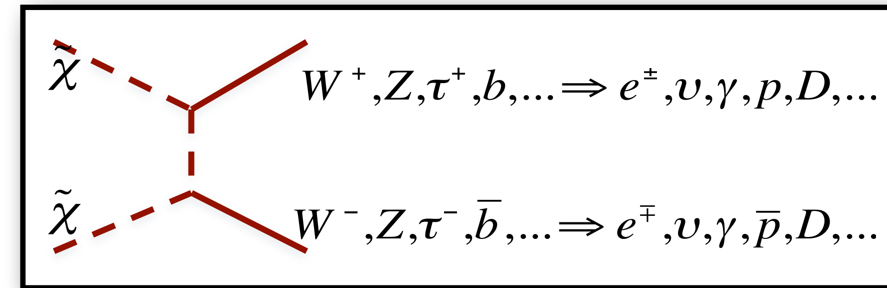

Colliders	Direct	Indirect

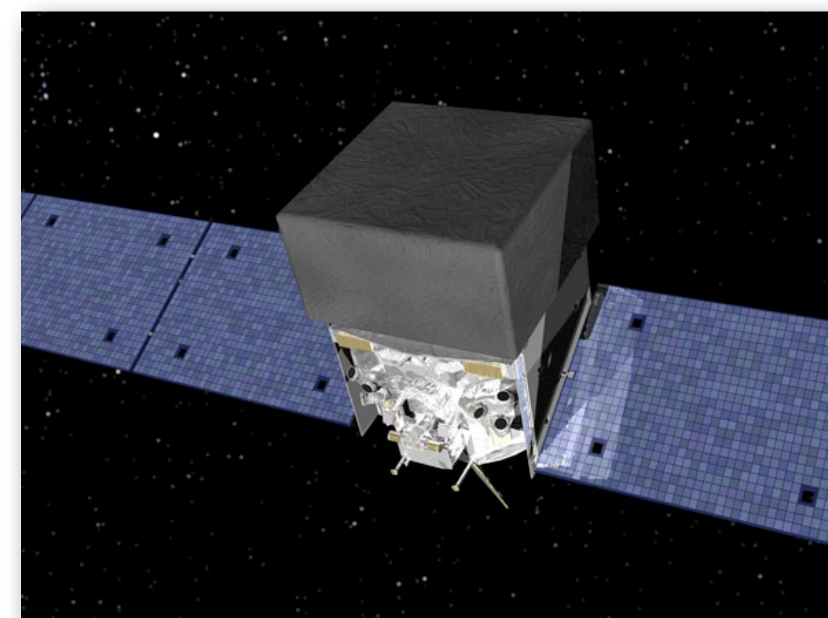

Dark Matter Annihilation Signals

- Interactions that determine the WIMP relic abundance also lead to self-annihilations in the present epoch
  - Identify overdense regions of Dark Matter ⇒self-annihilation can occur at significant rates
- Pick prominent Dark Matter target
- Understand backgrounds
- Features in the signal enhance to chance distinguish backgrounds
  - Line / End-point

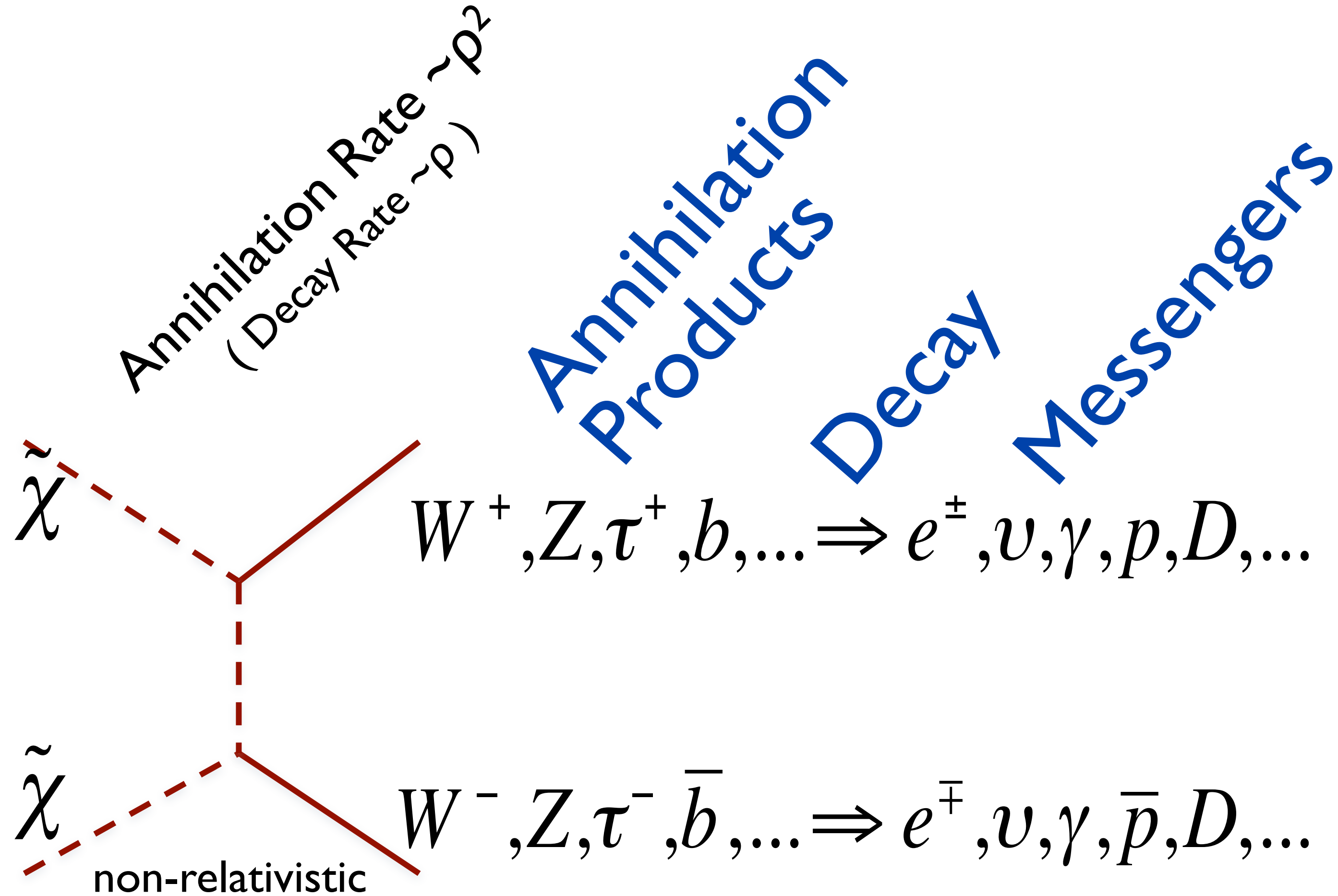

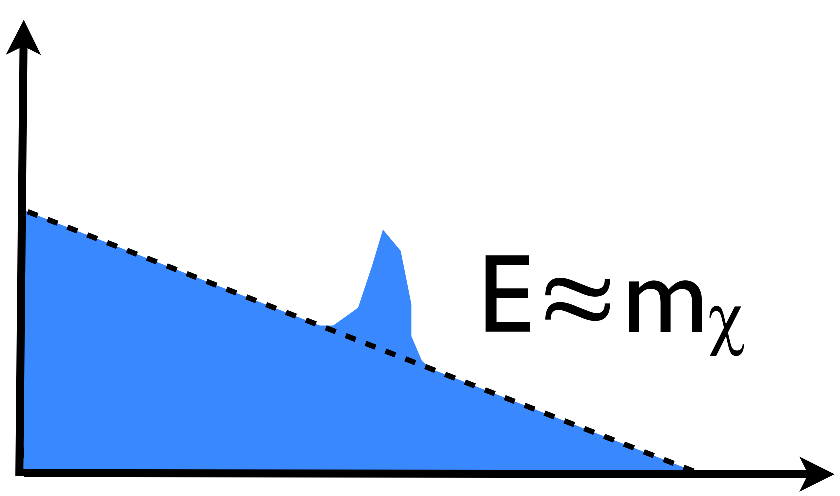

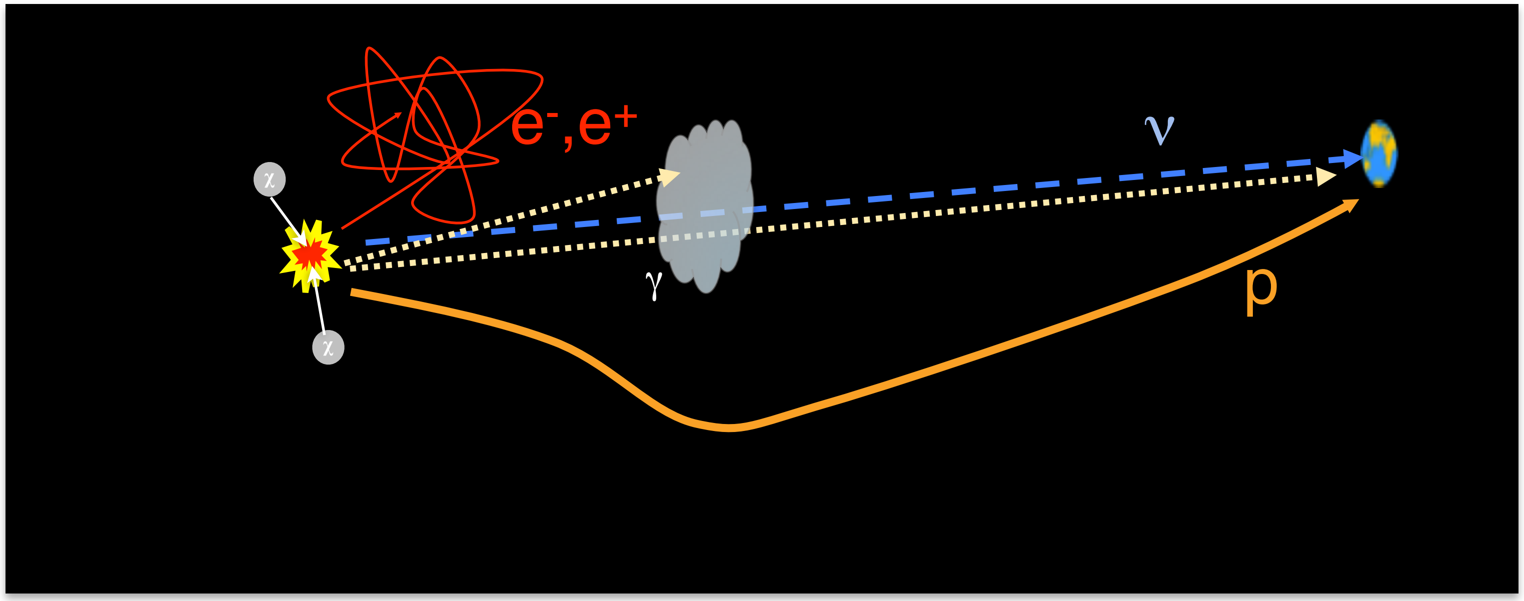

Dark Matter Signals

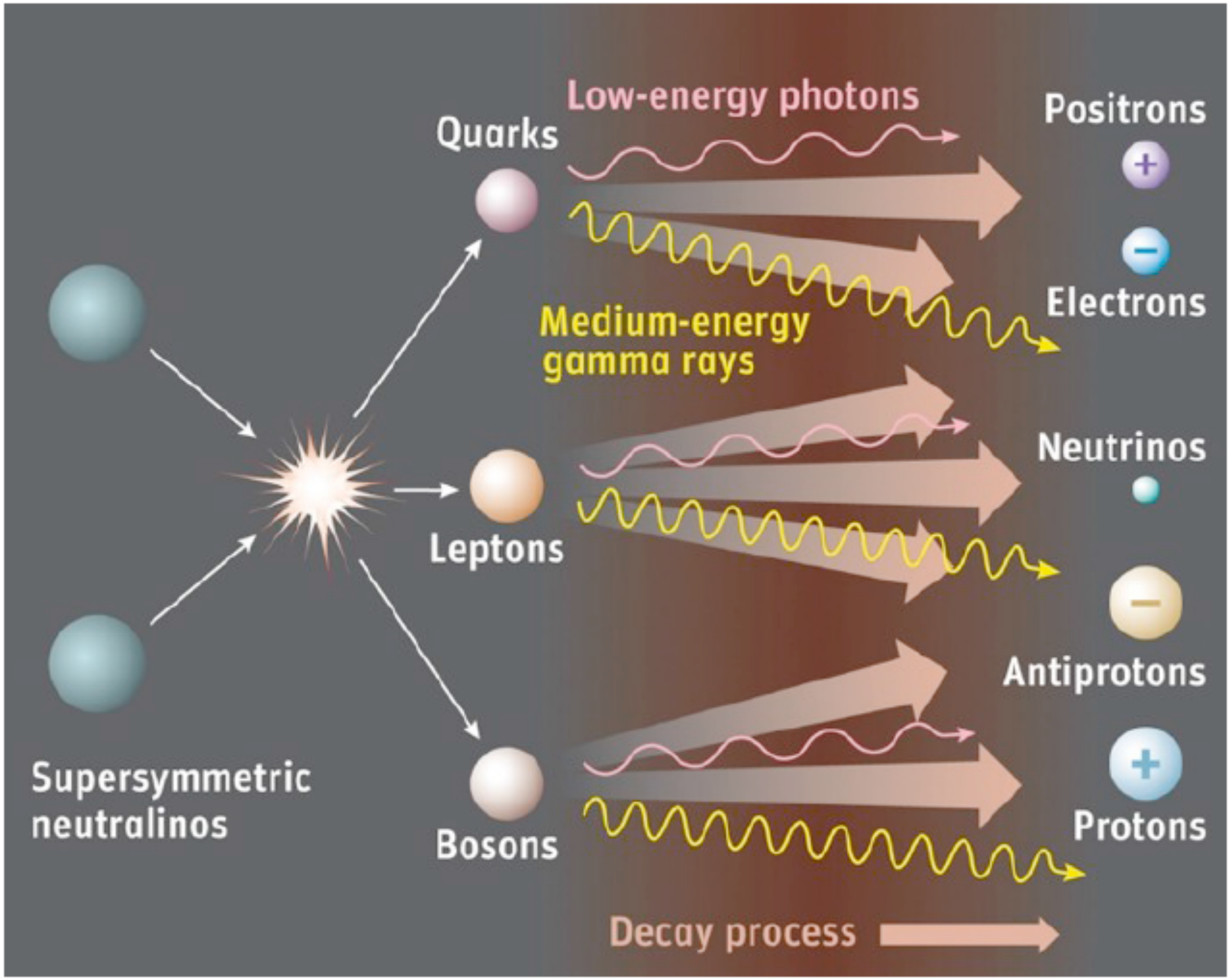

Credit: Sky & Telescope / Gregg Dinderman

Strategies and Targets

Dark Matter at all scales

“Evidence”

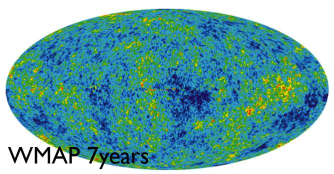

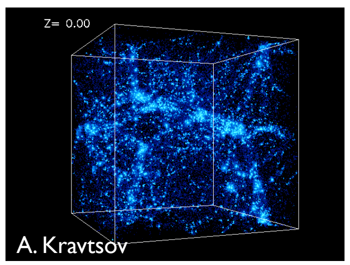

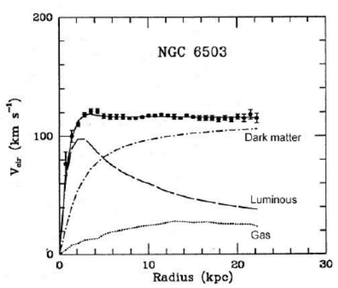

Begeman, Broels & Sanders (1991)

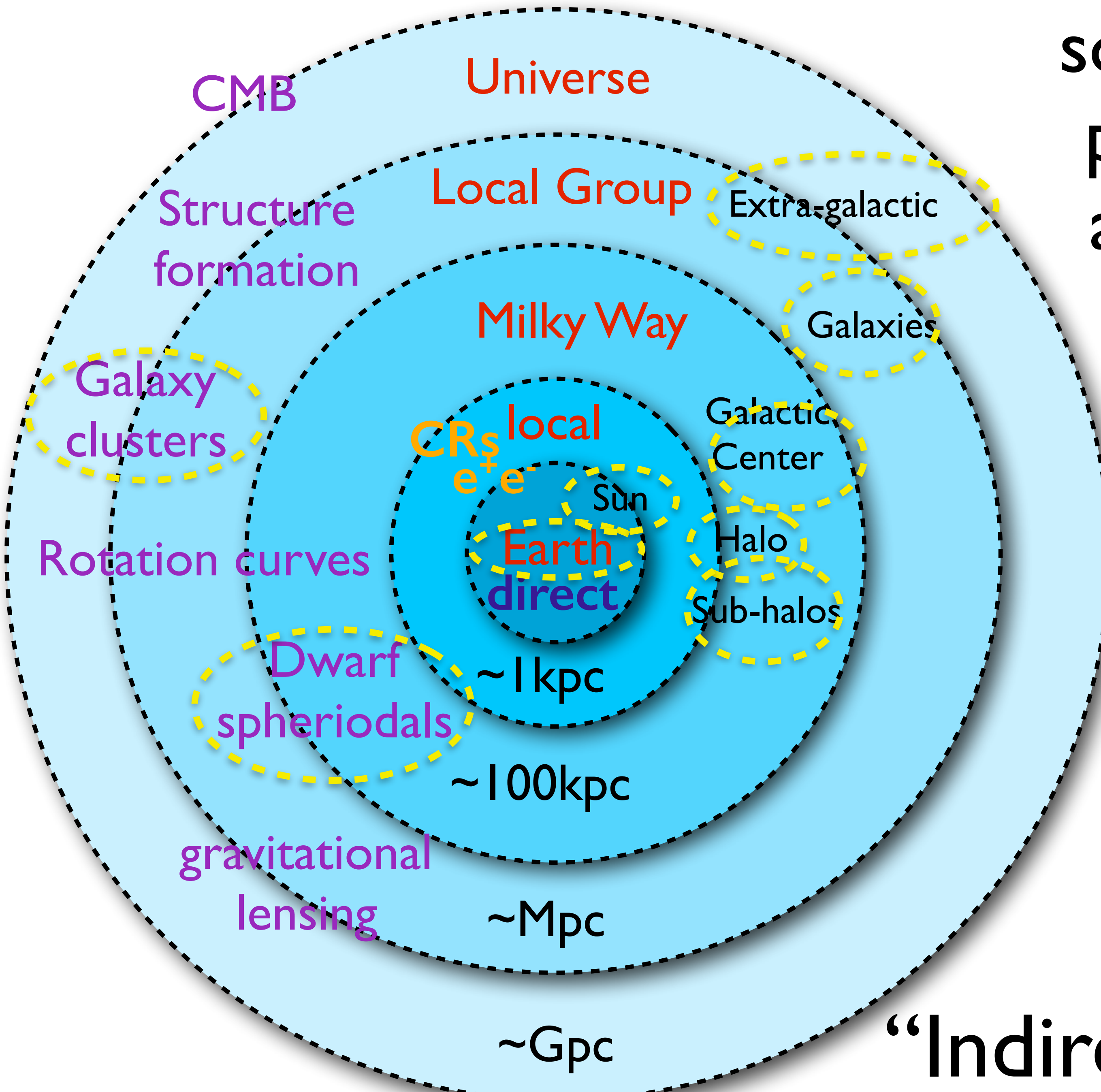

Other objects or sources expected to produce significant annihilation signals

“Indirect Targets” for ν,γ

Individual sources and diffuse

Sources of High Energy Neutrinos

Dark Matter self-annihilation or decay

Annihilation — K_{ann} — $J(\Psi)_{ann}$

$$\frac{d\Phi}{dE}(E,\phi,\theta) = \frac{1}{4\pi}\frac{\langle\sigma_A v\rangle}{2m_\chi^2}\sum_f Br(f)\frac{dN_f}{dE} \times \int_{\Delta\Omega(\phi,\theta)} d\Omega' \int_{\mathrm{los}} \rho^2(r(l,\phi'))dl(r,\phi')$$

Measure Flux — **Particle Physics** — **Dark Matter Distribution**

$$\frac{d\Phi}{dE}(E,\phi,\theta) = \frac{1}{4\pi}\frac{1}{m_\chi \tau_\chi}\sum_f Br(f)\frac{dN_f}{dE} \times \int_{\Delta\Omega(\phi,\theta)} d\Omega' \int_{los} \rho(r(l,\phi'))dl(r,\phi')$$

Decay — K_{decay} — $J(\Psi)_{decay}$

expected prompt signal
for particles propagating
directly to the observer
(gamma-rays, neutrinos)

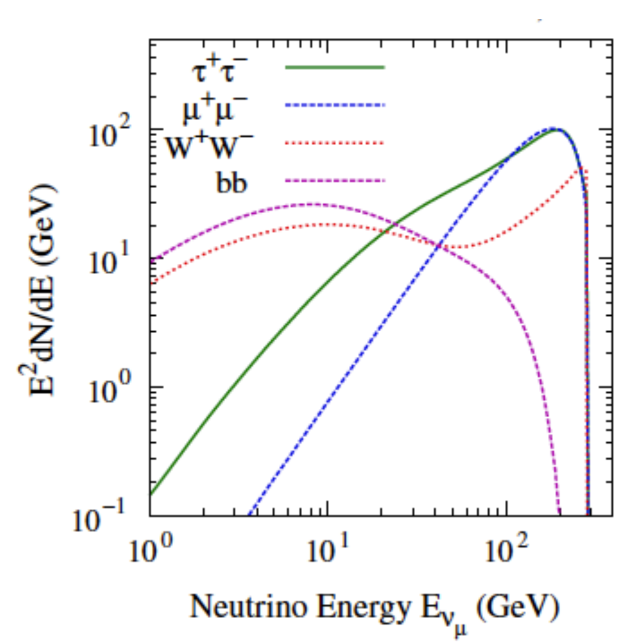

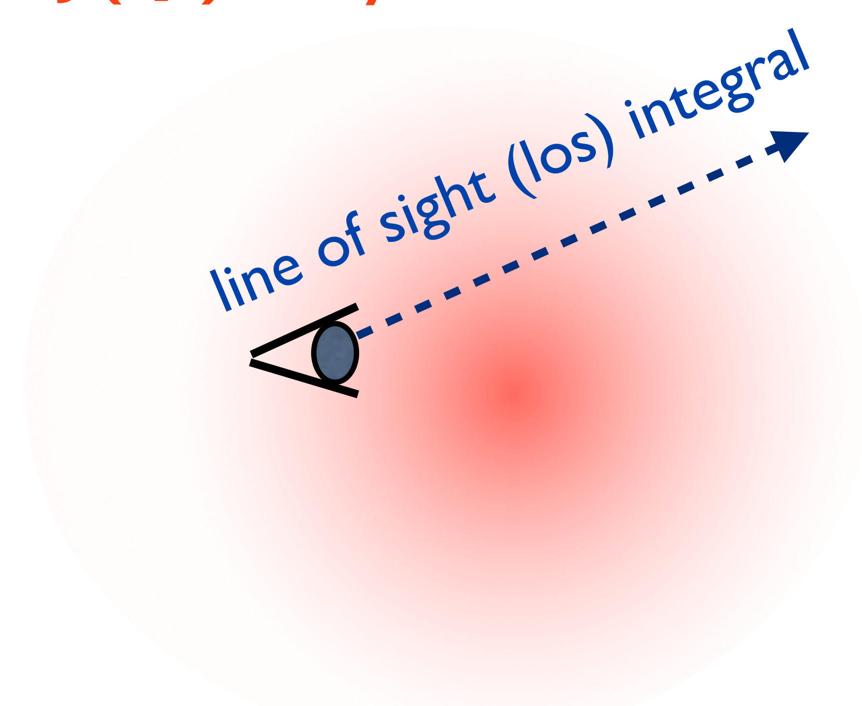

N-Body Simulations

These images show the six Milky-Way sized halos we simulated, at z=0. The resolution corresponds to our resolution level 2, which has between 160 and 224 million particles in the final halo.

Click to enlarge the images.

Links to some N-body movies of structure formation (DM-only):
Millennium run (Structure formation):
http://www.mpa-garching.mpg.de/galform/virgo/millennium/
Aquarius run (Milky Way halo):
http://www.mpa-garching.mpg.de/aquarius/

How Dark Matter is distributed

- N-body simulations of Milky Way like galaxies yield halo profiles ρ(r). Halo profiles described the average dark matter density (smooth)
- Two major difficulties
  - Inner halo shape (cuspy or cored ?)
  - Sub-structure in outer halo

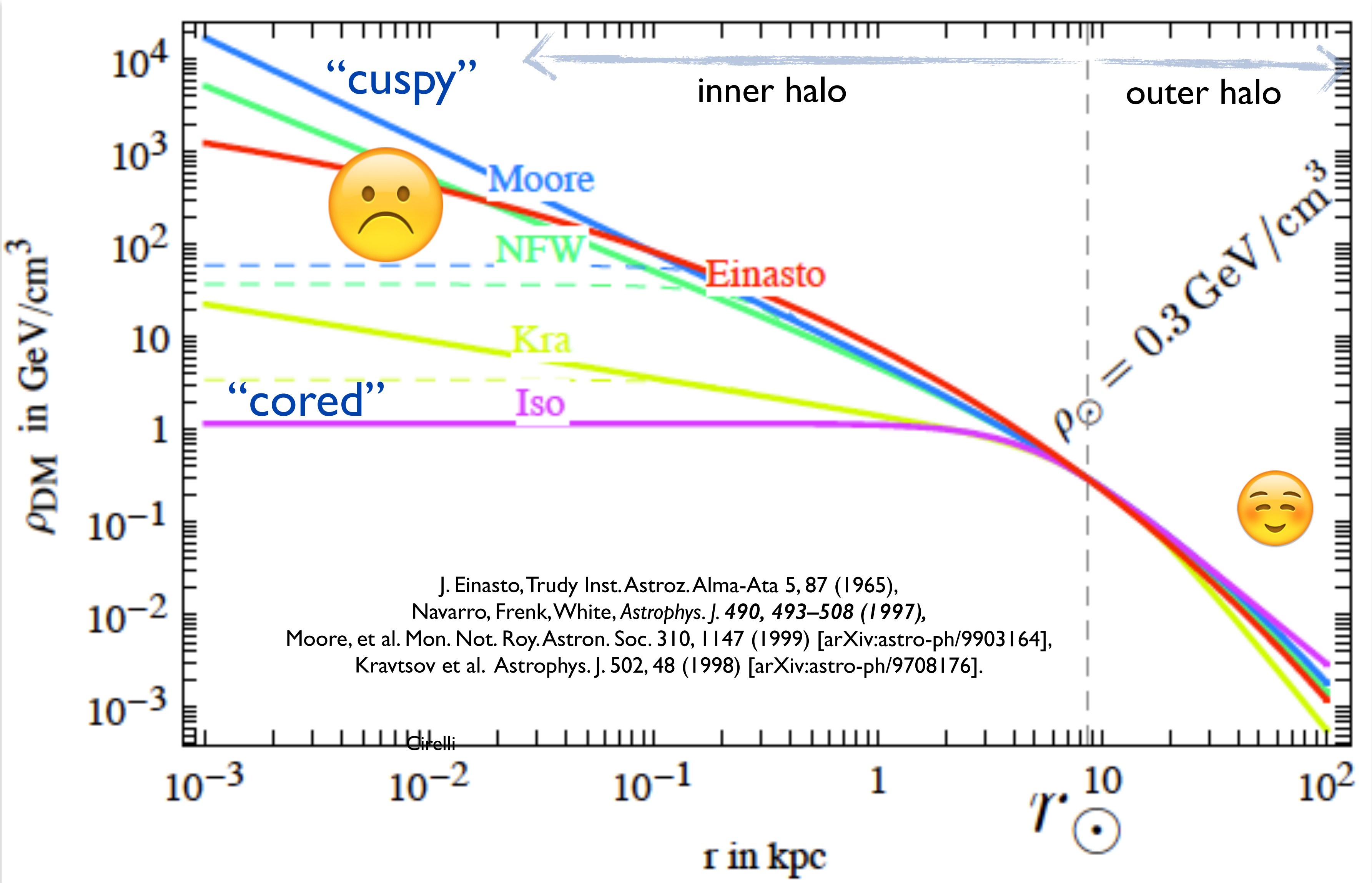

Dark Matter self-annihilation or decay

Annihilation — Measure Flux — K_{ann} (Particle Physics) — $J(\Psi)_{ann}$ (Dark Matter Distribution)

$$\frac{d\Phi}{dE}(E,\phi,\theta) = \frac{1}{4\pi}\frac{\langle\sigma_A v\rangle}{2m_\chi^2}\sum_f Br(f)\frac{dN_f}{dE} \times \int_{\Delta\Omega(\phi,\theta)} d\Omega' \int_{\rm los} \rho^2(r(l,\phi'))dl(r,\phi')$$

Measure Flux — Particle Physics — Dark Matter Distribution

$$\frac{d\Phi}{dE}(E,\phi,\theta) = \frac{1}{4\pi}\frac{1}{m_\chi \tau_\chi}\sum_f Br(f)\frac{dN_f}{dE} \times \int_{\Delta\Omega(\phi,\theta)} d\Omega' \int_{los} \rho(r(l,\phi'))dl(r,\phi')$$

Decay — K_{decay} — $J(\Psi)_{decay}$

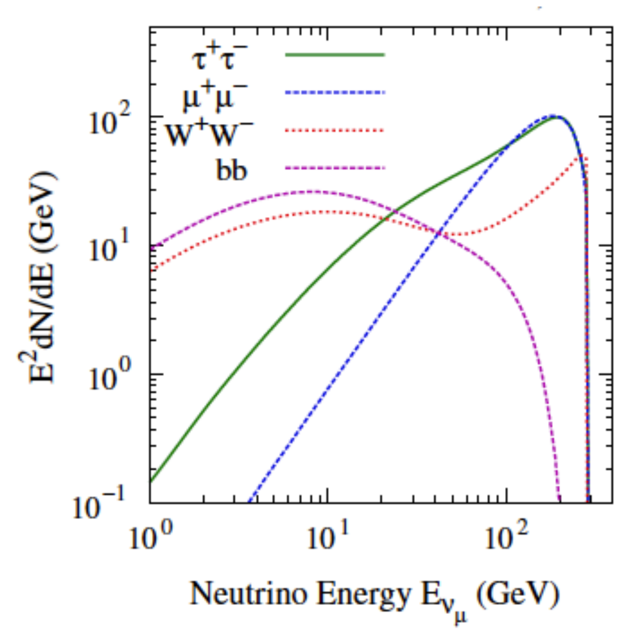

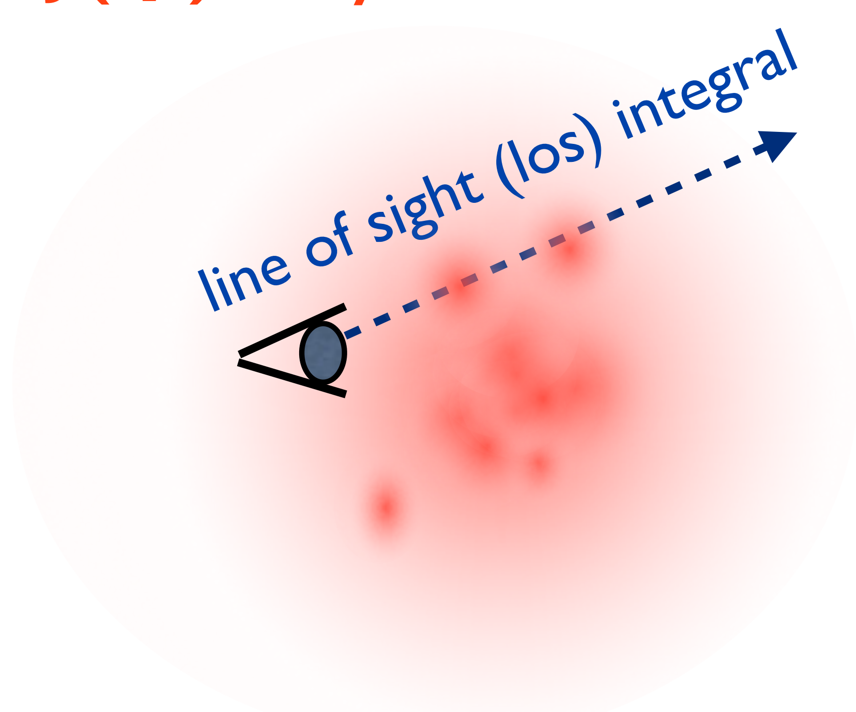

Sources of High Energy Neutrinos

Dark Matter self-annihilation or decay

Annihilation — K_{ann} — Boost x $J_{smooth}(\Psi)_{ann}$

$$\frac{d\Phi}{dE}(E,\phi,\theta) = \frac{1}{4\pi}\frac{\langle\sigma_A v\rangle}{2m_\chi^2}\sum_f Br(f)\frac{dN_f}{dE} \times \int_{\Delta\Omega(\phi,\theta)} d\Omega' \int_{los} b\times\rho^2_{smooth}(r(l,\phi'))dl(r,\phi')$$

Measure Flux — **Particle Physics** — **Dark Matter Distribution**

$$\frac{d\Phi}{dE}(E,\phi,\theta) = \frac{1}{4\pi}\frac{1}{m_\chi\tau_\chi}\sum_f Br(f)\frac{dN_f}{dE} \times \int_{\Delta\Omega(\phi,\theta)} d\Omega' \int_{los} \rho_{smooth}(r(l,\phi'))dl(r,\phi')$$

Decay — K_{decay} — $J_{smooth}(\Psi)_{decay}$

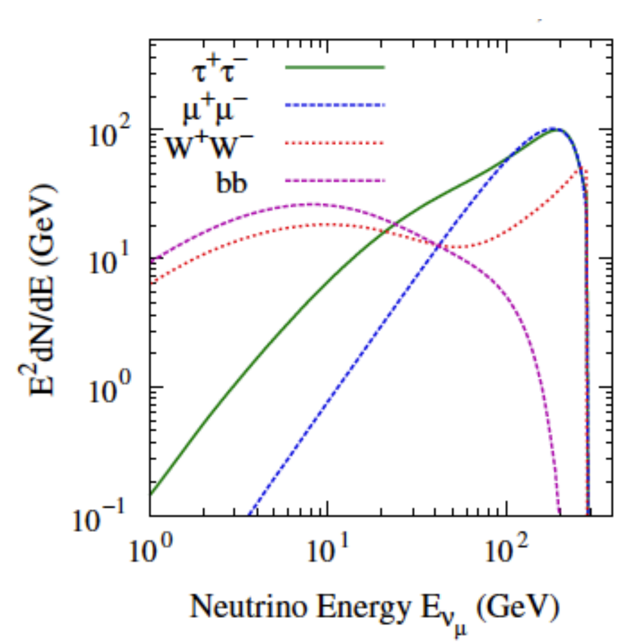

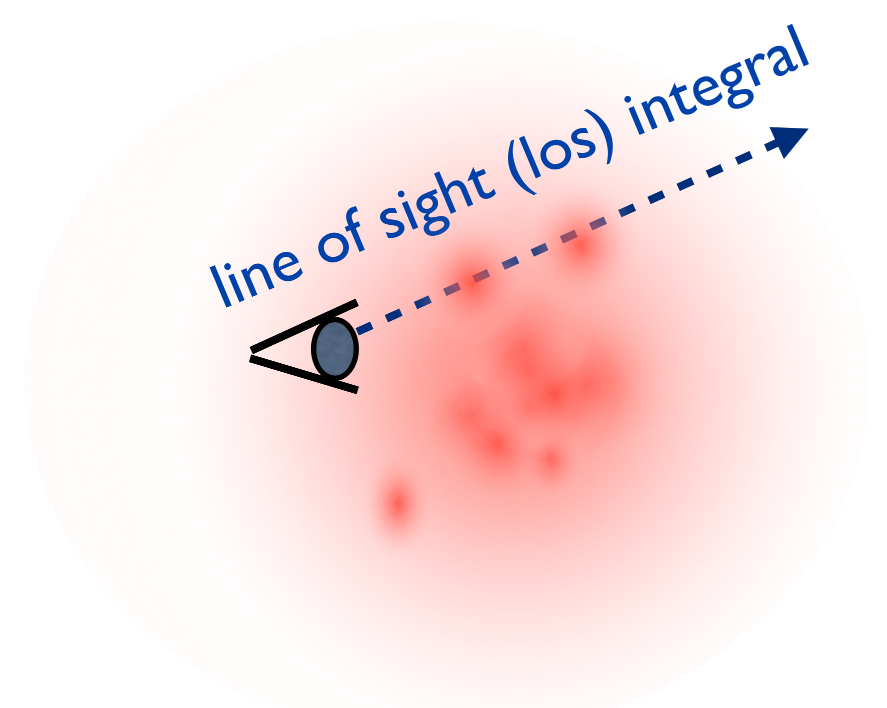

Boost factor

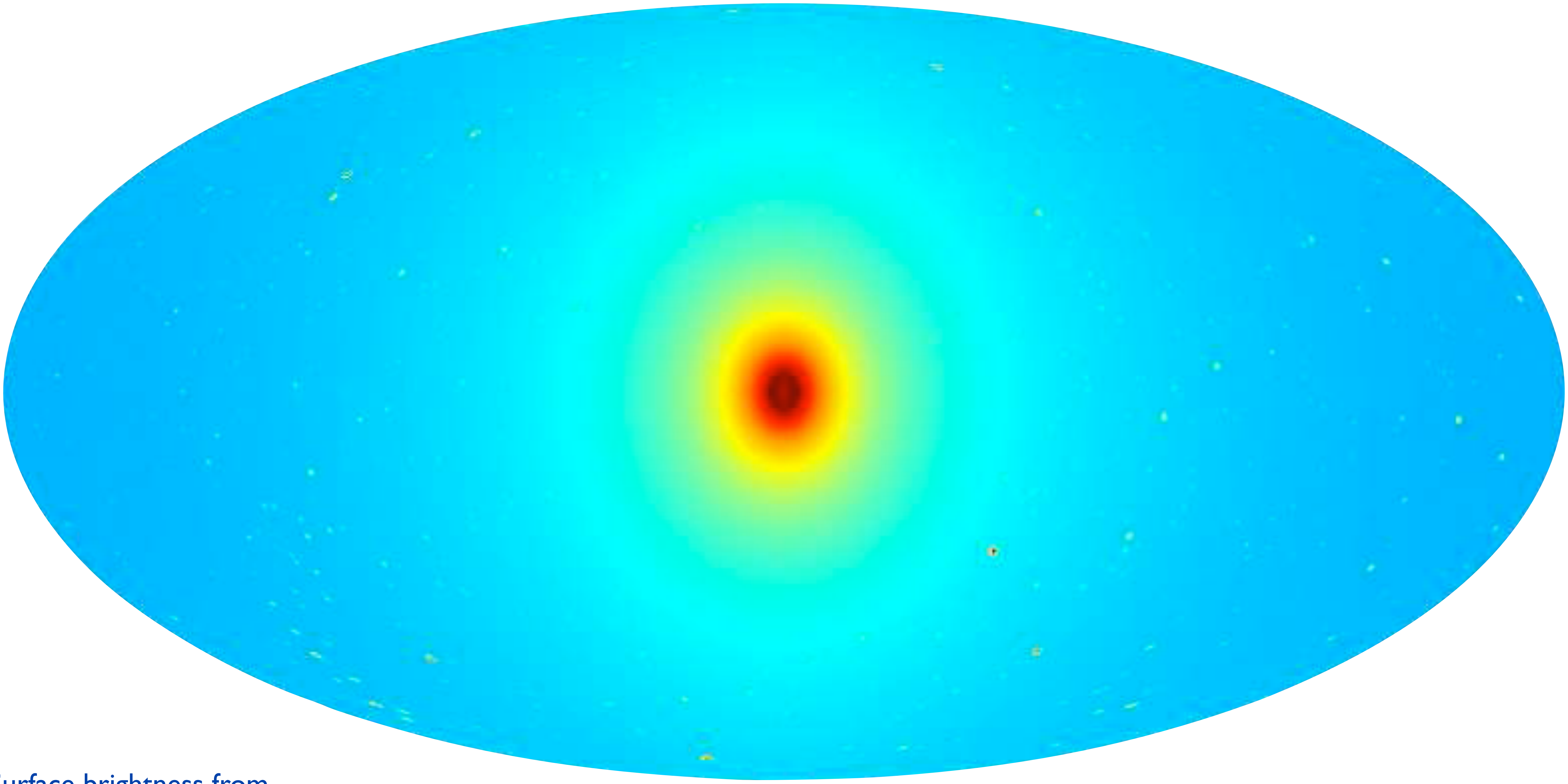

Surface brightness from dark matter annihilation at the position of the Sun, calculated directly from the Aq-A-1 simulation.

Astro-physical boost factor

- Local clumps in the DM halo enhance the density and boost the flux from annihilations:
  - Boost $B = \dfrac{\phi^{actual}(\vec{r})}{\phi^{smooth}(\vec{r})}$
- Typical boost factors are B~ 1-20 (simulations)
- Boost factor ~ 1 (for central halo region <10kpc) tidal stripping

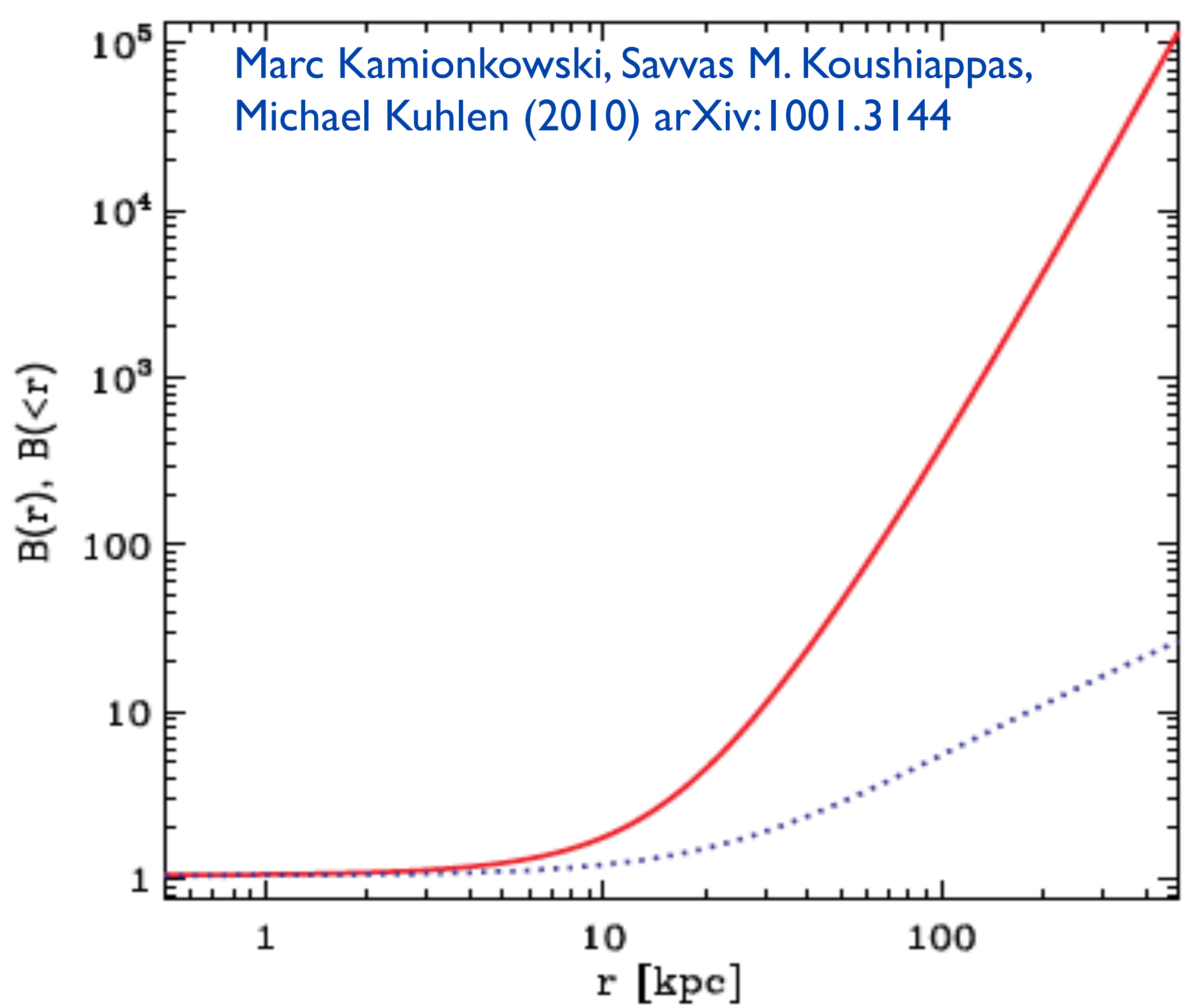

FIG. 4. The local substructure boost $B(r)$ (*solid*) and the cumulative luminosity boost $B(<r)$ (*dotted*), as a function of radius.

Boost factor

- Boost factor important for:
  - Galaxy clusters,
  - Diffuse extra galactic, ...
- Not important for:
  - Galactic Center
  - Solar circle
  - Dwarf Spheriodal Galaxies

$$B(r) = \frac{\int \rho^2 dV}{\int (\bar{\rho})^2 dV},$$

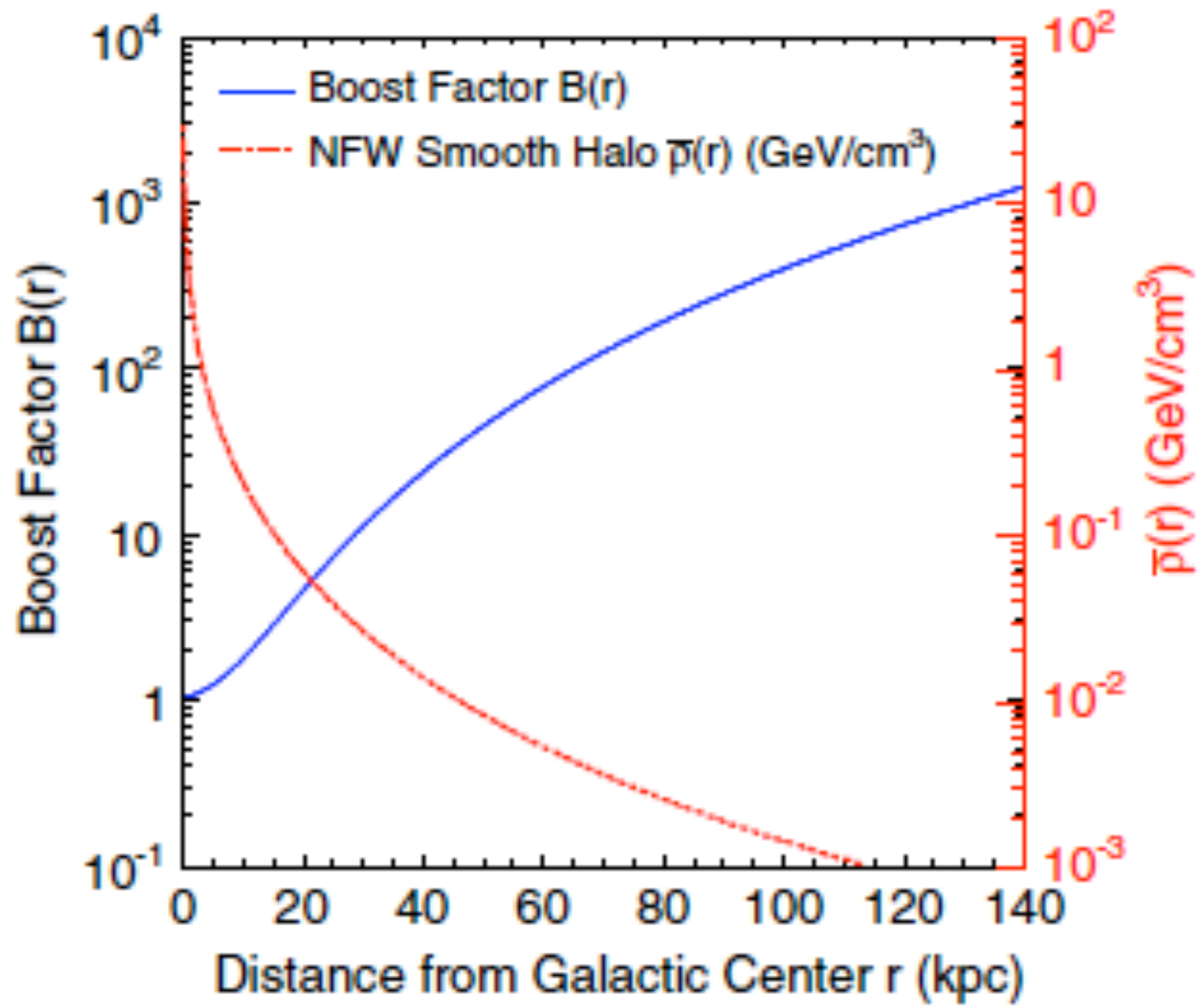

Sources

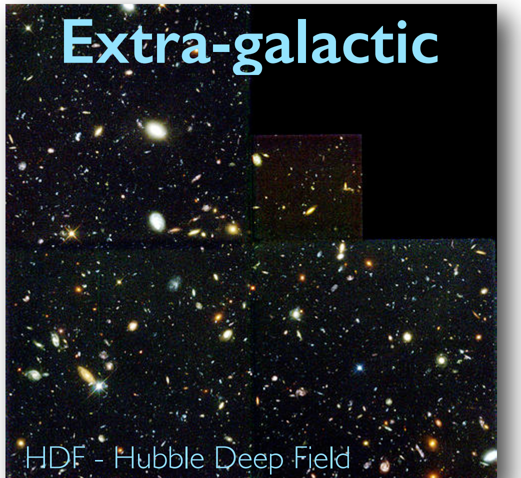

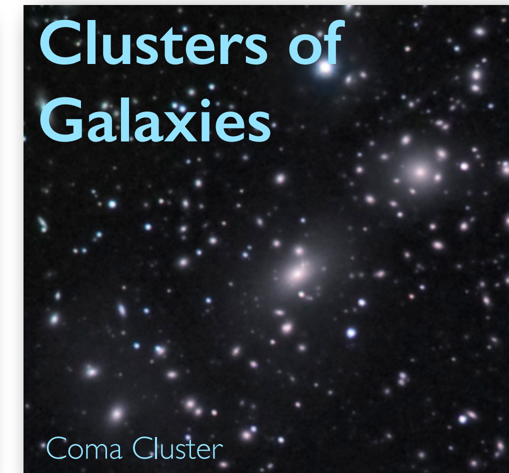

Small halo model dependence, boost factors	Large DM content, nearby source, O(10) larger flux than extra-galactic	Very dense DM accumulation, nearby source	No astrophysical backgrounds	Large DM content, high boost factors from sub structure
Diffuse flux, spectral feature	Anisotropy	Extended Source	Point source	Extended source
Signal weak compared to Galactic signal	Relatively independent from DM halo profile	Very strong dependence on DM density profile	Cored profiles favored, less flux	Understanding of boost factors

Experimental Searches

Indirect Searches - Instruments

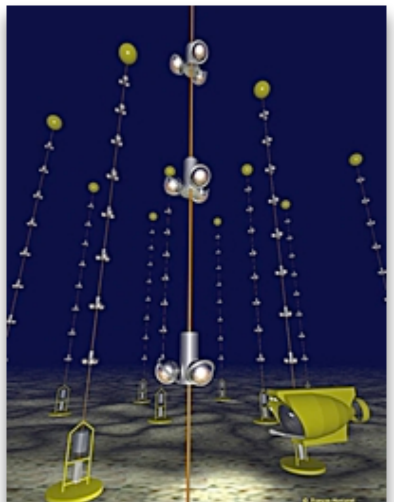

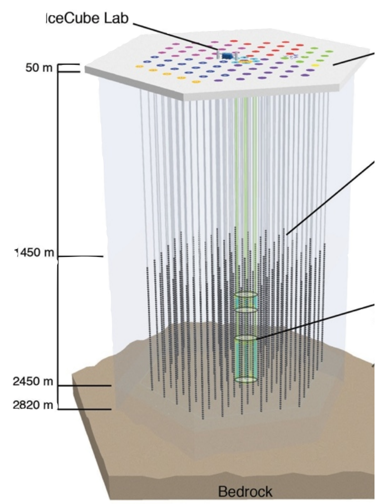

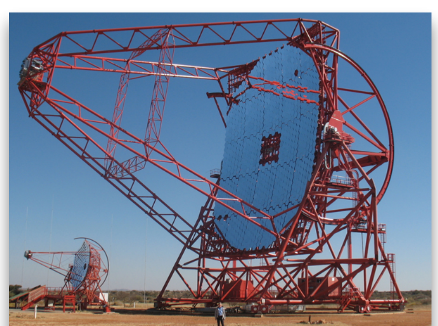

Neutrino Detectors
- ANTARES, NESTOR, NEMO, KM3Net...
- IceCube, PINGU, ORCA, ...
- Baikal, ...
- Super-K, KamLAND, Laguna-LBNO, Hyper-K, ...

Gamma Ray Telescopes
- MAGIC, H.E.S.S., VERITAS, ...
- Fermi, ...
- CTA, Gamma-400,...

Anti-Matter Satellites
- PAMELA, ATIC, PPB-Bets, ...
- AMS-02

Others
- x-ray, radio, ...

Cosmic rays

$\chi + \chi \rightarrow WW \rightarrow e + \nu\text{'s} + \ldots$

$b\bar{b} \rightarrow \nu + \gamma + ..$

qq

ZZ

...

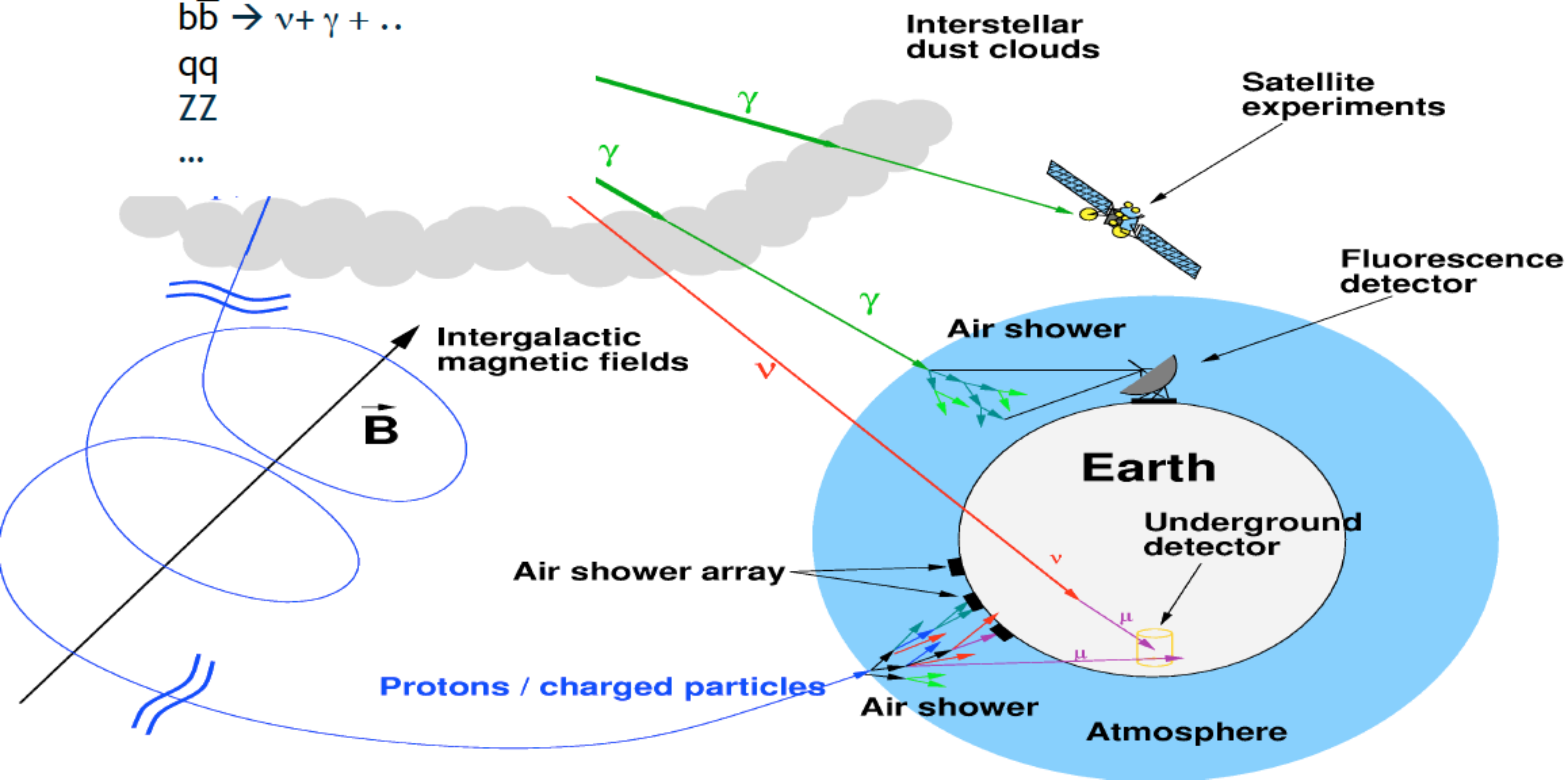

Larmor Radius and Rigidity

Larmor radius, or gyroradius, r_L, is the radius of the orbit of a charged particle moving in a uniform, perpendicular magnetic field, obtained by simply equating the Lorentz force with the centripetal force:

$$qvB = \frac{mv^2}{r_L} \Rightarrow r_L = \frac{p}{ZeB} \tag{1}$$

where p has replaced mv in the classical limit. However, this also holds for the relativistic generalization by considering p to be the relativistic 3-momentum. There are several adaptations of this formula, tuned to units natural to various scenarios. One such is

$$r_L = 33.36\,\text{km}\left(\frac{p}{\text{GeV}/c}\right)\left(\frac{1}{Z}\right)\left(\frac{G}{B}\right)$$

In cosmic ray physics, one often sees references in the literature to the *rigidity* of a particle, defined as

$$R \equiv r_L B c = \frac{pc}{Ze} \tag{2}$$

which has units Volts! A 10 GeV proton has a rigidity of 10 GV, etc ...

PAMELA – Payload for Anti-Matter Exploration and Light-nuclei Astrophysics

Low-earth elliptical orbit

- Launched: June 2006
- Satellite-born Magnetic spectrometer
- Size 70x70x130cm^3
- e$^+$(e$^-$) - 50 MeV –300GeV (600GeV)
- Protons up to ~1TeV

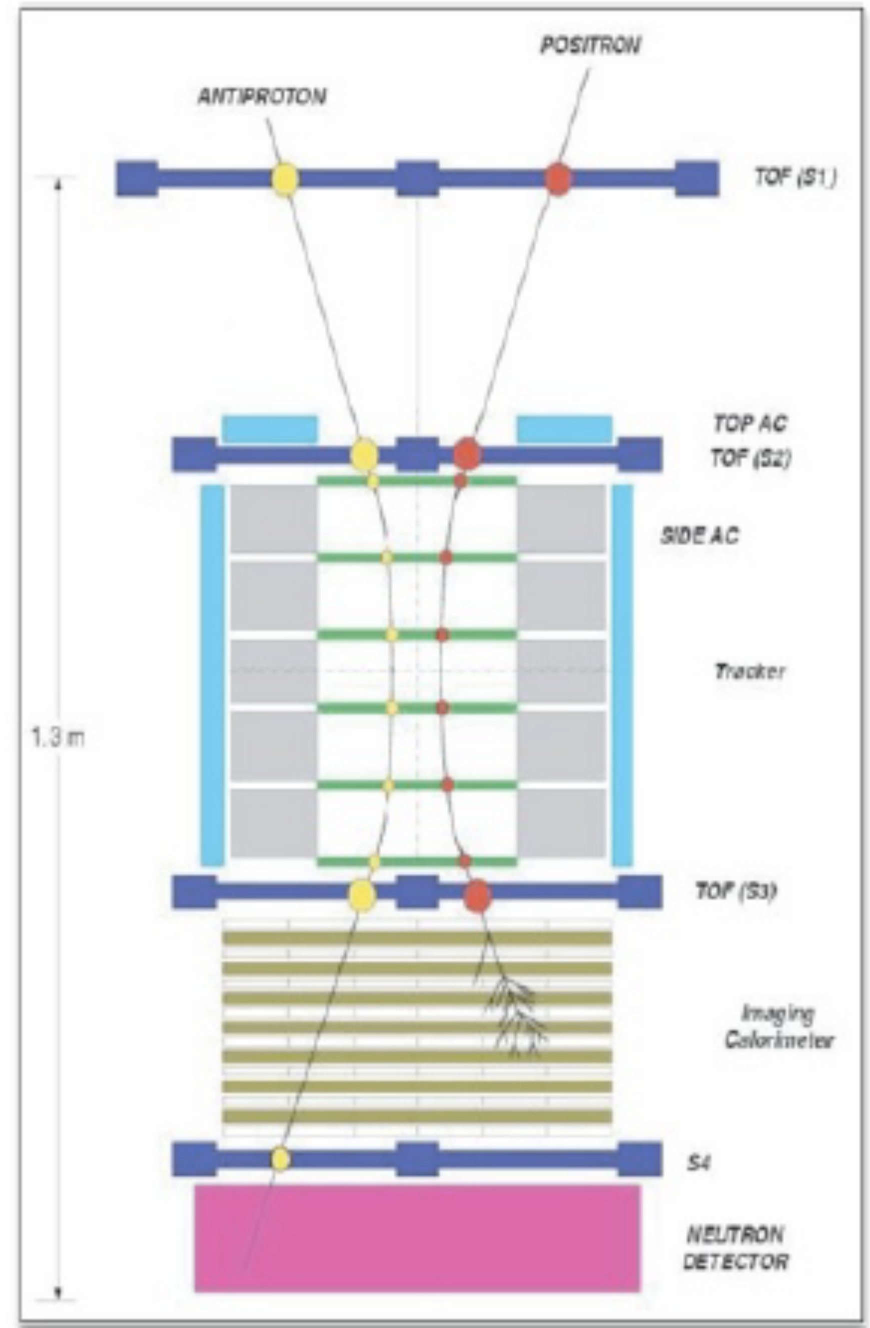

Astropart.Phys. 27 (2007) 296-315


AMS
AMS

AMS: A TeV precision, multipurpose spectrometer

Transition Radiation Detector
Identify e⁺, e⁻

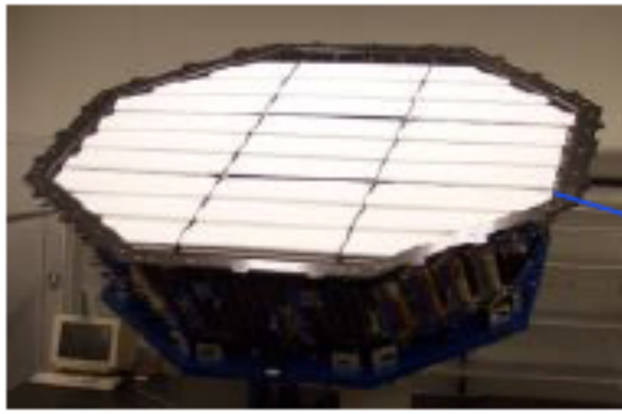

Silicon Tracker
Z, P

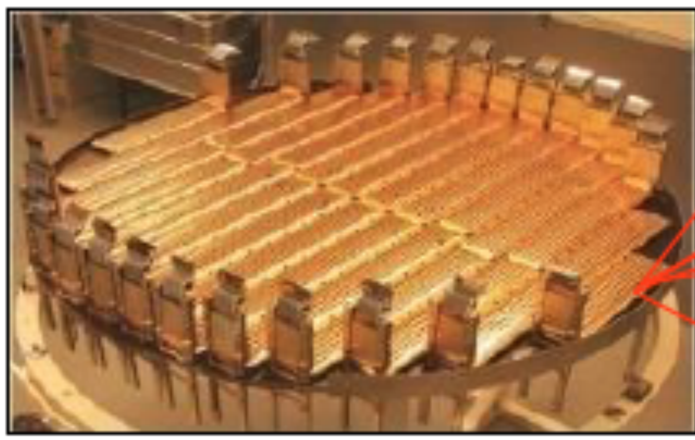

Electromagnetic Calorimeter
E of e^+, e^-

Particles and nuclei are defined by their charge (**Z**) and energy (**E**)

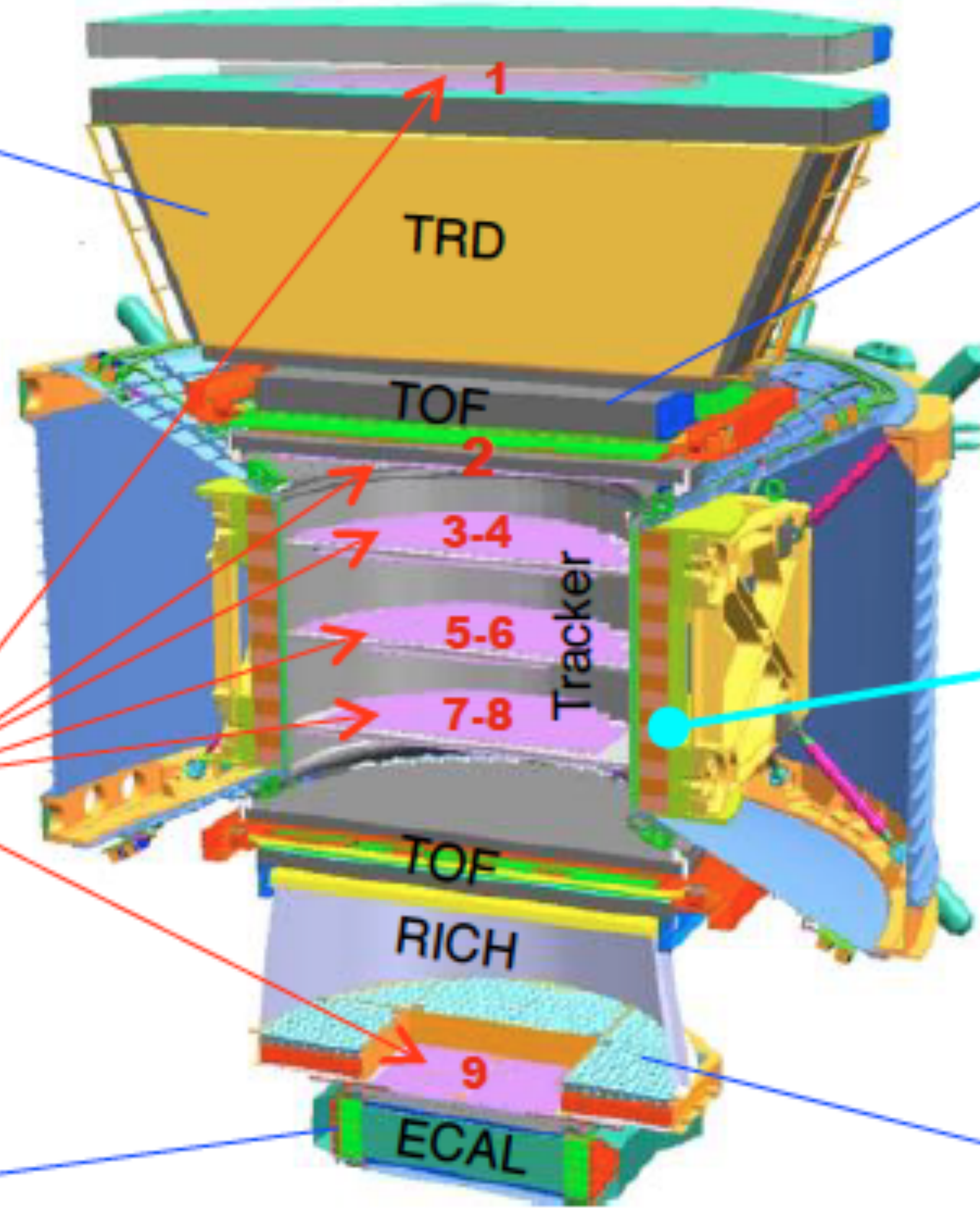

The Charge and Energy are measured independently by many detectors

Time of Flight
Z, E

Magnet
±Z

Ring Imaging Cherenkov
Z, E

4

Tests at CERN
AMS in accelerator test beams Feb 4-8 and Aug 8-20, 2010

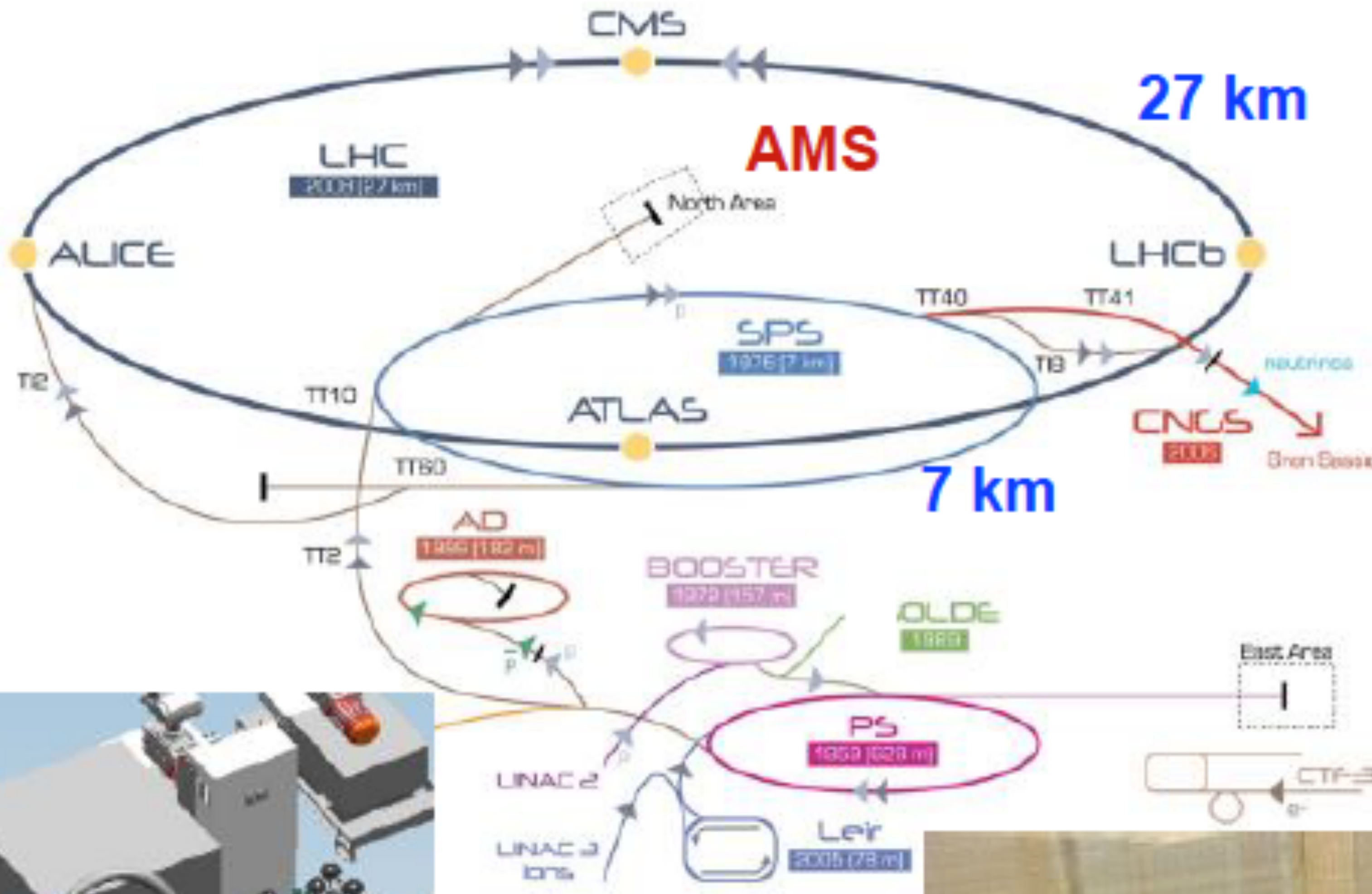

p, e+, e- ,π
10-400 GeV

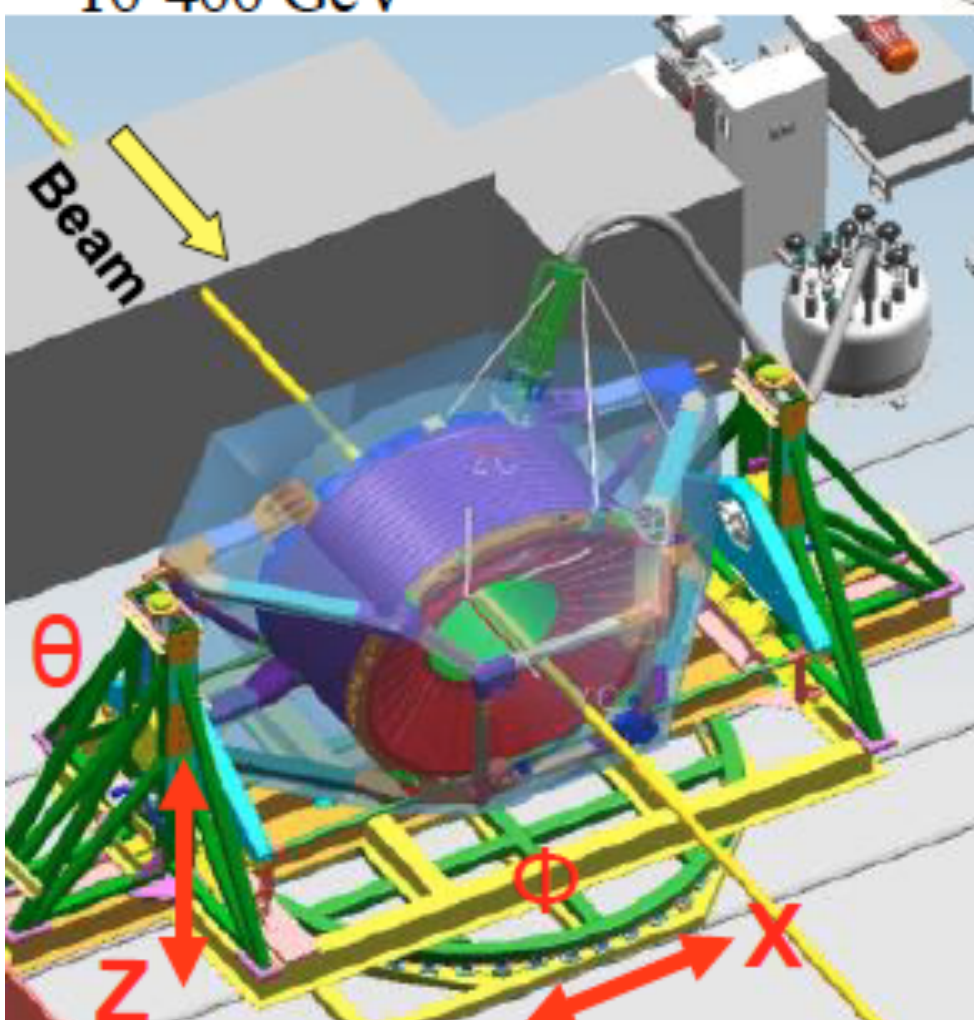

2000 positions


AMS installed on the ISS at
5:15 CDT May 19, 2011
AMS taking data since
9:35 CDT May 19, 2011

To date AMS collected over 85 billion events

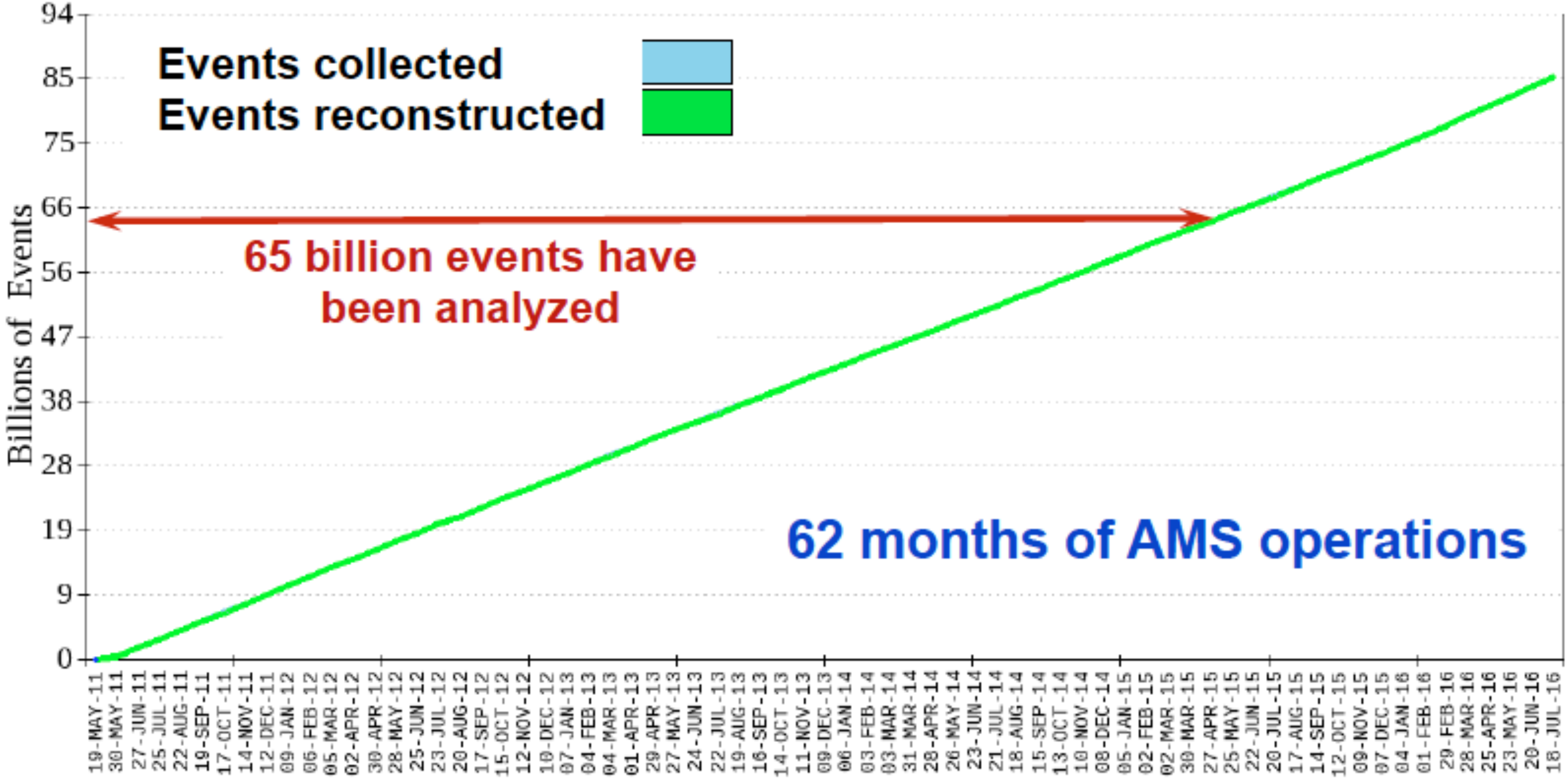

Dark Matter

Collision of "ordinary" Cosmic Rays produce e+, $\bar{p}$…

Annihilation of Dark Matter (neutralinos, χ) will produce additional e+, $\bar{p}$

M. Turner and F. Wilczek, Phys. Rev. D42 (1990) 1001

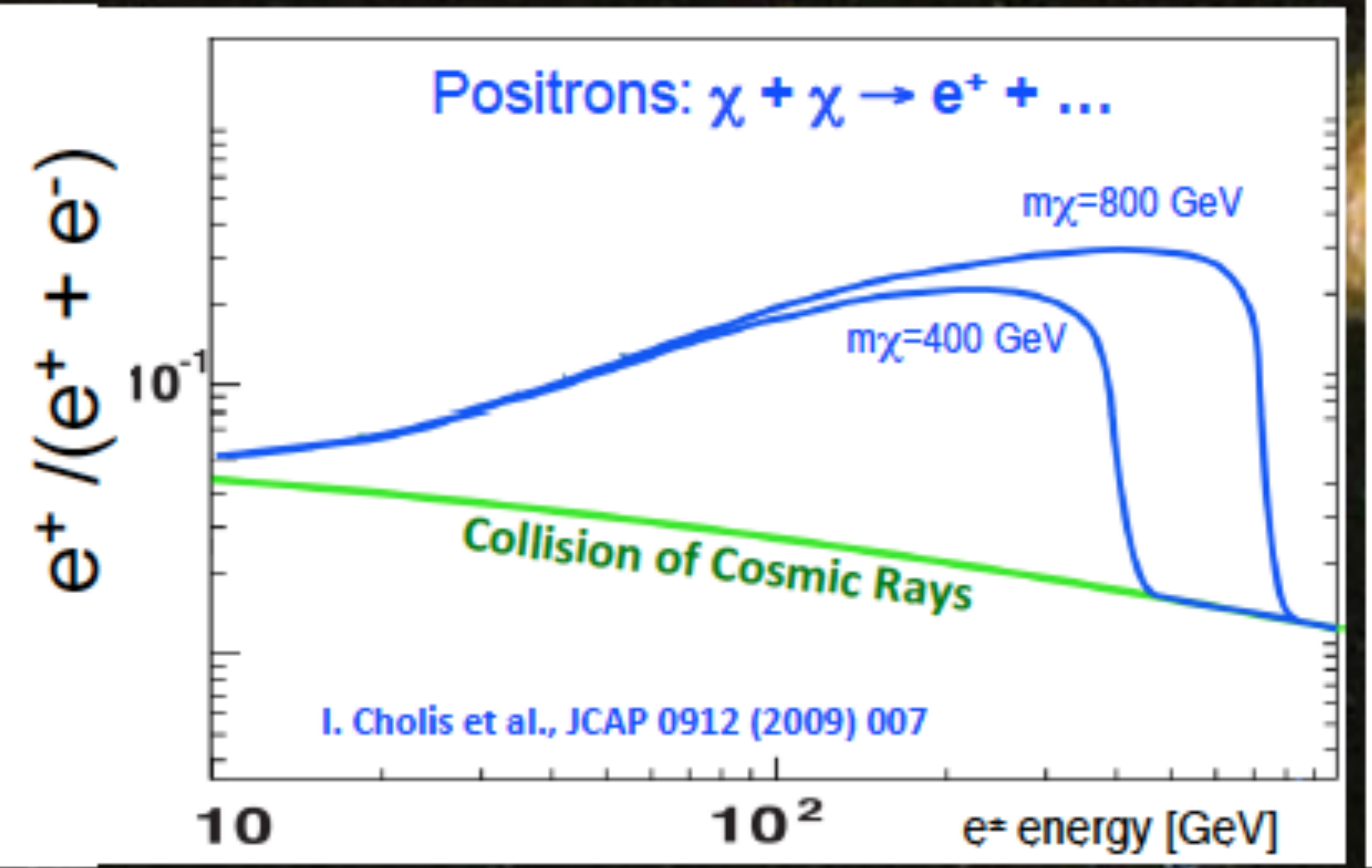

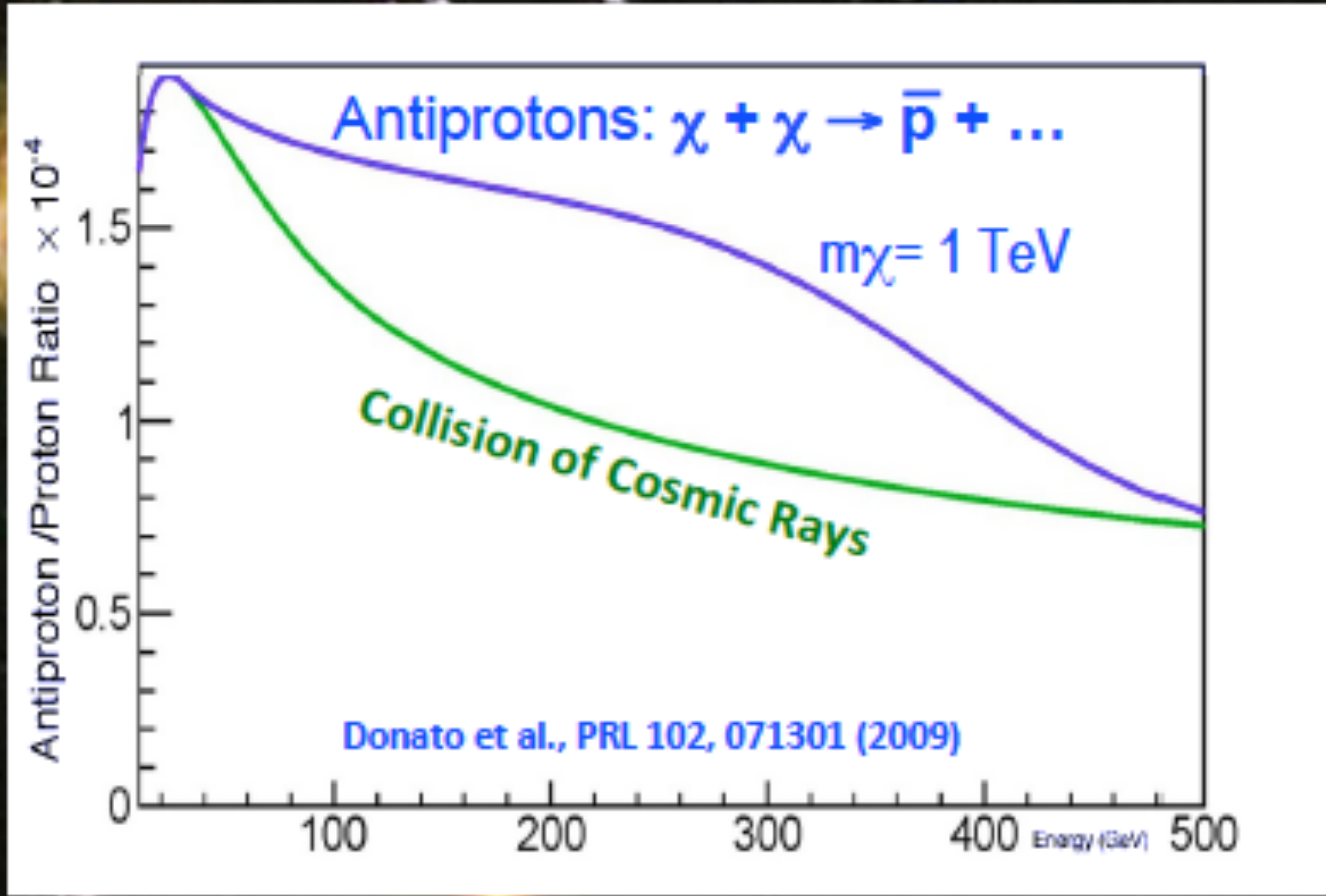

First Result from the AMS on the ISS: Precision Measurement of the Positron Fraction in Primary Cosmic Rays of 0.5-350 GeV, PRL 110 (2013) 141102

Selected by APS as a Highlight of the Year 2013

AMS positron fraction papers cited >700 times

Positron fraction analysis

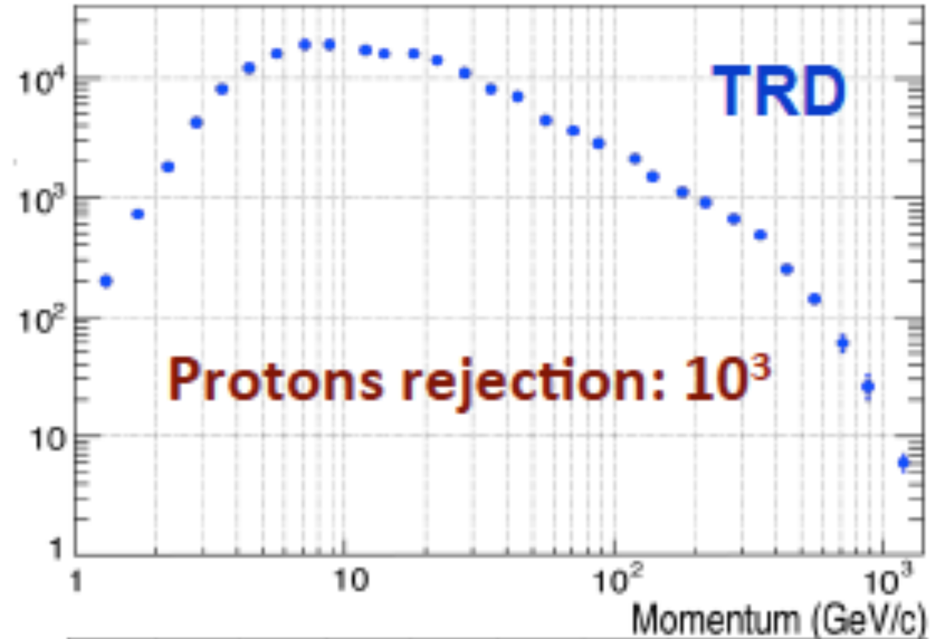

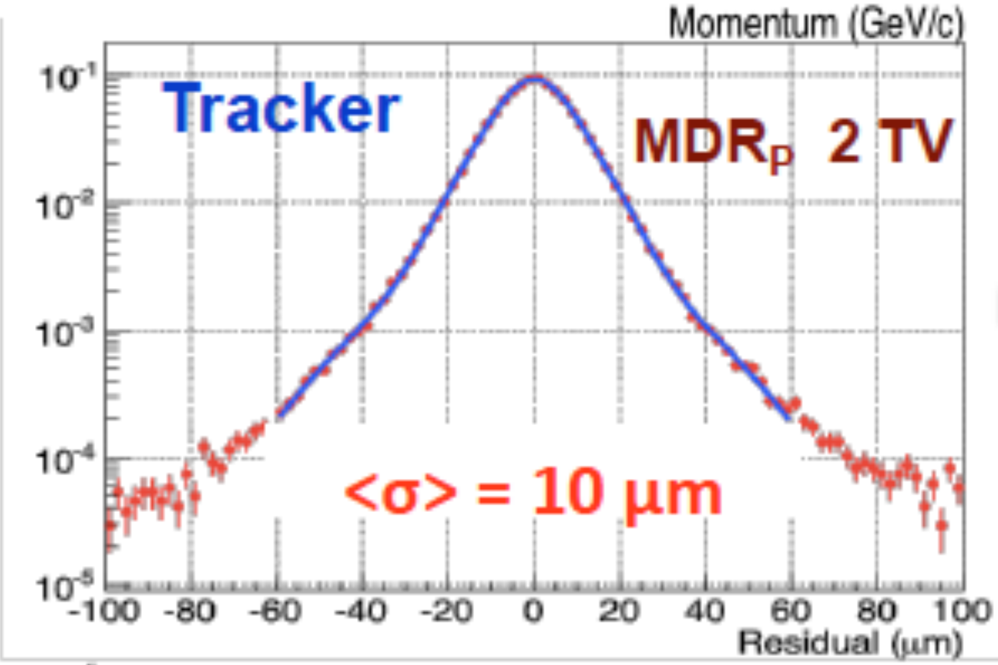

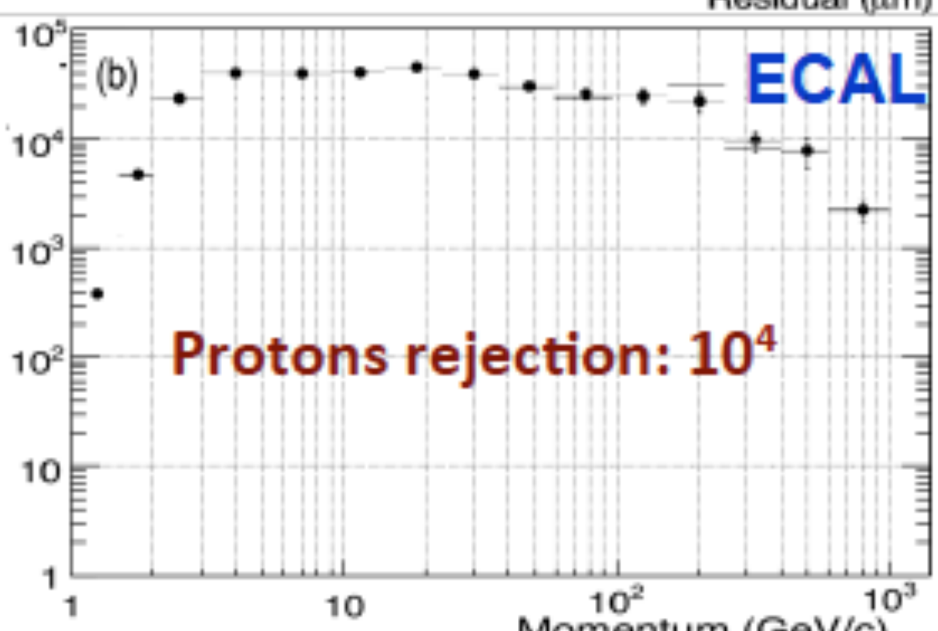

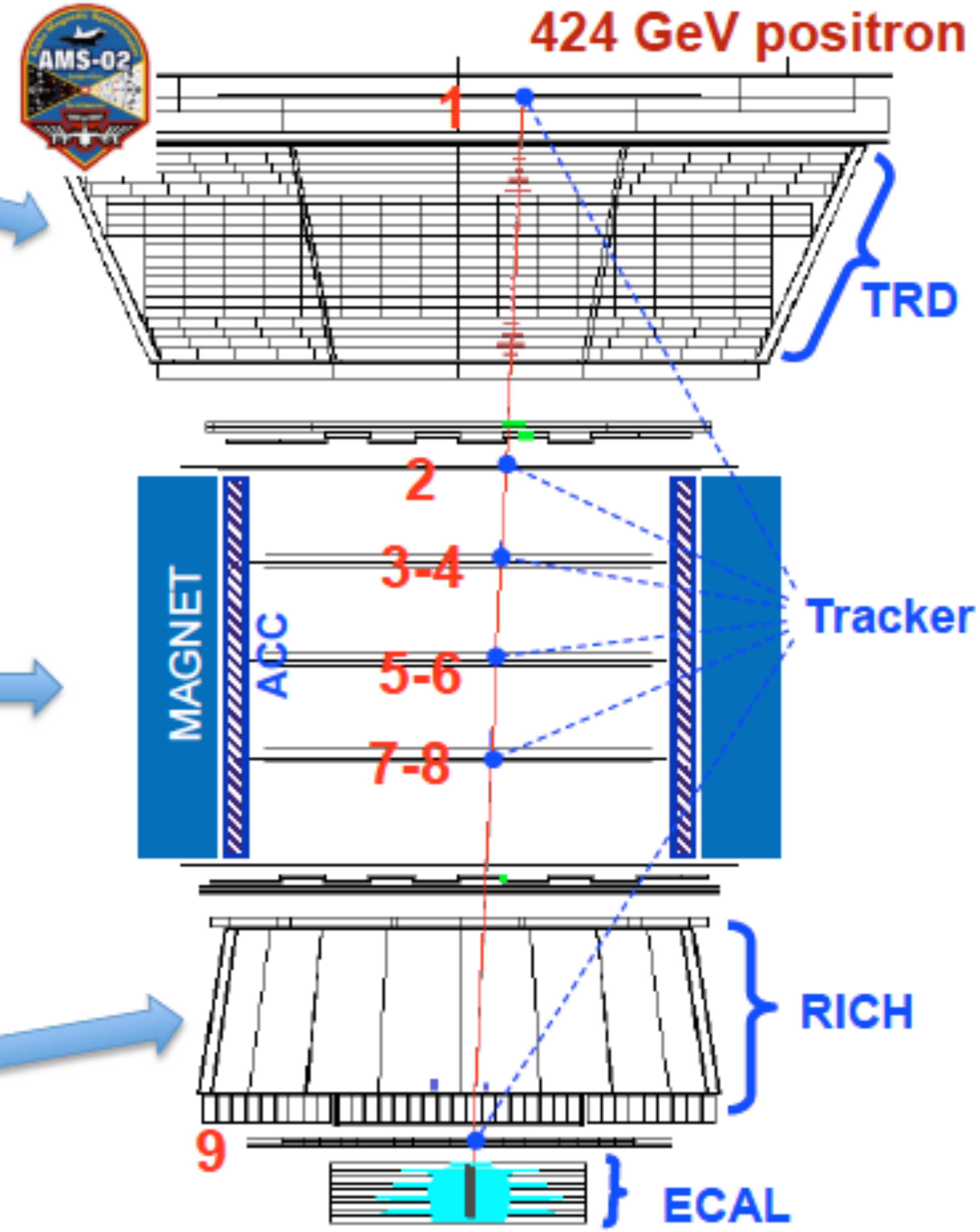

10.9 million of $e^{\pm}$ events are selected in the energy range 0.5–500 GeV

TRD Estimator shows clear separation between protons and positrons with a small charge confusion background

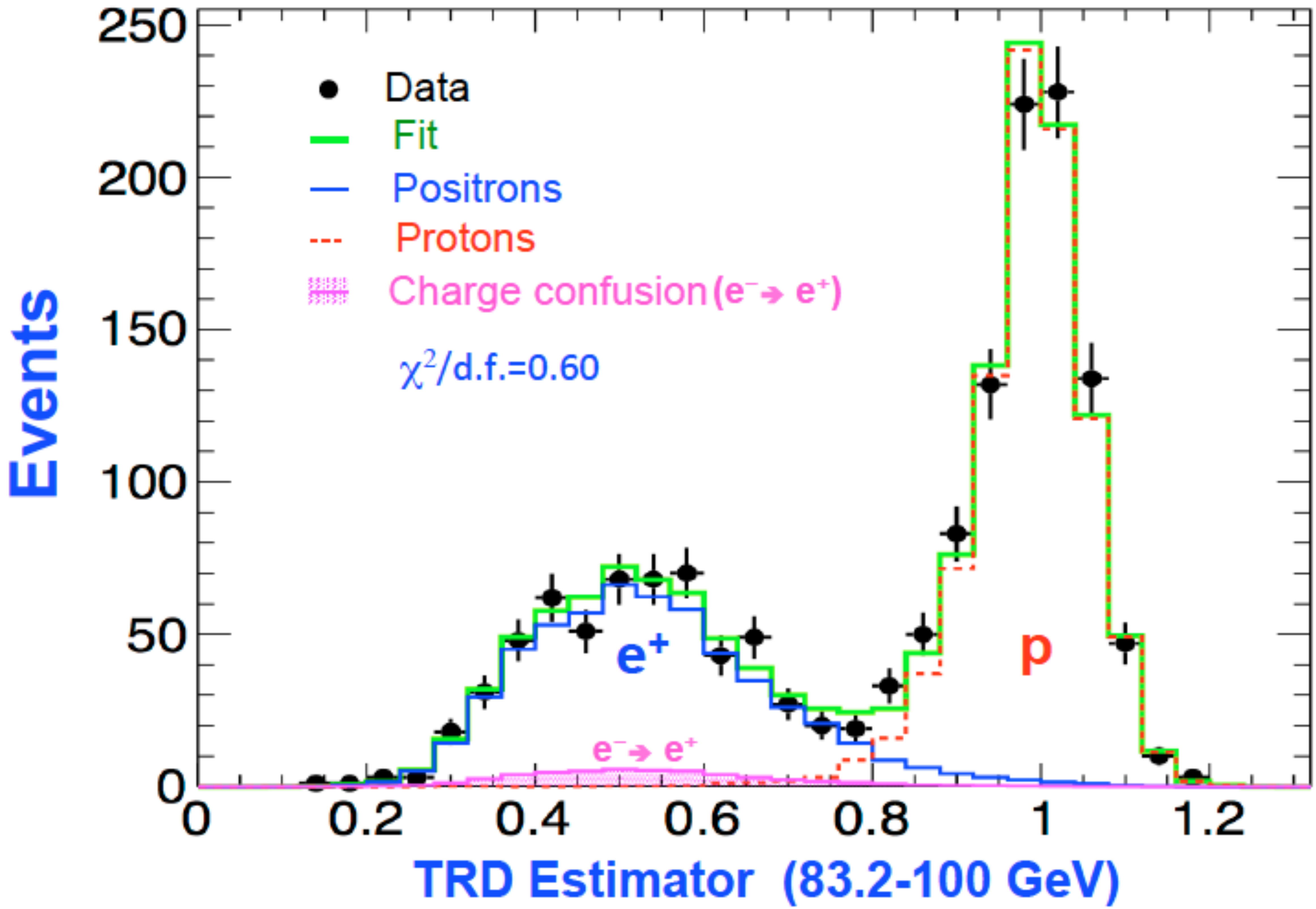

Results on the Positron Fraction from 11 million e±

PRL 113, 121101 (2014) PHYSICAL REVIEW LETTERS week ending 19 SEPTEMBER 2014

Editor's Suggestion

High Statistics Measurement of the Positron Fraction in Primary Cosmic Rays of 0.5–500 GeV with the Alpha Magnetic Spectrometer on the International Space Station

2. The rate of increase with energy compared with models

3. The energy beyond which it ceases to increase.

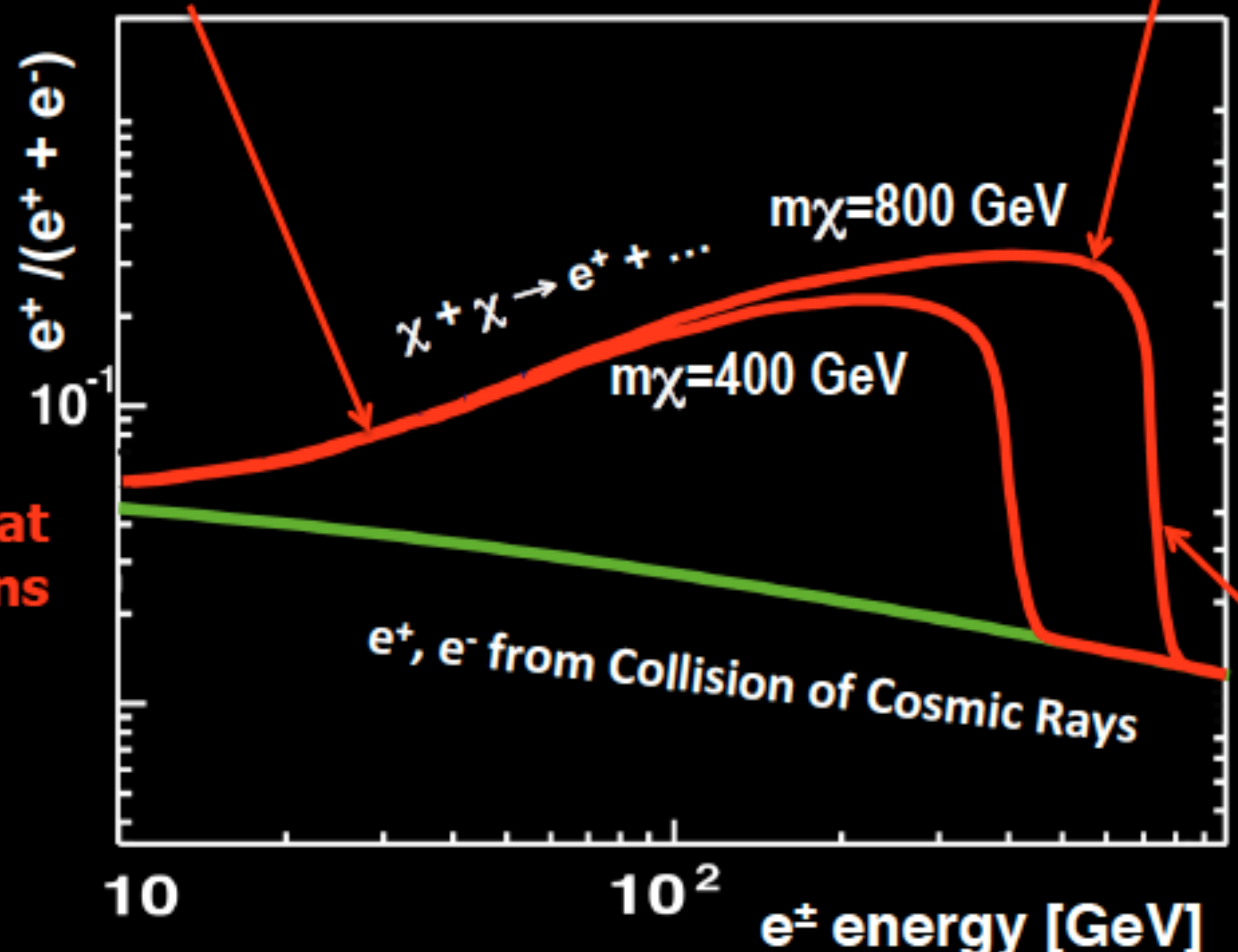

4. Isotropy.

1. The energy at which it begins to increase.

5. The rate at which it falls beyond the turning point.

1. The energy at which positron fraction begins to increase

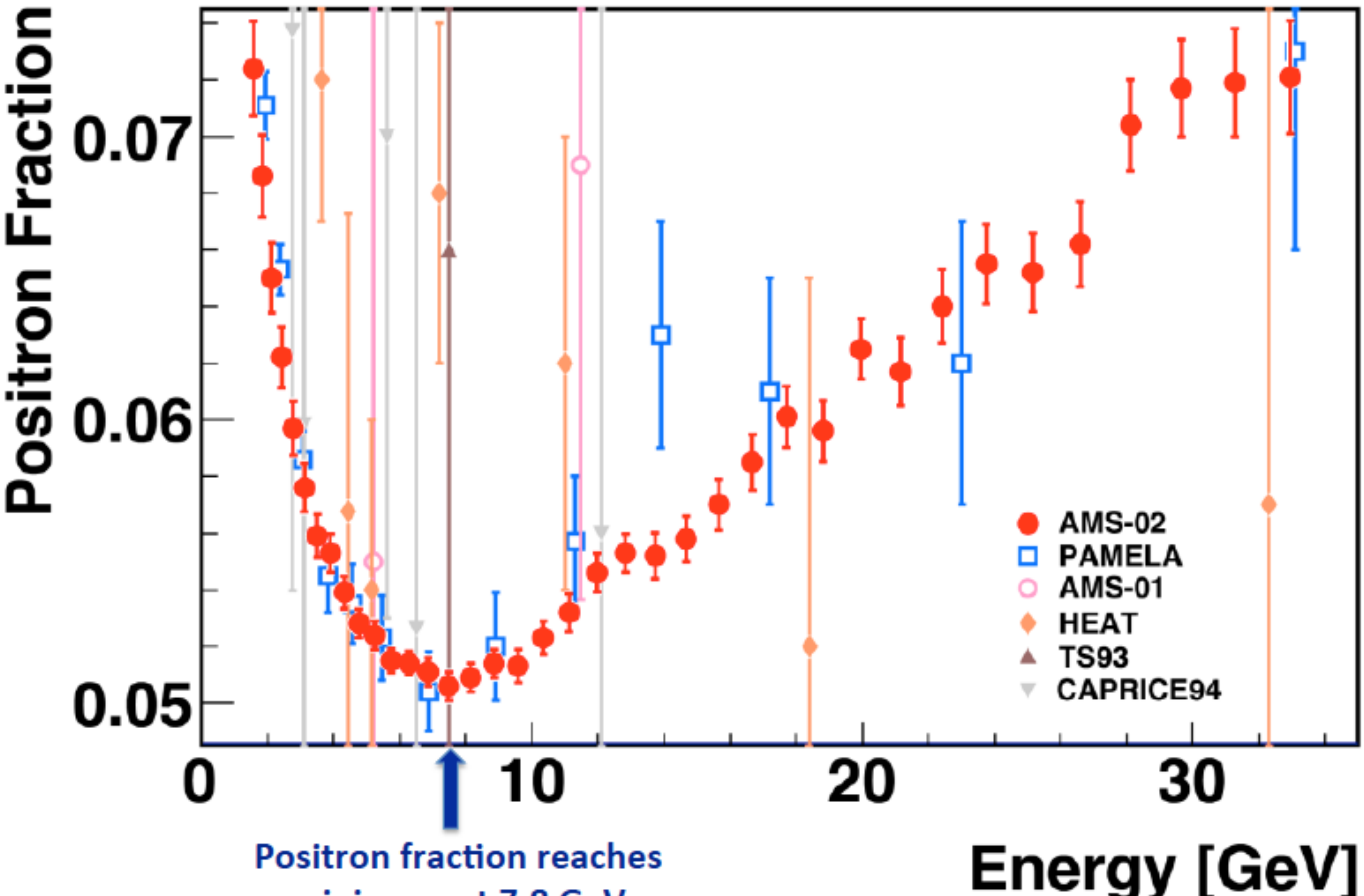

Positron fraction reaches minimum at 7.8 GeV

3. Behavior of the positron fraction at high energies

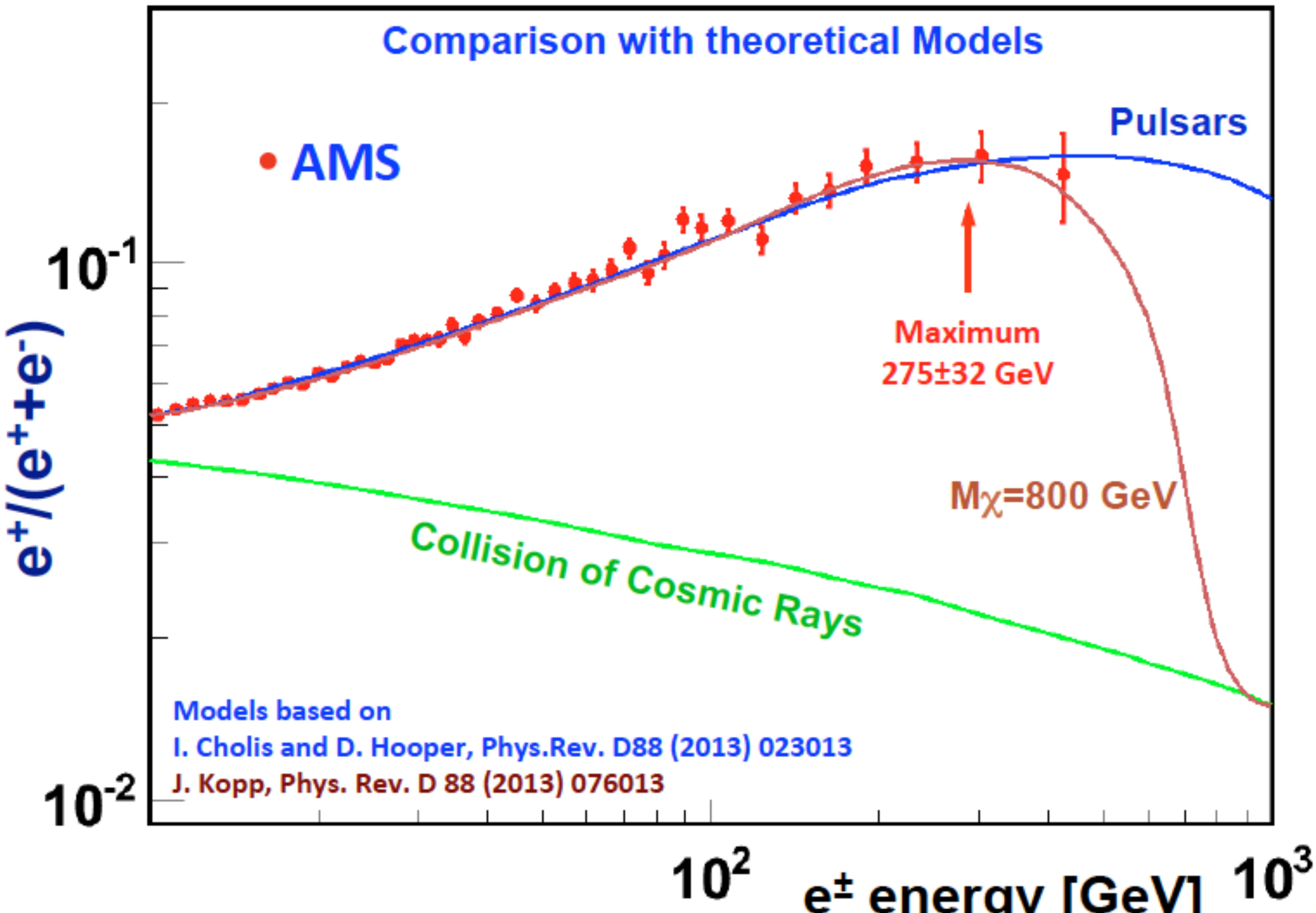

5. The expected rate at which it falls beyond the turning point.

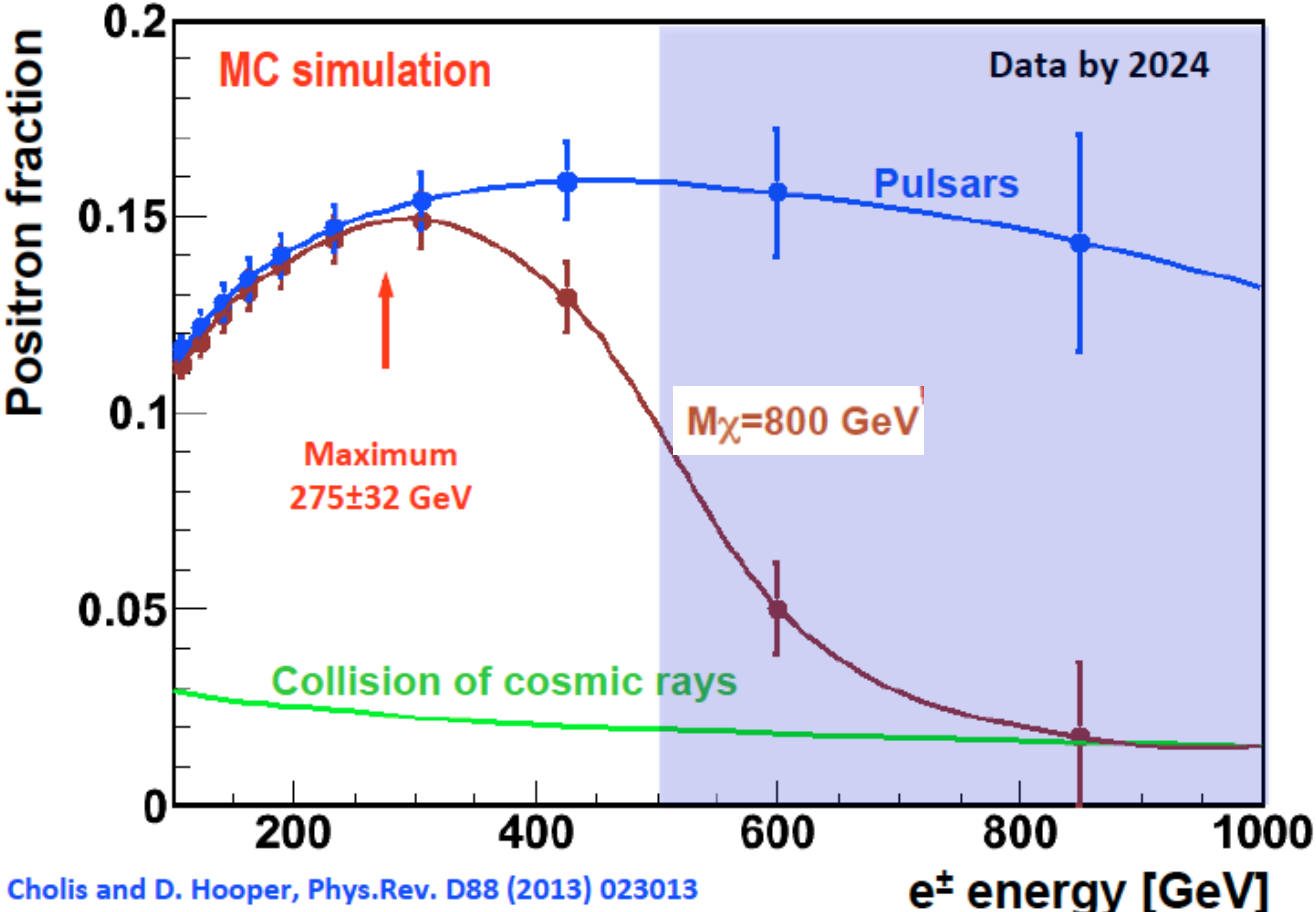

I. Cholis and D. Hooper, Phys.Rev. D88 (2013) 023013

J. Kopp, Phys. Rev. D 88 (2013) 076013

Boron / Carbon Ratio

- Carbon nuclei are primary particles produced in Stellar Nucleosynthesis and accelerated by supernova remnants, whereas
- Boron nuclei are considered to be secondary particles from spallation of heavier elements (Carbon, Nitrogen, Oxygen) in the interstellar medium

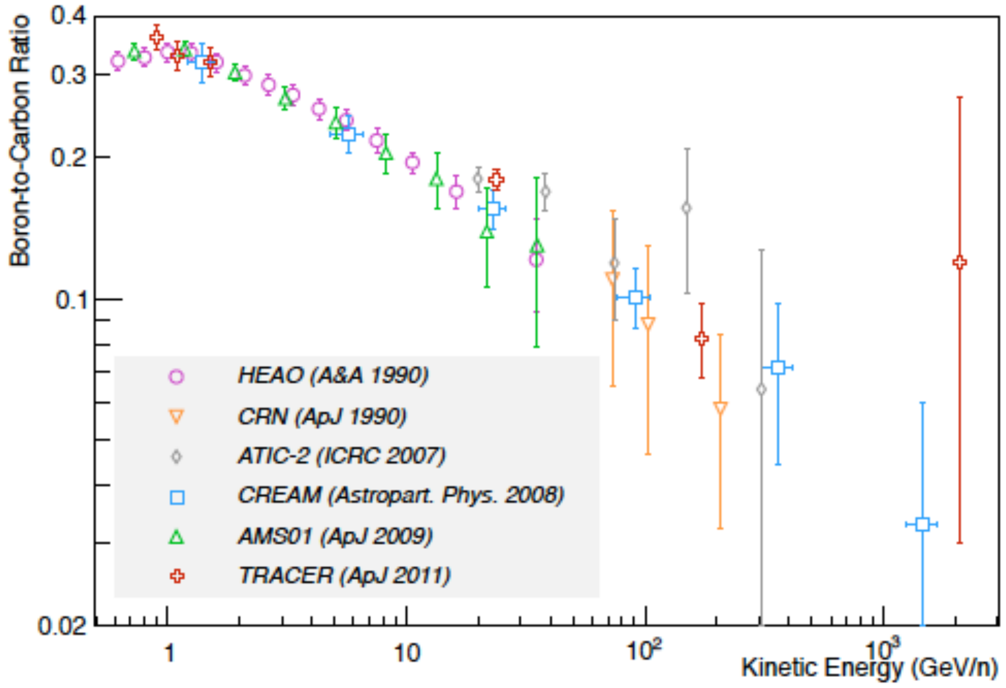

Figure 1-7: Previous measurements of the Boron to Carbon ratio in cosmic rays from HEAO [6], CNR [7], ATIC [8], CREAM [9], TRACER [10], and AMS-01 [11].

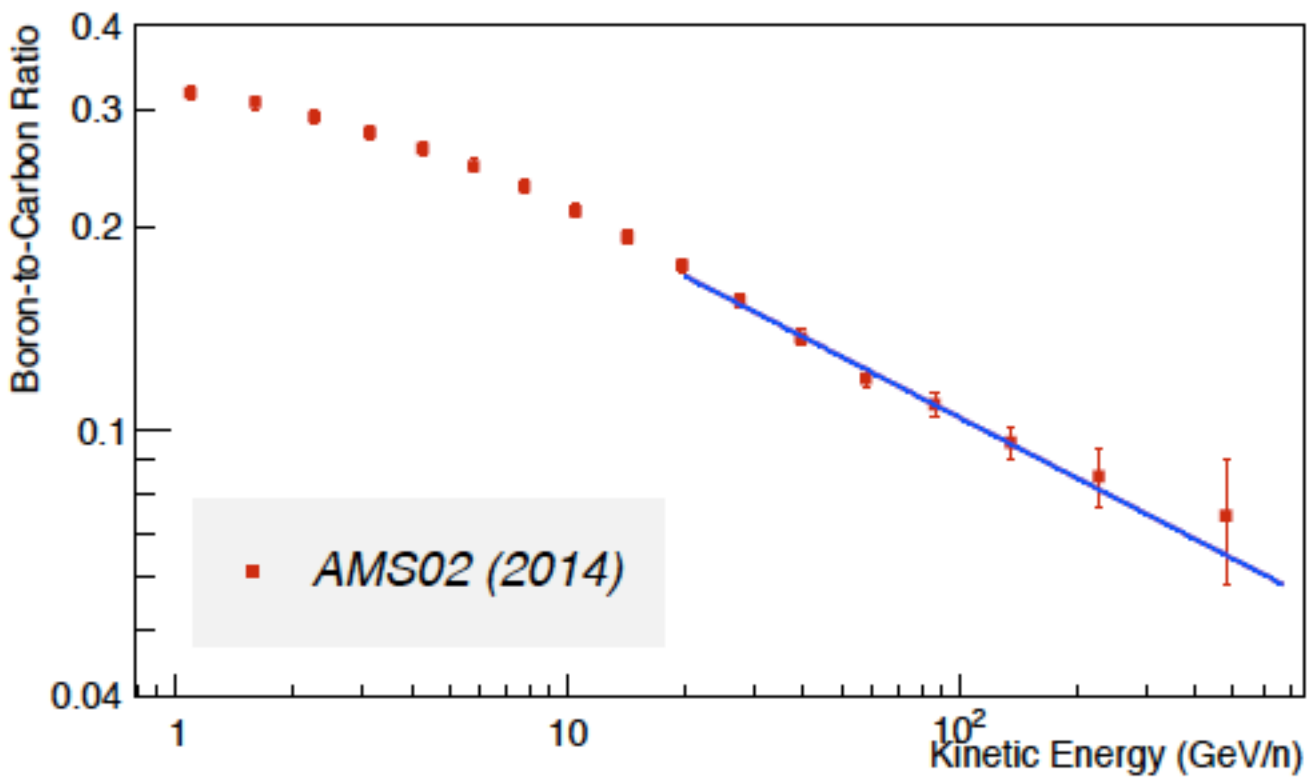

Conclusions cosmic rays

- Rise in positron fraction is unexpected and very interesting
  - It could hint at dark matter, but astrophysical origins seem more likely
  - With cosmic ray observations alone we will probably never be able to definitely identify a dark matter signal
  - If it is dark matter then heavy (~TeV) and leptophilic

Gamma-ray searches

Sources of Gamma-ray

- Production mechanisms of gamma-rays
  - Synchrotron radiation:
    - The deflection of charged particles in a magnetic field gives rise to an accelerated motion. An accelerated electrical charge radiates electromagnetic waves. This ‘bremsstrahlung’ of charged particles in magnetic fields is call synchrotron radiation.
    - The energy spectrum of synchrotron photons is continuous.
    - The power P radiated by an electron of energy E in a magnetic field of strength B is P ~E^2B^2

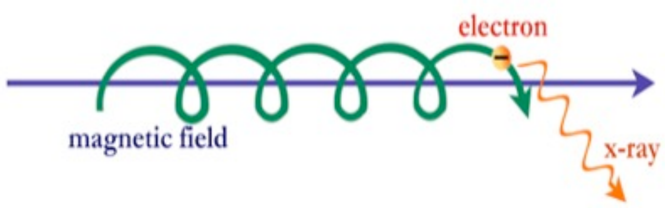

  - Bremsstrahlung
    - charged particle which is deflected in the Coulomb field of a charge (atomic nucleus or electron) emits bremsstrahlung photons
    - probability for bremsstrahlung φ depends on the projectile charge z, mass m, energy E, and depends on the target charge Z.
      - φ=z^2Z^2 E/m^2
    - Because of the smallness of the electron mass bremsstrahlung is predominantly created by electrons.
    - The energy spectrum of bremsstrahlung photons is continuous and the spectrum decreases like $1/E_\gamma$ to high energies.

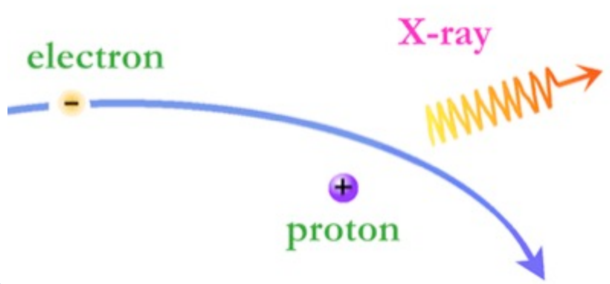

  - Inverse Compton
    - Energetic electrons transfer part of their energy to low energy photons in a collision
    - Numerous photons of
      - CMB / blackbody radiation ($E_\gamma \approx$ 250 μ eV, photon density $N_\gamma \approx$ 400/ cm^2)
      - Starlight photons ($E_\gamma \approx$ 1 eV, $N_\gamma \approx$ 1/ cm^3)

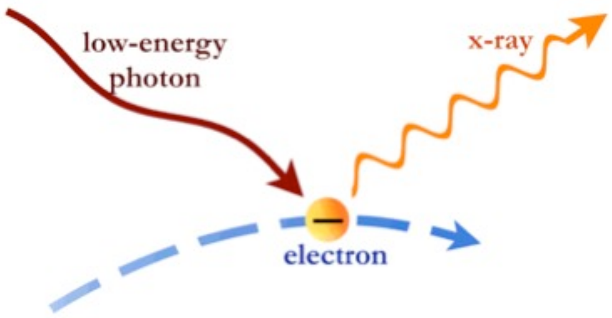

Sources of Gamma-ray ... continued

- Production mechanisms of gamma-rays
  - π^0-Decay
    - Neutral pions decay rapidly (τ = 8.4 x 10^{-17}s) into two γ ($\pi^0 \rightarrow \gamma+\gamma$)
    - p + nucleus $\rightarrow$ p + nucleus'+ π^++ π^-+ π^0
  - Matter–Antimatter Annihilation
    - $e^+ + e^- \rightarrow \gamma+\gamma$
    - p+pbar$\rightarrow \pi^+\pi^-\pi^0$
  - Nuclear decays
    - Radio active isotopes dec

$$
\begin{aligned}
{}^{60}\mathrm{Co} \rightarrow\ & {}^{60}\mathrm{Ni}^{**} + e^- + \bar{\nu}_e \\
& \hookrightarrow {}^{60}\mathrm{Ni}^{*} + \gamma\,(1.17\,\mathrm{MeV}) \\
& \qquad \hookrightarrow {}^{60}\mathrm{Ni} + \gamma\,(1.33\,\mathrm{MeV})
\end{aligned}
$$

gamma-rays

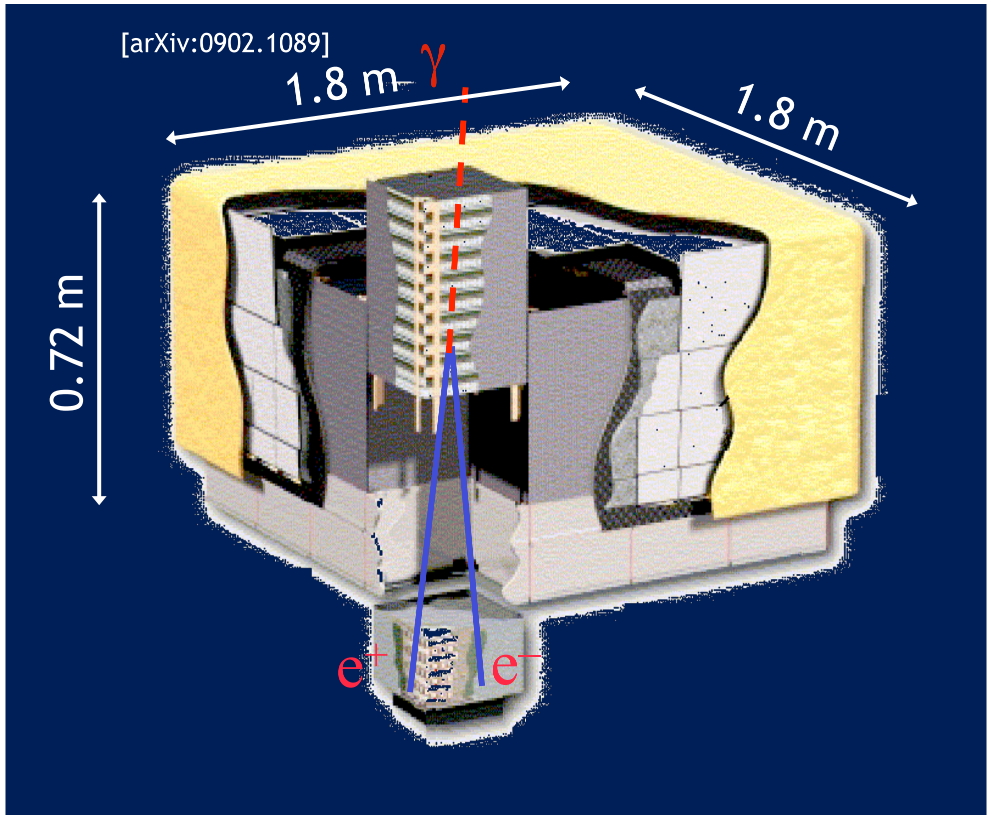

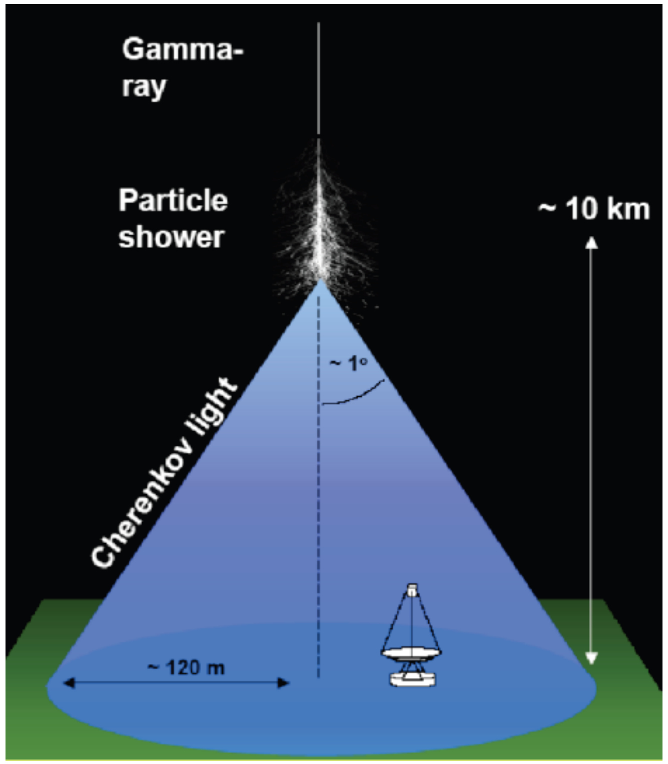

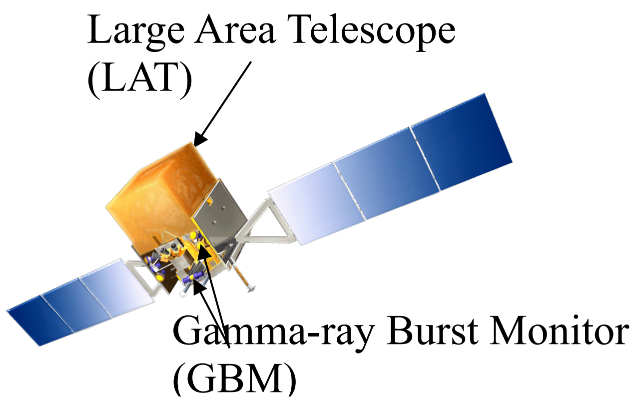

	Fermi-LAT	Imaging Air Cherenkov Telescopes
Detection Method	Pair conversion	Cherenkov light from particle shower
Effective Area	1m^2	~400-500m^2
Field of View (FOV)	2.5sr	3.5° - 5.0°
Duty cycle	~100%	~15%
Energy range	20MeV - 300GeV	>100GeV
Energy resolution	4% (@5GeV) 2% (@200GeV)	10% - 20%
Angular resolution	~0.1° (@10GeV) ~3.5°(@100MeV)	0.1° at 100 GeV

Fermi-LAT

Photons … Fermi

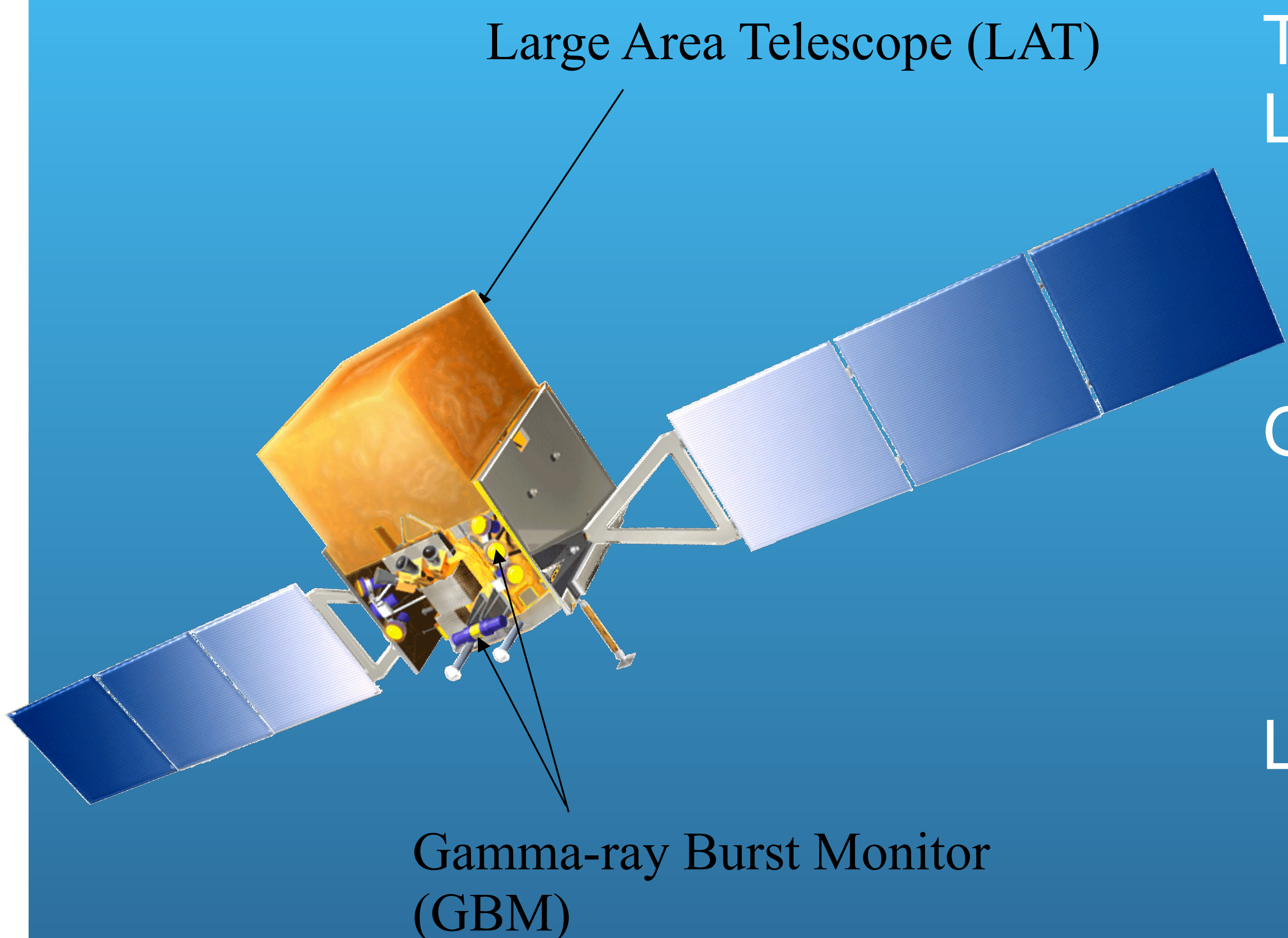

Two Instruments:

Large Area Telescope (LAT)

- 20 MeV - 300 GeV
- >2.5 sr FoV

Gamma-Ray Burst Monitor (GBM)

- 8 keV – 40 MeV
- 9 sr FoV

Launched: June 11 2008

	Years	Ang. Res. (100 MeV)	Ang. Res. (10 GeV)	Eng. Rng. (GeV)	$A_{eff}\,\Omega$ (cm^2 sr)	# γ-rays
EGRET	1991–00	5.8°	0.5°	0.03–10	750	1.4×10^6/yr
AGILE	2007–	4.7°	0.2°	0.03–50	1,500	4×10^6/yr
Fermi LAT	2008–	3.5°	0.1°	0.02–300	25,000	1×10^8/yr

Fermi Large Area Telescope (LAT)

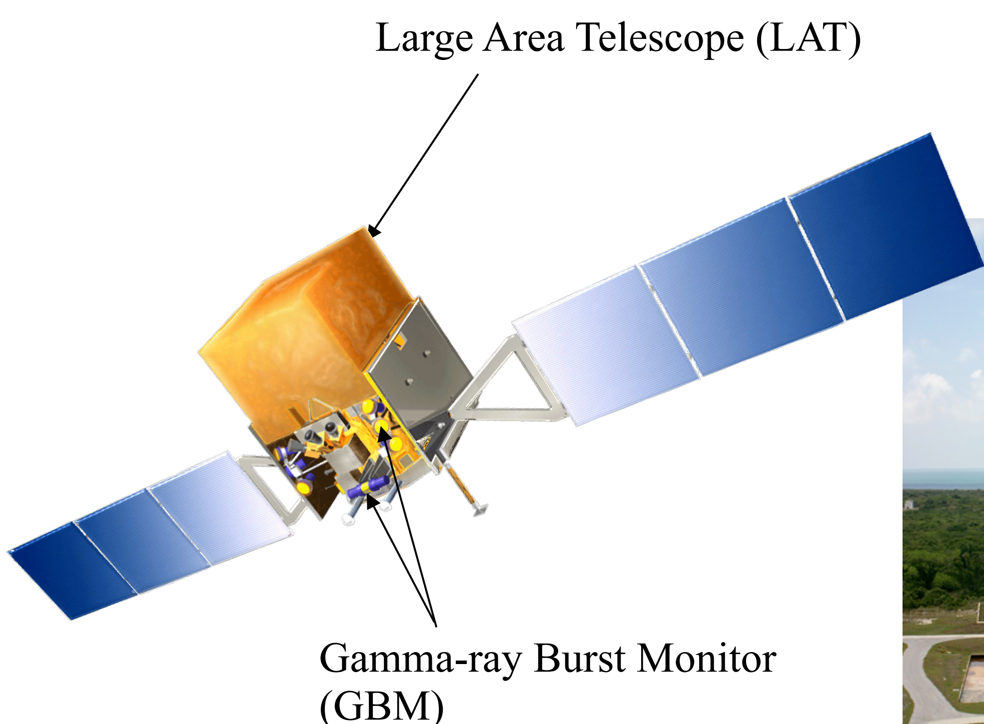

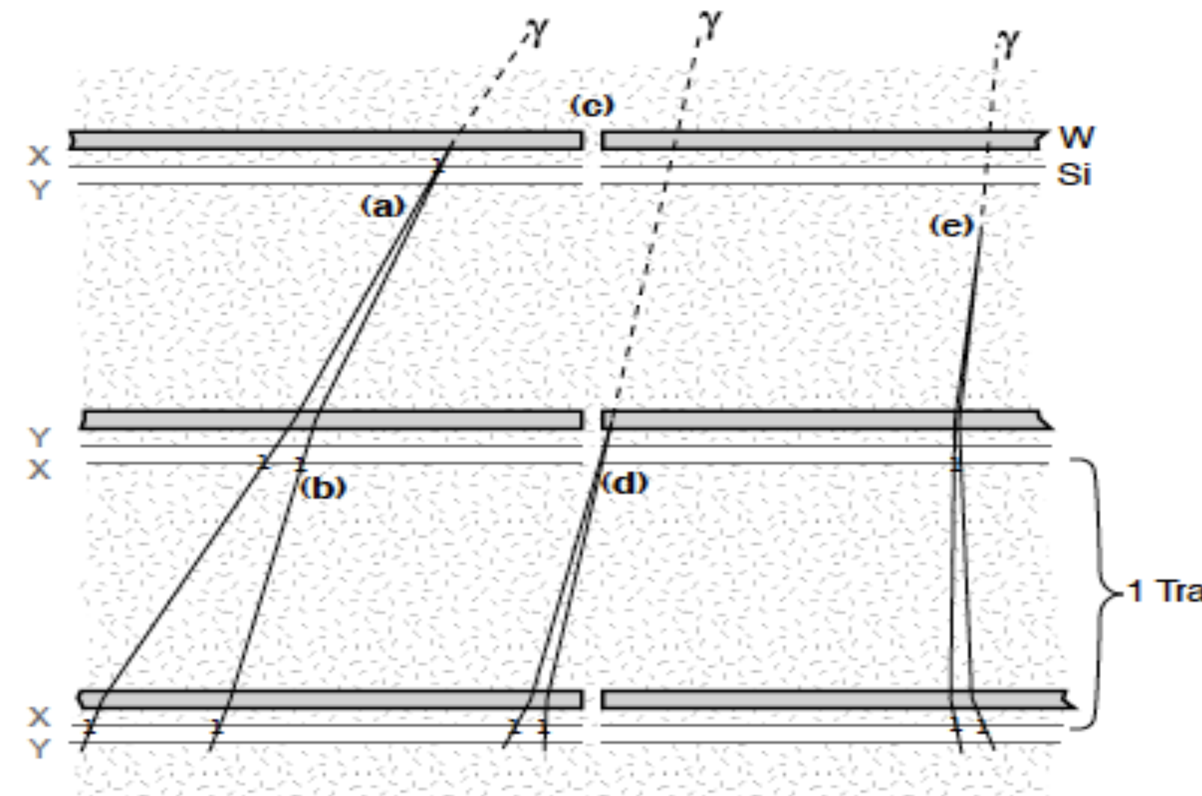

- Pair conversion telescope
- Launched June 11, 2008
- Energy range 20MeV - 300GeV
- γ-ray angular resolution ~0.1° (@10GeV) [~3.5° (@100MeV)]
- 2.5sr FoV
- Effective area ~ 1m^2

- Pair conversion telescope
- Tracking detector: 16 tungsten foils + 18 pairs of SI strip detectors
- Calorimeter: ~8.5 radiation length - 8 layers of CsI logs
- Anti-coincidence detector: 89 scintillating tiles ~99.97% efficient for MIPs

Fermi – Large Area Telescope (LAT)

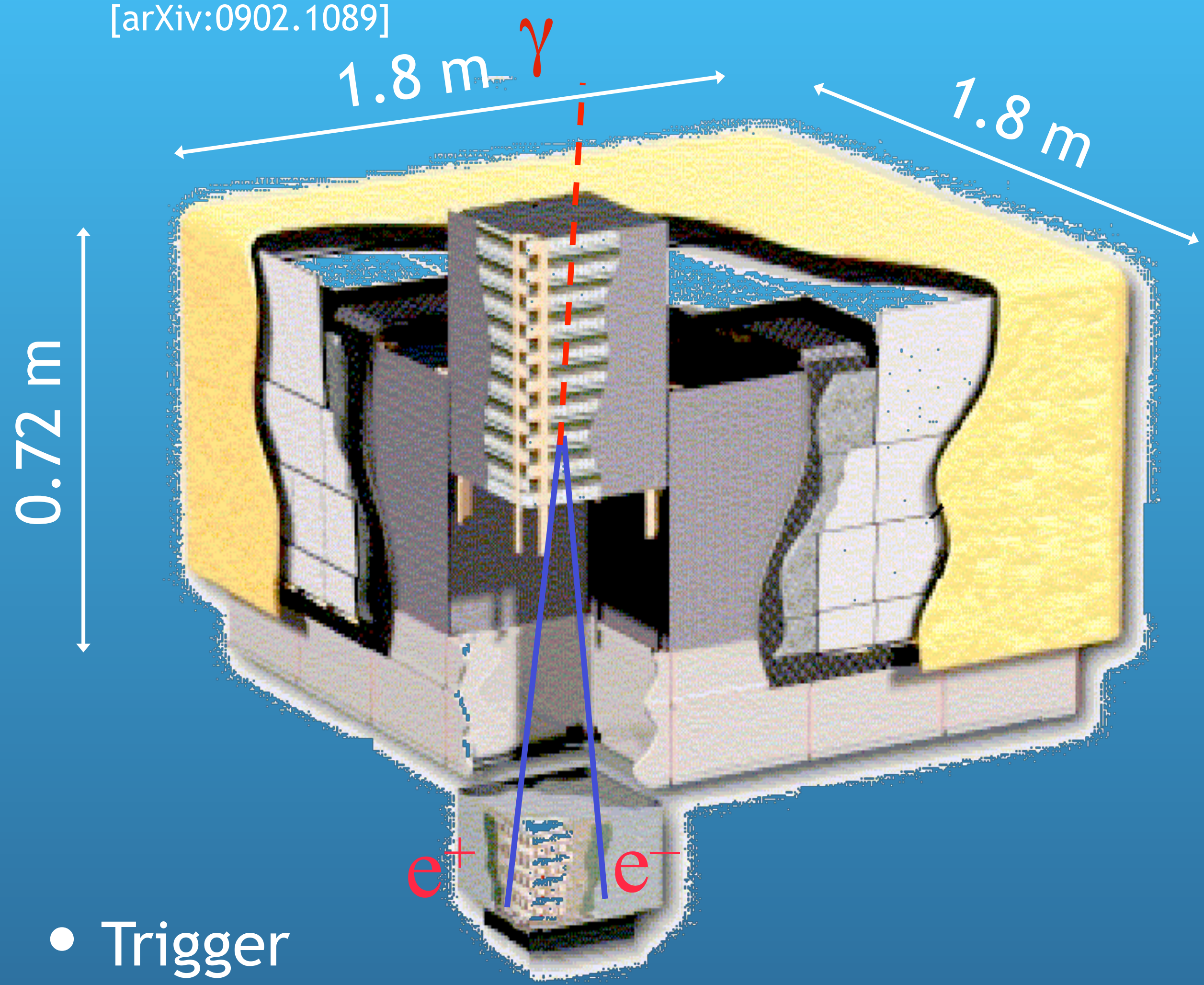

- Tracking detector
  - 16 tungsten foils
  - 18 pairs of SI strip detectors
- Calorimeter
  - ~8.5 radiation length
  - 8 layers of CsI logs
- Anti-coincidence detector
  - 89 scintillating tiles
  - ~99.97% efficient for MIPs

- Trigger
  - Overall HW Trigger rate ~few kHz
  - Filters reduce rate
  - Downlink ~ 400-500 Hz

Gamma-ray Energy Loss Mechanism

- For photons in matter above ~10 MeV, pair conversion is the dominant energy loss mechanism.
  - Pair conversion telescope

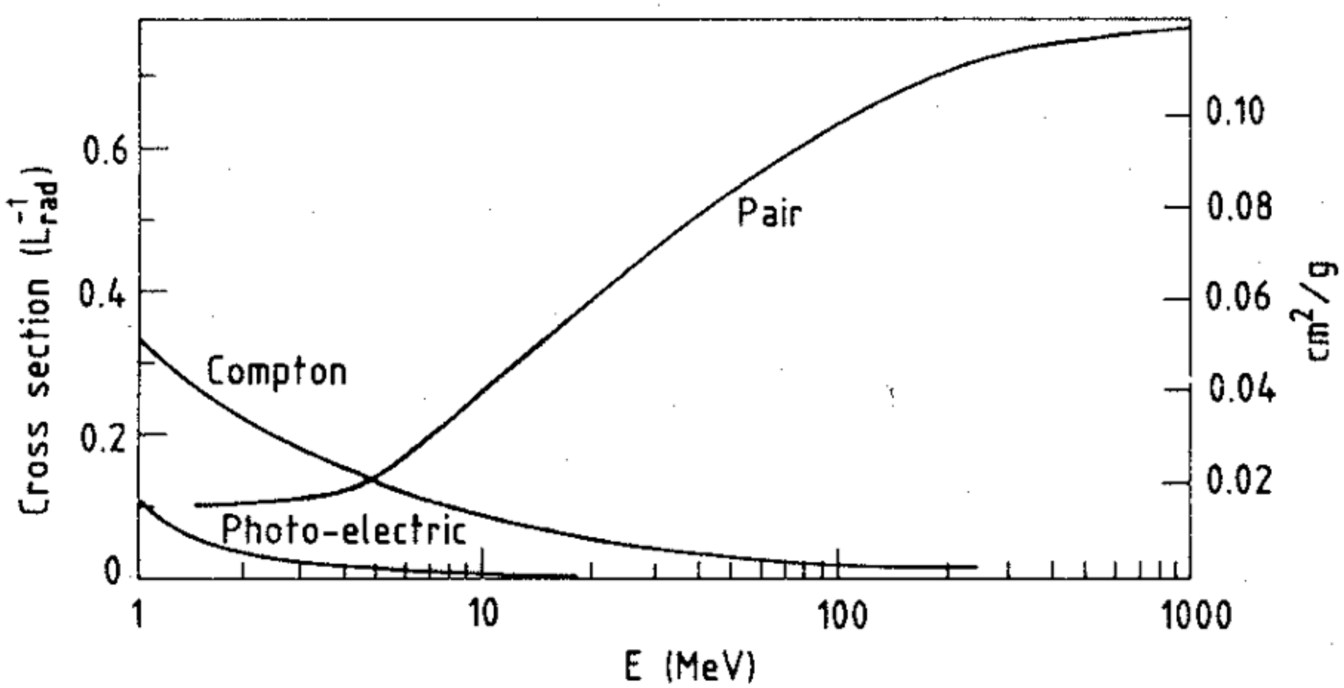

Fig. 2: Photon cross-section σ in lead as a function of photon energy. The intensity of photons can be expressed as $I = I_0 \exp(-\sigma x)$, where x is the path length in radiation lengths. (Review of Particle Properties, April 1980 edition).

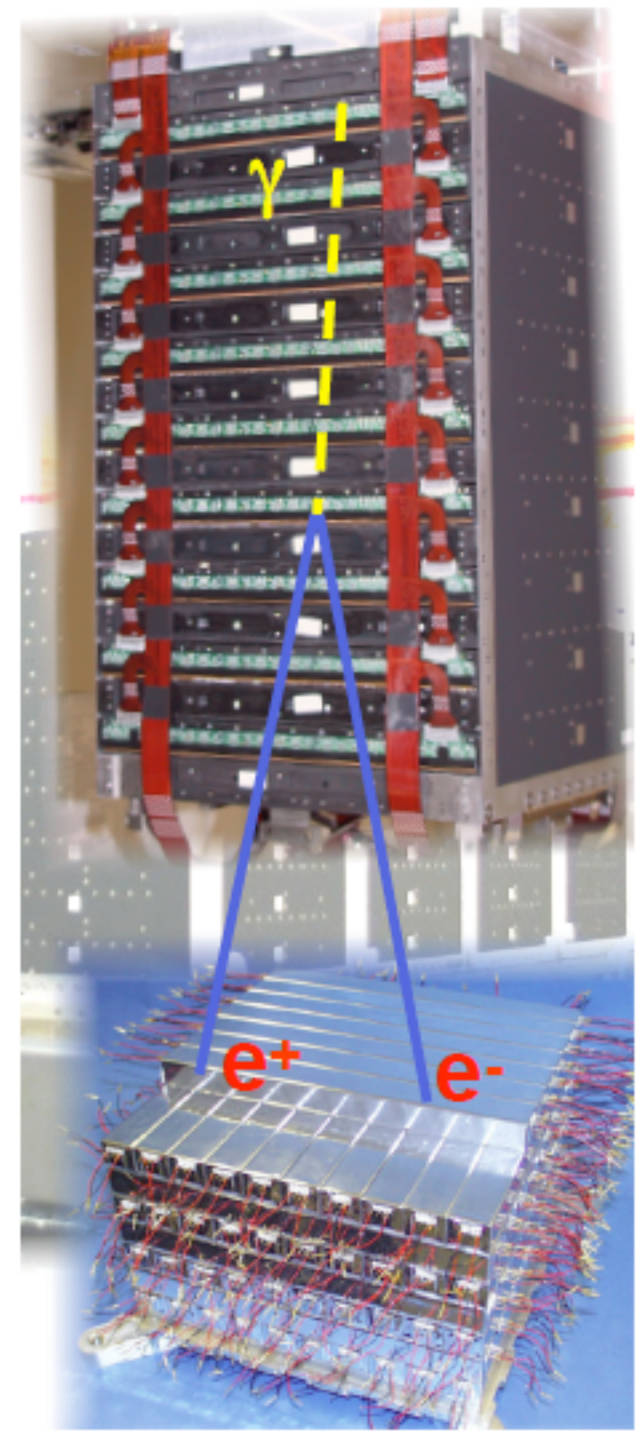

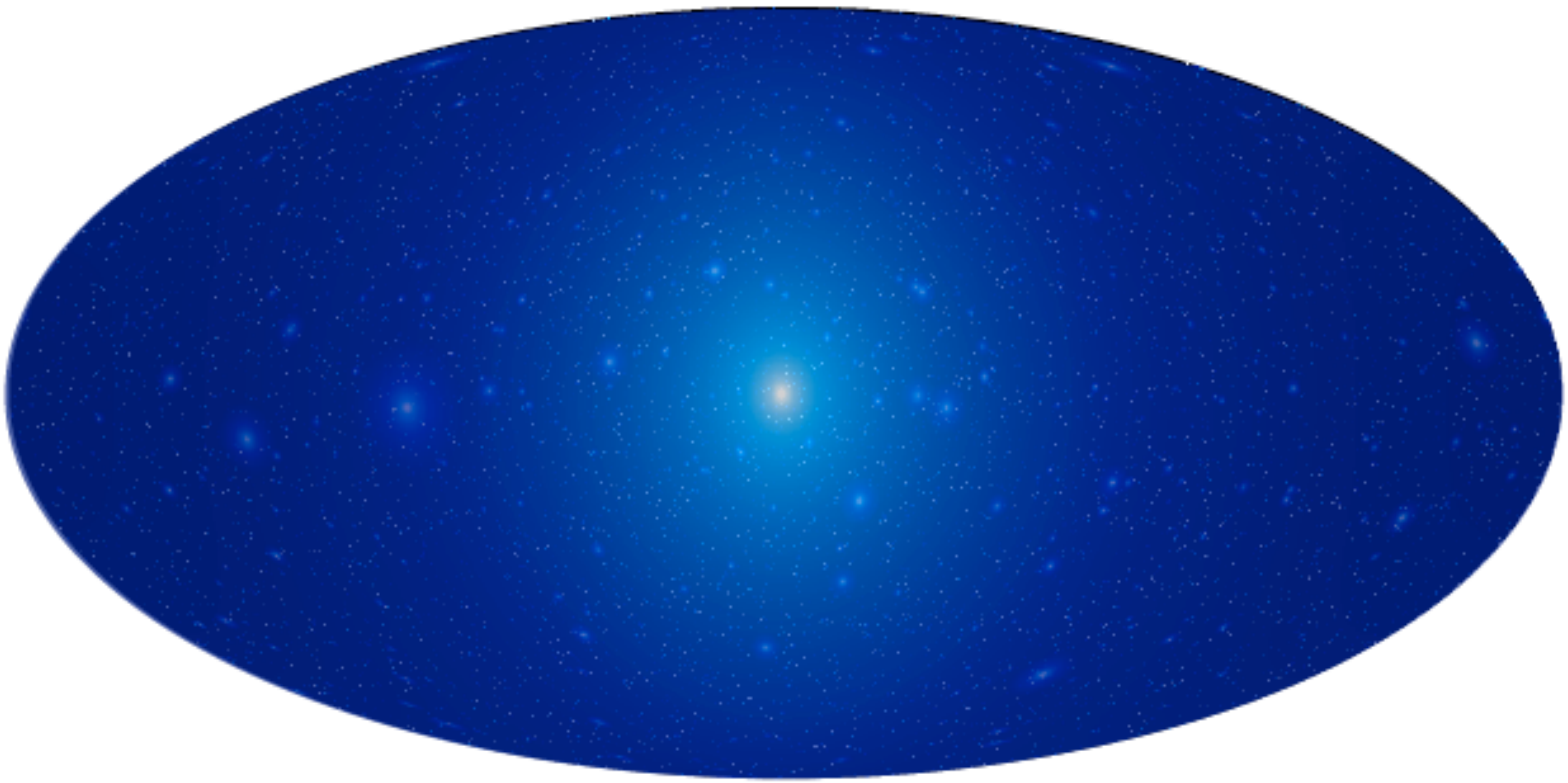

Gamma rays from dark matter annihilation

Fermi-LAT 5 Year Sky Map

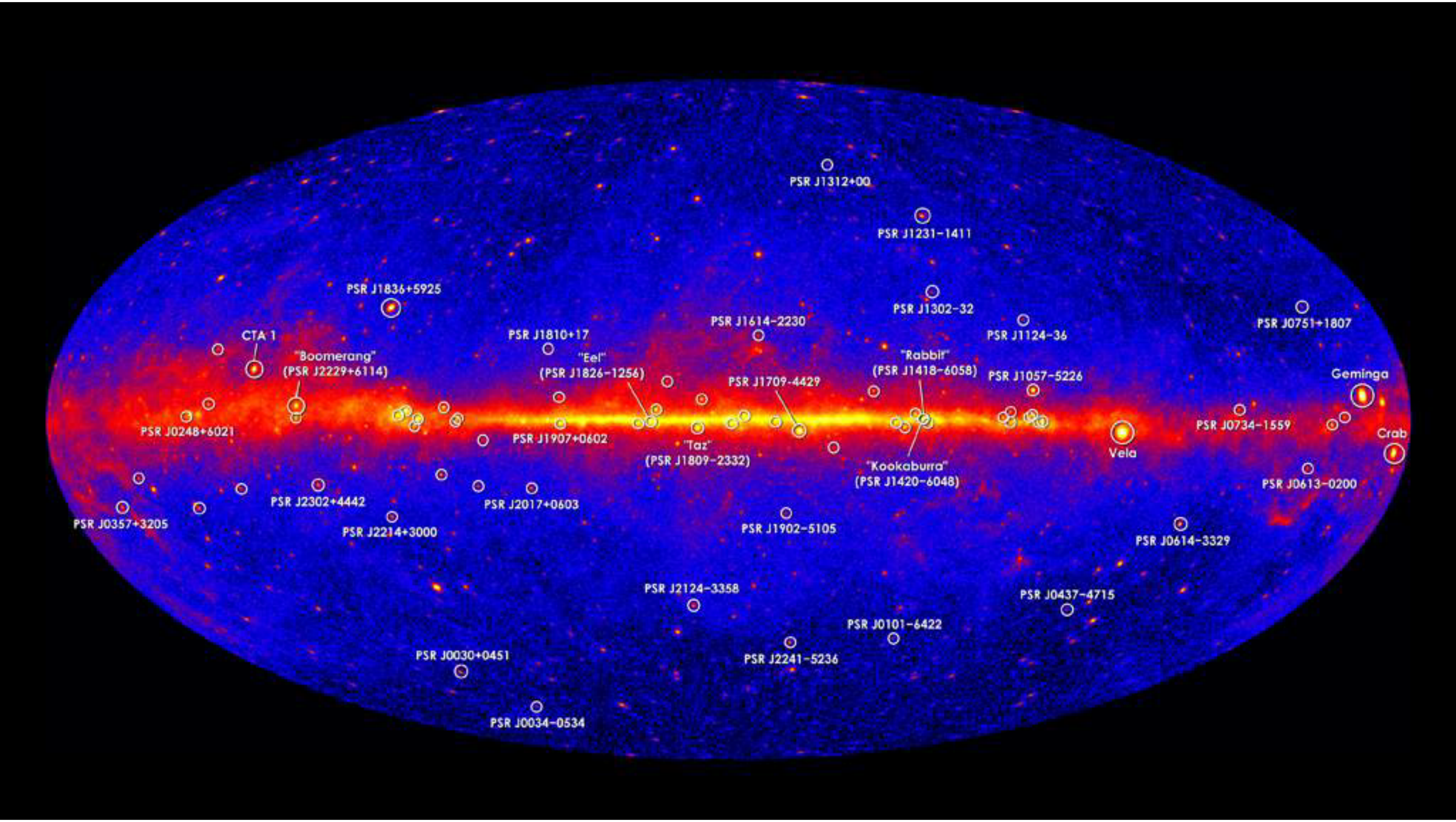

Halo analysis: background modeling

DM limits with simultaneous modeling of non-DM astrophysical signal:

- uncertainties from diffusion models and gas maps taken into account by scanning over a grid of GALPROP models
- for each GALPROP (+DM) model, maps of different components of diffuse emission are generated and fit to the Fermi LAT data, incorporating both morphology and spectra
- the distribution of CR sources is highly uncertain, so is left free to vary in radial Galactic bins. To get more conservative DM constraints, *the distribution is set to zero in the inner 3 kpc*
- the profile likelihood method is used to combine all the models in the grid, and to derive the DM limits marginalized over the astrophysical uncertainties

π^0 decay

bremss

IC

dark matter

isotropic

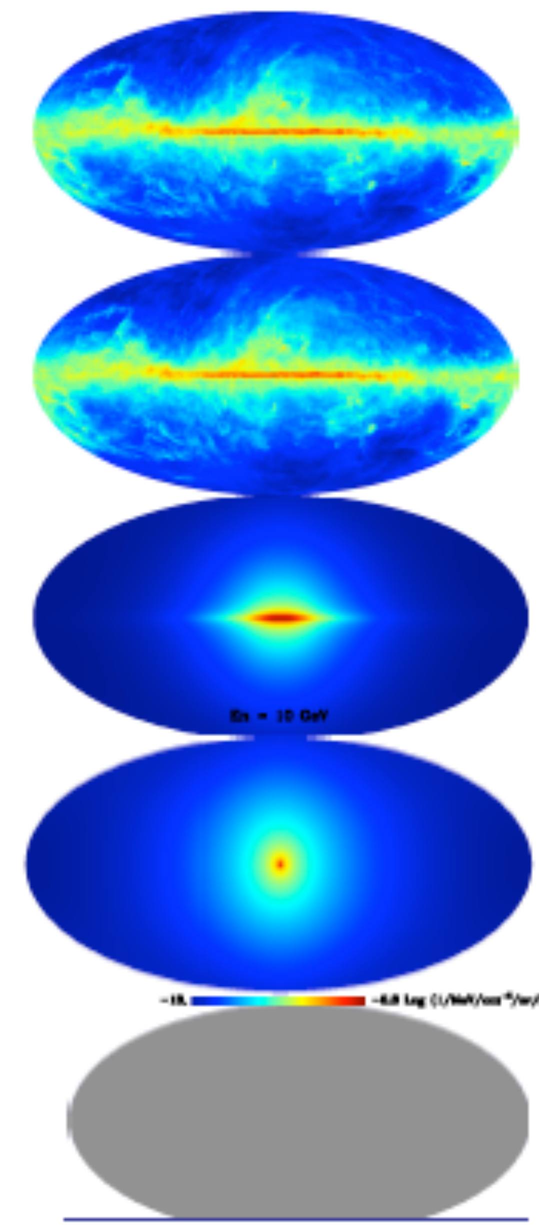

Dwarf Spheriodal Galaxies

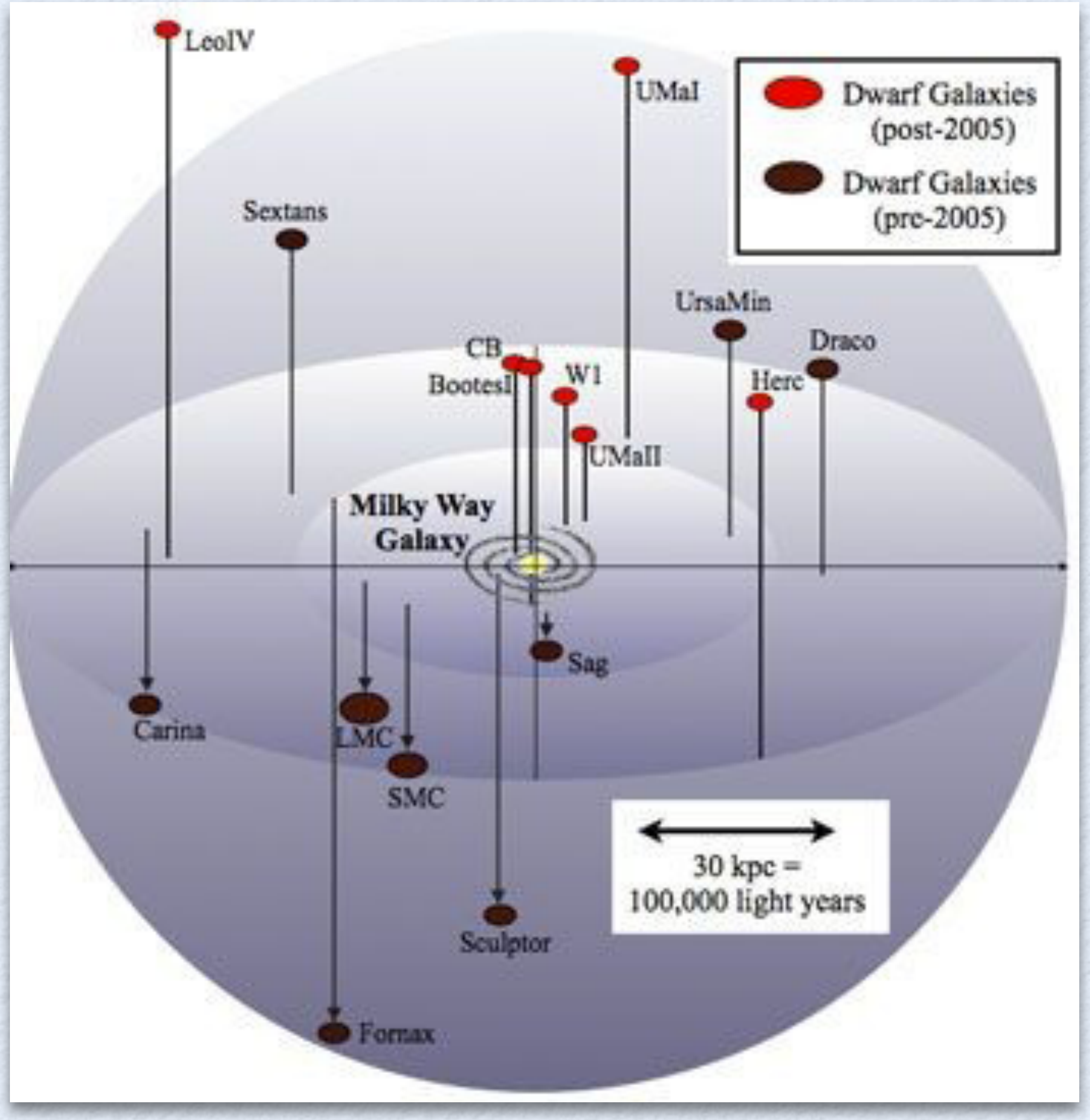

Source	Distance (kpc)	Mass (10^7 M_{Sun})	Right asc.	Dec.
Segue I	25	1.58	10 07’ 04”	+16 04’55”
Ursa Major II	32	1.09	08 51’ 30”	+63 07’48”
Willman I	38	0.77	10 49’ 22”	+51 03’04”
Coma Berenices	44	0.72	12 26’ 59”	+23 55’09”
Ursa Minor	66	1.79	15 09’ 09”	+67 13’21”
Draco	80	1.87	17 20’ 12”	+57 54’55”
…	…	…	..	…

- Roughly two dozen dwarf spheroidal satellite galaxies of the Milky Way
- Some of the most dark matter dominated objects in the Universe
- No astrophysical gamma-ray production expected
- Boost factor expected to be less than 10 [J.Diemand, et al., Nature 454,735 (2008) / V. Springel et al., Mon. Not. R. Astron. Soc., 391, 1685 (2008), ...]

Dwarf Galaxies

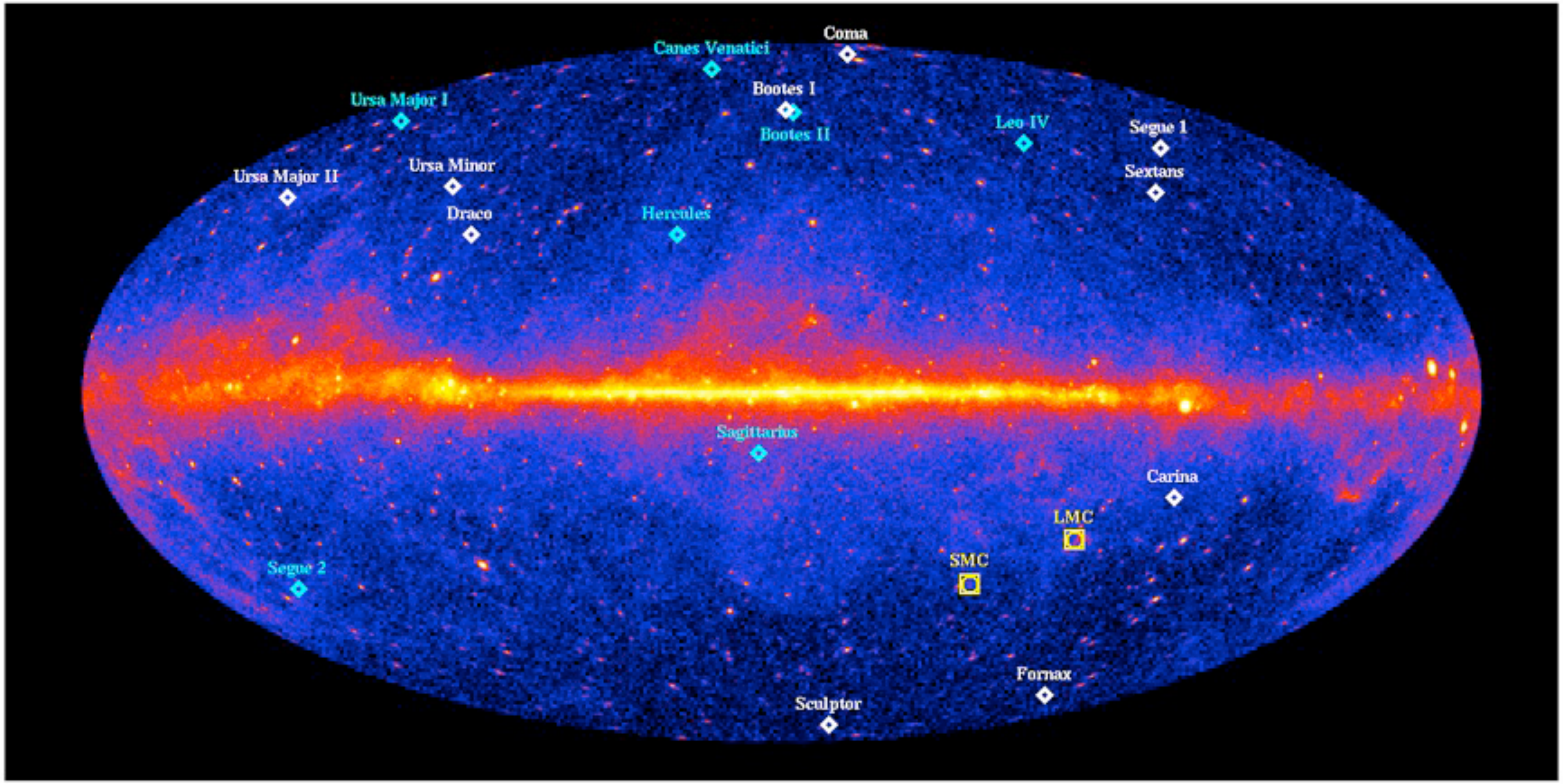

- there are roughly two dozen known dwarf spheroidal galaxies (dSphs) of the Milky Way
- some of the most dark-matter--dominated objects in the Universe
- no non-DM astrophysical gamma-ray production expected

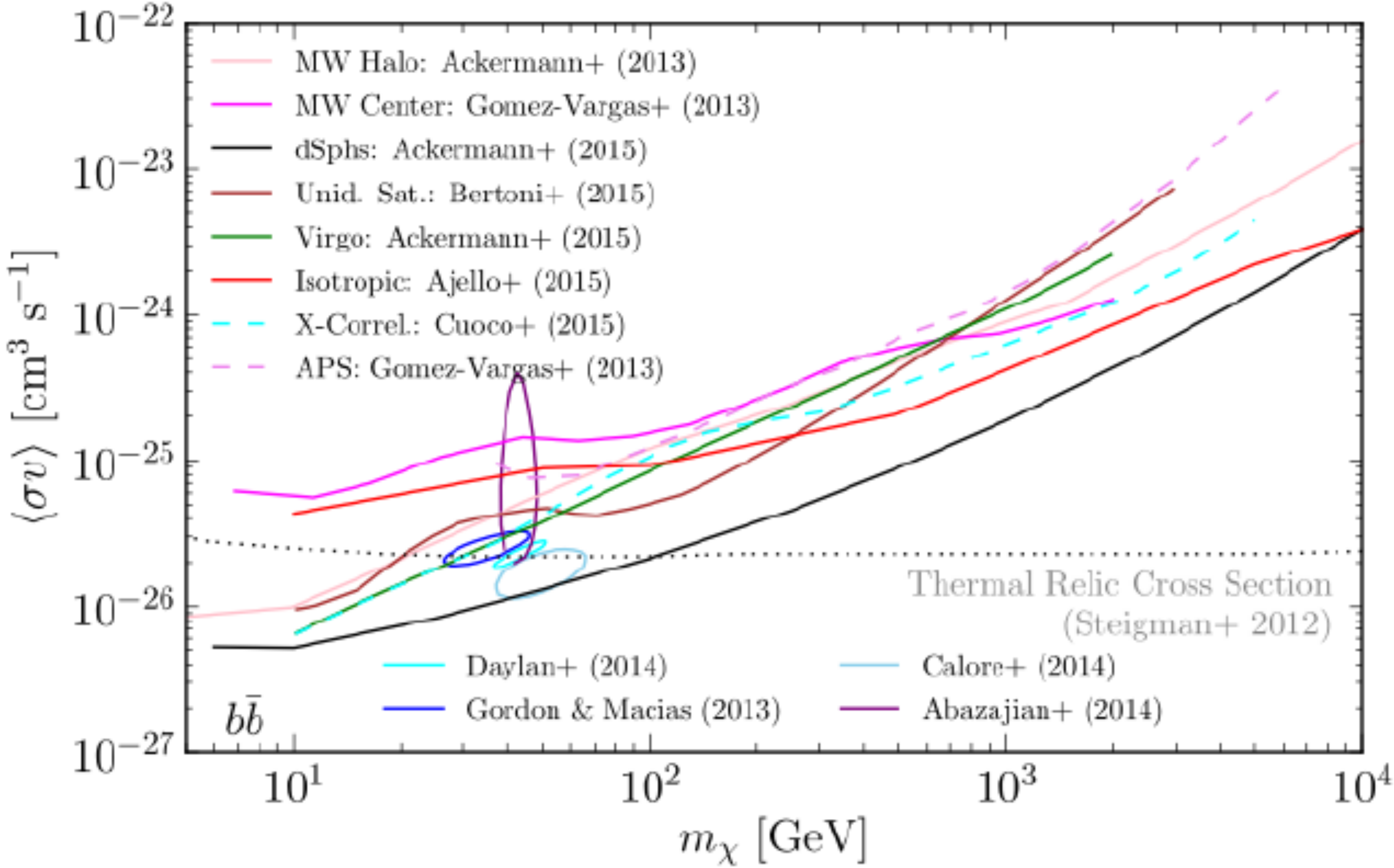
10^{-22}
10^{-23}
10^{-24}
10^{-25}
10^{-26}
10^{-27}
$\langle \sigma v \rangle$ [cm^3 s^{-1}]
MW Halo: Ackermann+ (2013)
MW Center: Gomez-Vargas+ (2013)
dSphs: Ackermann+ (2015)
Unid. Sat.: Bertoni+ (2015)
Virgo: Ackermann+ (2015)
Isotropic: Ajello+ (2015)
X-Correl.: Cuoco+ (2015)
APS: Gomez-Vargas+ (2013)
Thermal Relic Cross Section
(Steigman+ 2012)
Daylan+ (2014)
Gordon & Macias (2013)
Calore+ (2014)
Abazajian+ (2014)
$b\bar{b}$
10^1
10^2
10^3
10^4
m_χ [GeV]

Imaging Atmospheric Cherenkov Telescopes (IACTs)

- Large optical reflector focuses Cherenkov light emitted by particle air showers onto a camera

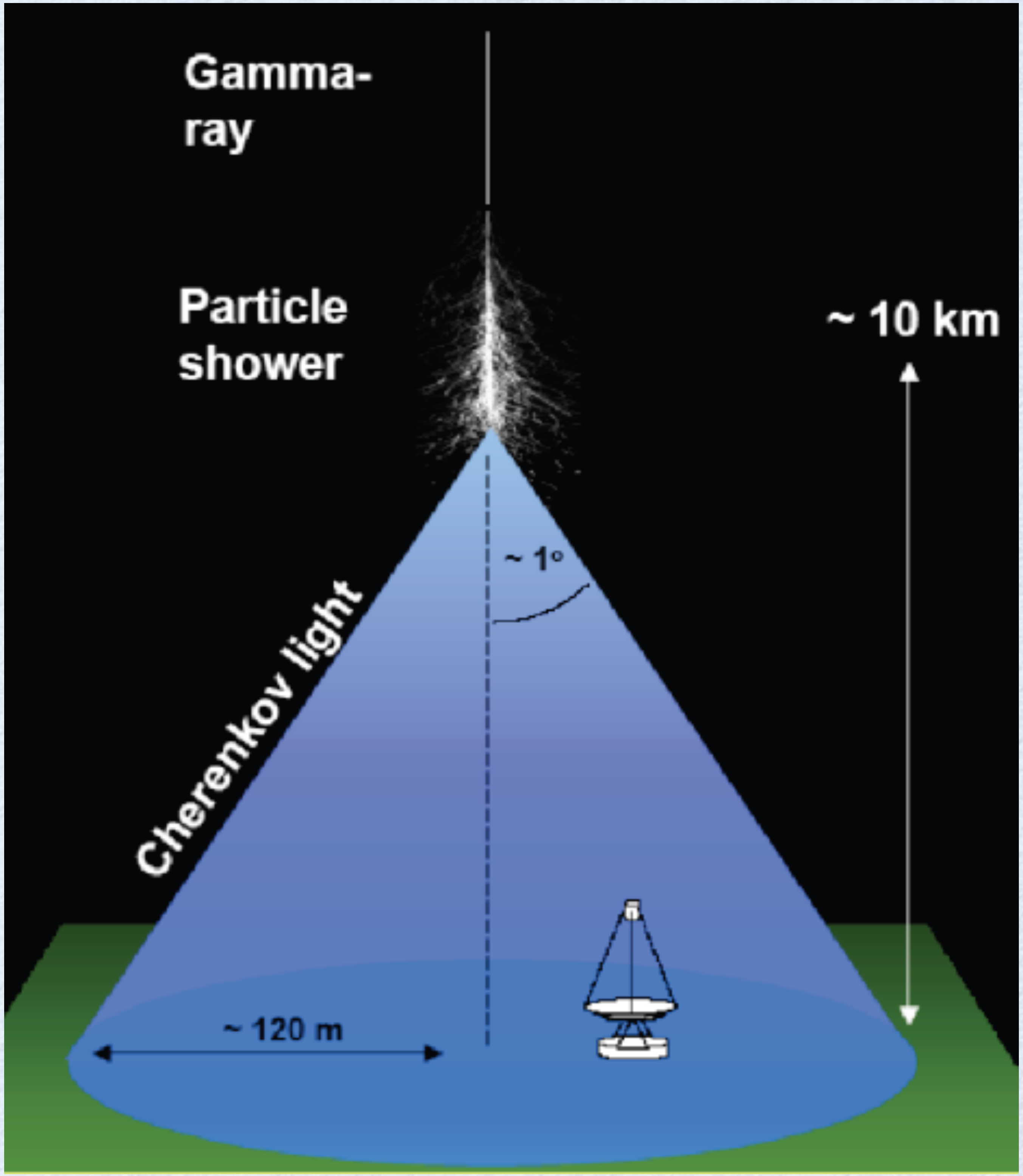

Technique: Cherenkov light is secondary radiation from Extensive Air Showers

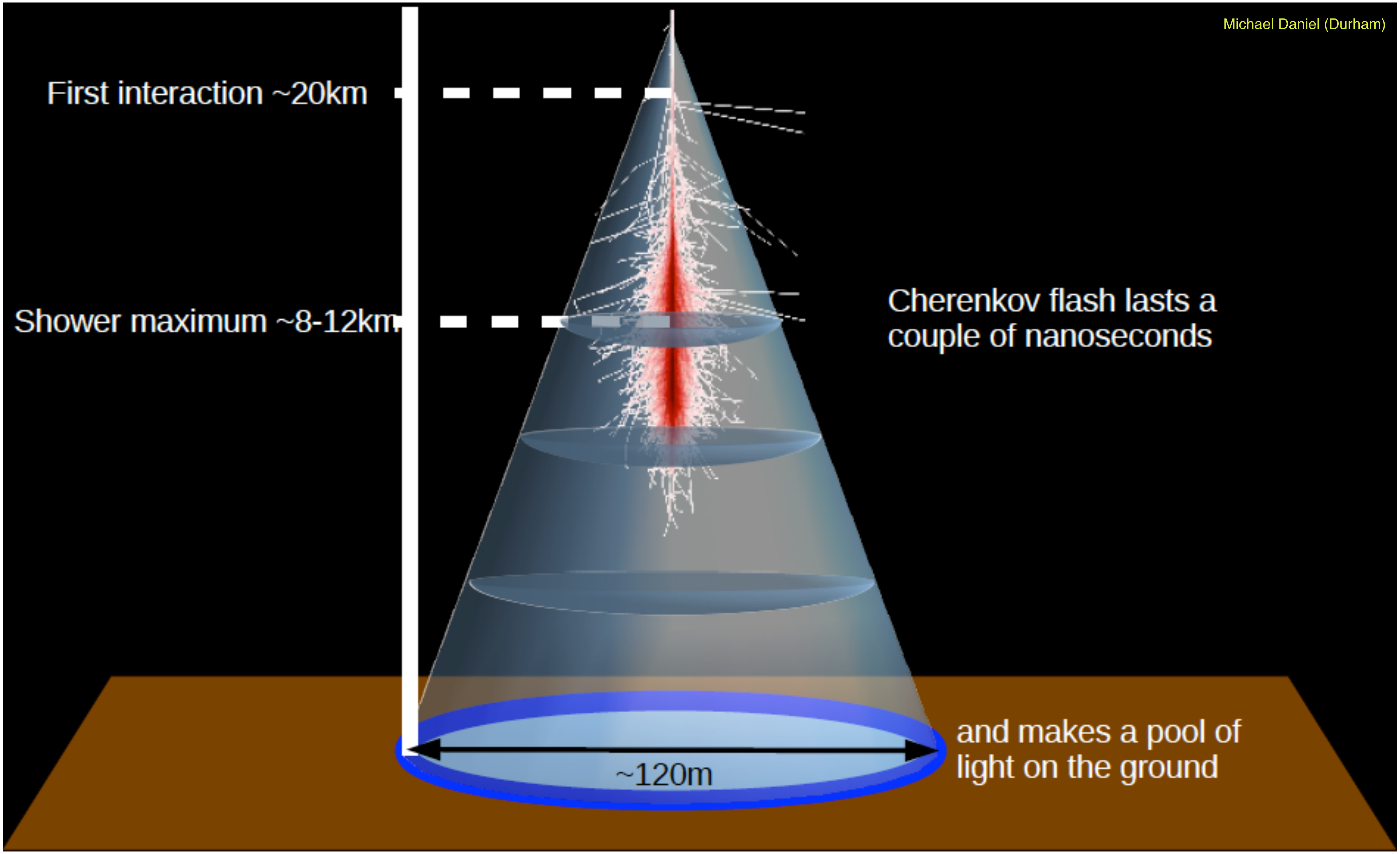

Technique: an imaging Cherenkov telescope

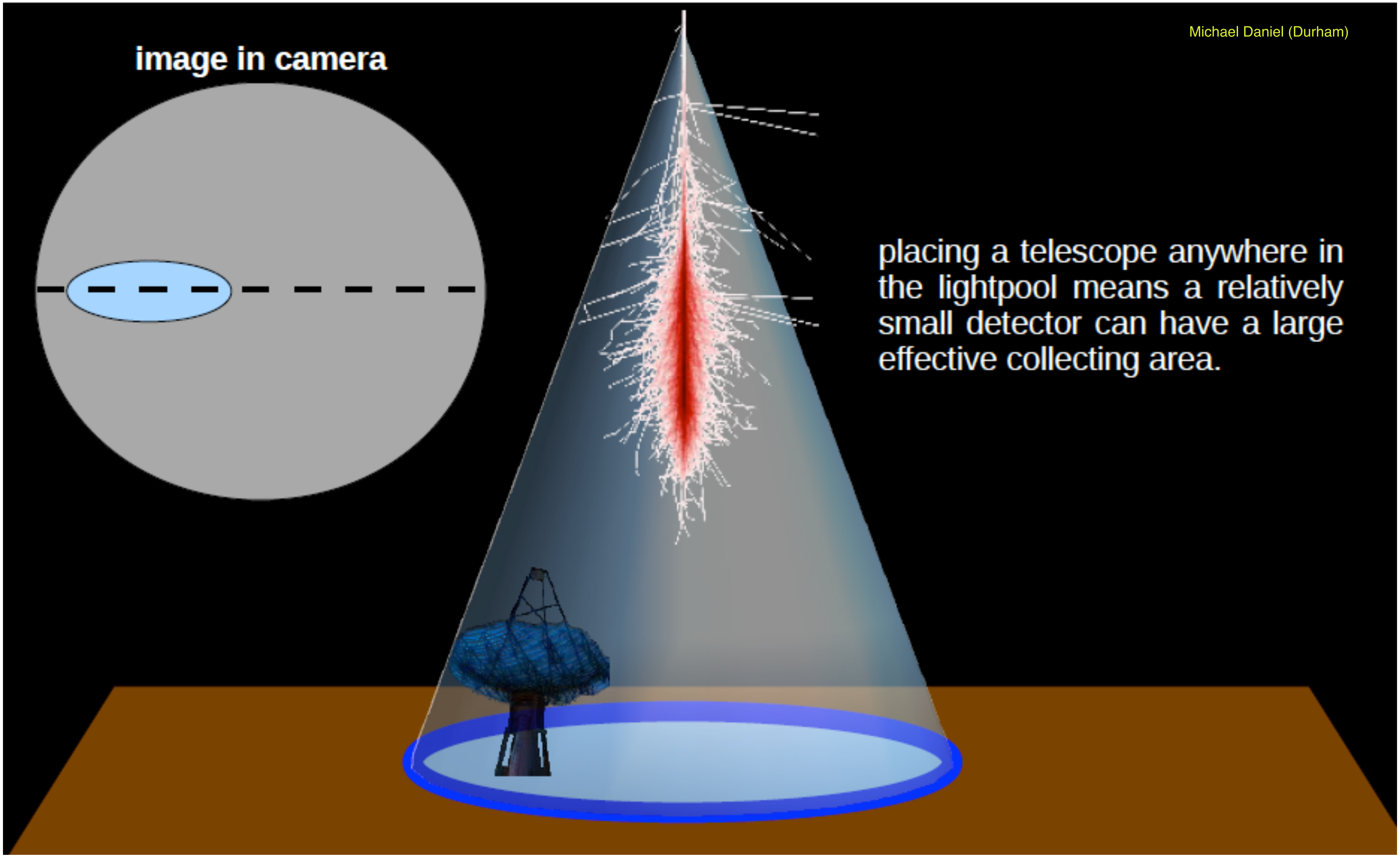

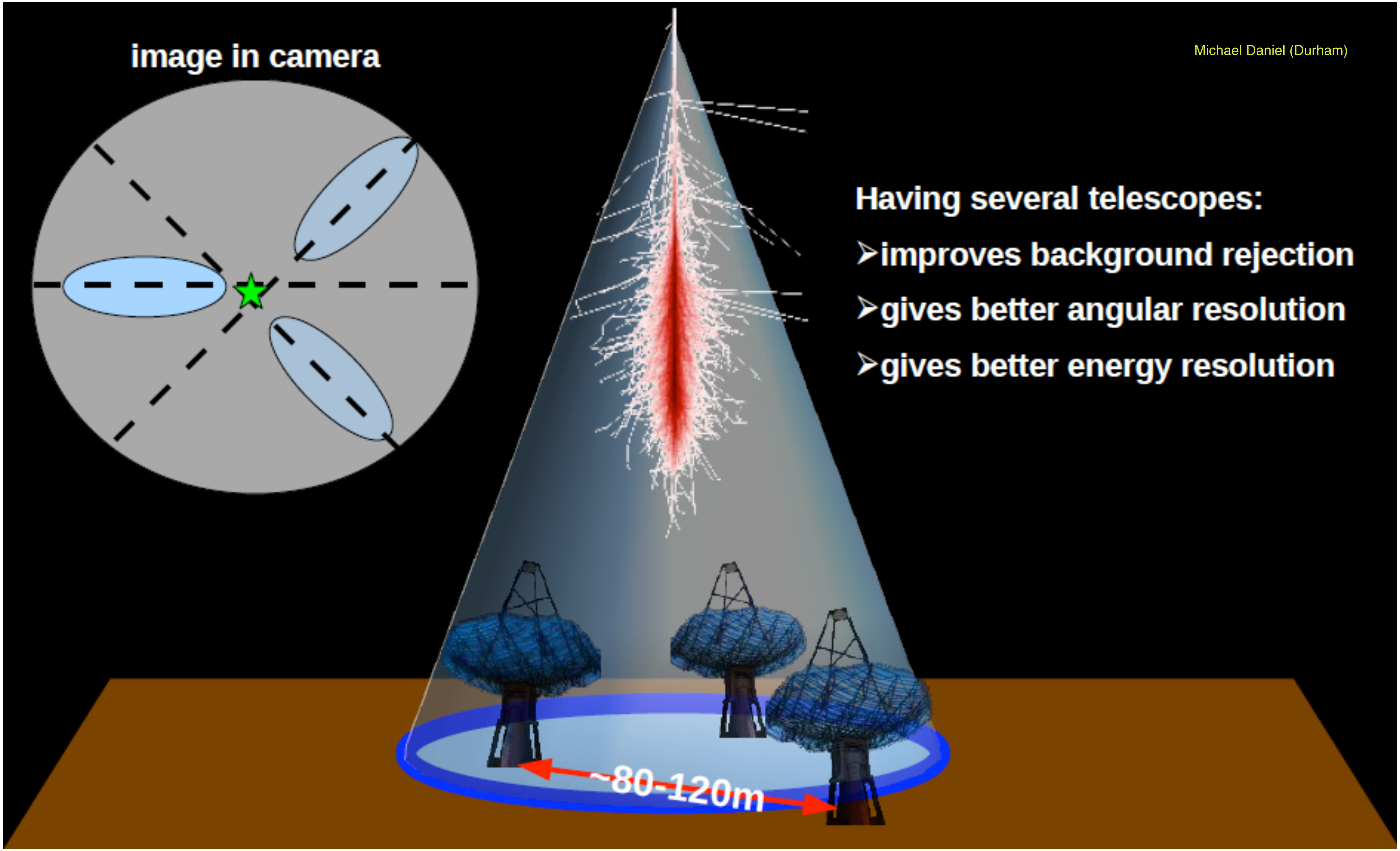
image in camera
Michael Daniel (Durham)
Having several telescopes:
➢improves background rejection
➢gives better angular resolution
➢gives better energy resolution
~80-120m

Focal Plane Instrumentation: an IACT camera

Cherenkov image is faint

200-600nm Cherenkov light density on ground from a 100 GeV primary

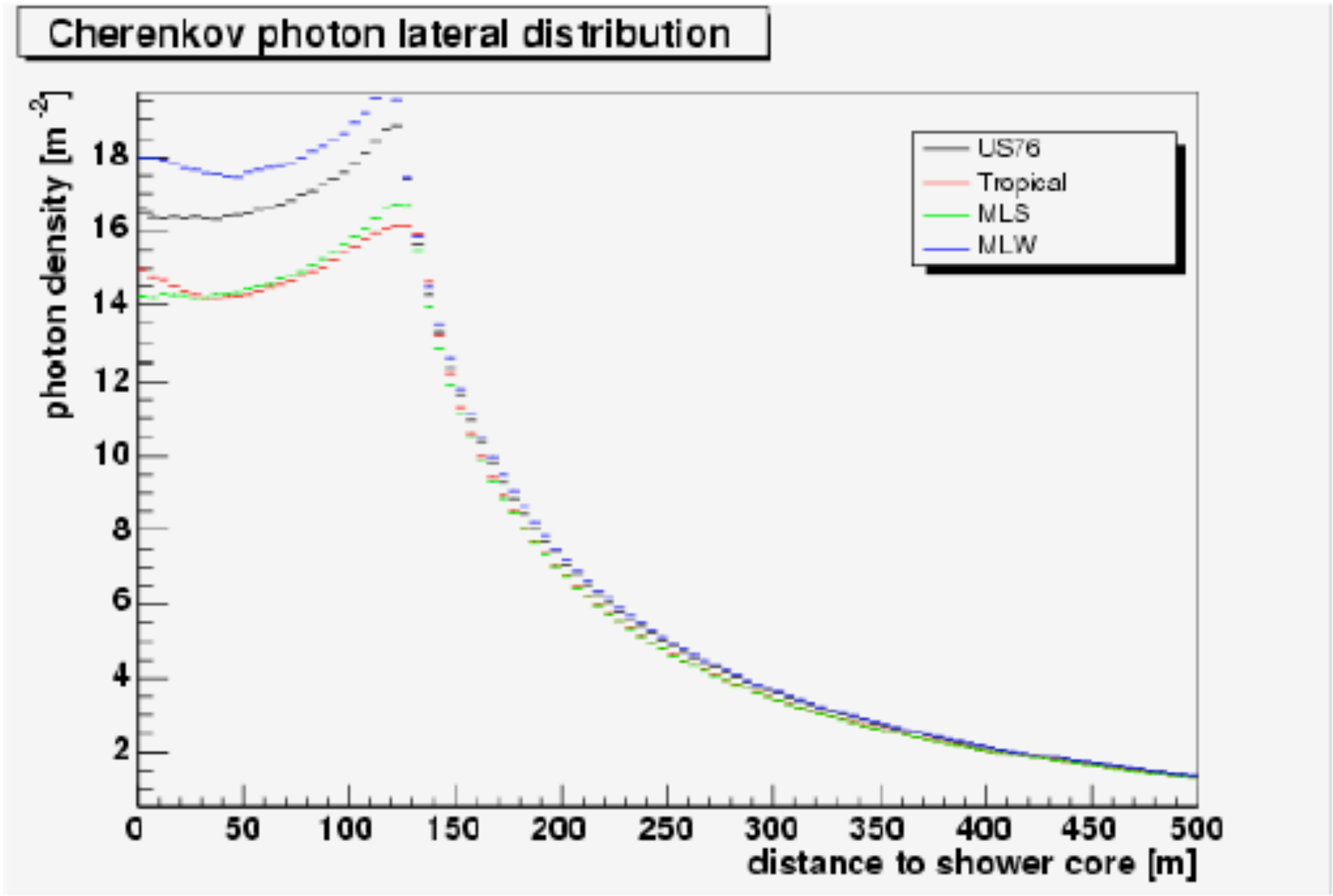

so large collectors (i.e. big mirrors) are needed

Focal Plane Instrumentation: an IACT camera

Cherenkov image is faint

The Cherenkov signal can easily be swamped by background light, so these instruments do not operate under bright conditions, i.e. under moonlight*

so duty cycle of an IACT can be as low as ~10%

*though some do run at reduced gain when the moon is far from full

Focal Plane Instrumentation: an IACT camera

Cherenkov image is faint, brief

lightpool contained in a pancake of a few nanoseconds duration

so using fast electronics with a narrow integration window increases signal/noise by reducing night sky background contamination.

Focal Plane Instrumentation: an IACT camera

Cherenkov image is faint, brief & blue

Spectrum of Cherenkov light

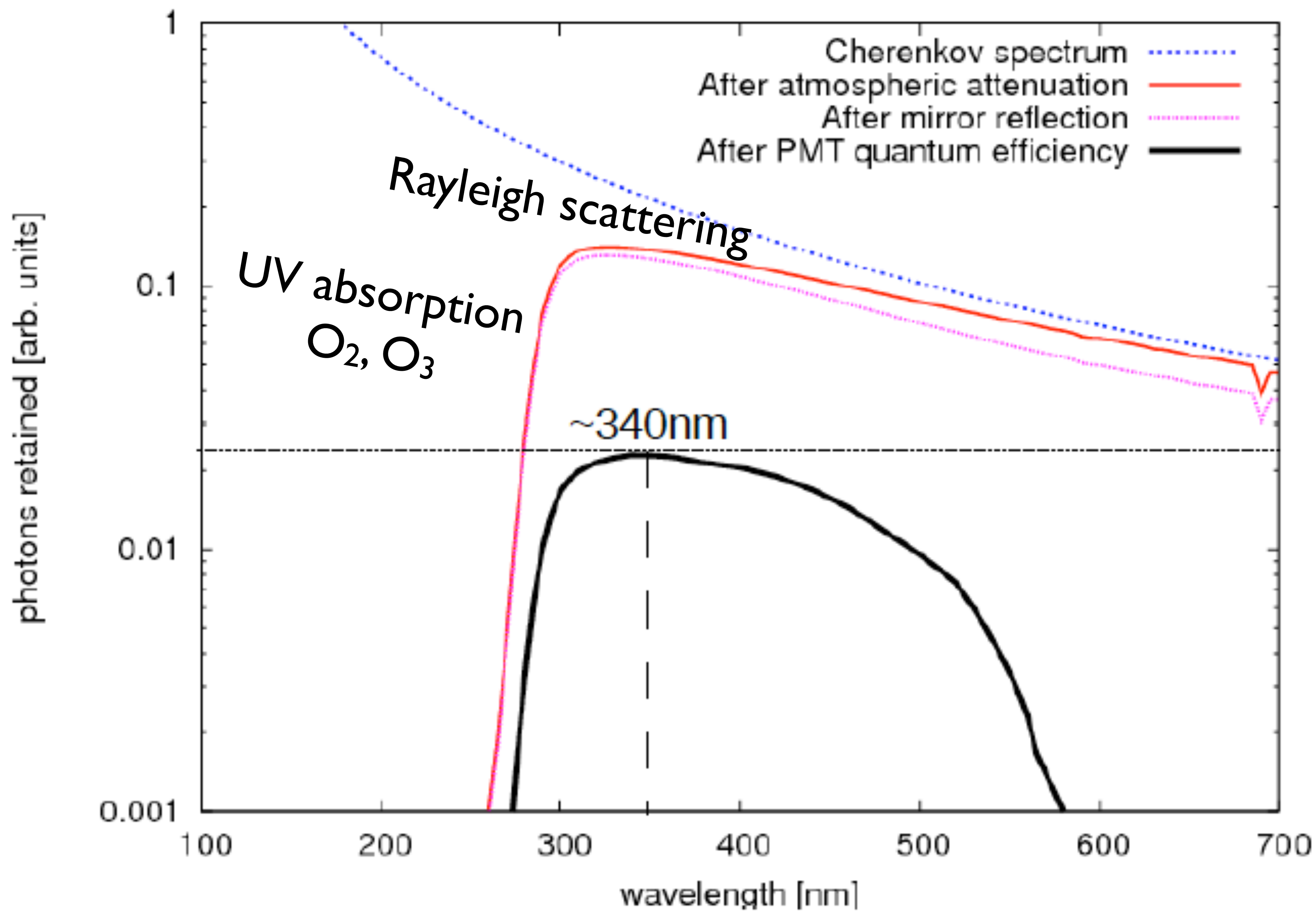

Focal Plane Instrumentation: an IACT camera

Cherenkov image is faint, brief & blue. It is also quite large.

so optical quality in the reflector and the pixel size can be quite modest (i.e. optical PSF relatively large at ~few arcminutes)

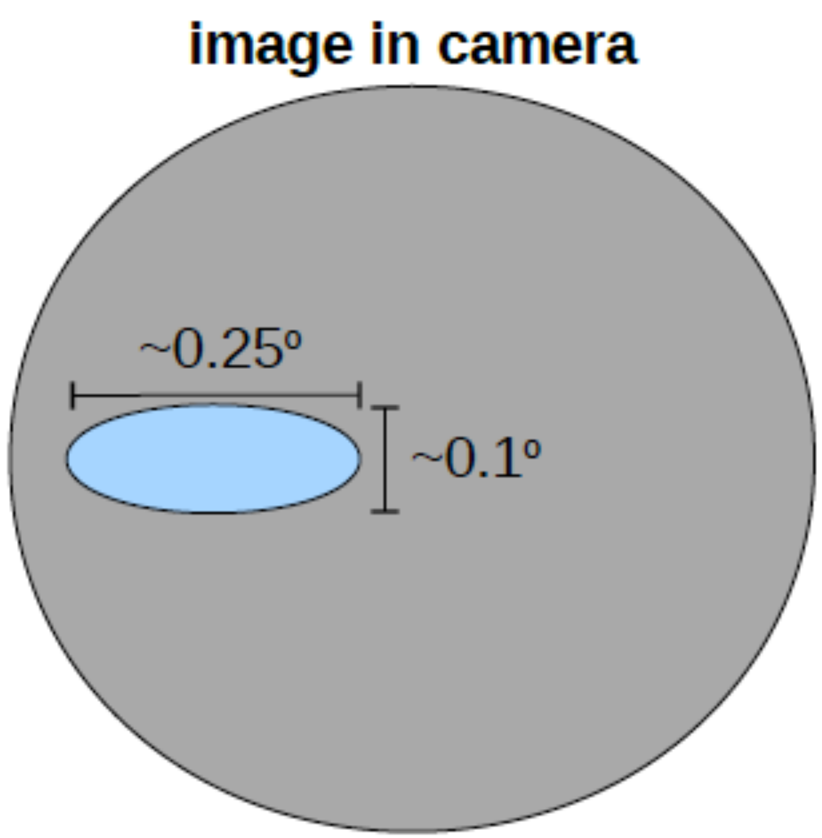

but reasonably good off-axis performance is needed since image is not centred in camera.

The optical support structure is usually of Davies-Cotton design as a compromise between timing and off-axis performance.

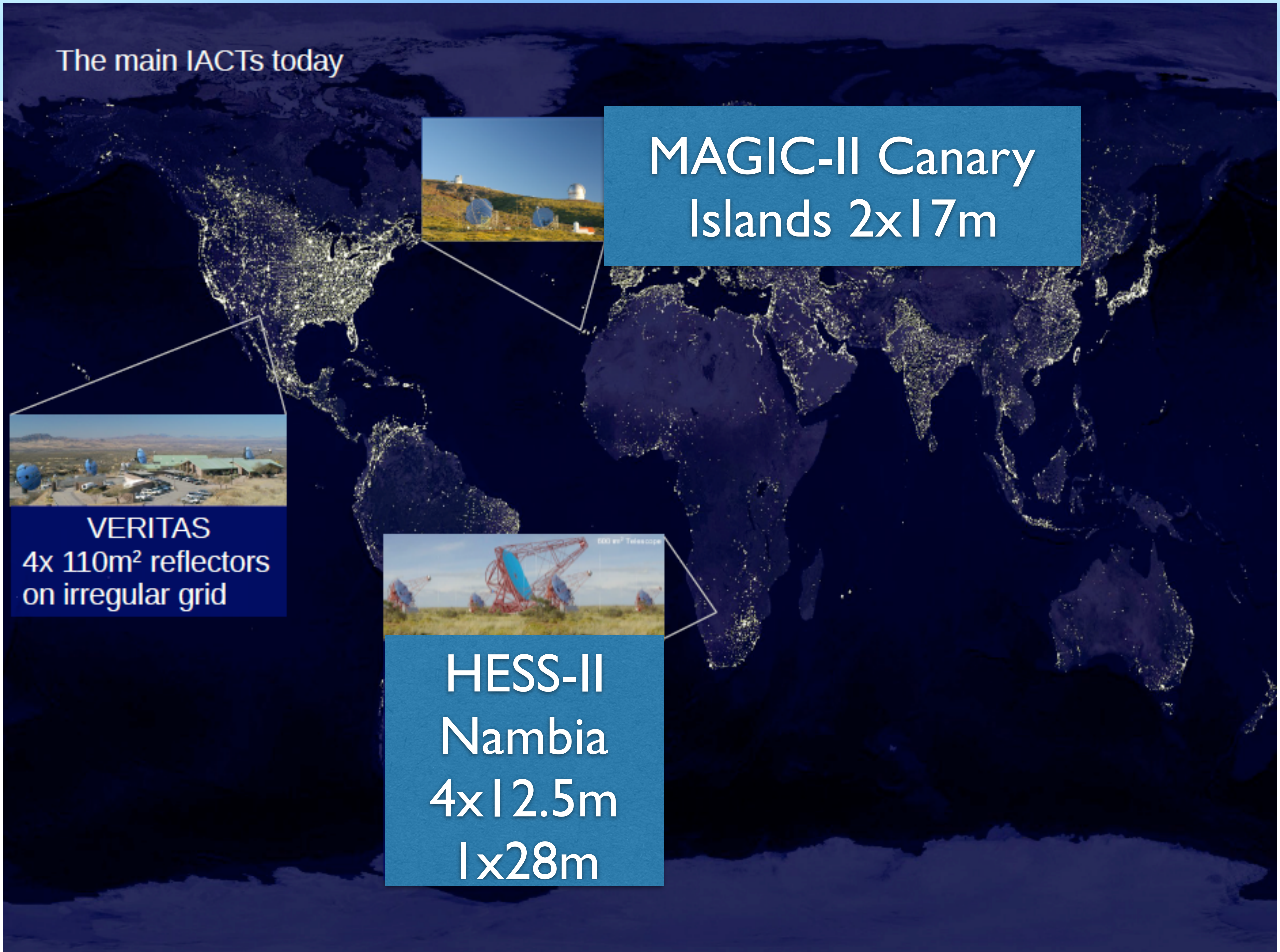
The main IACTs today
MAGIC-II Canary Islands 2x17m
VERITAS
4x 110m² reflectors on irregular grid
HESS-II
Nambia
4x12.5m
1x28m

Veritas

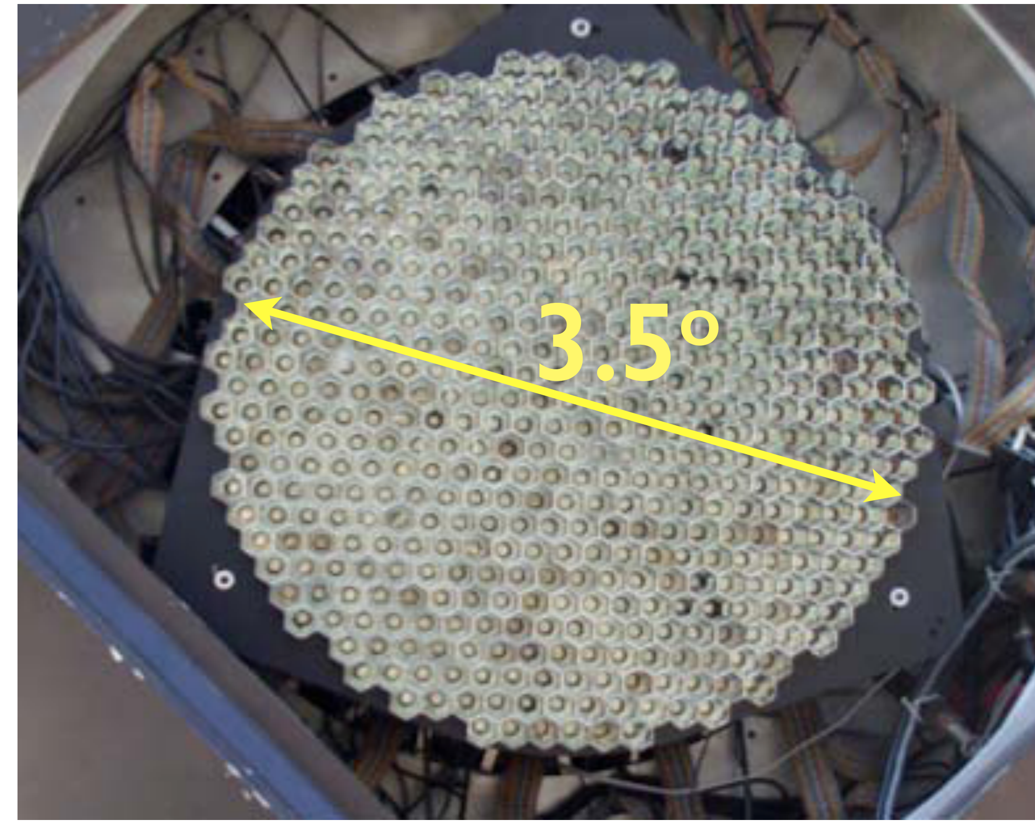

- Array of 4 12-meter IACTs
- Camera: 499 PMTs
- Operational since September 2007
- Sensitivity to a wide range of energies (150GeV - 30TeV) through stereoscopic imaging
- γ-ray reconstruction accuracy ~0.1 and energy resolution ~15%-20%
- Sensitivity 1% Crab at 5σ in 25h

lowest trigger en- ergy threshold among the existing IACTs

MAGIC-I has been in operation since 2004 and the stereoscopic system has been operation since 2009

high quantum efficiency photomulti- plier tubes (PMTs) from Hamamatsu (superbialkali type, QE ~ 32% at the peak wavelength) that we operate at rather low gain of 3·10^4

- Stereo IACT with 2 x 17mØ
- Camera: 577pixels (upgrading to 1039)
- Regular stereo observations since Fall 2009
- Energy threshold ~ 50GeV
- Angular resolution: 0.1° at 100 GeV, down to 0.04° at >1 TeV.
- Energy resolution: 20% at 100 GeV, down to 15% around 1 TeV.
- Sensitivity <0.8% Crab at 5σ in 50h above 300GeV

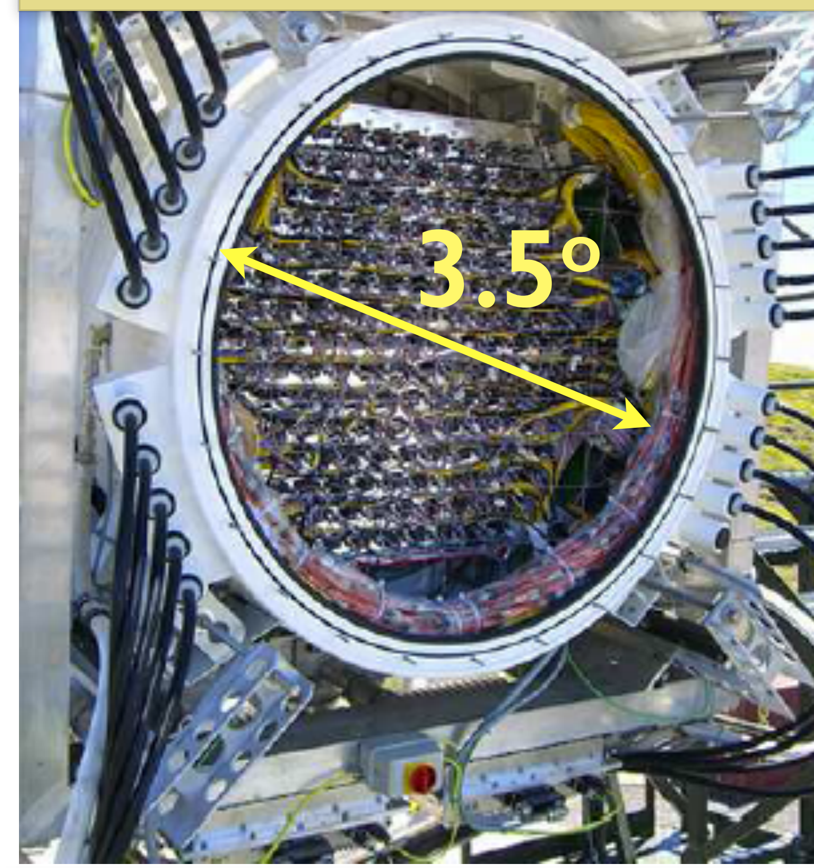

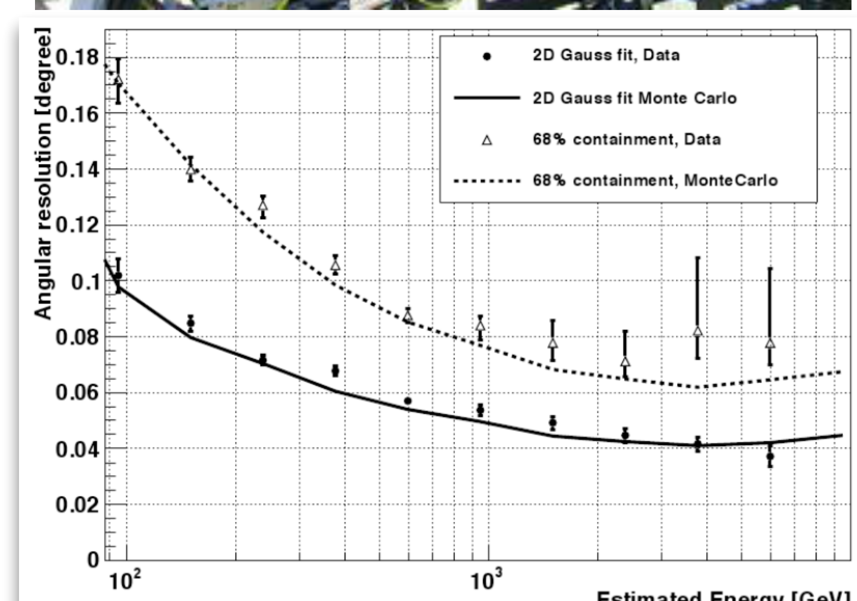

Fermi+MAGIC

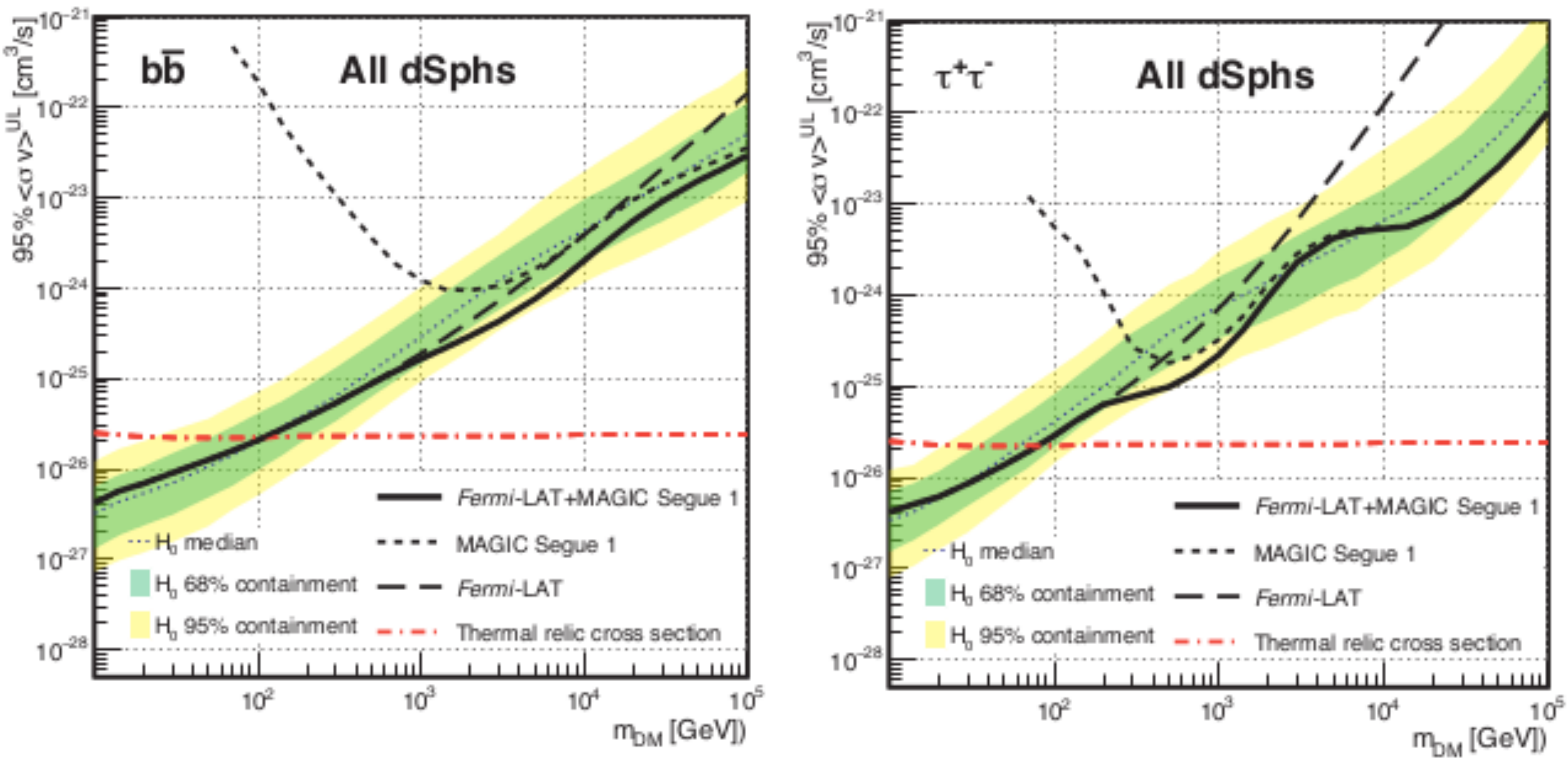

$b\bar{b}$
All dSphs
95% $<\sigma v>^{UL}$ [cm^3/s]
m_{DM} [GeV])
Fermi-LAT+MAGIC Segue 1
MAGIC Segue 1
Fermi-LAT
Thermal relic cross section
H_0 median
H_0 68% containment
H_0 95% containment
$\tau^+\tau^-$
All dSphs
95% $<\sigma v>^{UL}$ [cm^3/s]
m_{DM} [GeV])
Fermi-LAT+MAGIC Segue 1
MAGIC Segue 1
Fermi-LAT
Thermal relic cross section
H_0 median
H_0 68% containment
H_0 95% containment

Gamma-rays future

Gamma-400

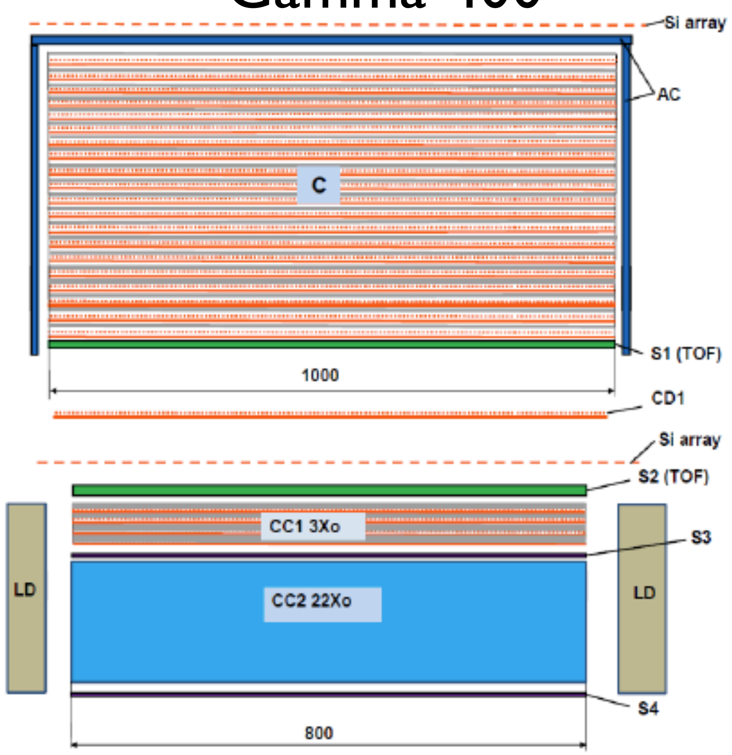

- Follow up to Fermi
- extend energy range to 3TeV
- Improve angular resolution
- Launch of the GAMMA-400 space observatory is planned in 2018

Cherenkov Telescope Array (CTA)

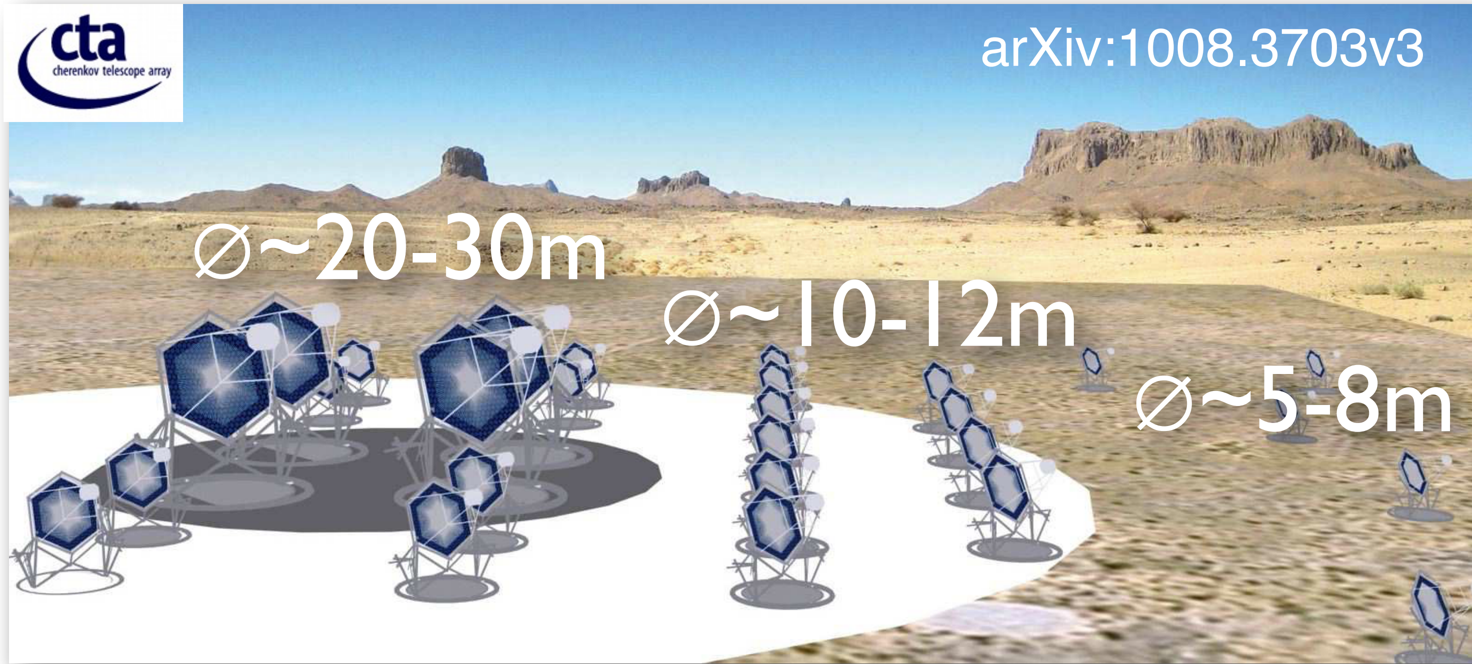

- Energy range: a few tens of GeV to above 100 TeV)
- Baseline design consists of three single-mirror telescopes: Small/Medium/Large size telescopes.
- Improvement in flux sensitivity of 1-2 orders of magnitude over current instruments is expected

CTA Prospects

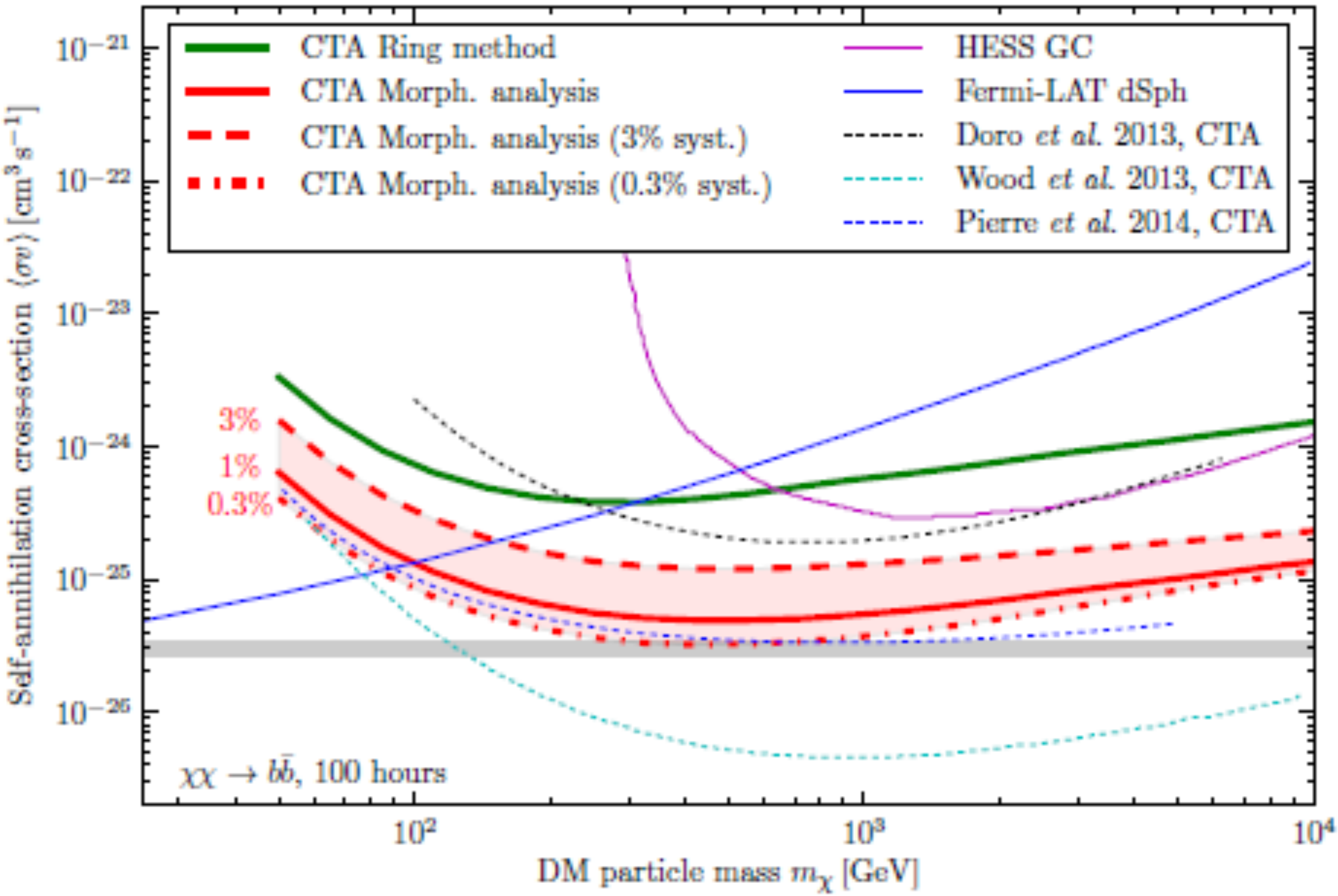

Neutrinos

Principle of an optical Neutrino Telescope

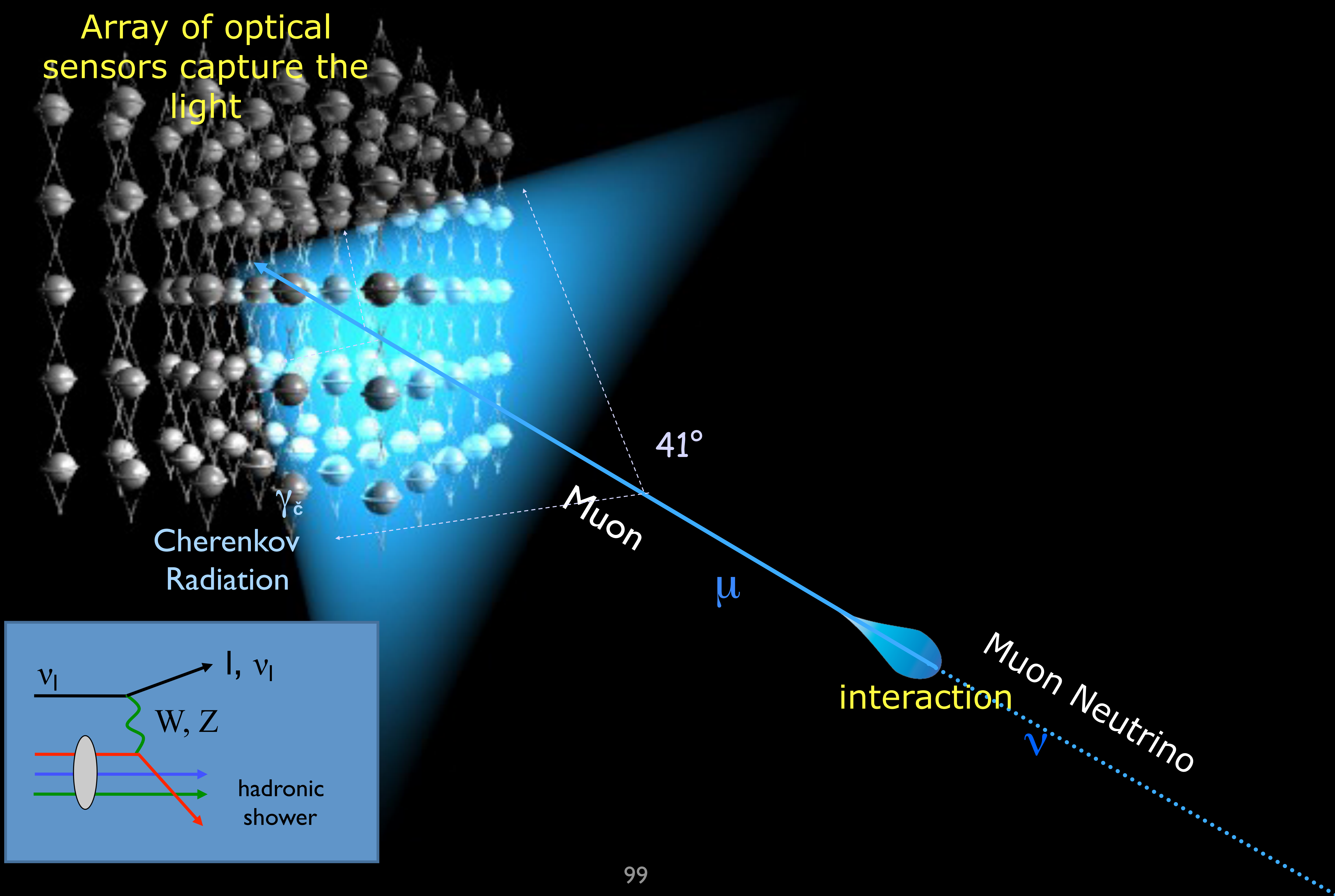

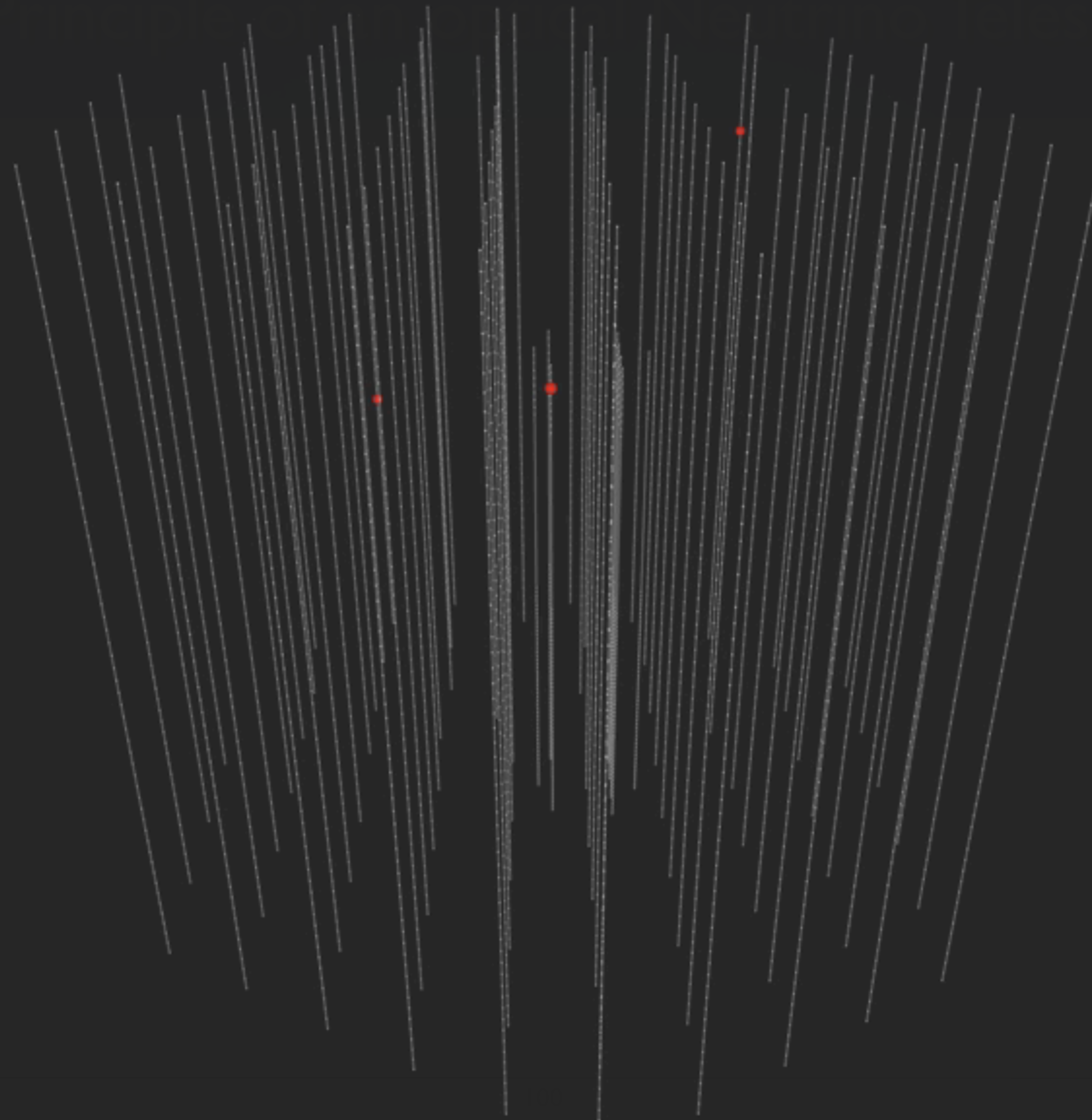

Neutrino Telescopes

Large Water Cherenkov Neutrino Detectors

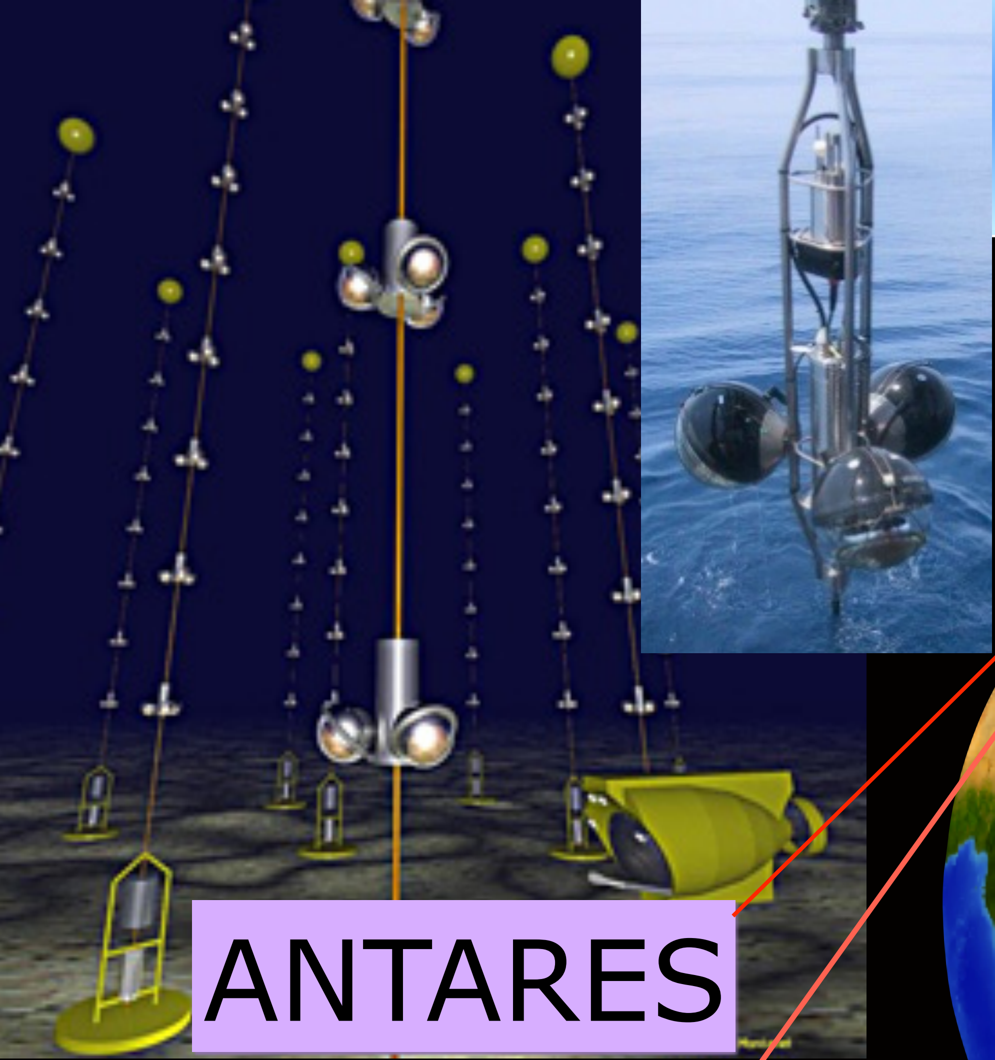

ANTARES

KM3Net

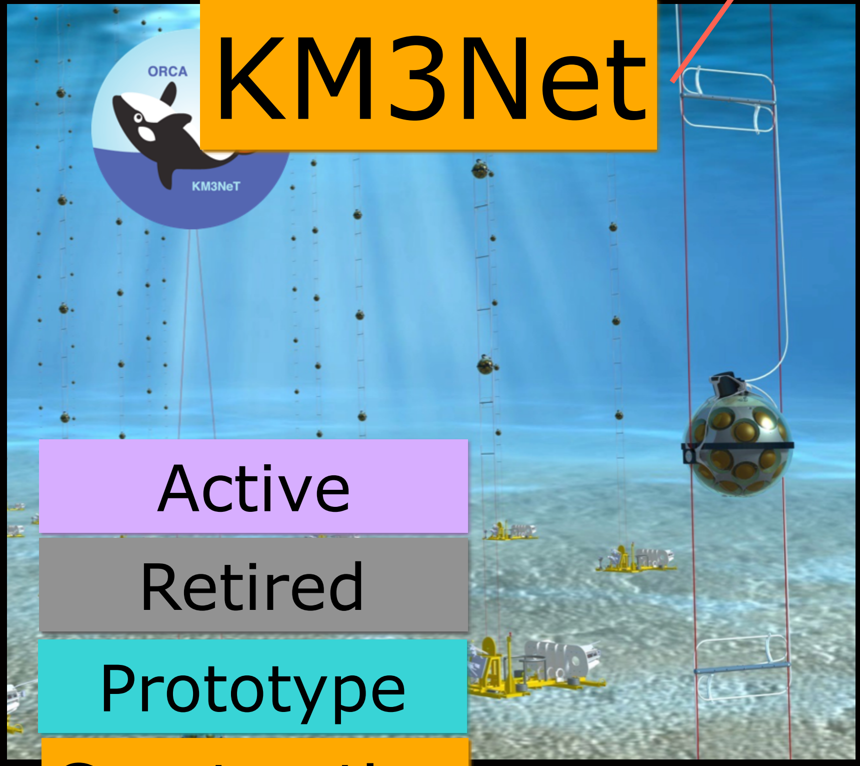

Active

Retired

Prototype

Construction

Planned

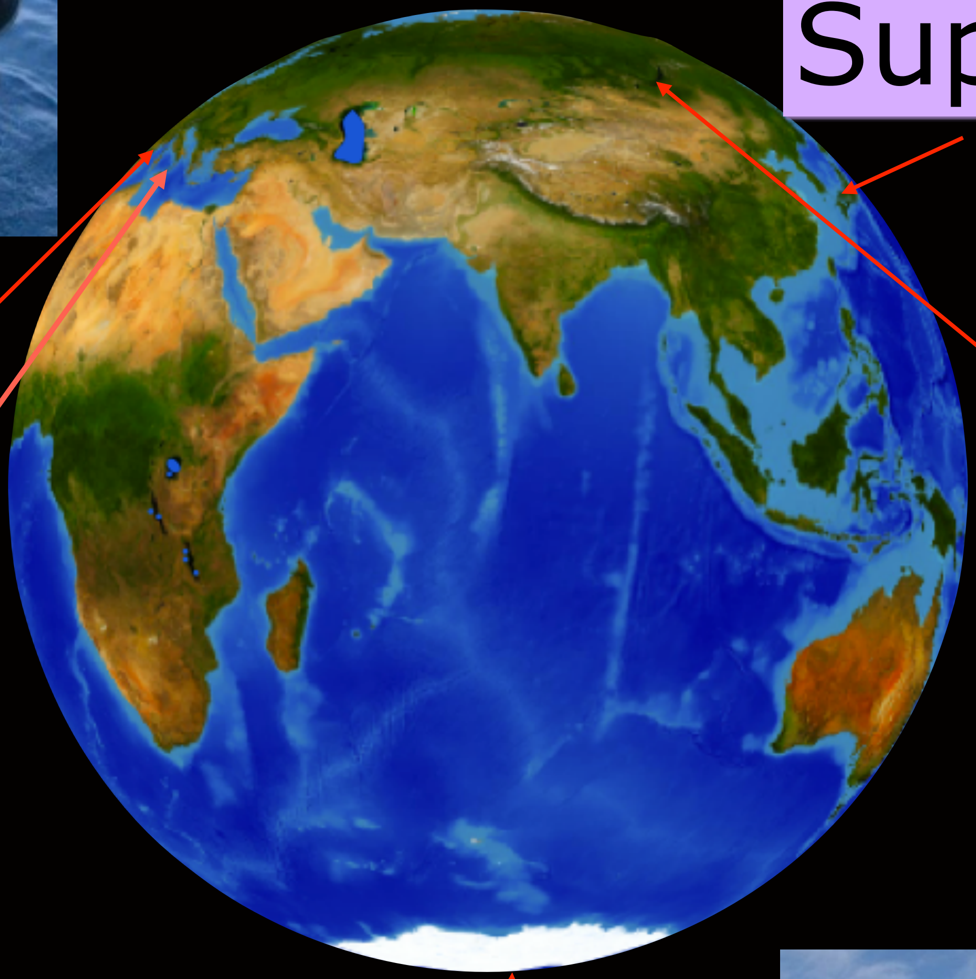

Hyper-K

Super-K

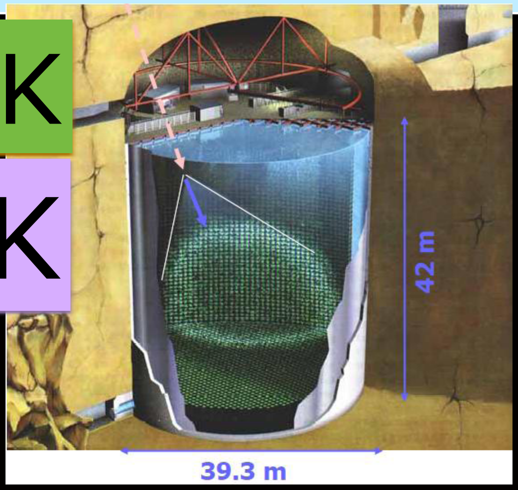

Lake Baikal

GVD

IceCube

Gen2/PINGU

Neutrino Telescopes / Detectors

- **ANTARES** is located at a depth of 2475 m in the Mediterranean Sea, 40 km offshore from Toulon
- Consists 885 10”PMTs on 12 lines with 25 storeys each.
- Detector was competed in May 2008

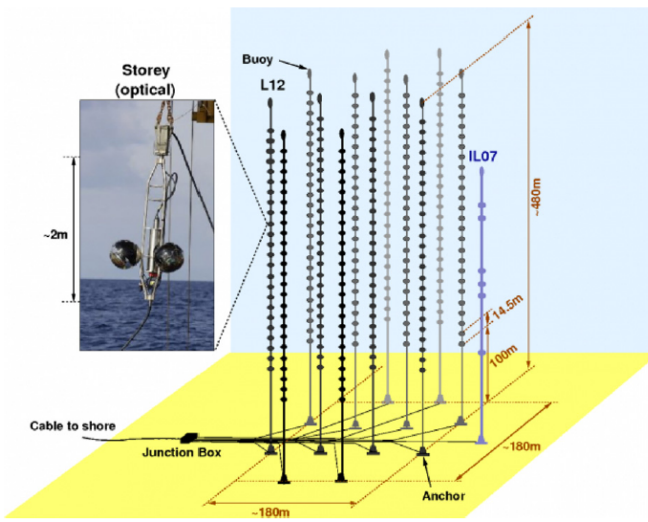

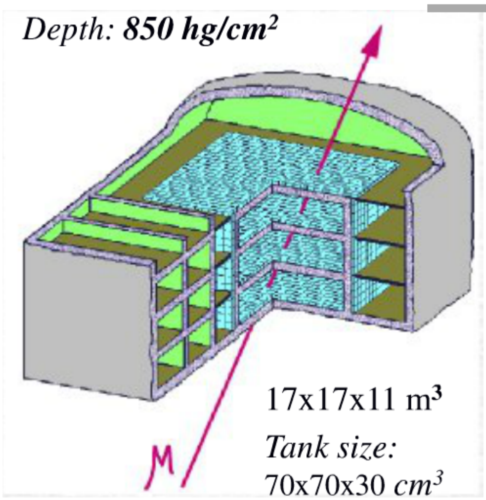

- **Baksan** Underground Scintillator Telescope with muon energy threshold about 1 GeV using 3,150 liquid scintillation counters
- Operating since Dec 1978 ; More than 34 years of continuous operation

- Lake **Baikal**, Siberia, at a depth 1.1 km NT36 in 1993
- NT200 (since Apr 1998) consists of one central and seven peripheral strings of 70m length

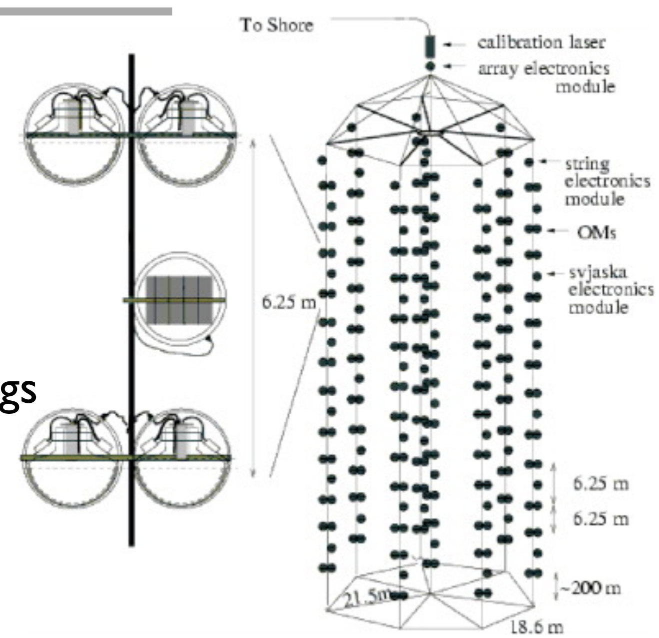

- **IceCube** at the Geographic South Pole
- 5160 10”PMTs in Digital optical modules distributed over 86 strings instrumenting ~1km^3
- Physics data taking since 2007 ; Completed in December 2010, including **DeepCore** low-energy extension

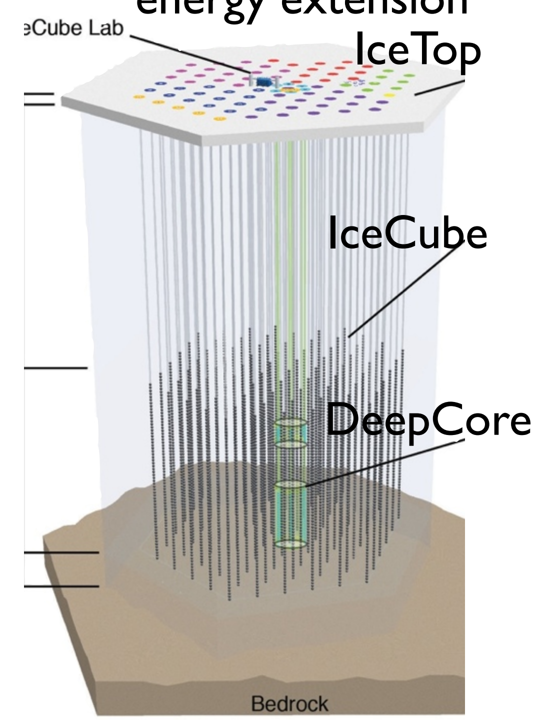

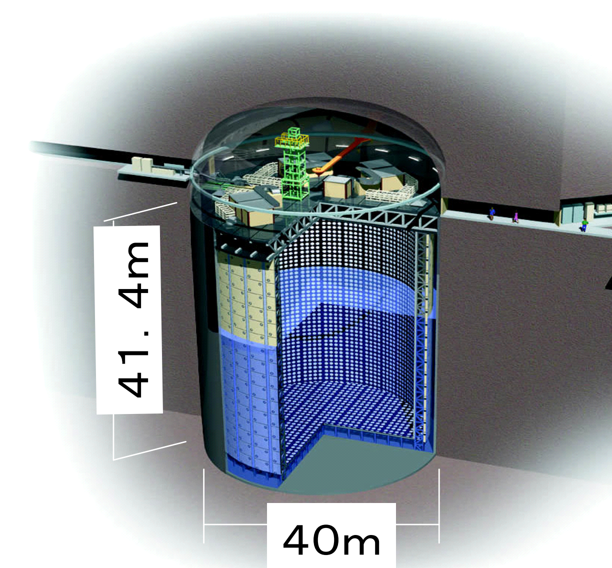

- **Super-Kamiokande** at Kamioka uses 11K 20” PMTs
- 50kt pure water (22.5kt fiducial) water-cherenkov detector
- Operating since 1996

ANTARES

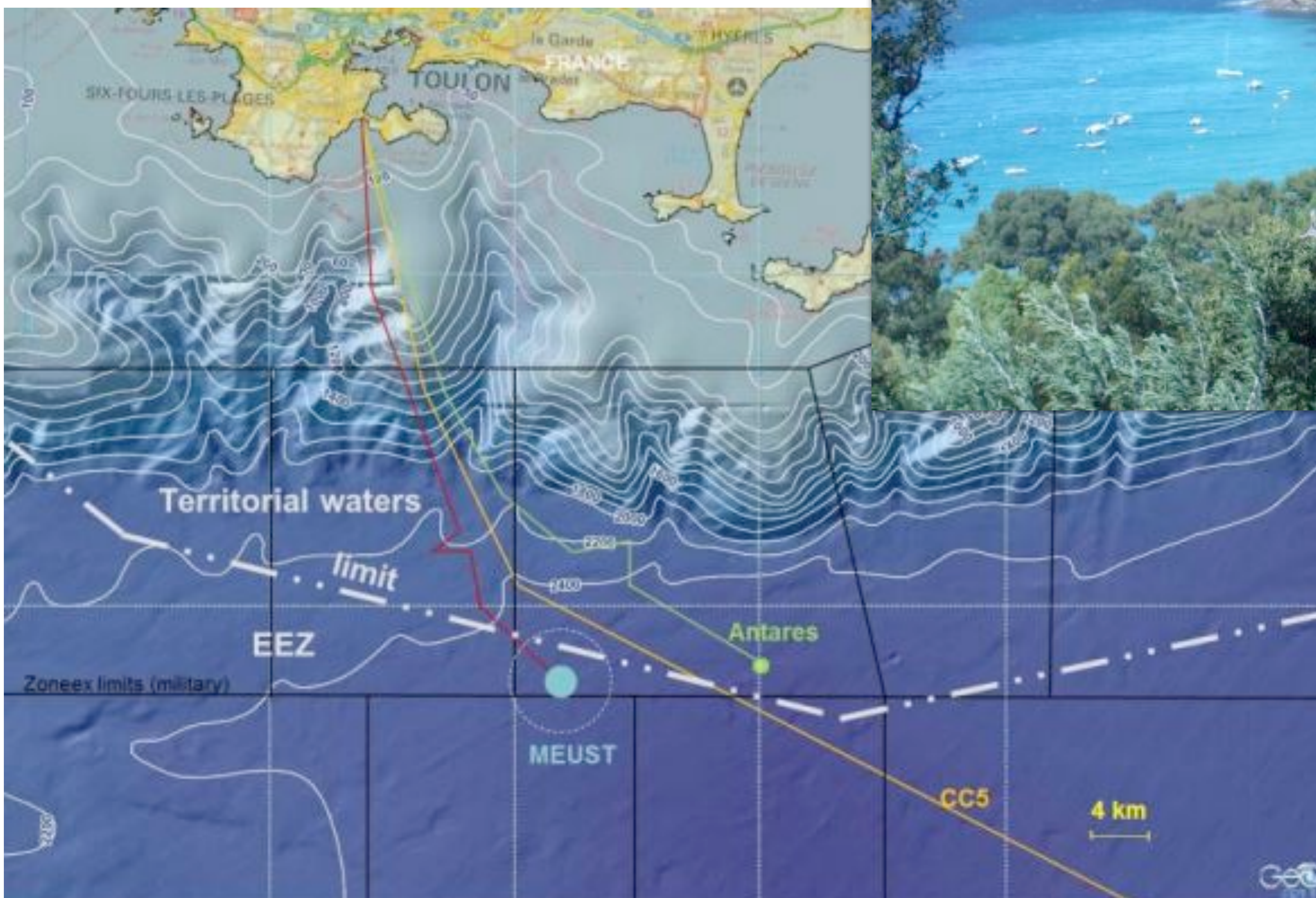
SIX-FOURS-LES-PLAGES
TOULON
FRANCE
HYERES
Territorial waters
limit
EEZ
Zoneex limits (military)
Antares
MEUST
CC5
4 km

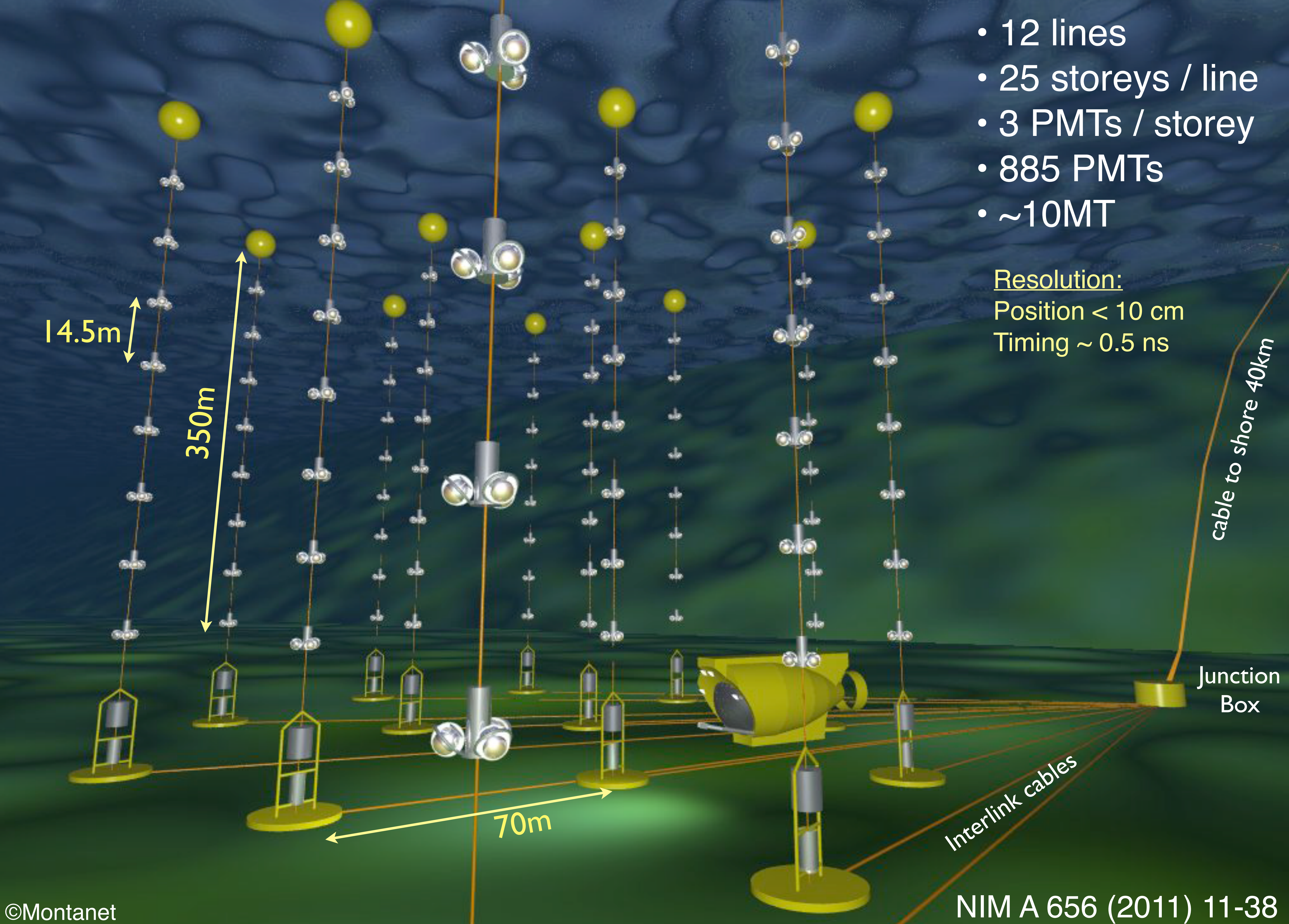
• 12 lines
• 25 storeys / line
• 3 PMTs / storey
• 885 PMTs
• ~10MT
Resolution:
Position < 10 cm
Timing ~ 0.5 ns
14.5m
350m
70m
cable to shore 40km
Junction Box
Interlink cables
©Montanet
NIM A 656 (2011) 11-38

Storey with 3OMs

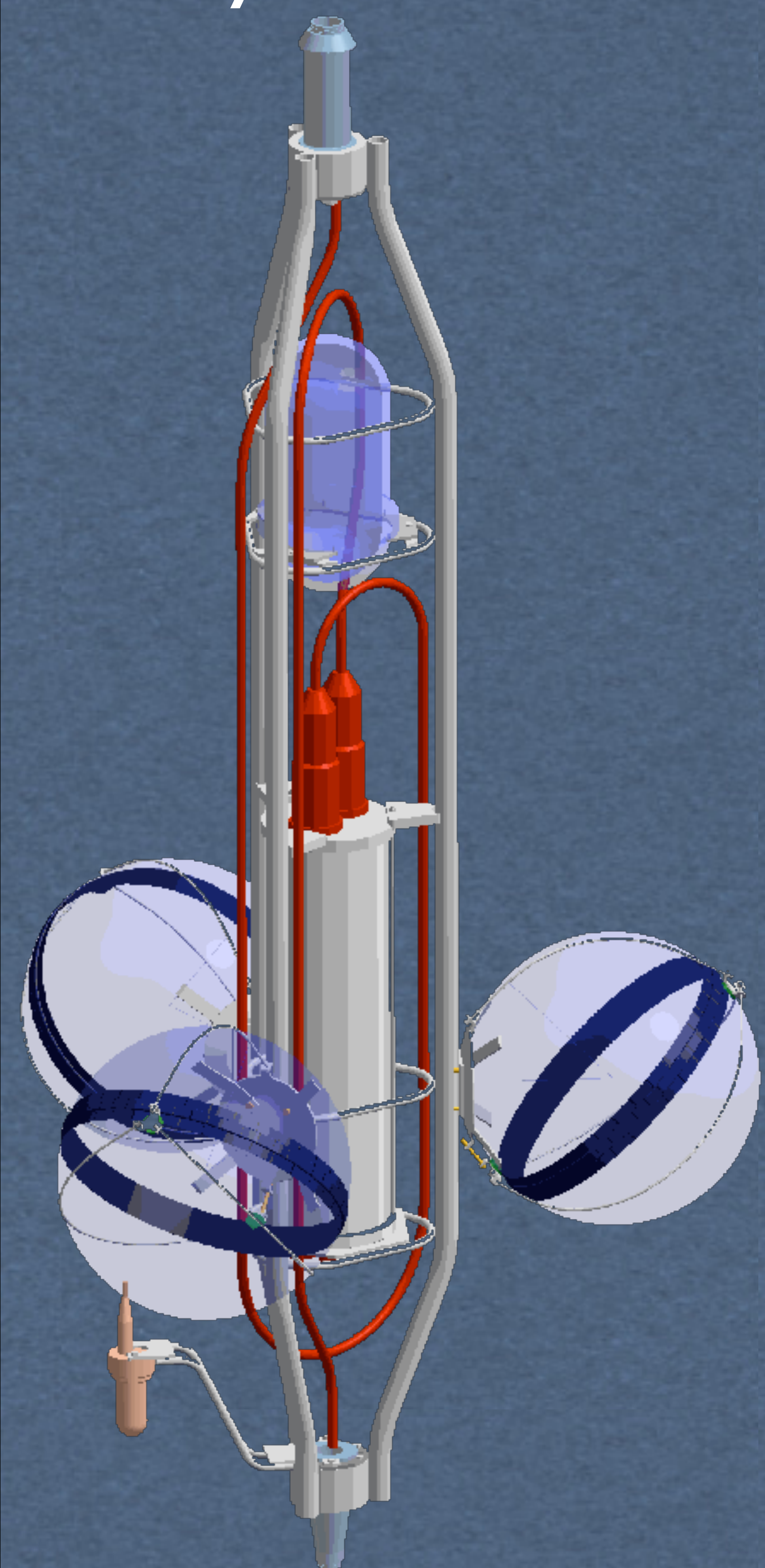

- 12 lines
- 25 storeys / line
- 3 PMTs / storey
- 885 PMTs
- ~10MT

Resolution:
Position < 10 cm
Timing ~ 0.5 ns

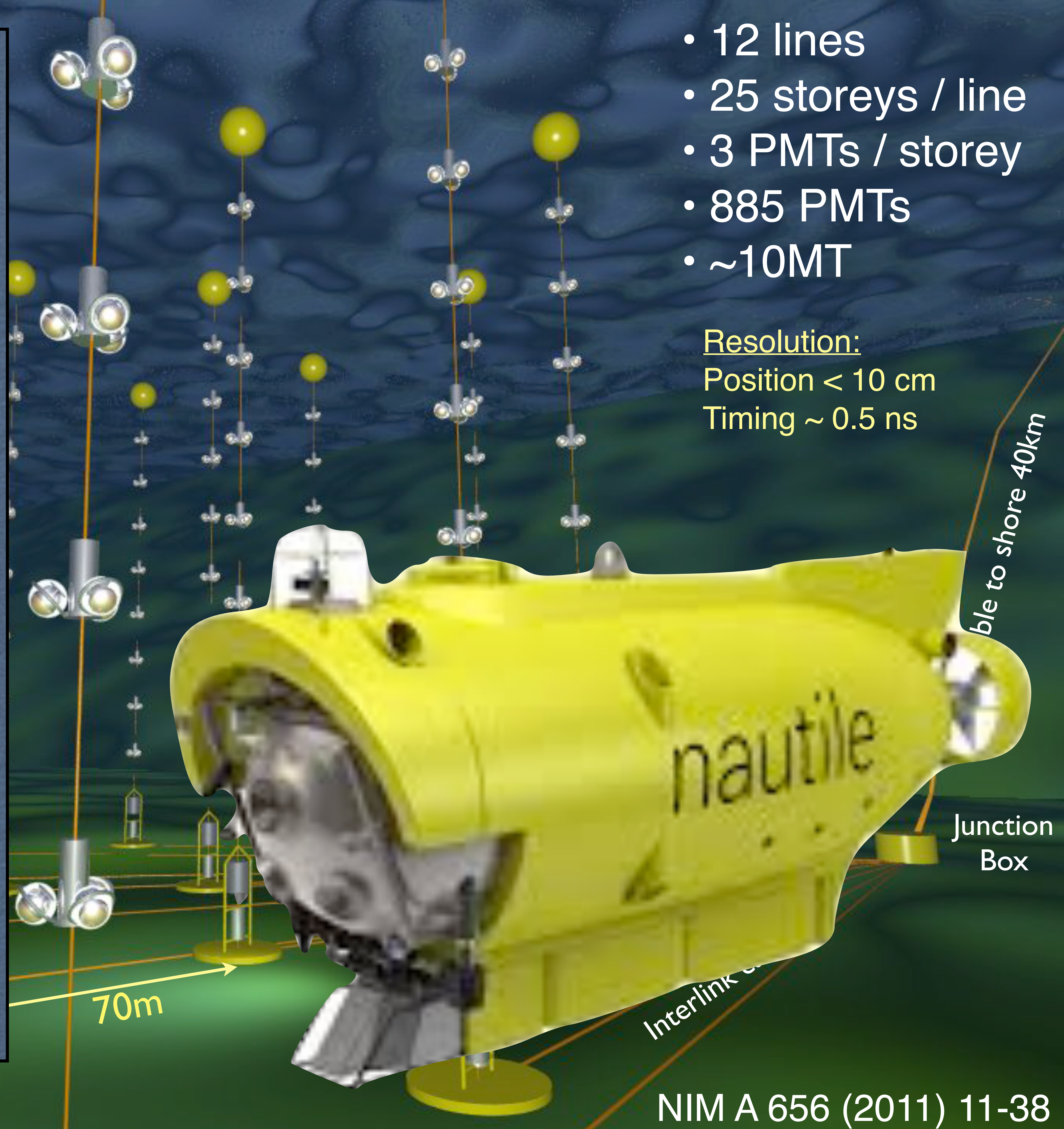

©Montanet

NIM A 656 (2011) 11-38

The IceCube Neutrino Telescope

Laboratory at the South Pole

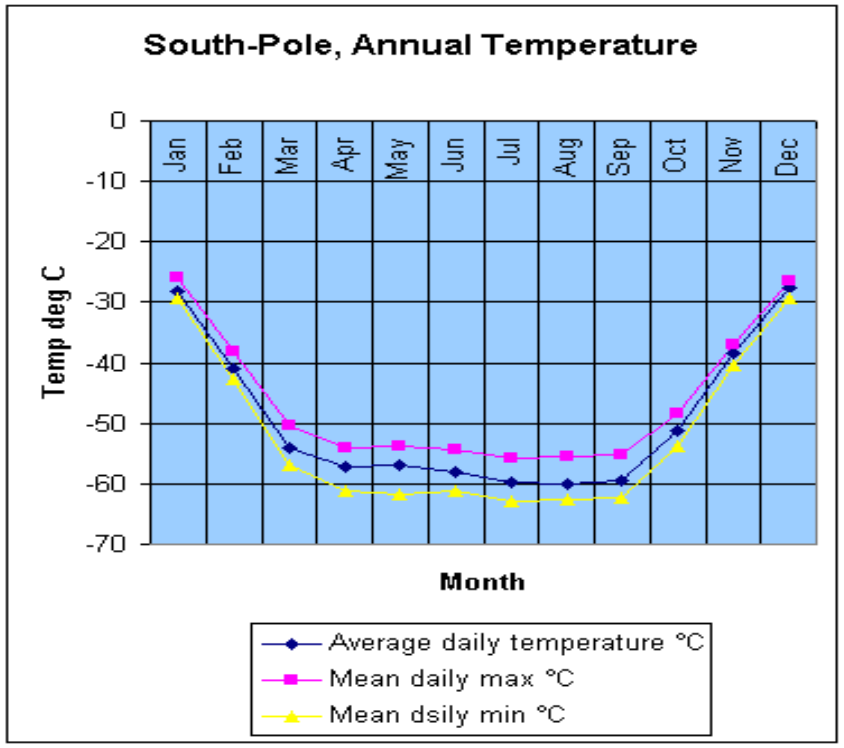

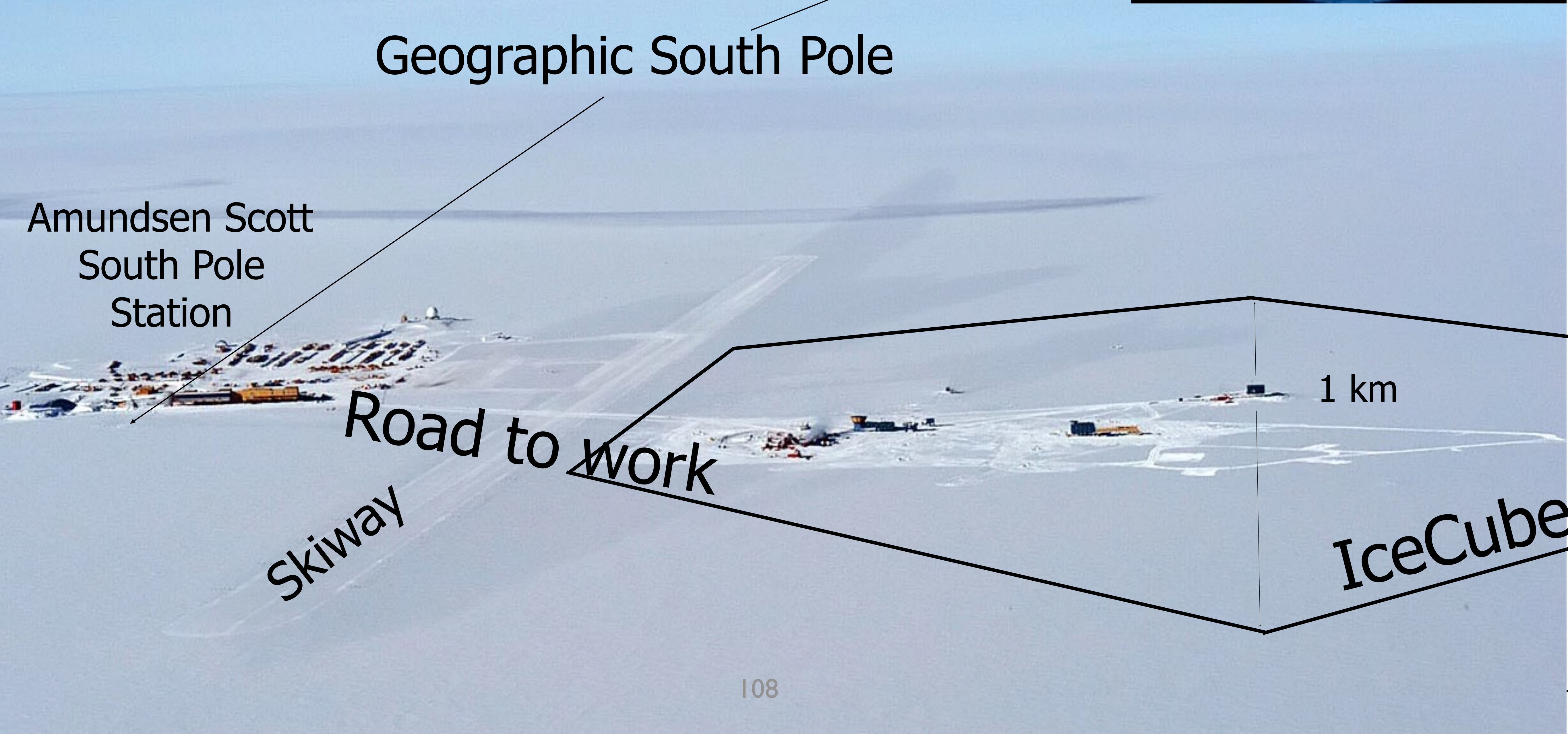

The IceCube Neutrino Telescope

- Gigaton Neutrino Detector at the Geographic South Pole
- 5160 Digital optical modules distributed over 86 strings
- Completed in December 2010, start of data taking with full detector May 2011
- Data acquired during the construction phase has been analyzed
- Neutrinos are identified through Cherenkov light emission from secondary particles produced in the neutrino interaction with the ice

Strings	Dataset
1	2005-2006
9	2006-2007
22	2007-2008
40	2008-2009
59	2009-2010
73 + 6	2010-2011
78 + 8	2011 - .....

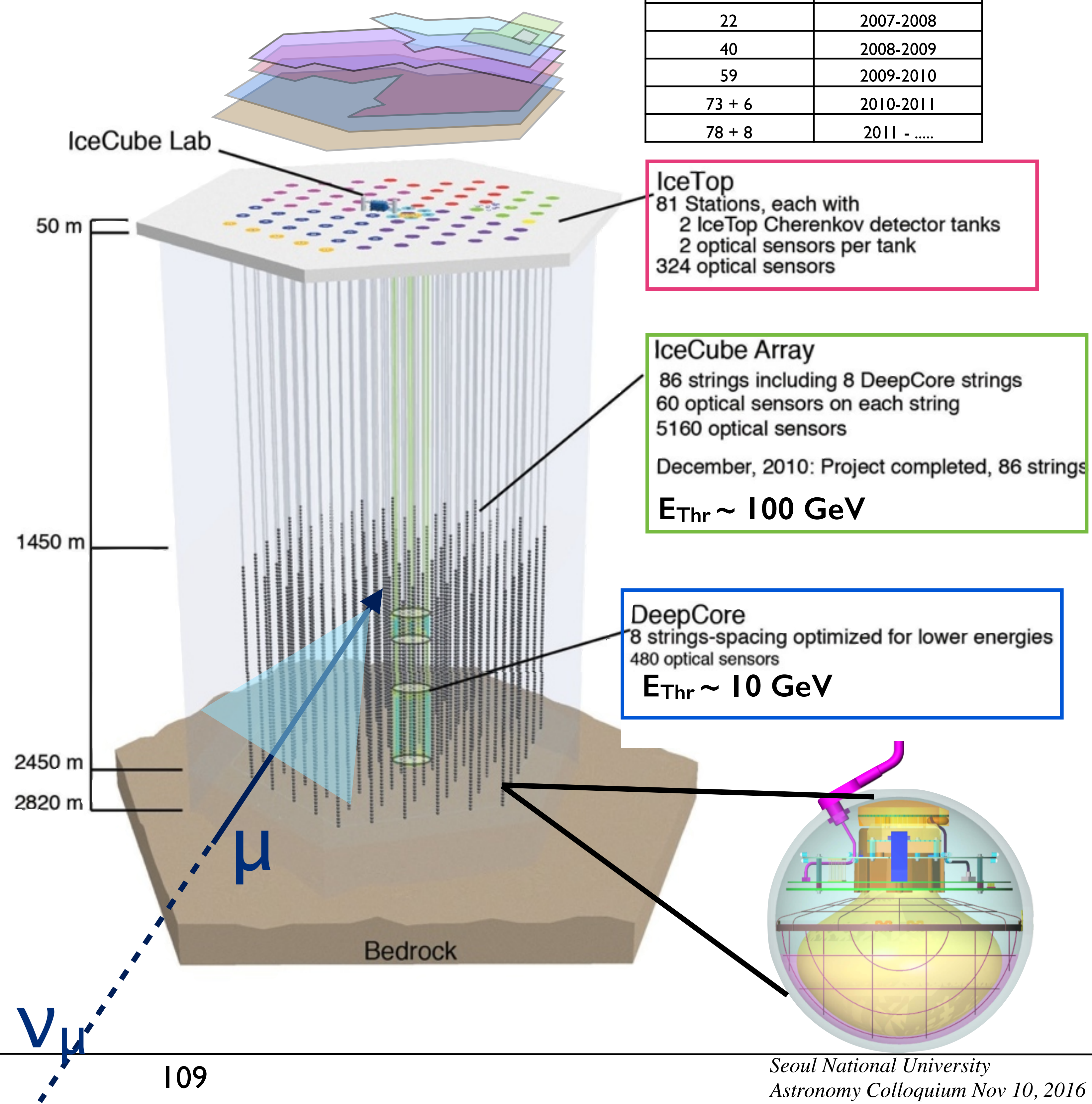

The Ice

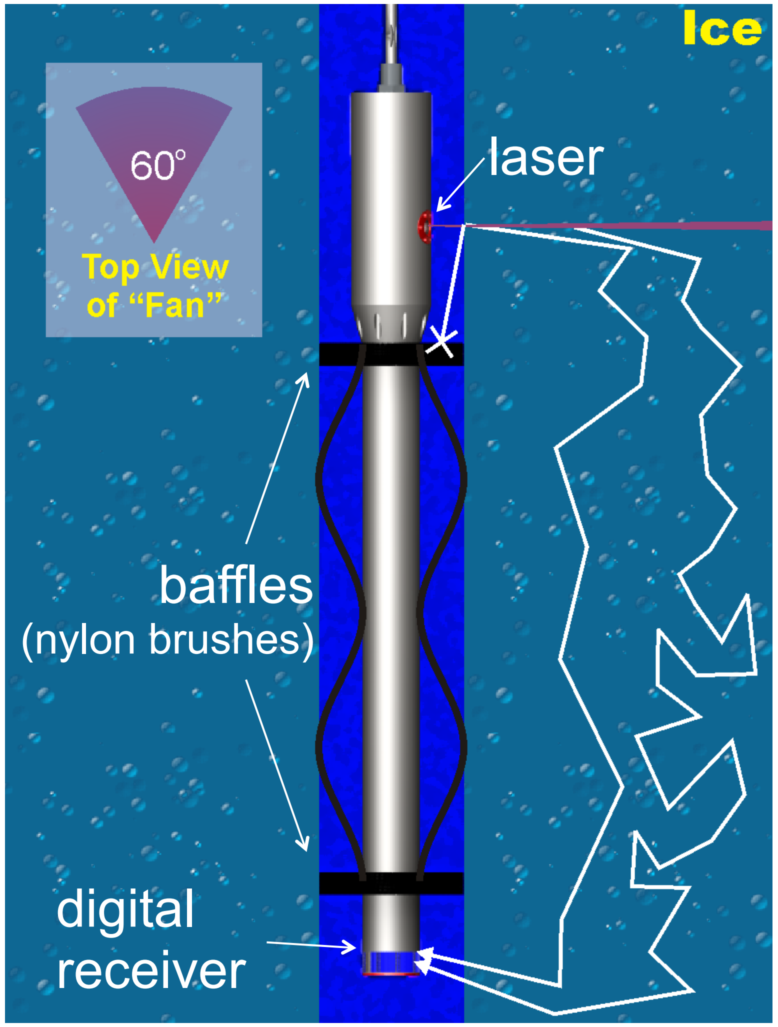

Major calibration efforts resulted in a very precise understanding of the ice surrounding the IceCube detector

- Calibration Sources:
  - 12 LED flashers on each DOM
  - In-Ice Calibration Laser
  - Cosmic Rays
  - One pair of Camera DOMs

absorption length ~ 210m
scattering length ~20-40m

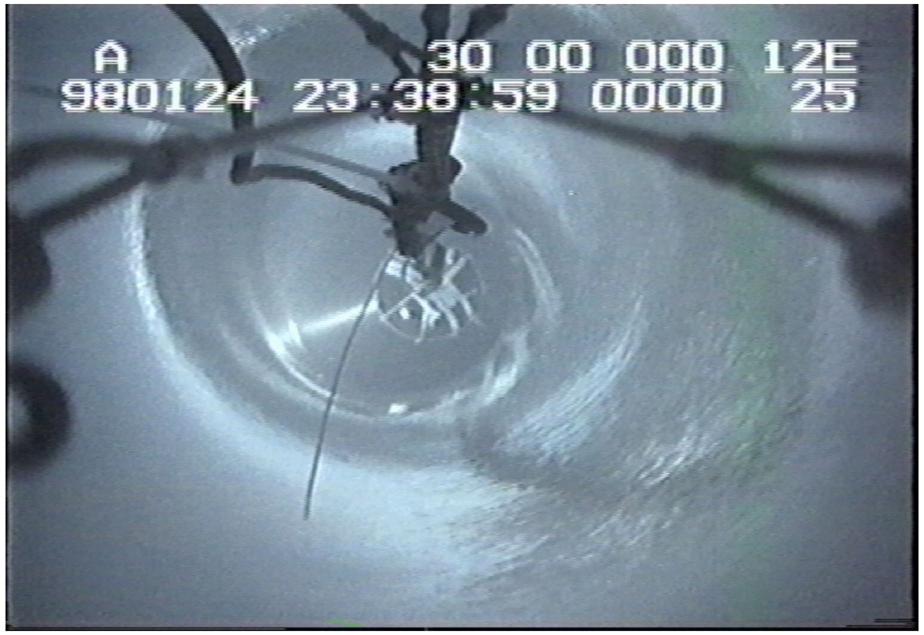

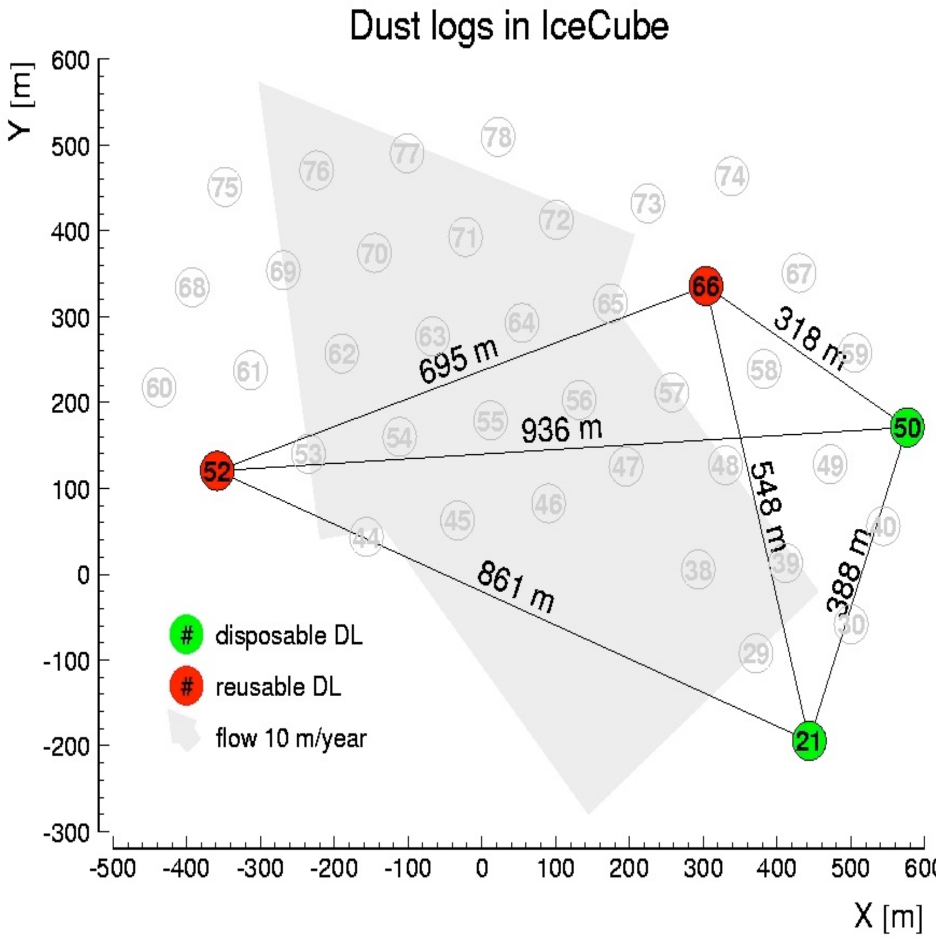

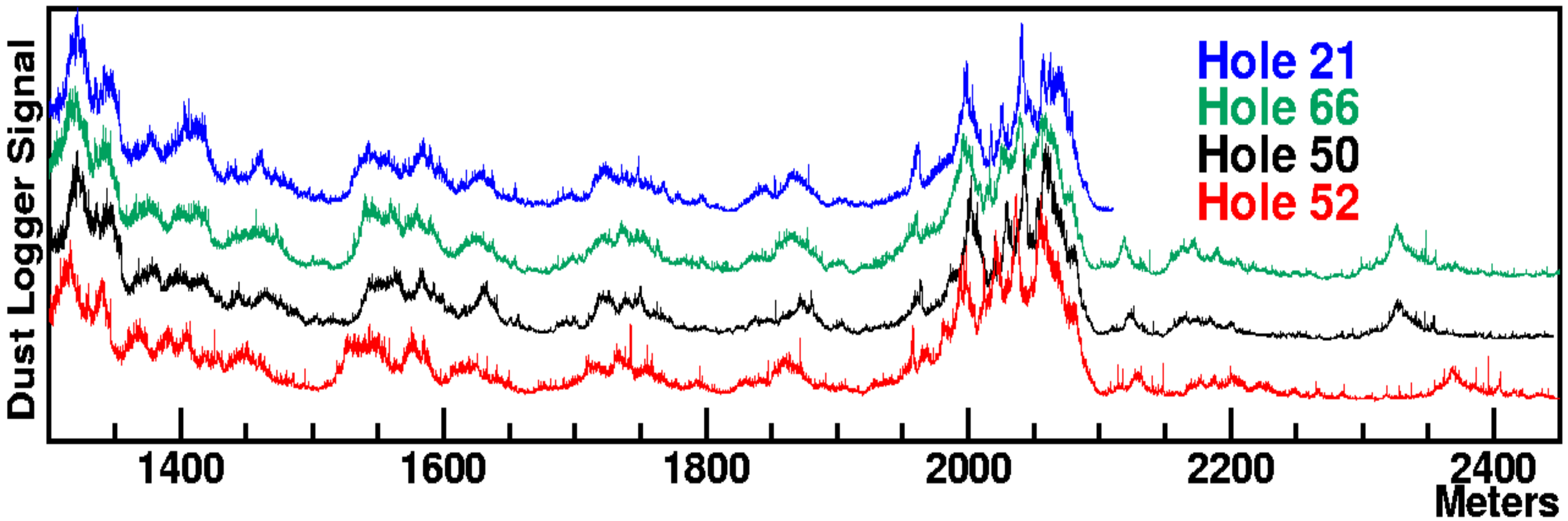

DOM @ SKKU

South Pole Summer / Winter


TEX

South Pole Summer / Winter

Signals in IceCube

$p + A \rightarrow \pi^{\pm} (K^{\pm})$ + other hadrons ... $\pi^{+} \rightarrow \mu^{+}\nu_{\mu} \rightarrow e^{+}\nu_{e}\nu_{\mu}\nu_{\mu}$

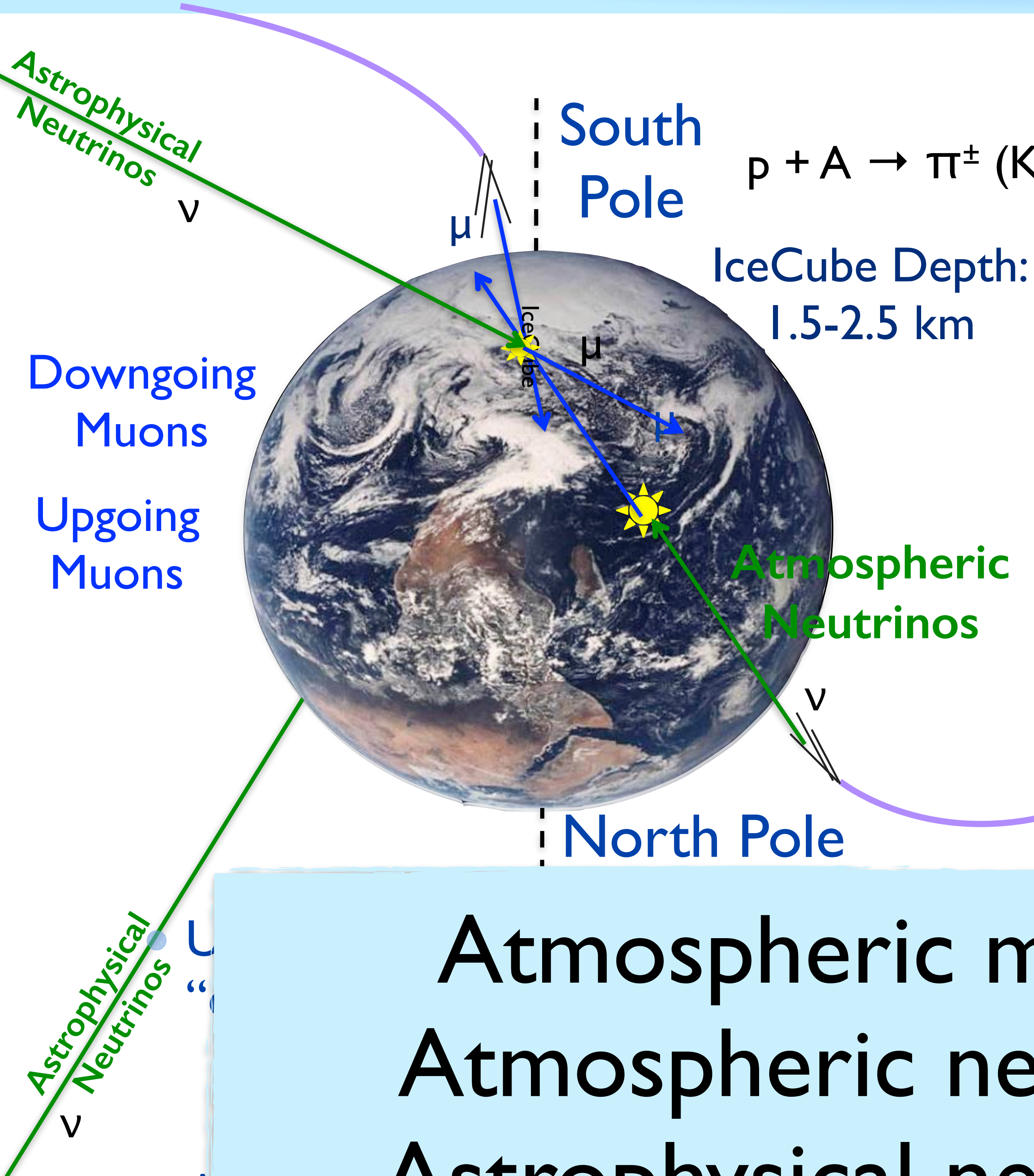

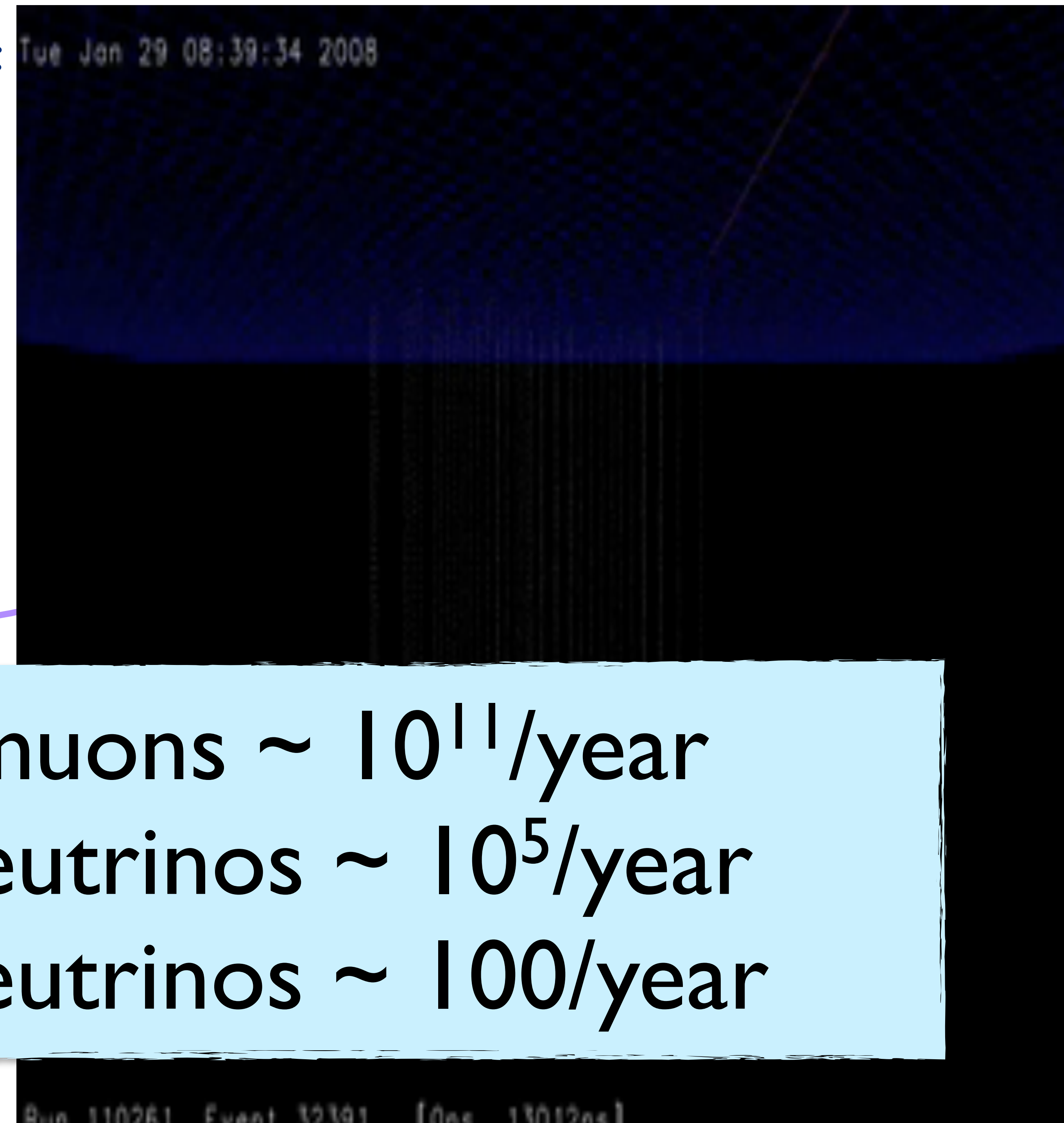

Atmospheric muons ~ 10^{11}/year
Atmospheric neutrinos ~ 10^{5}/year
Astrophysical neutrinos ~ 100/year

- U
- A ... irreducible neutrino background to extra terrestrial neutrino fluxes

Event Topologies in IceCube

Track topology

(e.g. induced by muon neutrino)

CC: ν_μ

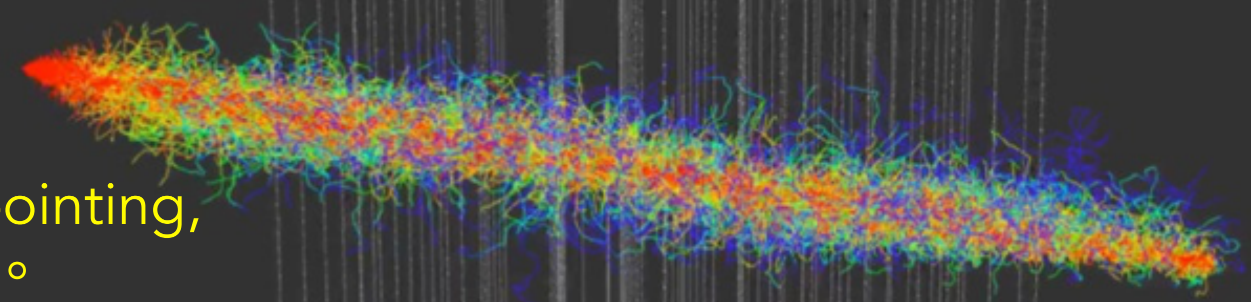

Good pointing,
0.2° - 1°

Lower bound on energy for through-going events

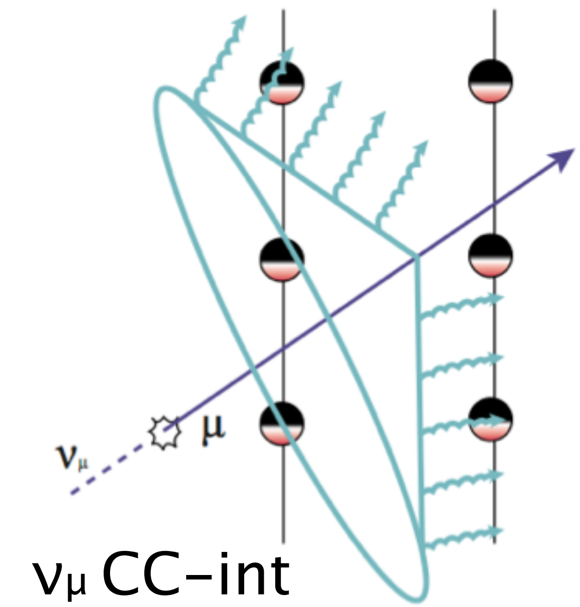

ν_μ CC–int

CC: ν_e ν_τ

NC: ν_e ν_μ ν_τ

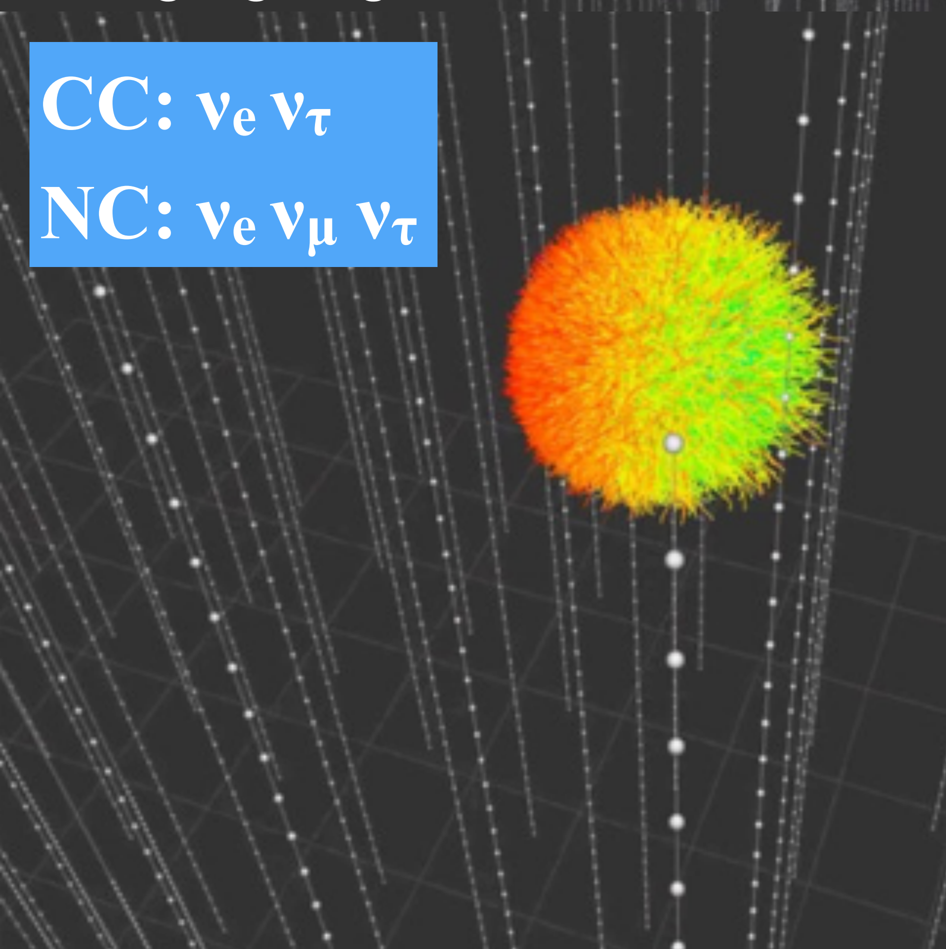

Cascade topology

(e.g. induced by electron neutrino)

Good energy resolution, 15%

Some pointing,
10° - 15°

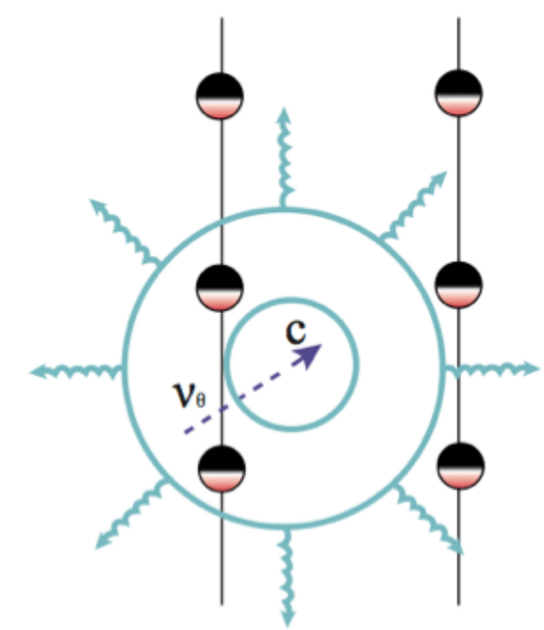

ν_e ν_τ CC–int & ν_i NC–int

IceCube Science

Cosmic Rays	Atmospheric neutrinos	Particle Physics	Astronomy	Applied science	Cosmology

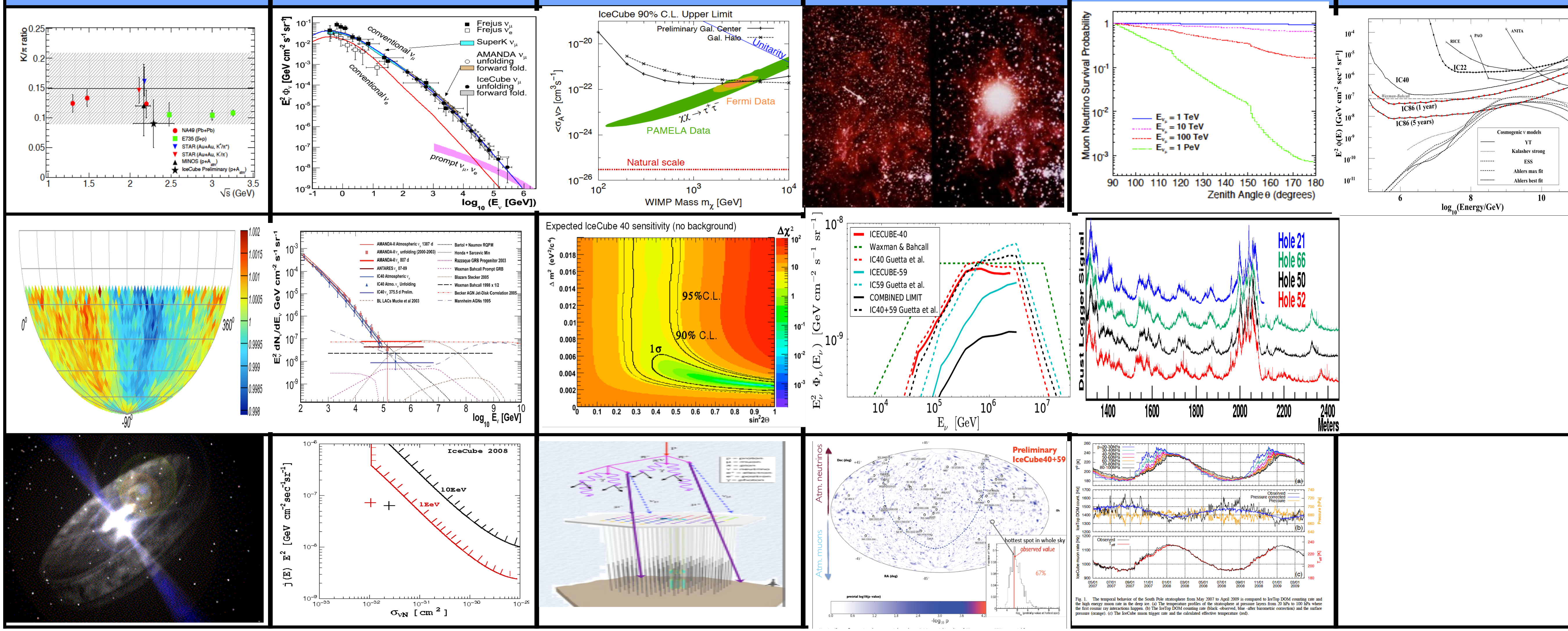

Very diverse science program, with neutrinos from 10GeV to EeV, and MeV burst neutrinos

Dark Matter Self-annihilations

$\langle \sigma_A v \rangle$

Dark Matter in the Milky Way

Dark Matter Annihilation

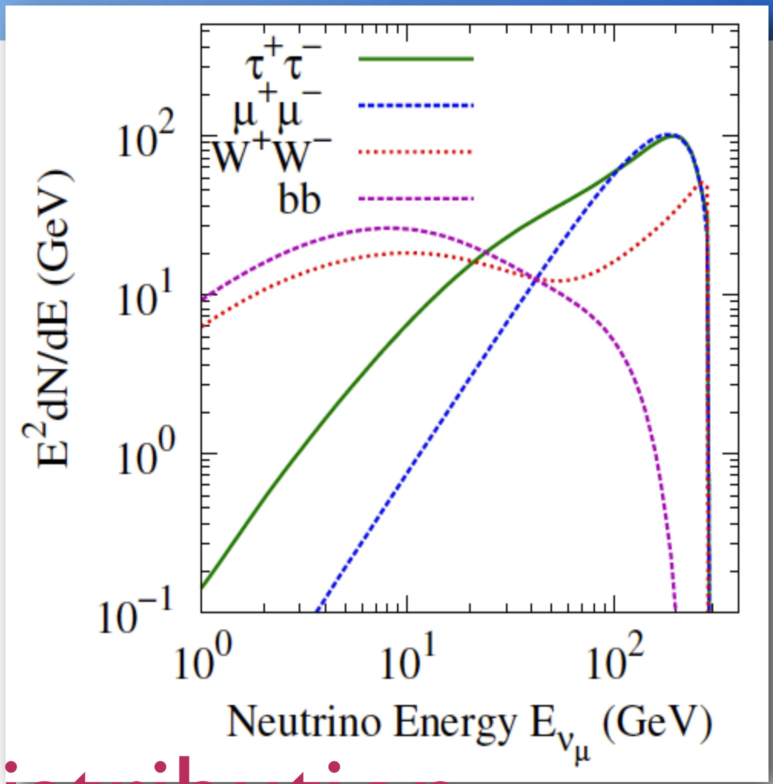

Measure Flux

$$\frac{d\Phi}{dE}(E,\phi,\theta) = \frac{1}{4\pi}\frac{\langle\sigma_A v\rangle}{2m_\chi^2}\Sigma_f \frac{dN}{dE}B_f$$

Particle Physics

x

Dark Matter Distribution

line of sight (los) integral

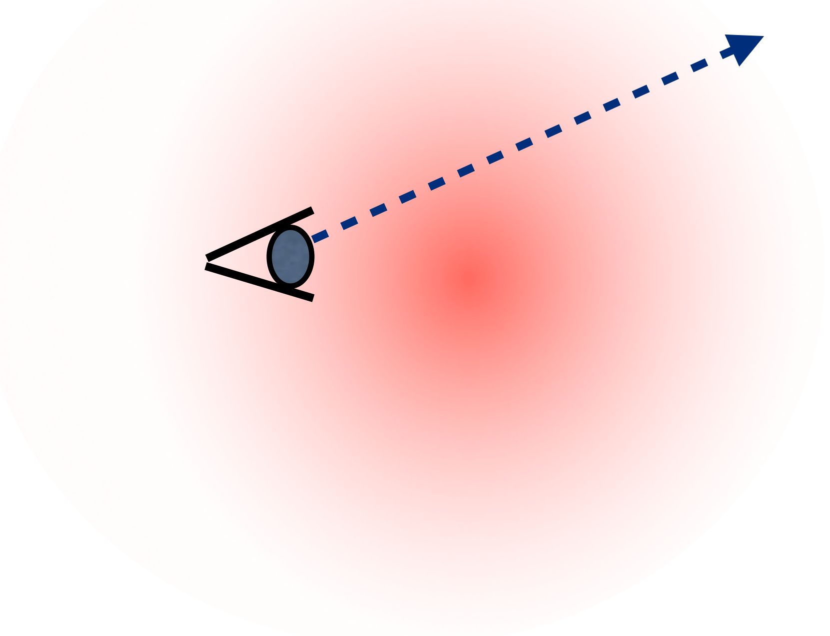

$$\int_{\Delta\Omega(\phi,\theta)} d\Omega' \int_{\text{los}} \rho^2(r(l,\phi'))dl(r,\phi')$$

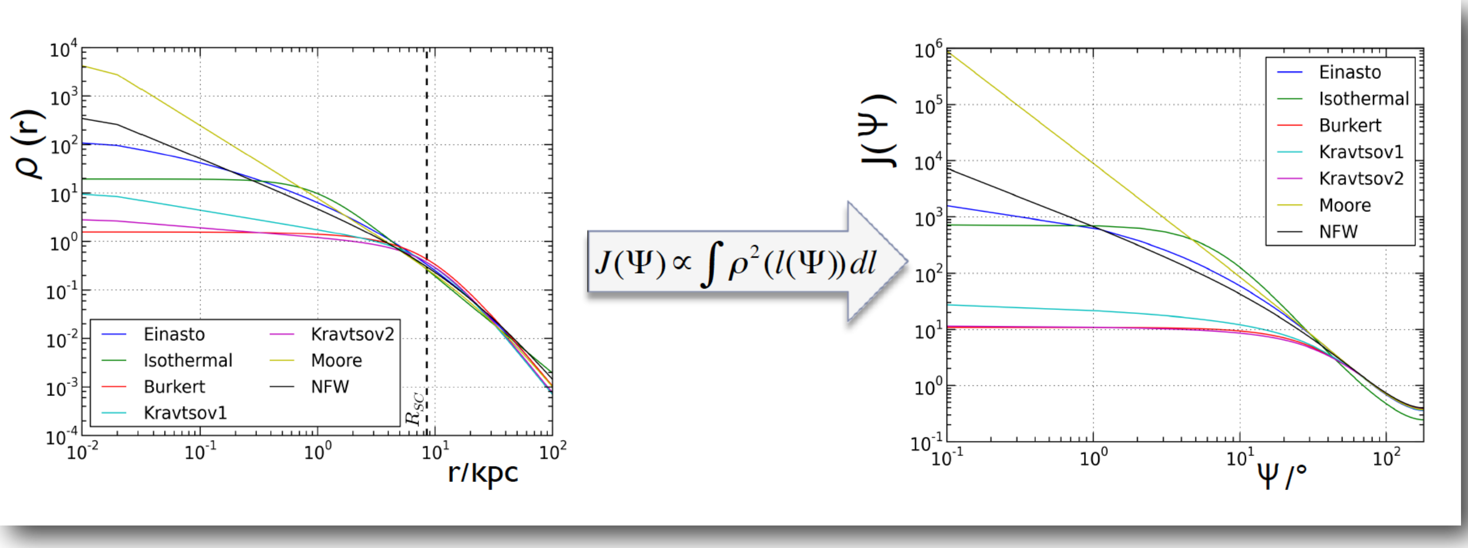

IceCube Collaboration
arXiv1505.07259
Eur.Phys.J. C75 (2015) 10, 492

Galactic Center

Use IceCube external strings as a veto:
- 3 complete layers around DeepCore (~ 375m)
- Full sky sensitivity: access to southern hemisphere

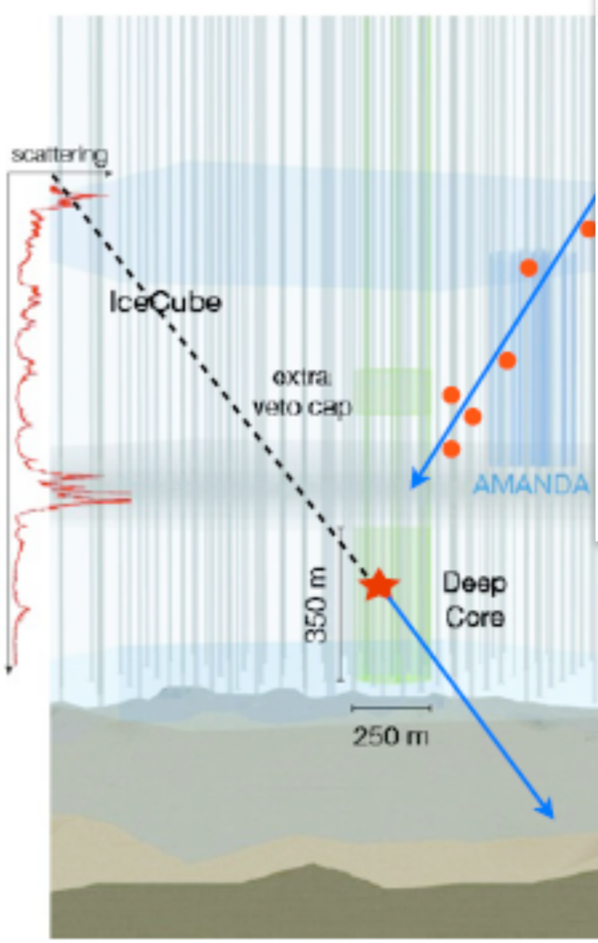

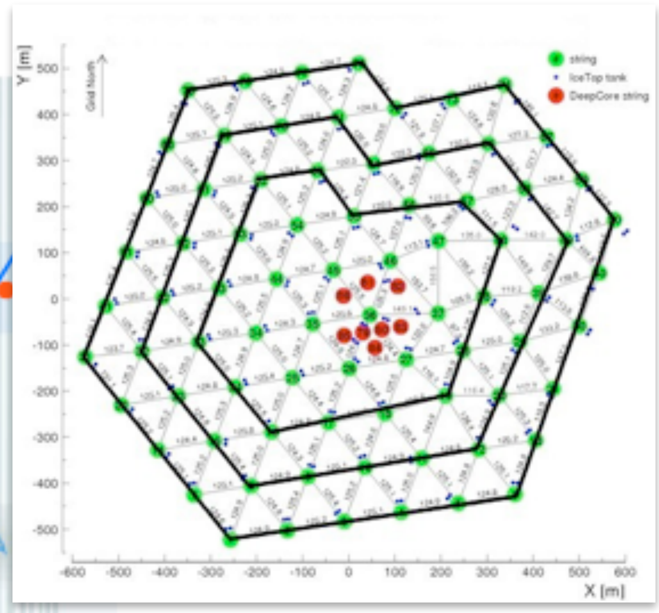

Two analyses, combined based on best sensitivity (dotted).

Both analyses observed underfluctuations

"High energy" analysis: 0.5 σ

"Low energy" analysis: 2σ

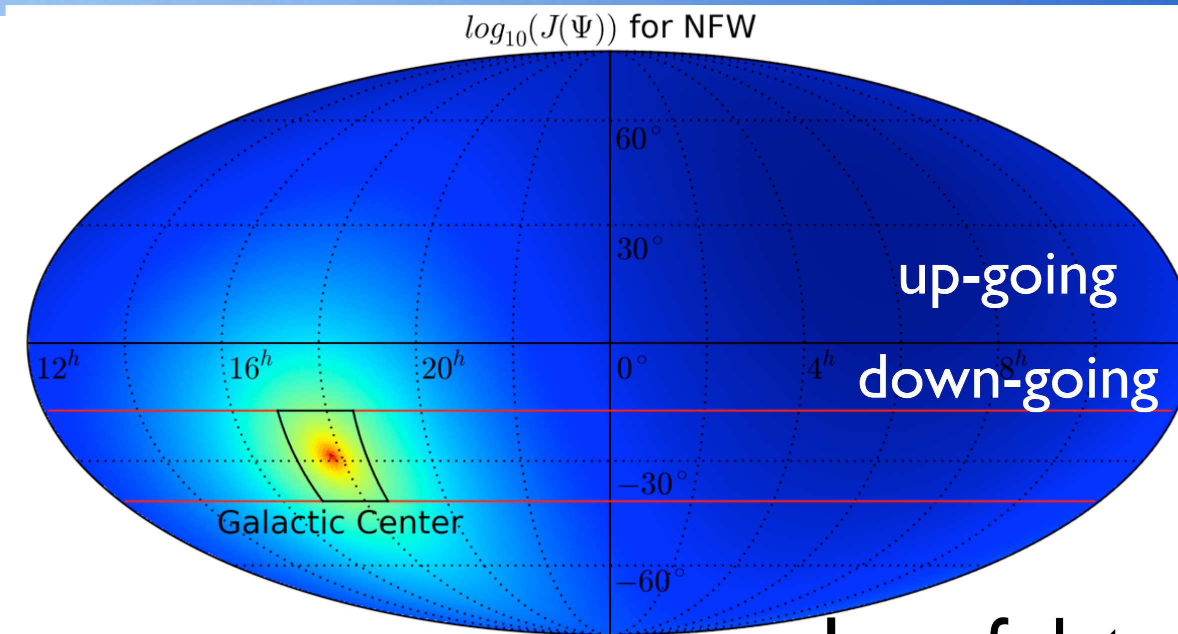

1yr of data

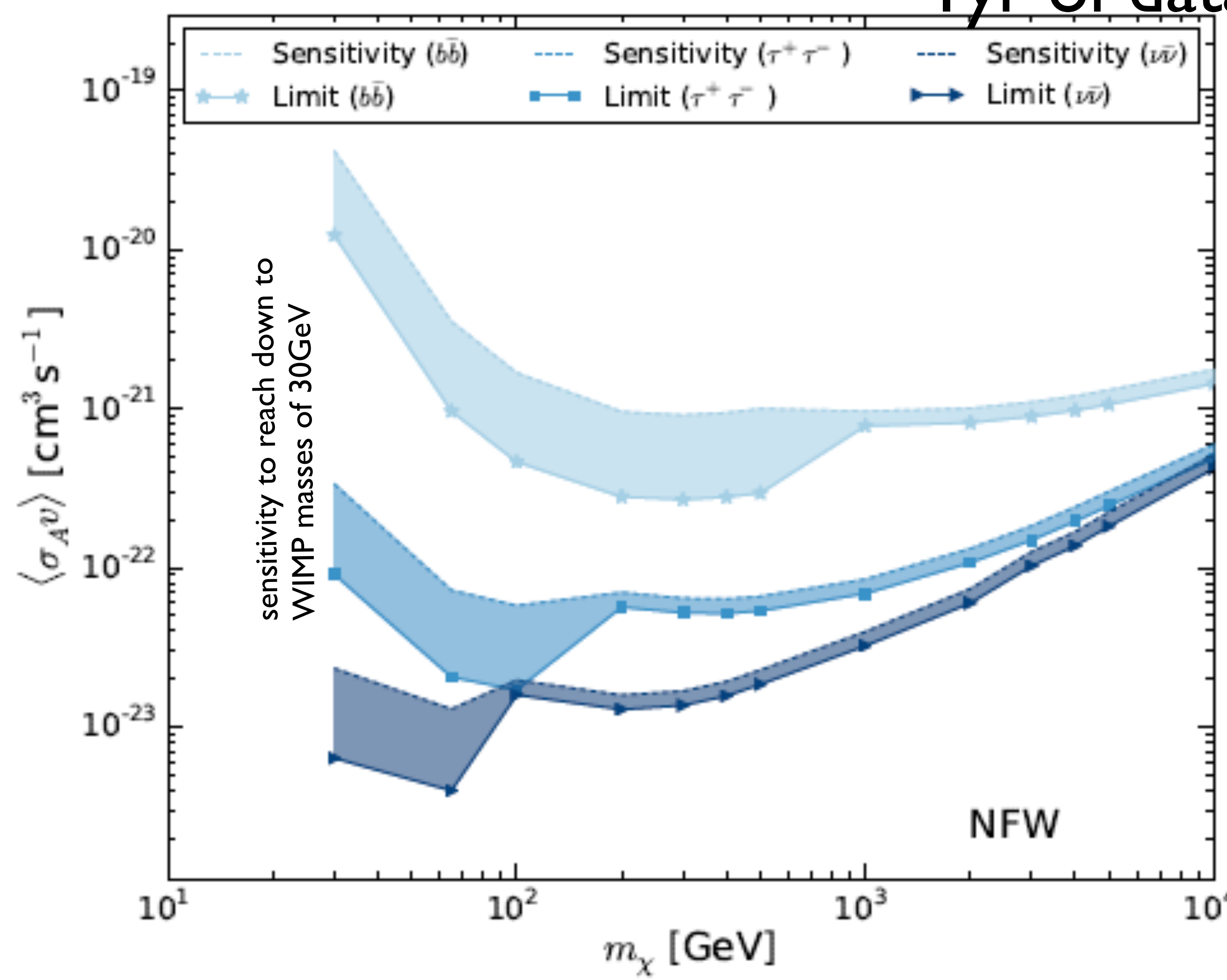

Separate Low energy and High energy optimizations:
GC is above the horizon
→ Fiducial volume in central strings
→ refined muon veto from surrounding layers
Use scrambled data for background estimation

Neutrinos test lepton anomalies

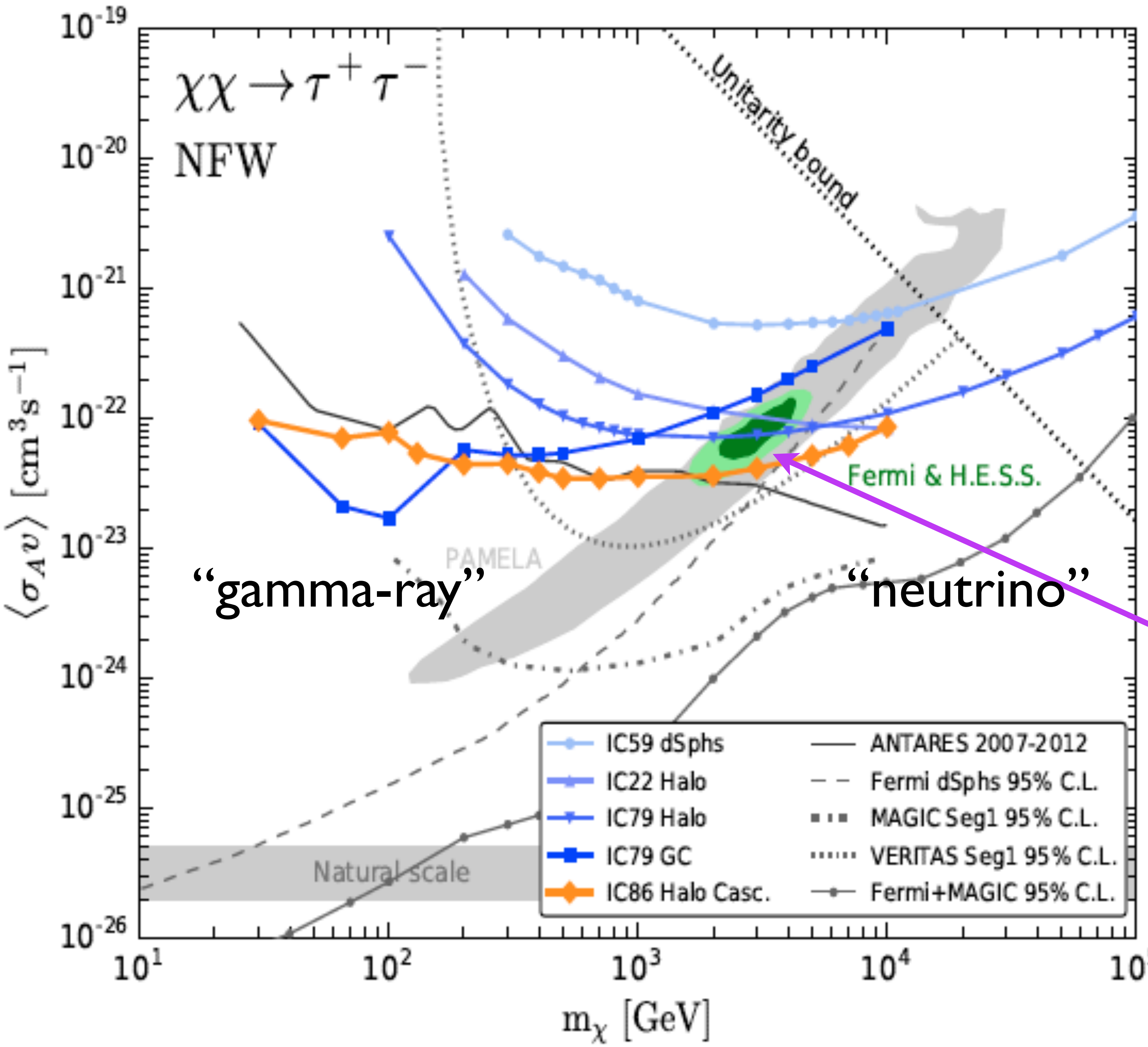

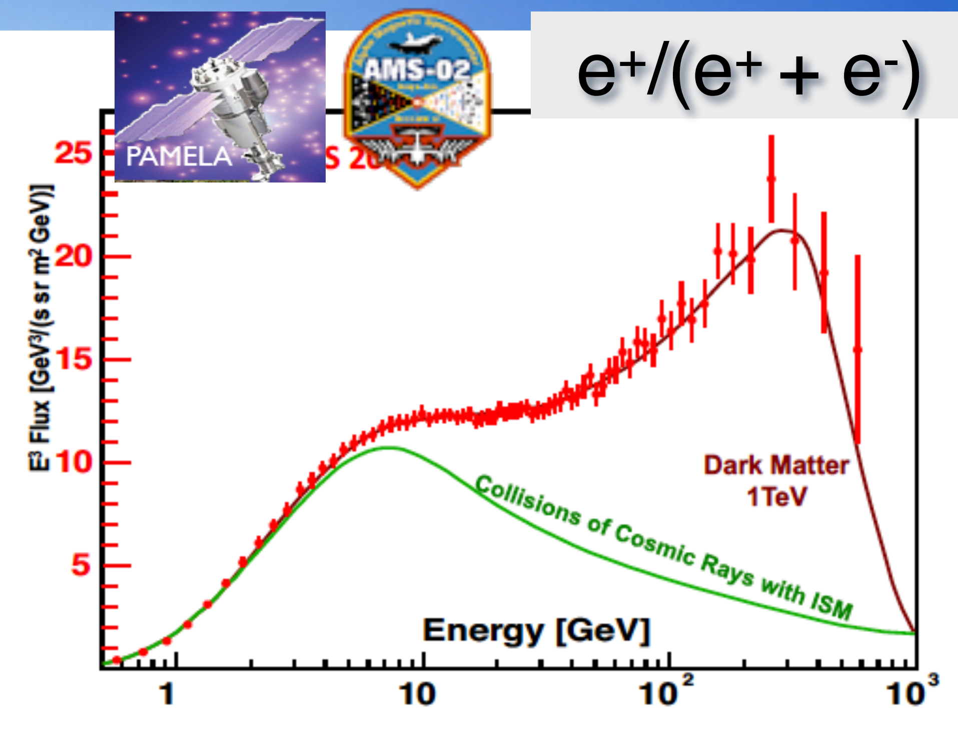

Figure 4. The current AMS positron flux measurement compared with theoretical models.

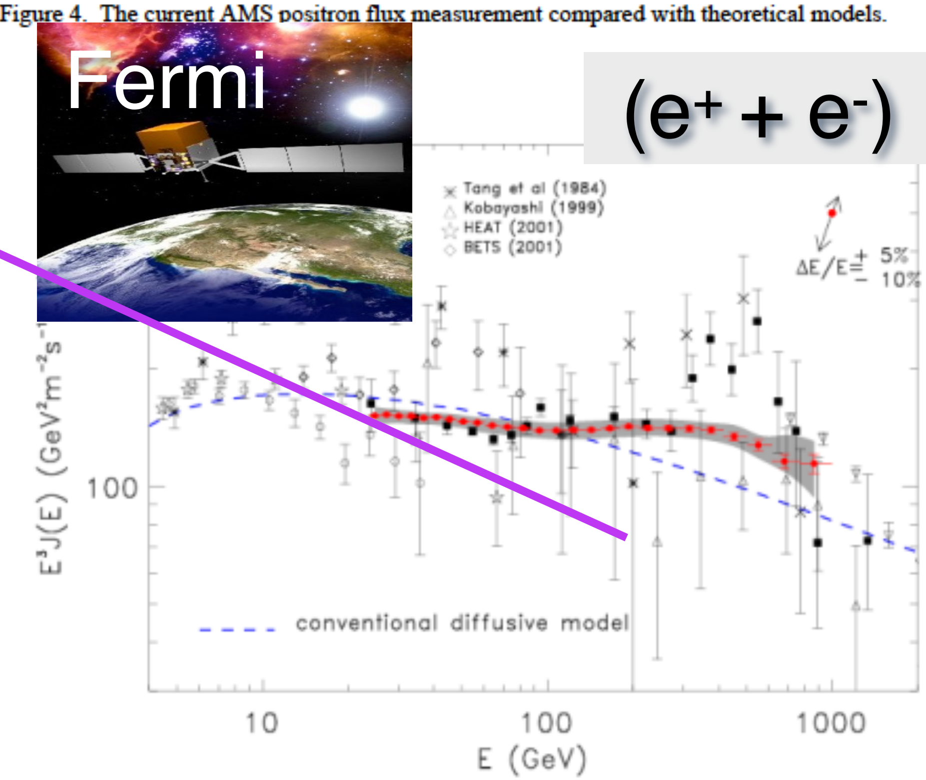

Neutrino Telescopes can probe models motivated by the observed lepton anomalies arXiv:1612.04595

ANTARES 9yrs GC analysis

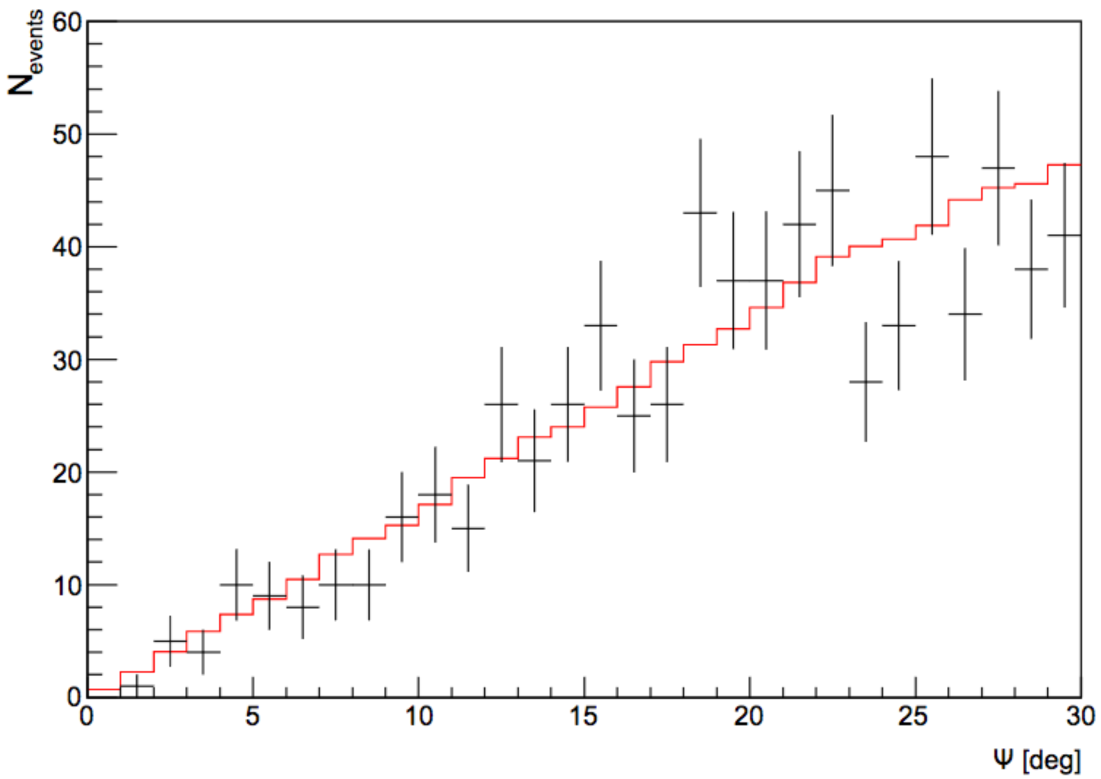

Combining 9yrs of ANTARES Data

$$\mathcal{A}^j(M_{\mathrm{WIMP}}) = \int A^j_{\mathrm{eff}}(E_{\nu_\mu}) \left.\frac{d\Phi_{\nu_\mu}}{dE_{\nu_\mu}}\right|_{ch,M_{\mathrm{WIMP}}} dE_{\nu_\mu} \cdot T^j_{\mathrm{eff}} + \int A^j_{\mathrm{eff}}(E_{\bar{\nu}_\mu}) \left.\frac{d\Phi_{\bar{\nu}_\mu}}{dE_{\bar{\nu}_\mu}}\right|_{ch,M_{\mathrm{WIMP}}} dE_{\bar{\nu}_\mu} \cdot T^j_{\mathrm{eff}},$$

Galactic Center observable in up-going muon neutrino sample for ANTARES

Impressive new limits

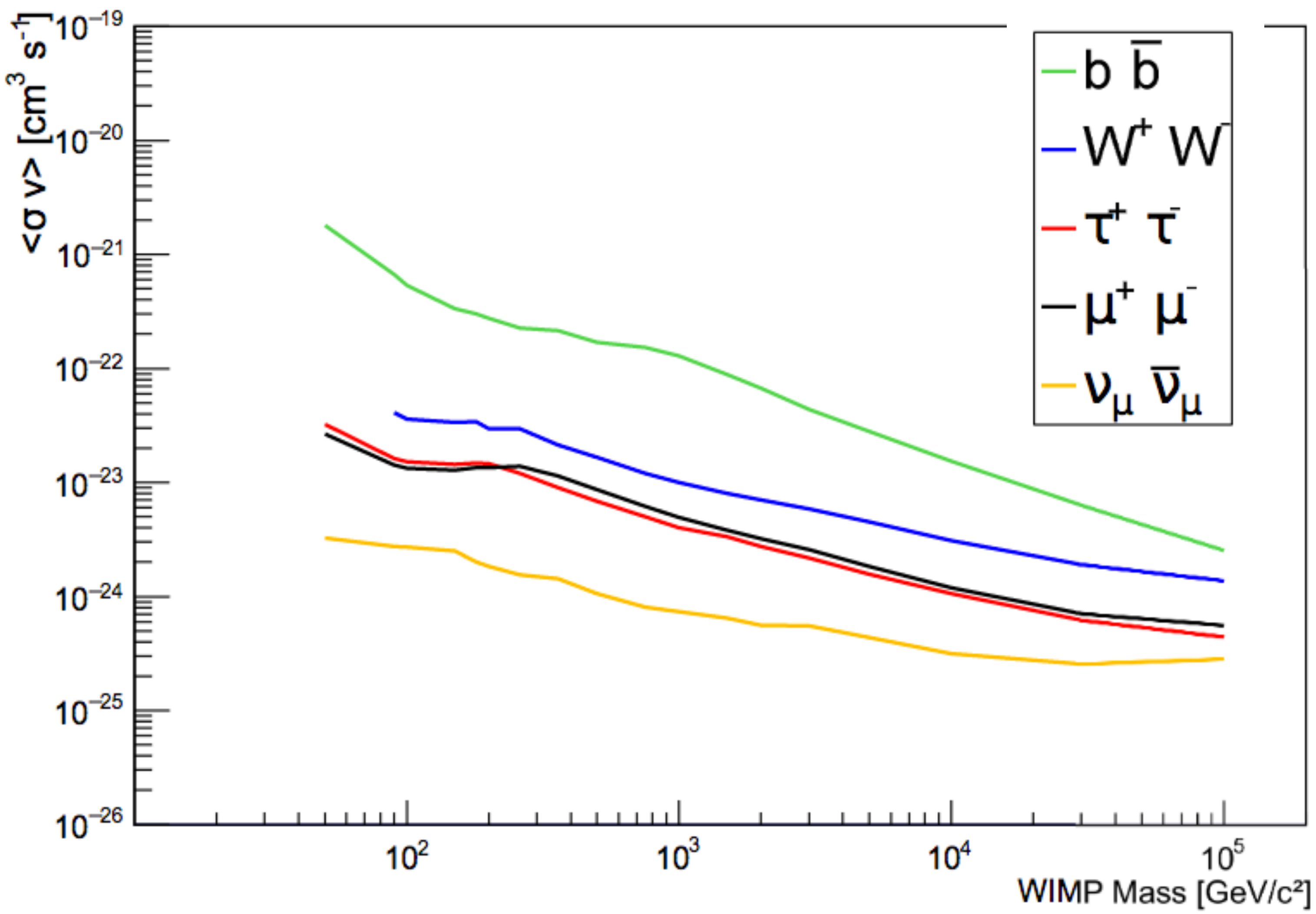

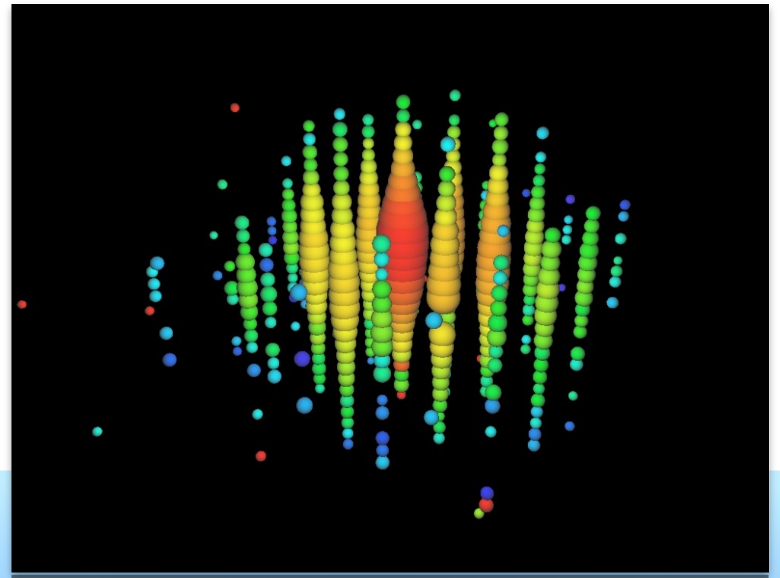

Dark Matter Decay / Astro-physical Neutrinos

Search for highest energy neutrinos

IceCube Coll. Phys.Rev.Lett. 111 (2013) 021103 / arXiv 1304.5356

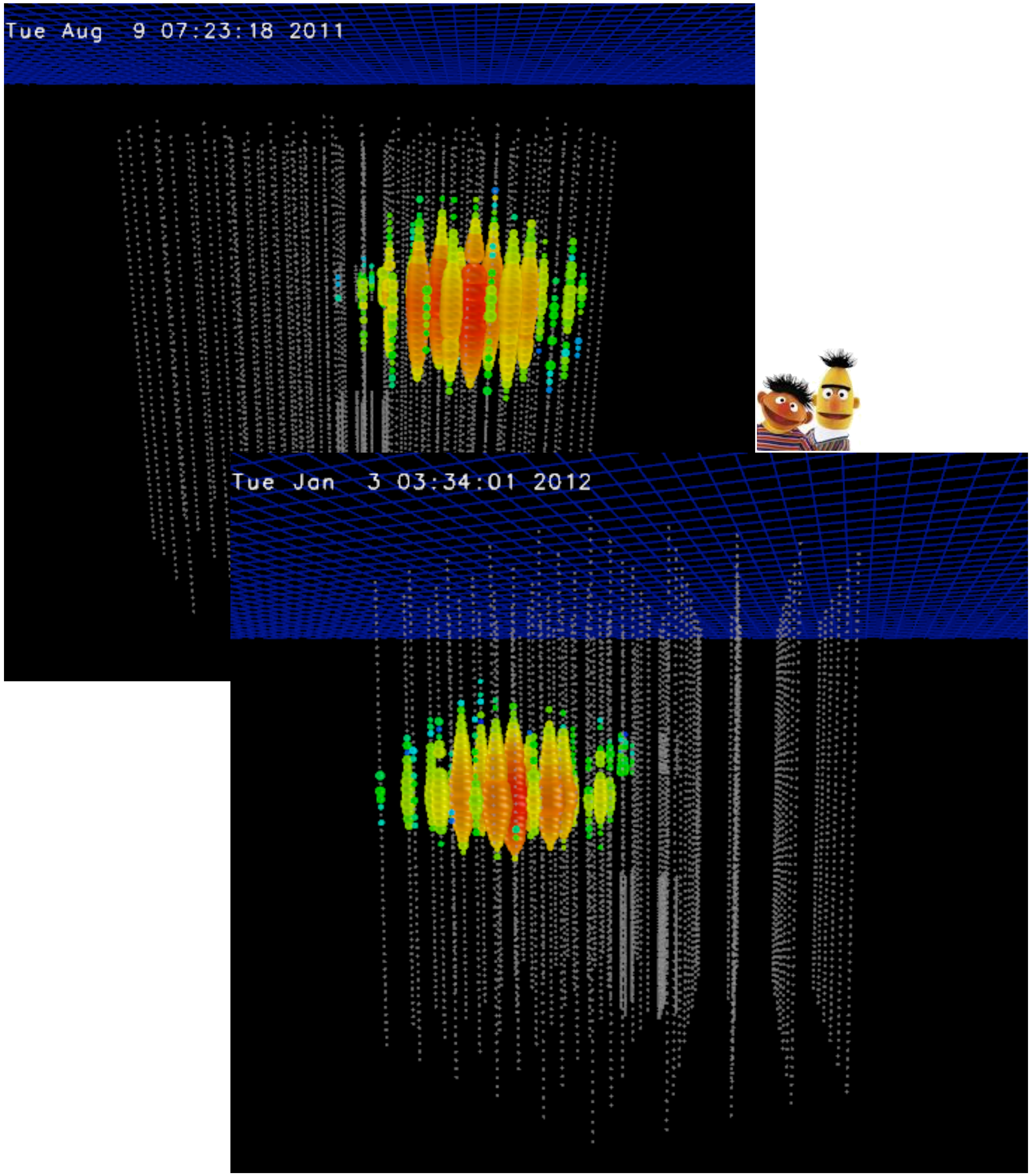

Dataset / Results
(670days of IC79/IC86 data)
expected 0.08 events
observed 2 events ($\rightarrow$ 2.7σ)

- Ernie ~1.15 PeV (~$1.9 \cdot 10^{-4}$ J)
- Bert ~ 1.05 PeV (~$1.7 \cdot 10^{-4}$ J)
- Energy is the visible energy of the cascade, could originate from NC event, ν_τ CC, or ν_e CC
- Angular resolution on cascade events at this energy ~10
- Energy resolution is about 15% on the deposited energy

Ernie & Bert are not GZK, but ...

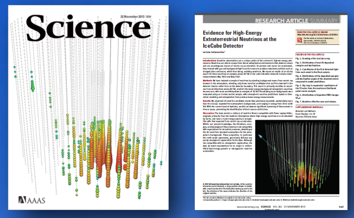

High-energy neutrino search 4yrs

54 events (15 track-like, 39 showers) observed

Expectation from conventional atm. muons and neutrinos ~21.6

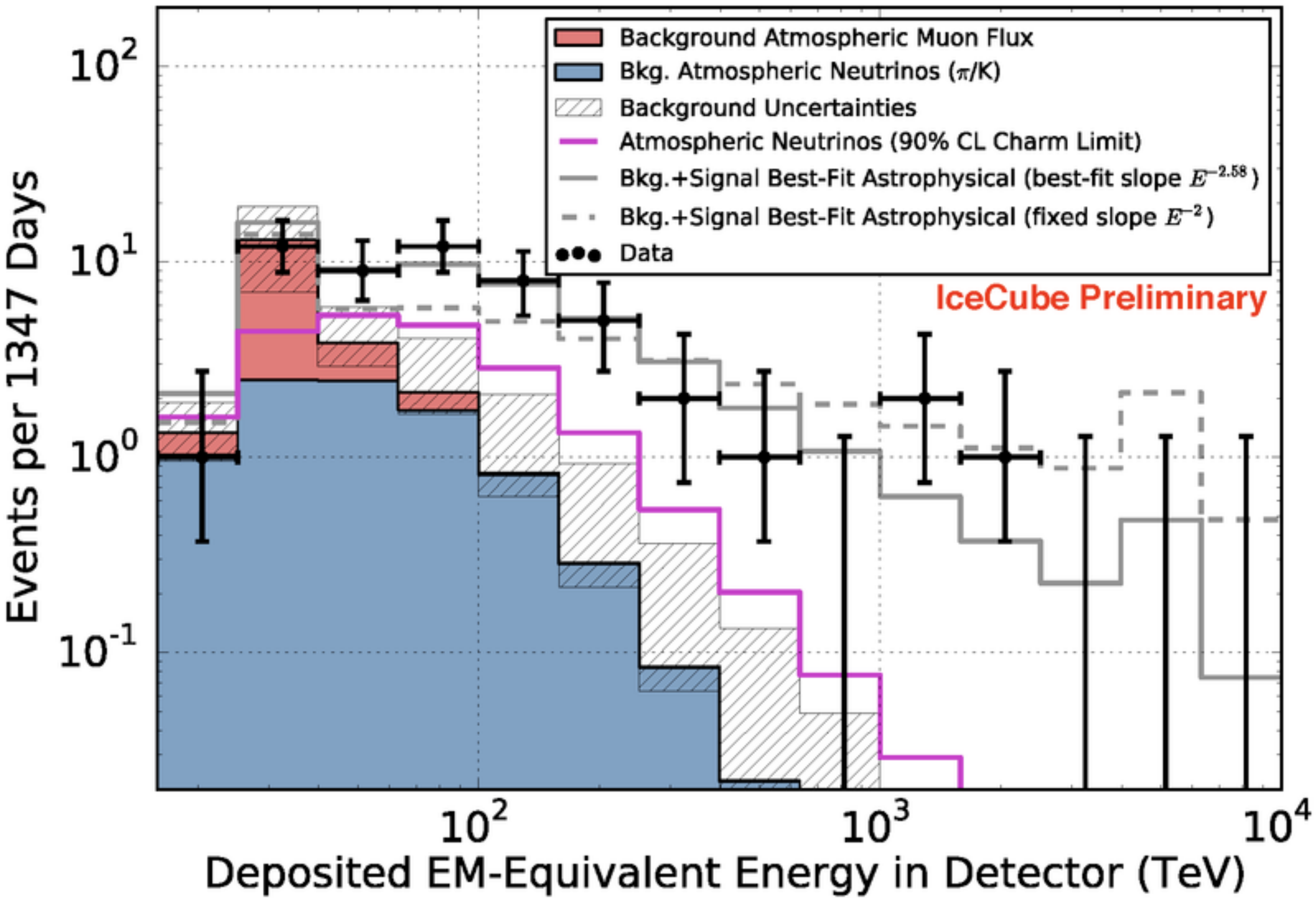

ICRC 2015 proceedings
IceCube Collaboration, *Science 342, 1242856 (2013)*,
IceCube Collaboration, *Phys. Rev. Lett 113, 101101 (2014)*

- Mesons including charm quarks in the atmosphere decay immediately to produce neutrinos, known as prompt neutrinos which are not observed yet.
- ERS, or Enberg et al. Phys. Rev. D 78, 043005 (2008) is used as a baseline prompt model
- Significance are based on the exact neutrino flux model, not including the uncertainty of the model.
- Atmospheric Bkg : CR Muon (12.6±5.1), Conv. Neutrino ($9.0^{+8.0}_{-2.2}$),
- Over 60 TeV < E < 2000 TeV, the spectrum best fit with $E^{-2.58}$
- E^{-2} spectrum predicts too may neutrinos above ~2 PeV. So, a cutoff or steeper spectrum needed.

~7 sigma rejection of atmospheric-only hypothesis

Skymap HESE-4yrs

IceCube Collaboration, *Science* 342, 1242856 (2013)

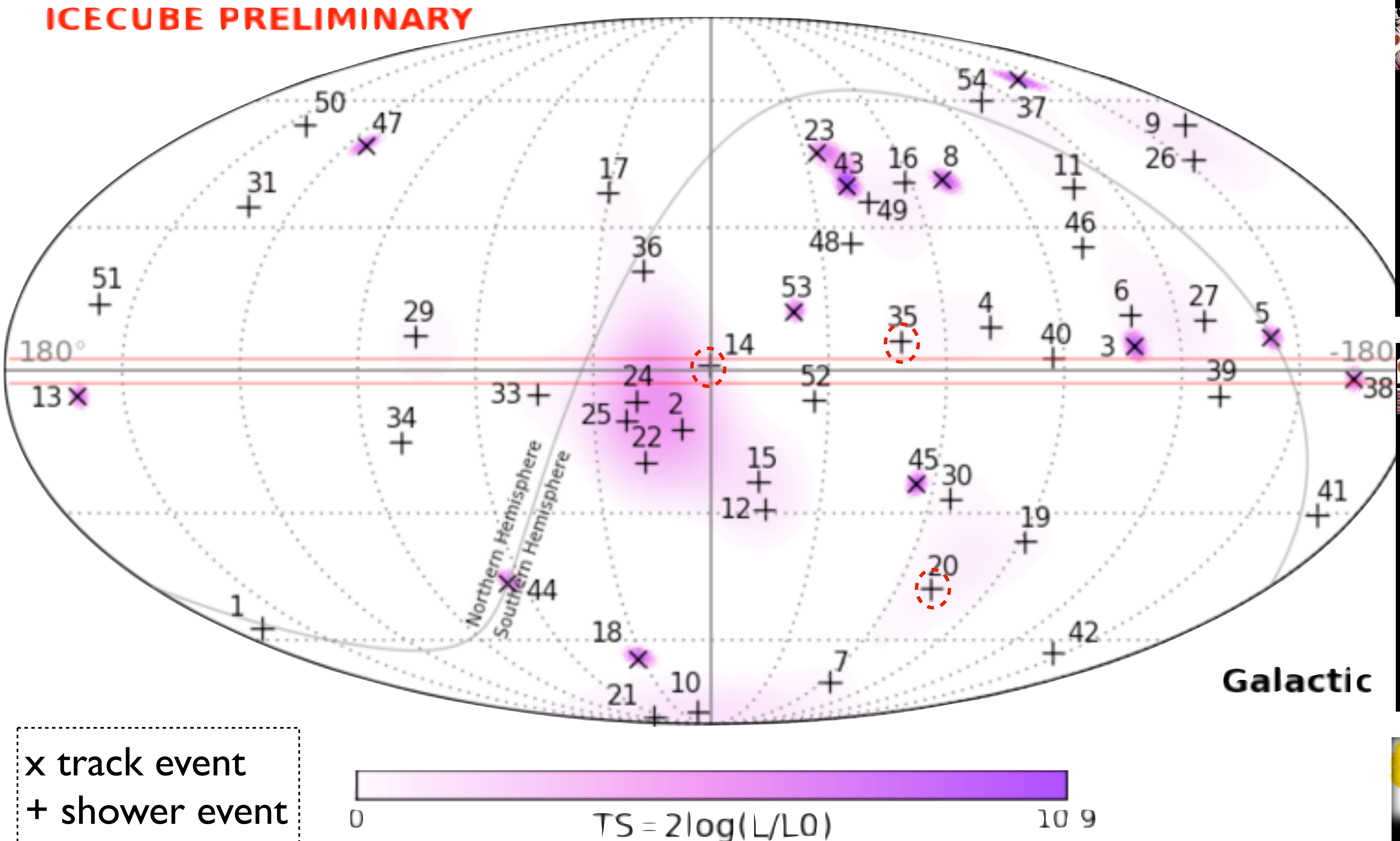

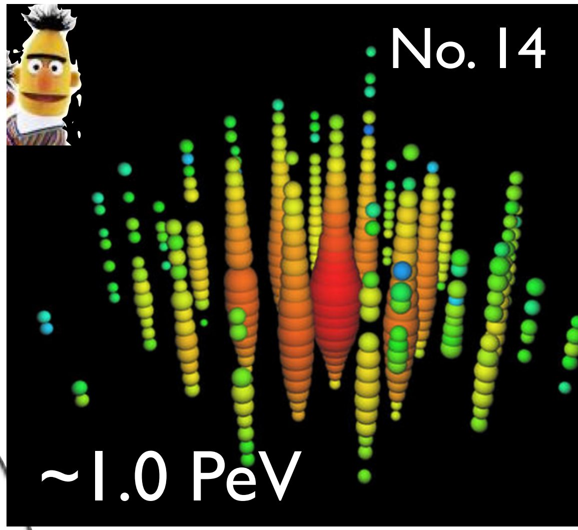

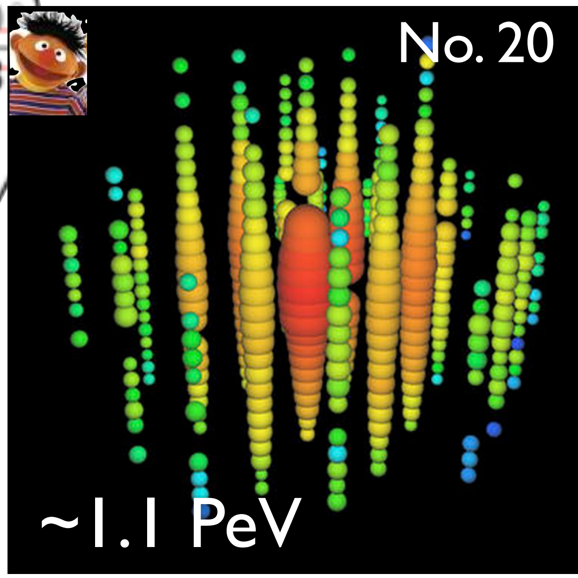

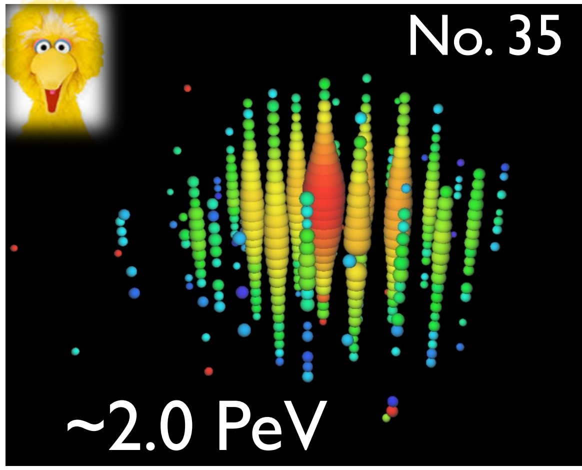

no significant correlations -- spacial or temporal

p-value for cascade events "clustering" 44%

Origin of the high-energy neutrinos ?

Extra Galactic

Gamma Ray Burst

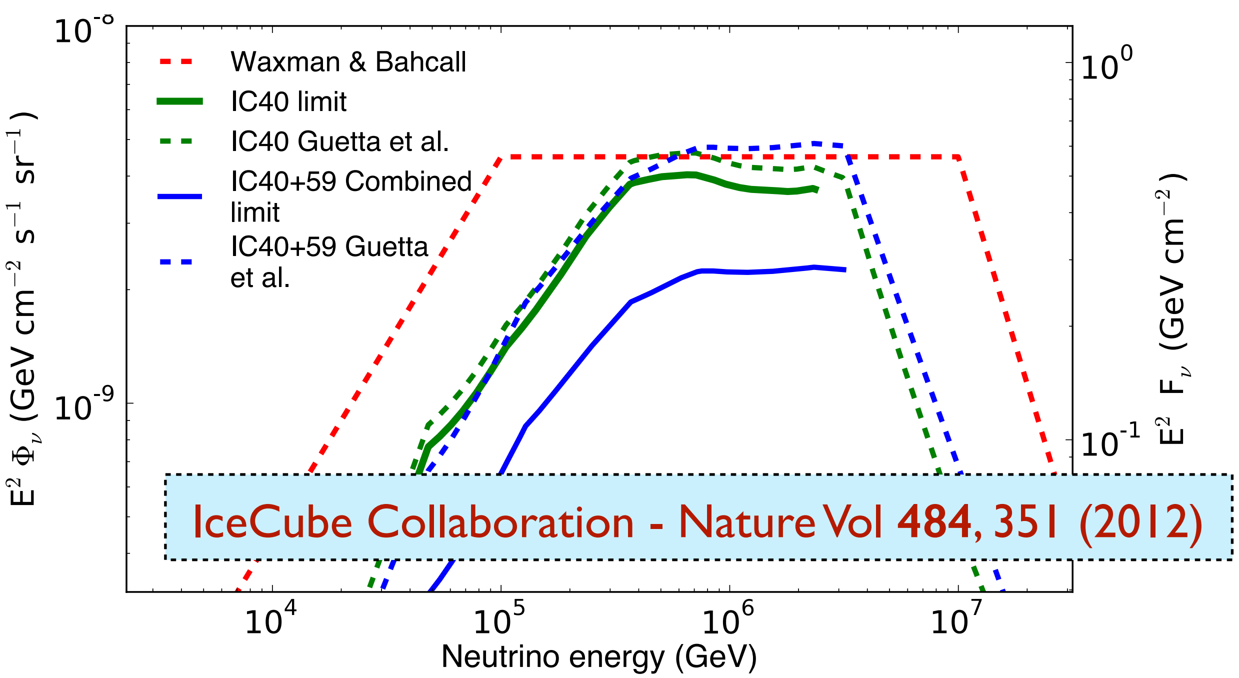

IceCube Collaboration - Nature Vol **484**, 351 (2012)

Active Galactic Nuclei / Starburst Galaxies

Starburst	M82	148.97	69.68	0.07	0.15
Radio	NGC 1275	49.95	41.51	0.0	–
Galaxies	Cyg A	299.87	40.73	0.9	0.03
	3C 123.0	69.27	29.67	0.0	–
	M87	187.71	12.39	0.0	–
	Cen A	201.37	-43.02	0.03	0.49

Galactic

Galactic Center

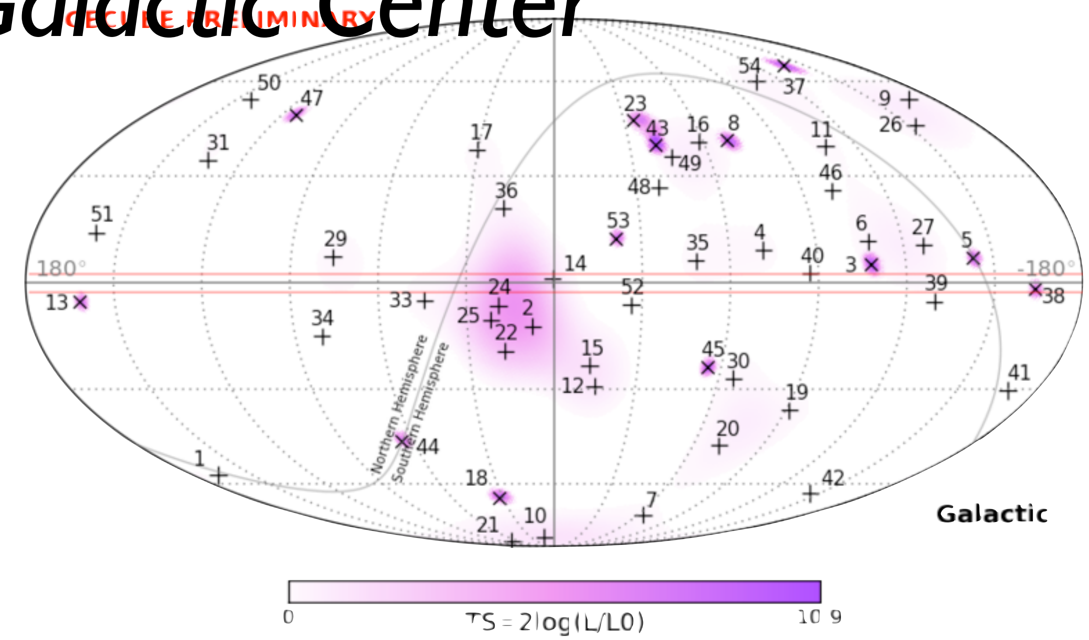

Galactic Plane

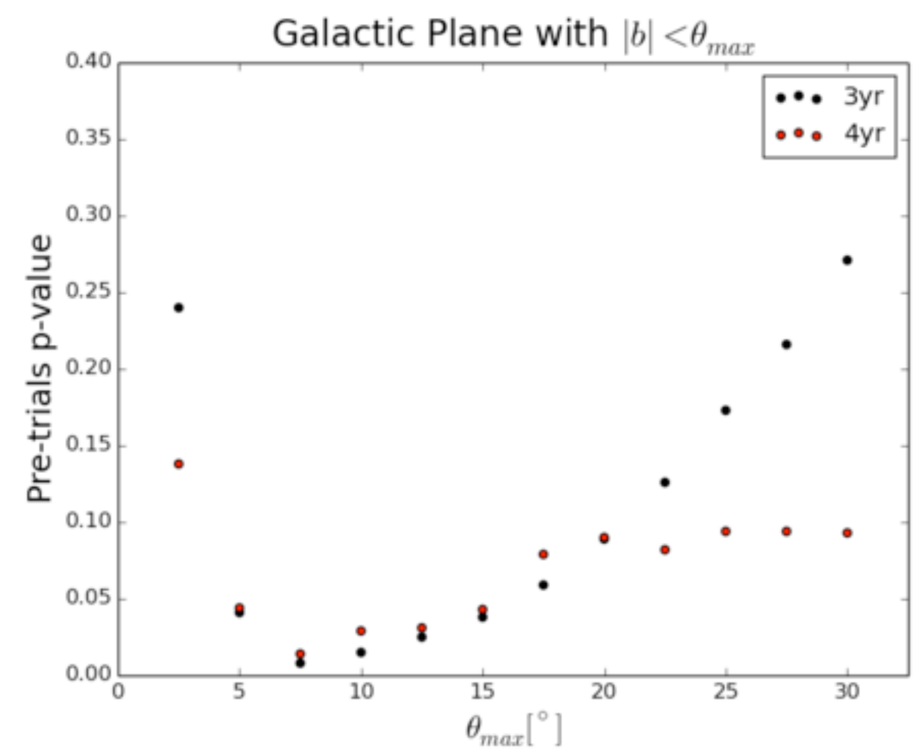

Heavy Dark Matter

- Intriguing overlap in energy of the two 1 PeV cascade events of IceCube high energy event sample

Could this be dark matter ?

example: B. Feldstein, A. Kusenko, S. Matsumoto, and T. Yanagida arXiv:1303.7320v1 / Phys.Rev. D88 (2013) 1, 015004

Evidence:
- 2.4PeV Dark Matter Particle mass
- Flux can be related to the lifetime τ_{DM}

$$\tau_{DM} \simeq 1.9 N_\nu \times 10^{28} \text{ s}$$

- Models
  - Singlet fermion in an extra dimension
  - Hidden Sector Gauge Boson
  - Gravitino Dark Matter with R-Parity Violation

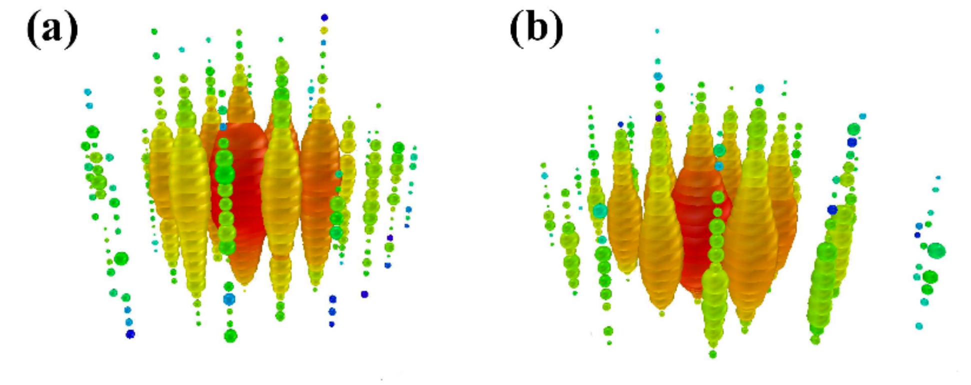

FIG. 4. The two observed events from (a) August 2011 and (b) January 2012. Each sphere represents a DOM. Colors represent the arrival times of the photons where red indicates early and blue late times. The size of the spheres is a measure for the recorded number of photo-electrons.

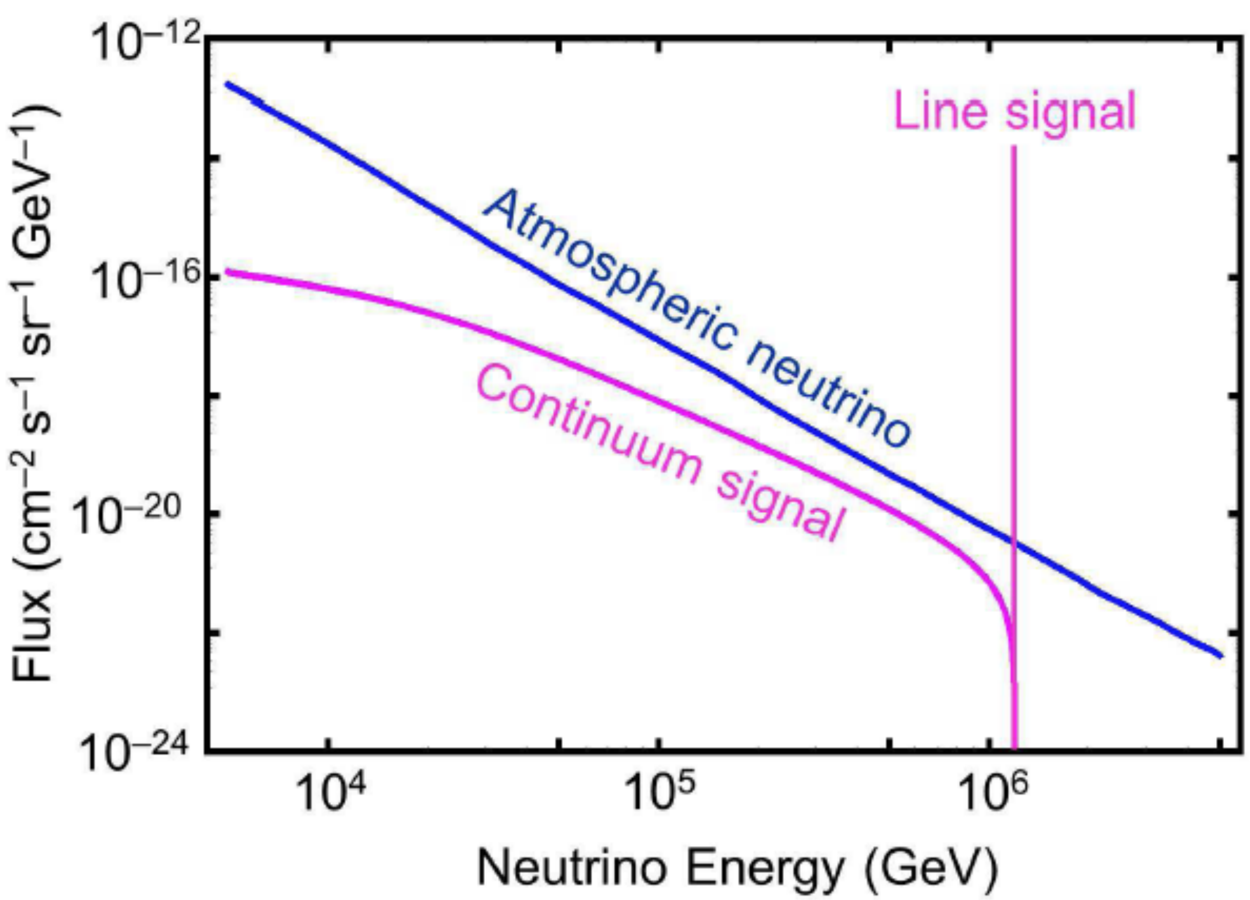

Heavy Dark Matter Decay

- Heavy Decaying Dark Matter (example $\chi\rightarrow\nu h$)
- Focus on most detectable feature (neutrino line)
- Backgrounds steeply falling with energy, highest energy events provide best sensitivity
- Continuum and spacial distribution could help identify a signal
- Bounds from Fermi-LAT and PAMELA derived from search for bb annihilation channel (dominant decay channel of Higgs).

Dedicated IceCube analysis should improve on these bounds
Analyses on-going

Bound on lifetime ~10^{28}s derived with IceCube data

PRD 92, 123515 (2015)

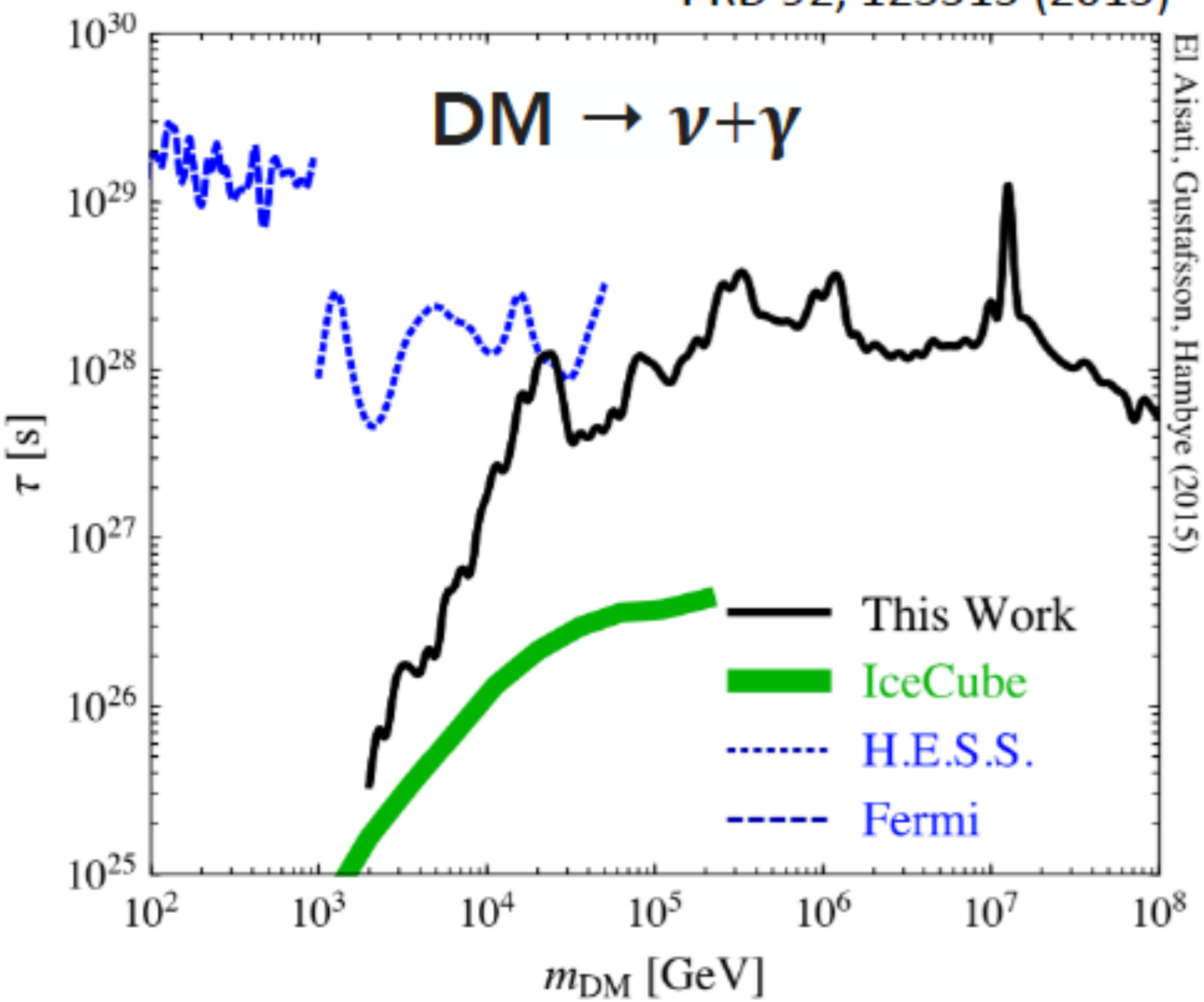

Heavy DM bounds with neutrinos, see also
Murase and Beacom JCAP 1210 (2012) 043
Esmaili, Ibarra, and Perez JCAP 1211 (2012) 034
El Aisati, Gustafsson, Hambye 1506.02657

Dark Matter Capture in the Sun

Solar WIMPs

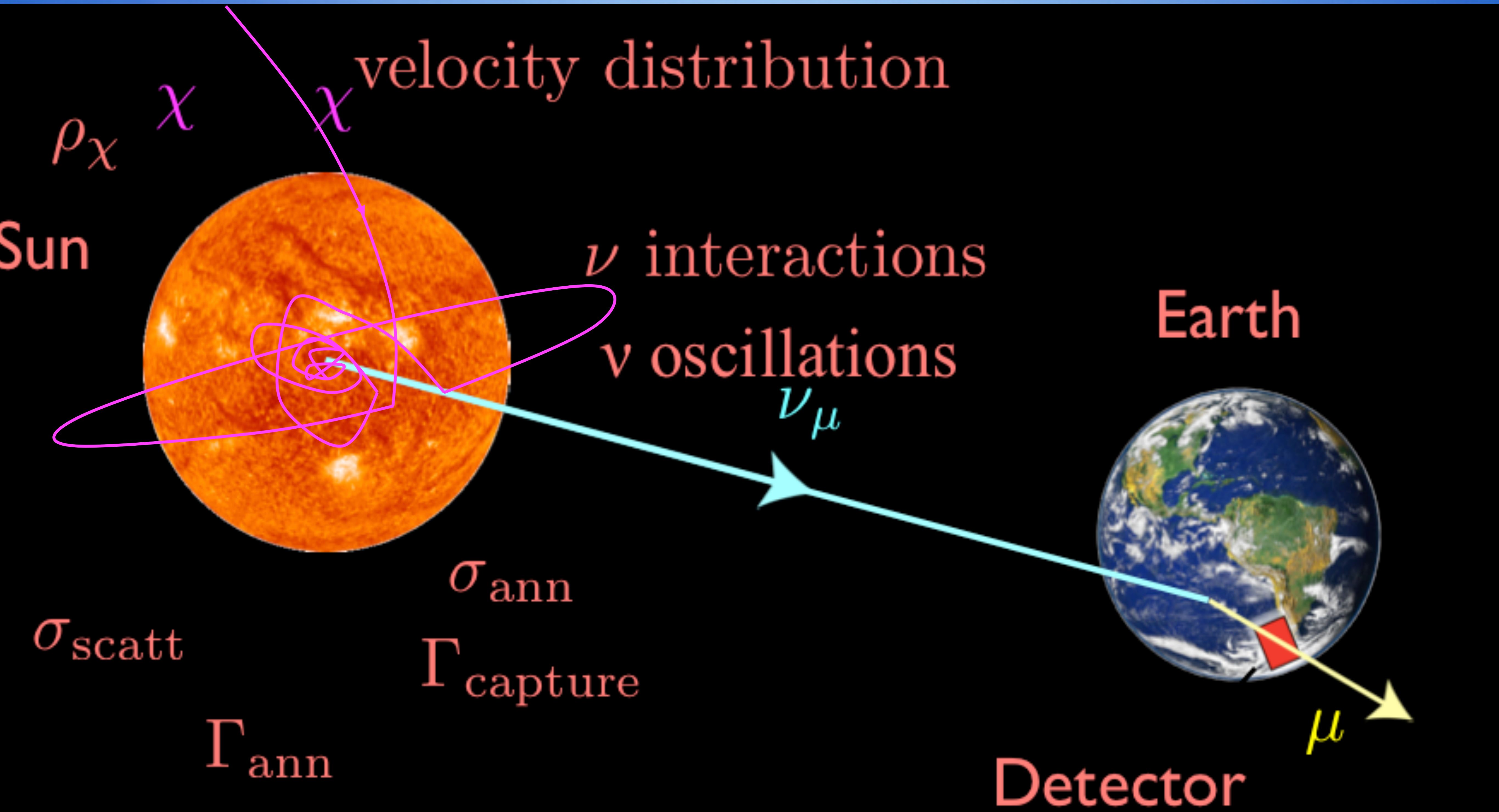

Freese '86

Silk, Olive and Srednicki '85

Gaisser, Steigman & Tilav '86

Krauss, Srednicki & Wilczek '86

Gaisser, Steigman & Tilav '86

Dark Matter Capture

Annihilation Rate ←→ Cross section

$$\frac{dN}{dt} = C_C - C_A N^2 - C_E N$$

C_C – Capture Rate
$C_A N^2$ – Annihilation Rate (2x)
$C_E N$ - Evaporation Rate (can often be neglected but should not be forgotten)

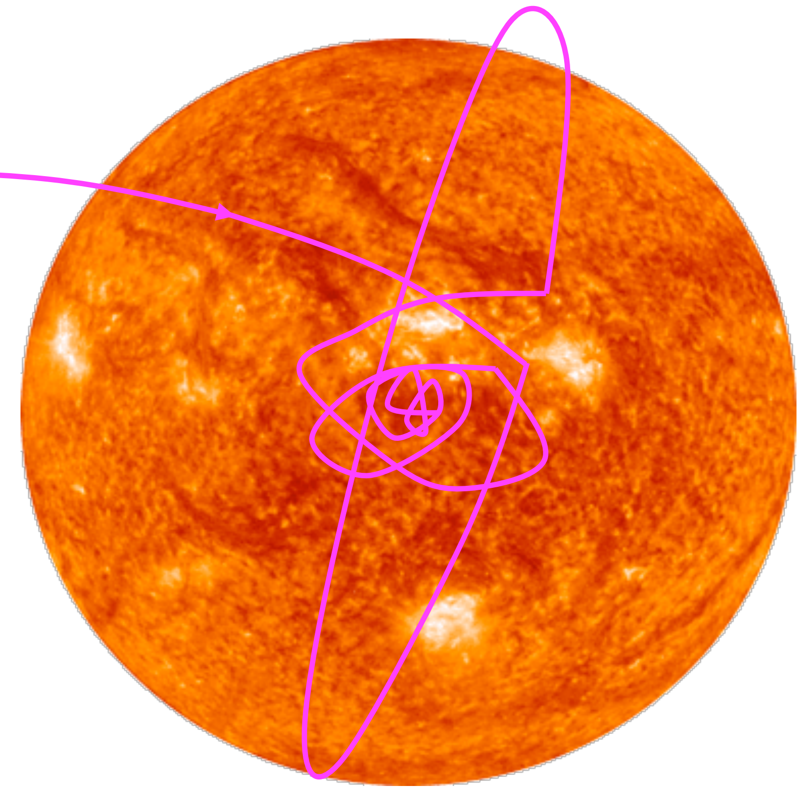

$$\Gamma_A = \frac{1}{2} C_A N^2 = \frac{1}{2} C_C \tanh^2\left(\frac{t}{\tau}\right) \quad \tau = \frac{1}{\sqrt{C_C C_A}}$$

Equilibrium for $t/\tau \gg 1$

$$\Gamma_A = \frac{1}{2} C_C , \frac{dN}{dt} = 0$$

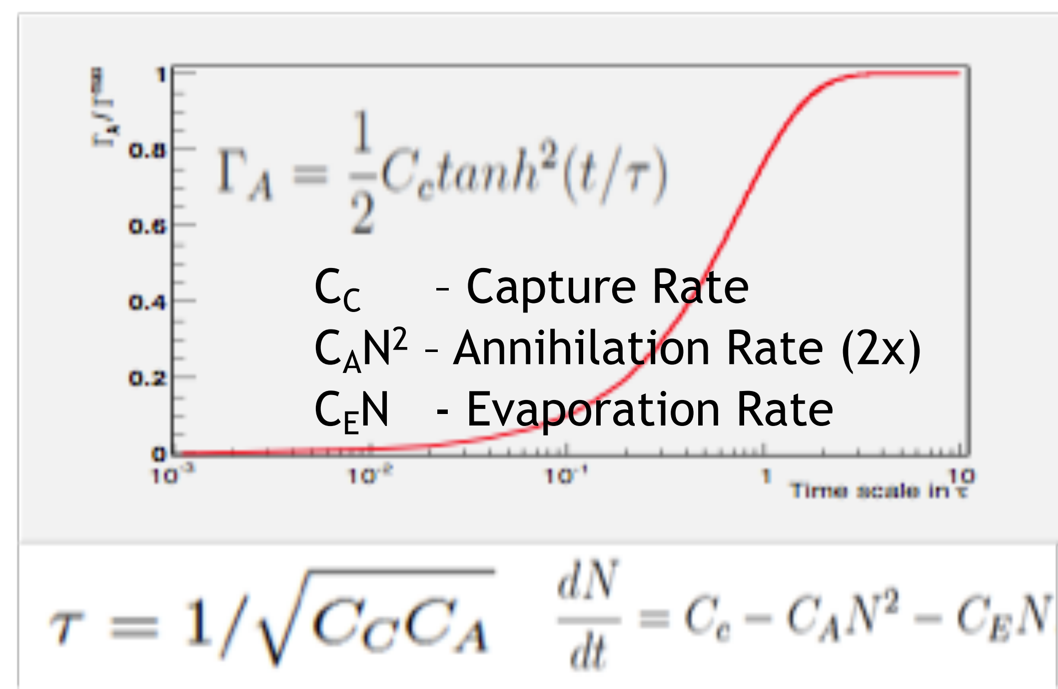

Solar WIMP Capture

- WIMPs can get gravitationally captured by the Sun
  - Capture rate, Γ_C ,depends on WIMP-nucleon scattering cross section
- Dark Matter accumulates and starts annihilating
  - → Only neutrinos can make it out
- Equilibrium: The capture rate regulates the annihilation rate ($\Gamma_A = \Gamma_C/2$)
  - The neutrino flux only depends on the WIMP-Nucleon scattering cross section

Rott, Siegal-Gaskins, Beacom PHYSICAL REVIEW D 88, 055005 (2013)

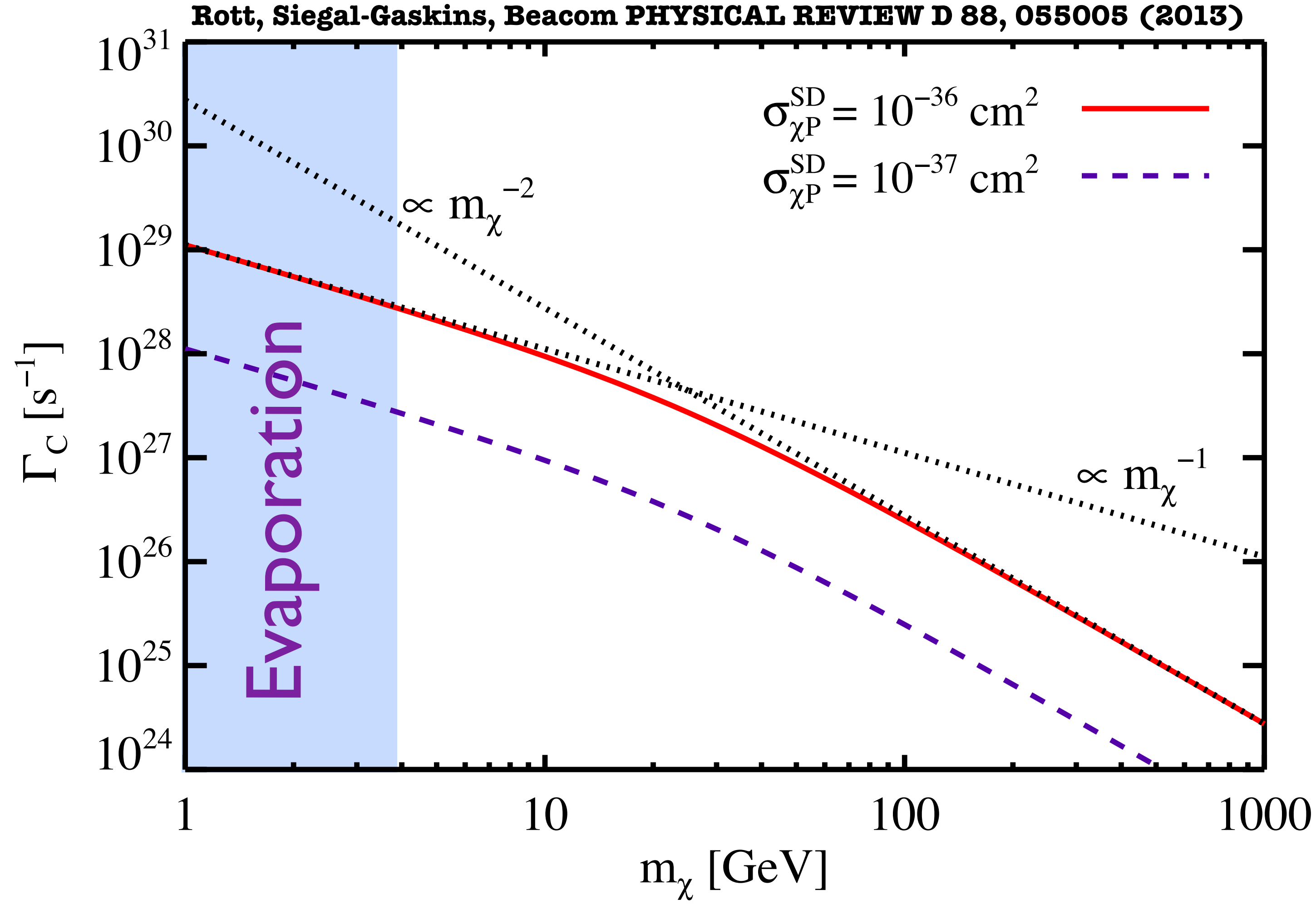

The capture rates scales as:

$\Gamma_C \sim \rho_\chi m_\chi^{-1} \sigma_A$ for $m_\chi \sim m_A$

$\Gamma_C \sim \rho_\chi m_\chi^{-2} \sigma_A$ for $m_\chi >> m_A$

number density + kinematic suppression

m_A - is the target mass

JCAP 08 2013 011

Dark Matter Distribution in the Sun

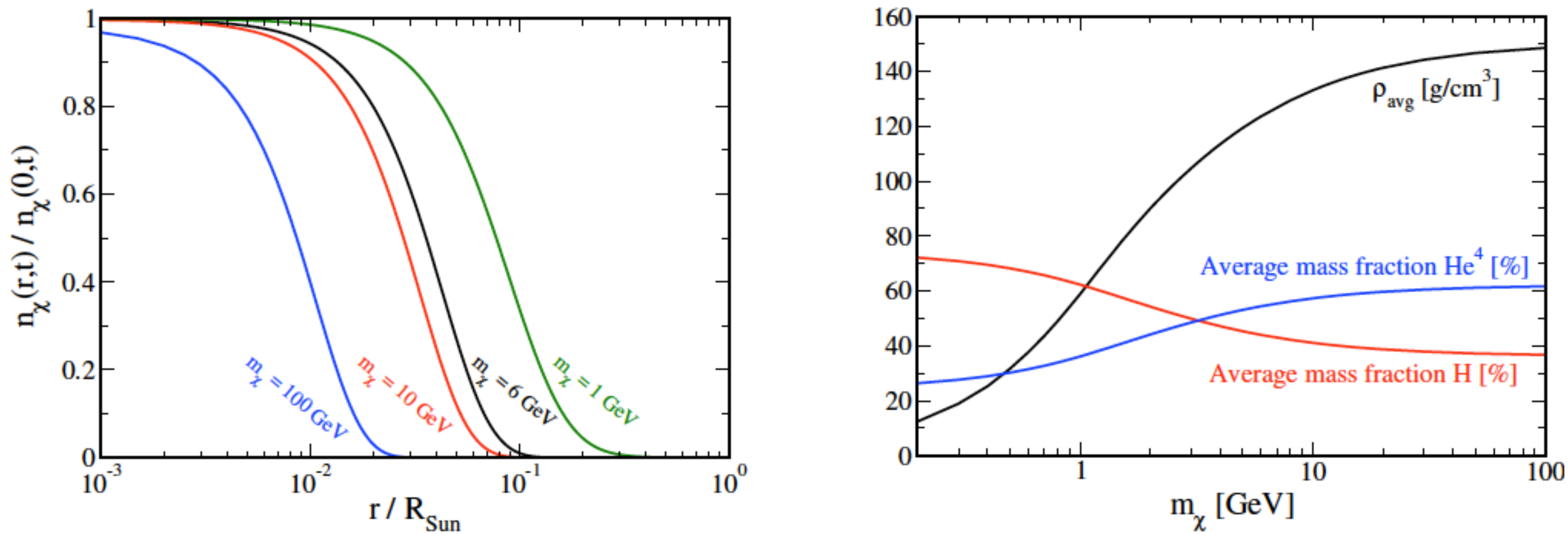

Figure 1. *Left panel: distribution of the number density of WIMPs in the Sun* (normalized to the density at the center of the Sun), $n_\chi(r,t)/n_\chi(0,t)$, as a function of the distance to the center of the Sun for four WIMP masses. *Right panel: weighted density and composition of the Sun*, according to the SSM [27, 28] and to the distribution of WIMPs (left panel), as a function of the WIMP mass. We only show the two main elements, He^4 and H. Here, we have assumed a spin-dependent cross section, $\sigma_\mathrm{p}^\mathrm{SD} = 10^{-40}$ cm^2, although the results are almost the same for any other case.

Dark Matter Annihilation in the Sun

Model i: Br(ττ)$_i$ + Br(WW)$_i$ + Br(bb)$_i$ + Br(qq)$_i$ + ... = 1

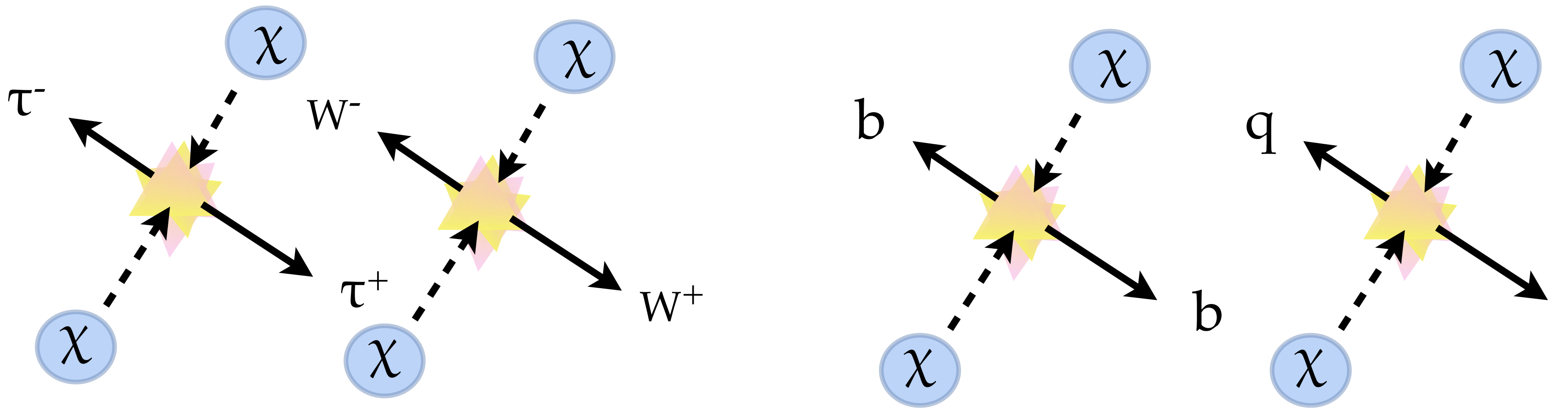

Hard channel

Soft channel

high energy neutrinos from annihilation / decay products

νν τ- τ+ W- W+ bb qq e+e-

highest energy neutrinos

fewest neutrinos

low energy neutrinos from hadronic shower

see: Rott, Siegal-Gaskins, Beacom arXiv1208.0827
N. Bernal, J. Martin-Albo and S. Palomares-Ruiz, arXiv:1208.0834

$$\tau^- \rightarrow \bar{\nu}_\mu \nu_\tau \mu^-$$
$$\tau^- \rightarrow \bar{\nu}_e \nu_\tau e^-$$
$$\tau^- \rightarrow hadrons$$

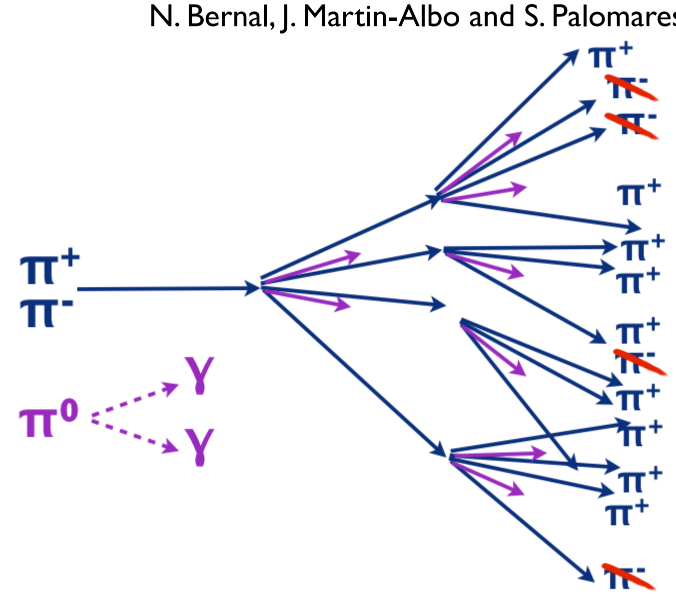

Charged pions decay at rest producing neutrinos up to E=52.8MeV

$$\pi^+ \rightarrow \mu^+ \nu_\mu$$

$$\mu^+ \rightarrow e^+ \nu_e \bar{\nu}_\mu$$

Annihilation Channels

Hard channel

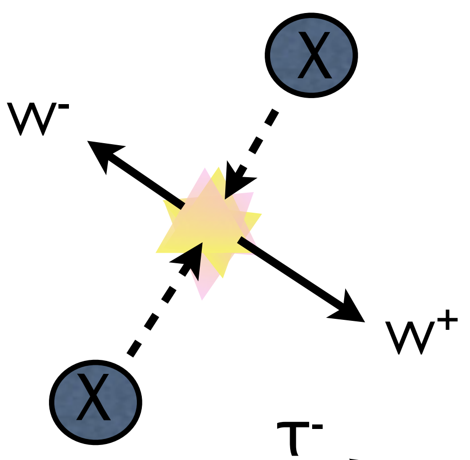

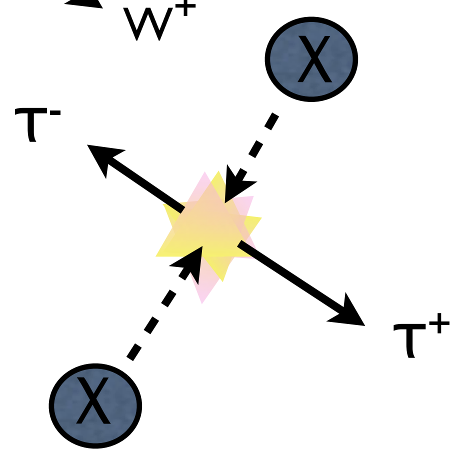

W^+ DECAY MODES		Fraction (Γ_i/Γ)	Confidence level	p (MeV/c)
$\ell^+\nu$	[b]	(10.80 ± 0.09) %		–
$e^+\nu$		(10.75 ± 0.13) %		40199
$\mu^+\nu$		(10.57 ± 0.15) %		40199
$\tau^+\nu$		(11.25 ± 0.20) %		40180
hadrons		(67.60 ± 0.27) %		–

τ^- DECAY MODES		Fraction (Γ_i/Γ)	Scale factor/ Confidence level	p (MeV/c)
Modes with one charged particle				
particle$^-$ ≥ 0 neutrals $\geq 0K^0\nu_\tau$ ("1-prong")		(85.36 ± 0.07) %	S=1.3	–
particle$^-$ ≥ 0 neutrals $\geq 0K^0_L\nu_\tau$		(84.72 ± 0.08) %	S=1.3	–
$\mu^-\overline{\nu}_\mu\nu_\tau$	[g]	(17.39 ± 0.04) %	S=1.1	885
$\mu^-\overline{\nu}_\mu\nu_\tau\gamma$	[e]	$(3.6\ \pm0.4\ )\times 10^{-3}$		885
$e^-\overline{\nu}_e\nu_\tau$	[g]	(17.82 ± 0.04) %	S=1.1	888
$e^-\overline{\nu}_e\nu_\tau\gamma$	[e]	(1.75 ± 0.18) %		888
$h^- \geq 0K^0_L\ \nu_\tau$		(12.13 ± 0.07) %	S=1.1	883
$h^-\nu_\tau$		(11.61 ± 0.06) %	S=1.1	883

Soft channel

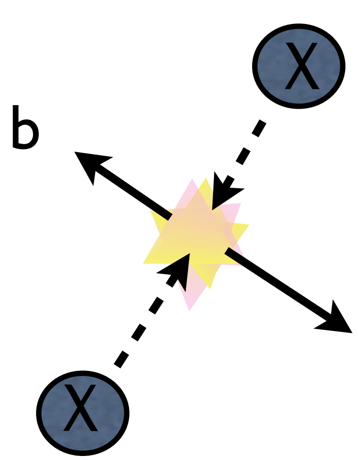

B^+ DECAY MODES		Fraction (Γ_i/Γ)	Scale factor/ Confidence level	p (MeV/c)
Semileptonic and leptonic modes				
$\ell^+\nu_\ell$ anything	[a]	$(\ 10.99\ \pm0.28\ )$ %		–
$e^+\nu_e X_c$		$(\ 10.8\ \pm0.4\ )$ %		–
$D\ell^+\nu_\ell$ anything		$(\ 9.8\ \pm0.7\ )$ %		–
$\overline{D}^0\ell^+\nu_\ell$	[a]	$(\ 2.23\ \pm0.11\ )$ %		2310
$\overline{D}^0\tau^+\nu_\tau$		$(\ 7.7\ \pm2.5\ )\times 10^{-3}$		1911
$\overline{D}^*(2007)^0\ell^+\nu_\ell$	[a]	$(\ 5.68\ \pm0.19\ )$ %		2258
$\overline{D}^*(2007)^0\tau^+\nu_\tau$		$(\ 2.1\ \pm0.4\ )$ %		1839
$D^-\pi^+\ell^+\nu_\ell$		$(\ 4.2\ \pm0.5\ )\times 10^{-3}$		2306
$\overline{D}^*_0(2420)^0\ell^+\nu_\ell\times$		$(\ 2.5\ \pm0.5\ )\times 10^{-3}$		–

- High energy neutrinos (1TeV) do not escape the Sun → Indirect dark matter searches from the **Sun** are "low-energy" analysis in neutrino telescopes.
- Utilize data when the Sun is below the horizon to reduce atmospheric muon background
- Consider different annihilation channels
  - hard neutrino spectrum $\tau\tau$, W^+W^-
  - Soft neutrino spectrum $b\bar{b}$
- Off-source region can be used to estimate background from data itself

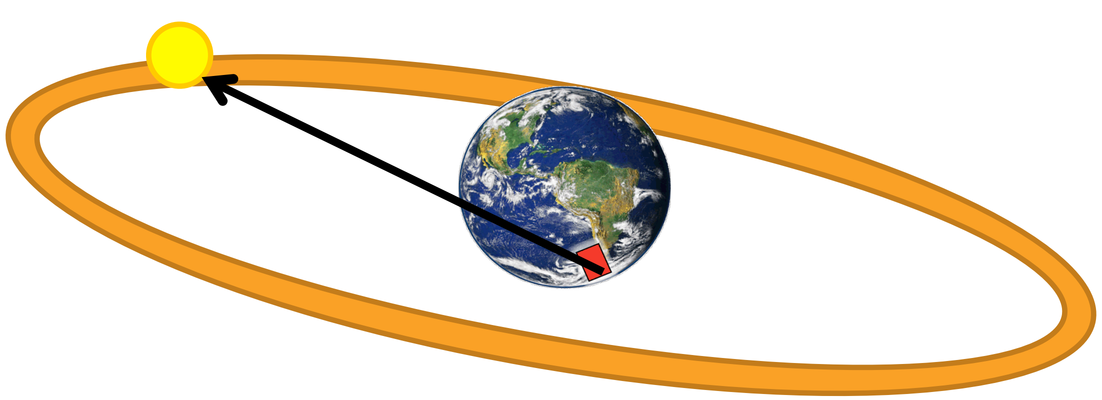

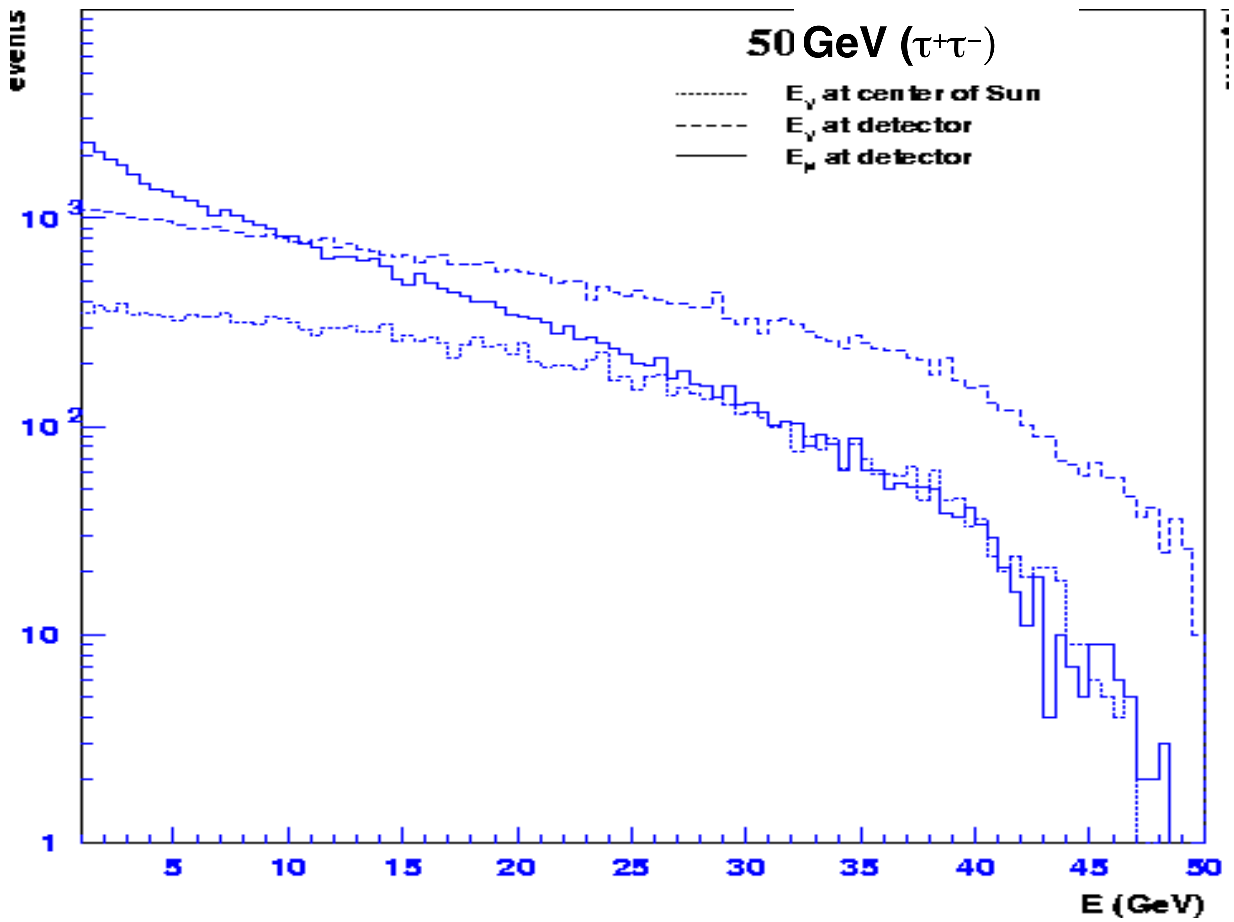

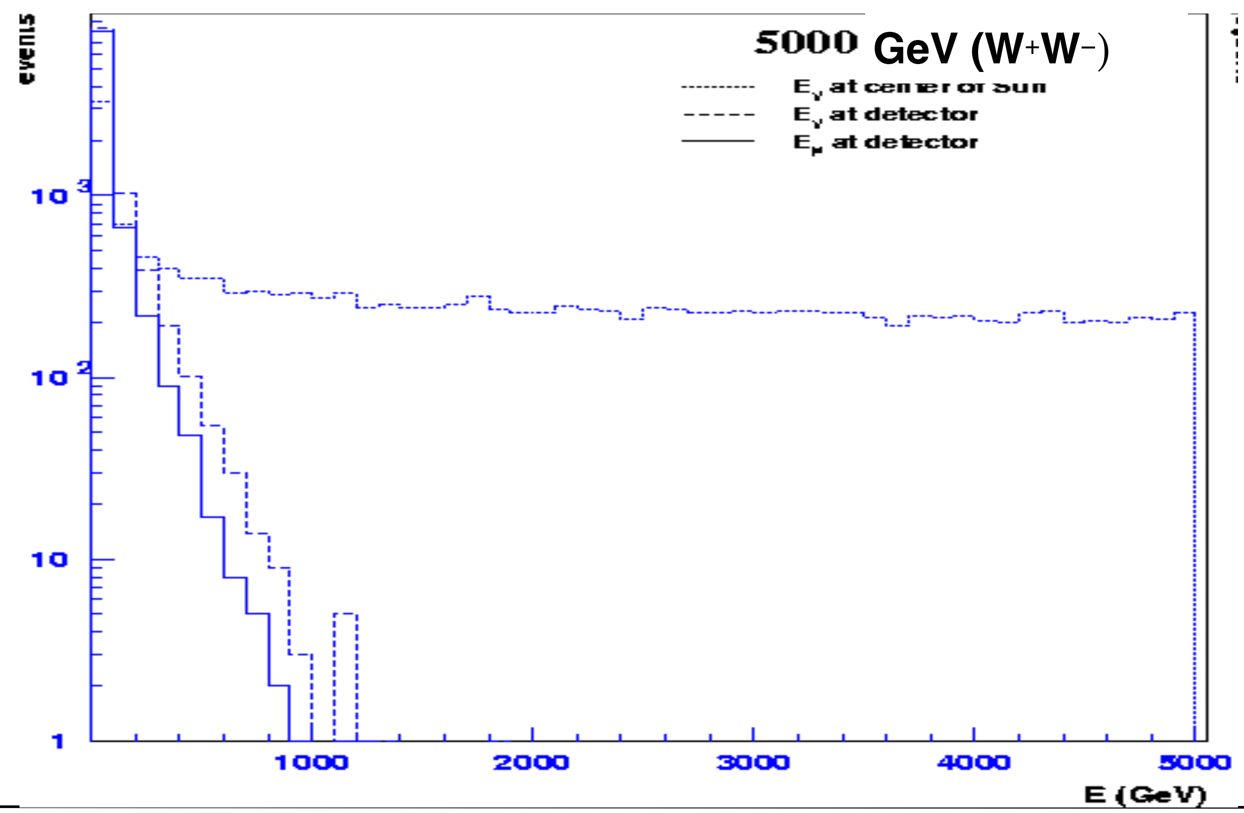

WIMPSim

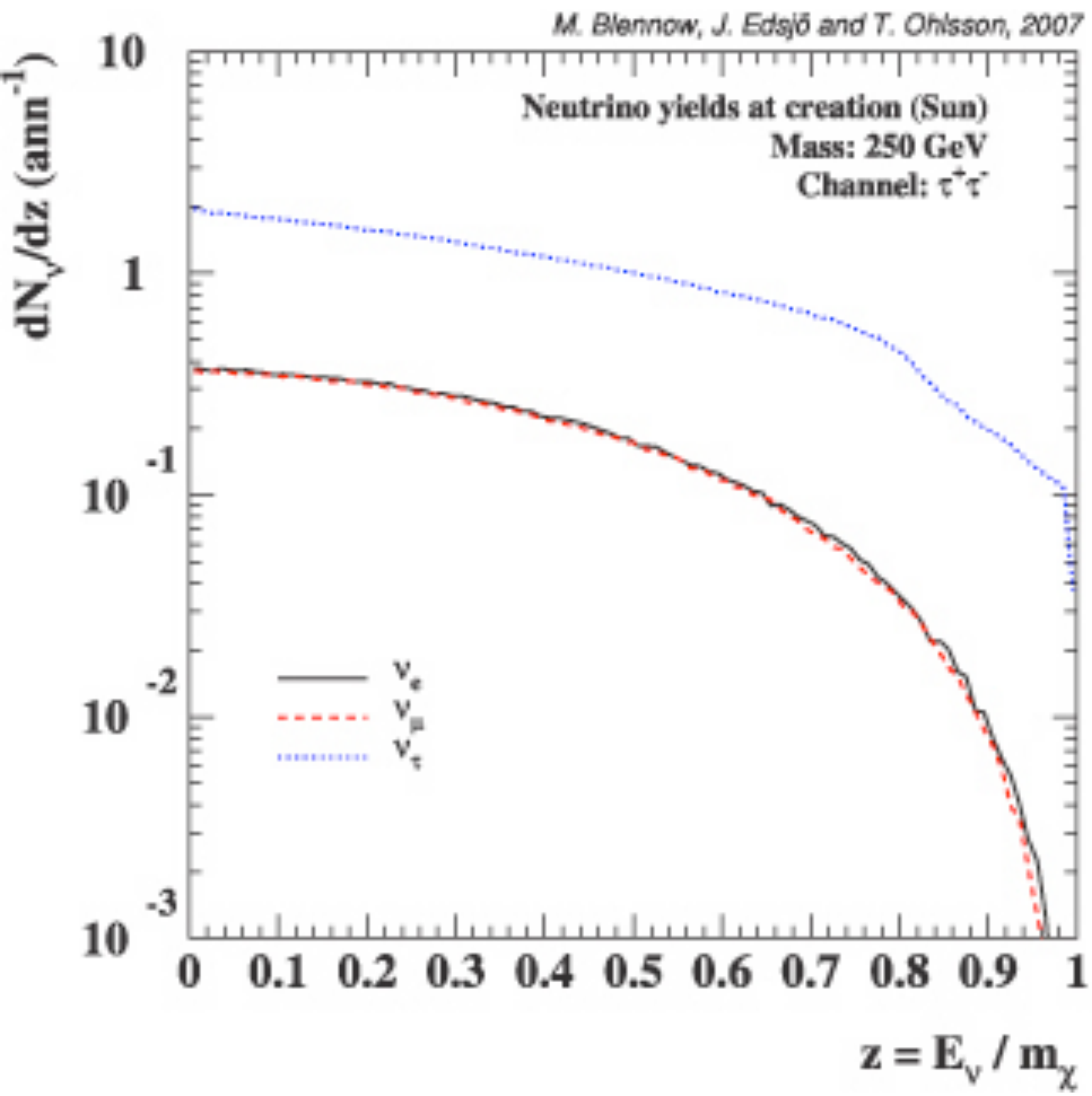

M. Blennow, J. Edsjö and T. Ohlsson, 2007
Neutrino yields at creation (Sun)
Mass: 250 GeV
Channel: $\tau^+\tau^-$
ν_e
ν_μ
ν_τ
dN_ν/dz (ann^{-1})
$z = E_\nu / m_\chi$

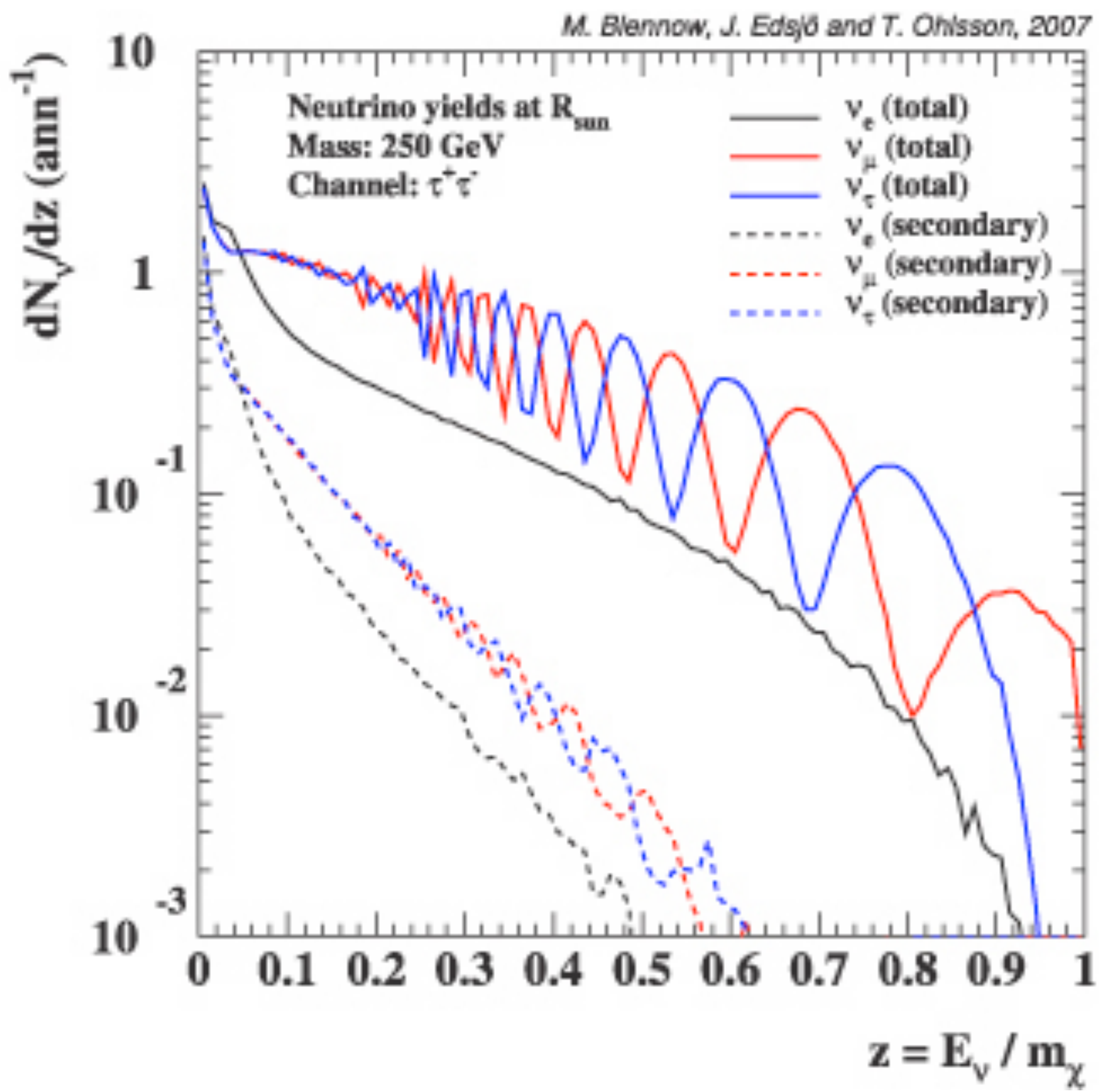

M. Blennow, J. Edsjö and T. Ohlsson, 2007
Neutrino yields at R_{sun}
Mass: 250 GeV
Channel: $\tau^+\tau^-$
ν_e (total)
ν_μ (total)
ν_τ (total)
ν_e (secondary)
ν_μ (secondary)
ν_τ (secondary)
dN_ν/dz (ann^{-1})
$z = E_\nu / m_\chi$

3yrs IceCube Solar WIMP Analysis

IceCubeColl., arXiv:1612.05949v1

- Three years of data in 86-string configuration used (**May 2011 - May 2014**)
  - Only **up-going** events (Sun below the horizon) results in **532days of livetime**
- Two independent analysis performed
  - ① **IceCube**: Higher energy focus (m_χ > 100GeV)
  - ② **DeepCore**: Low-energy focus (m_χ = 30GeV - 100GeV)

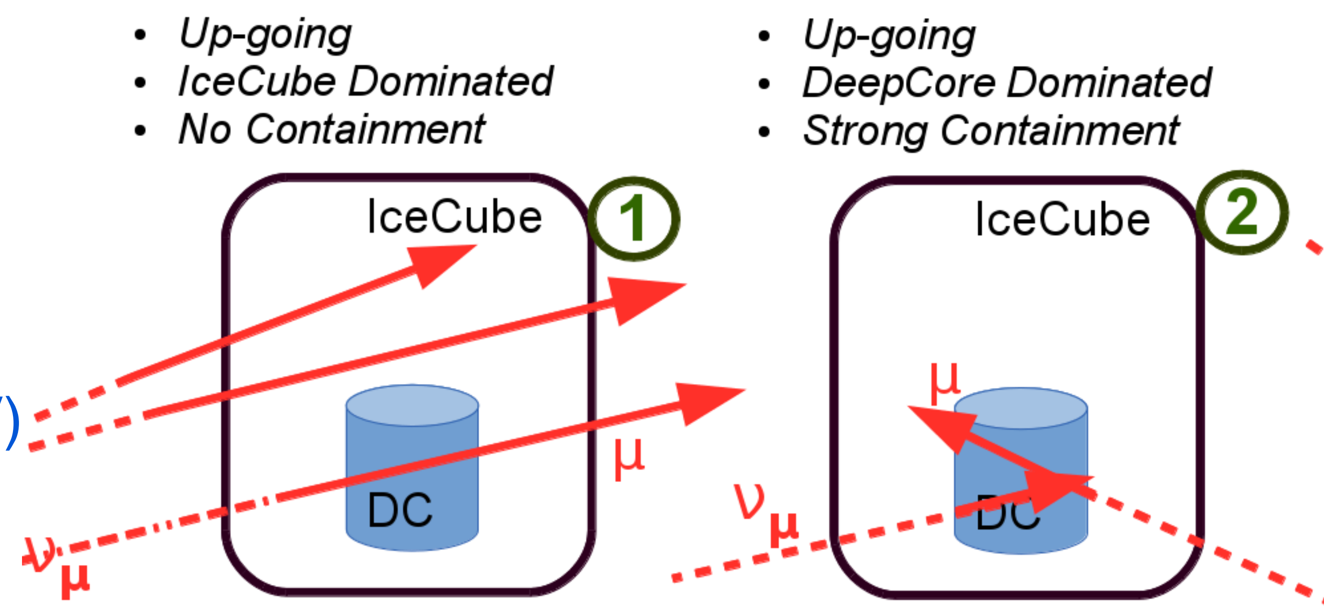

Median angular resolutions

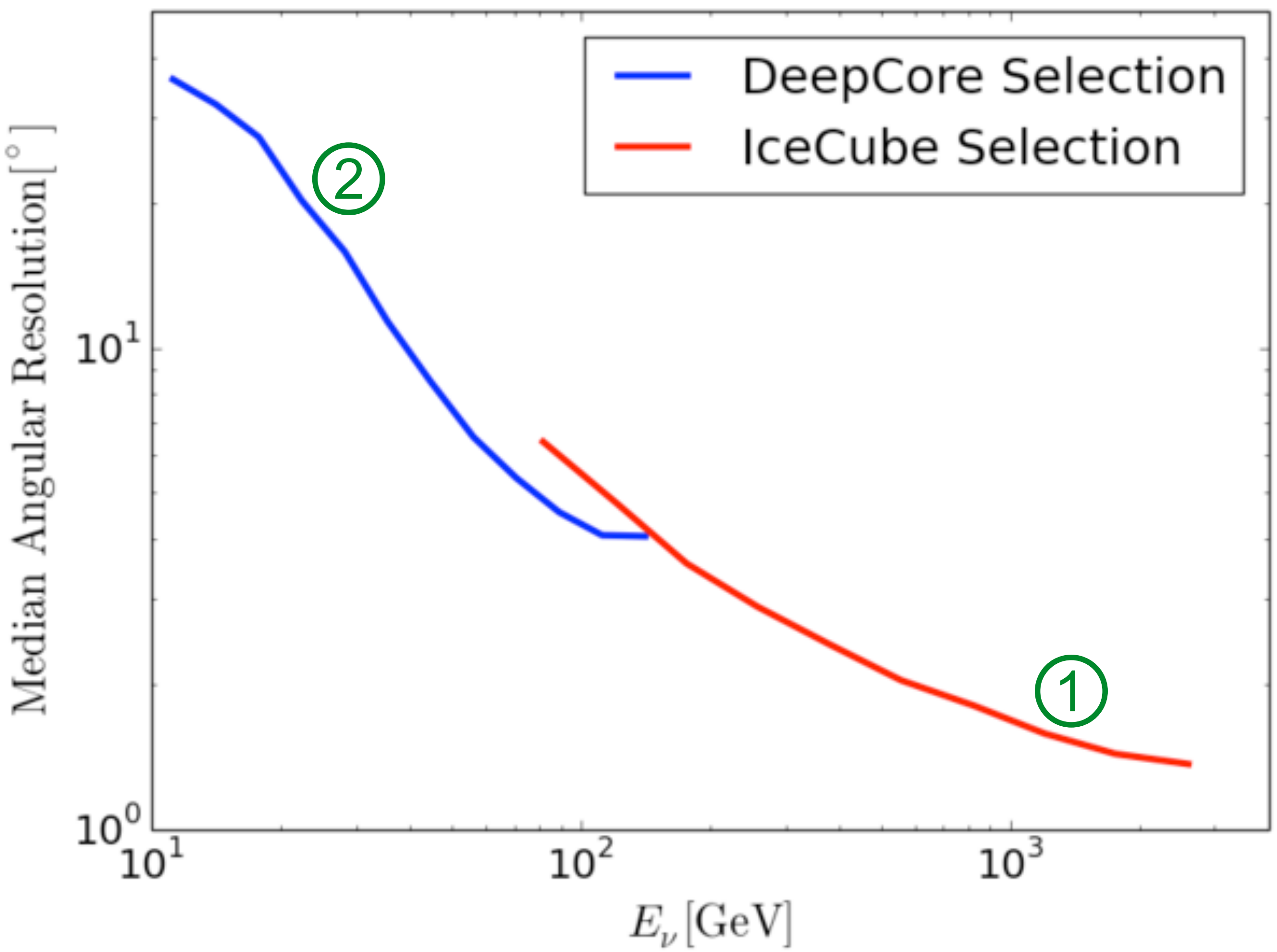

Effective Areas

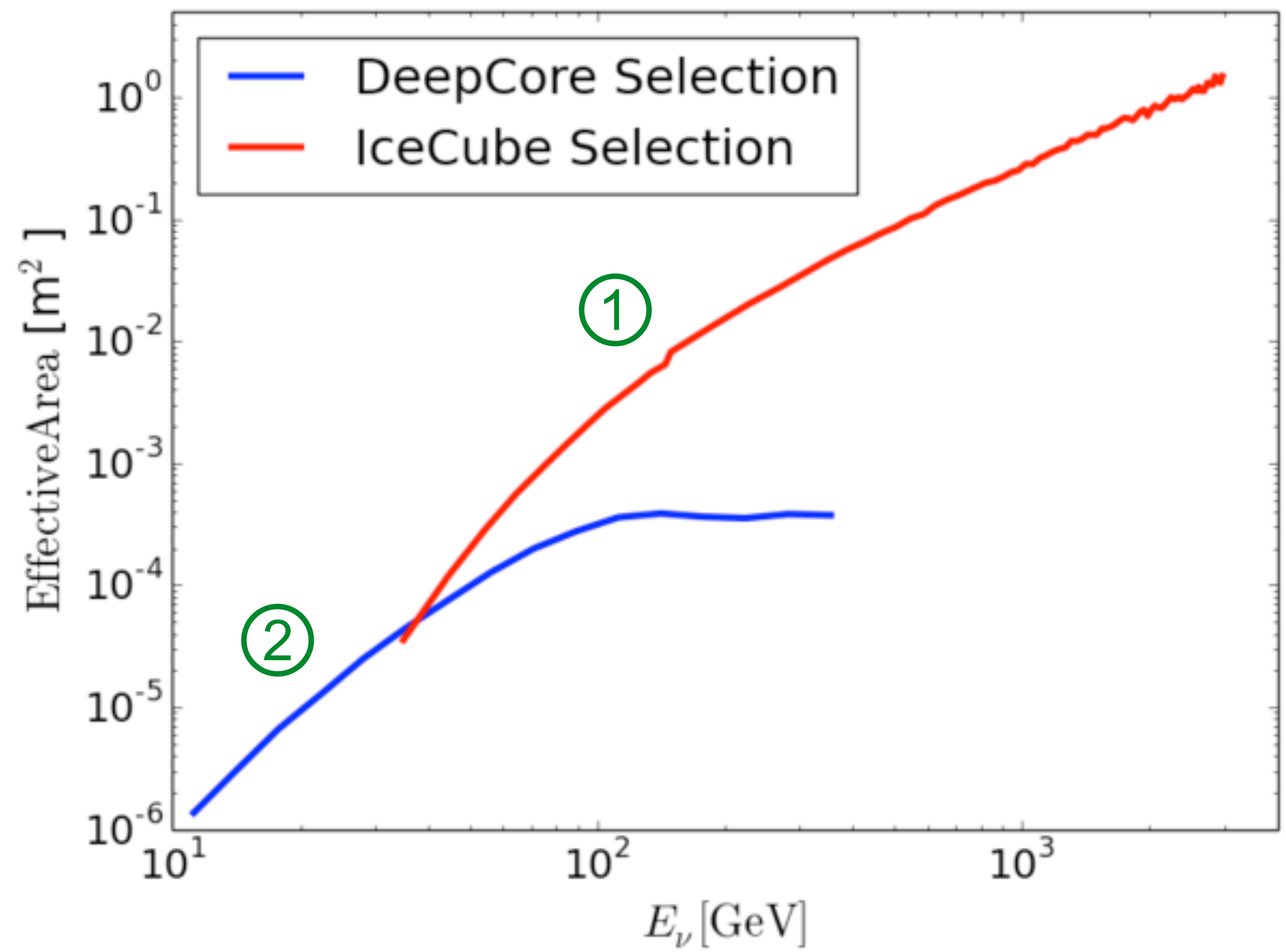

3yrs IceCube Solar WIMP Analysis

IceCubeColl., arXiv:1612.05949v1

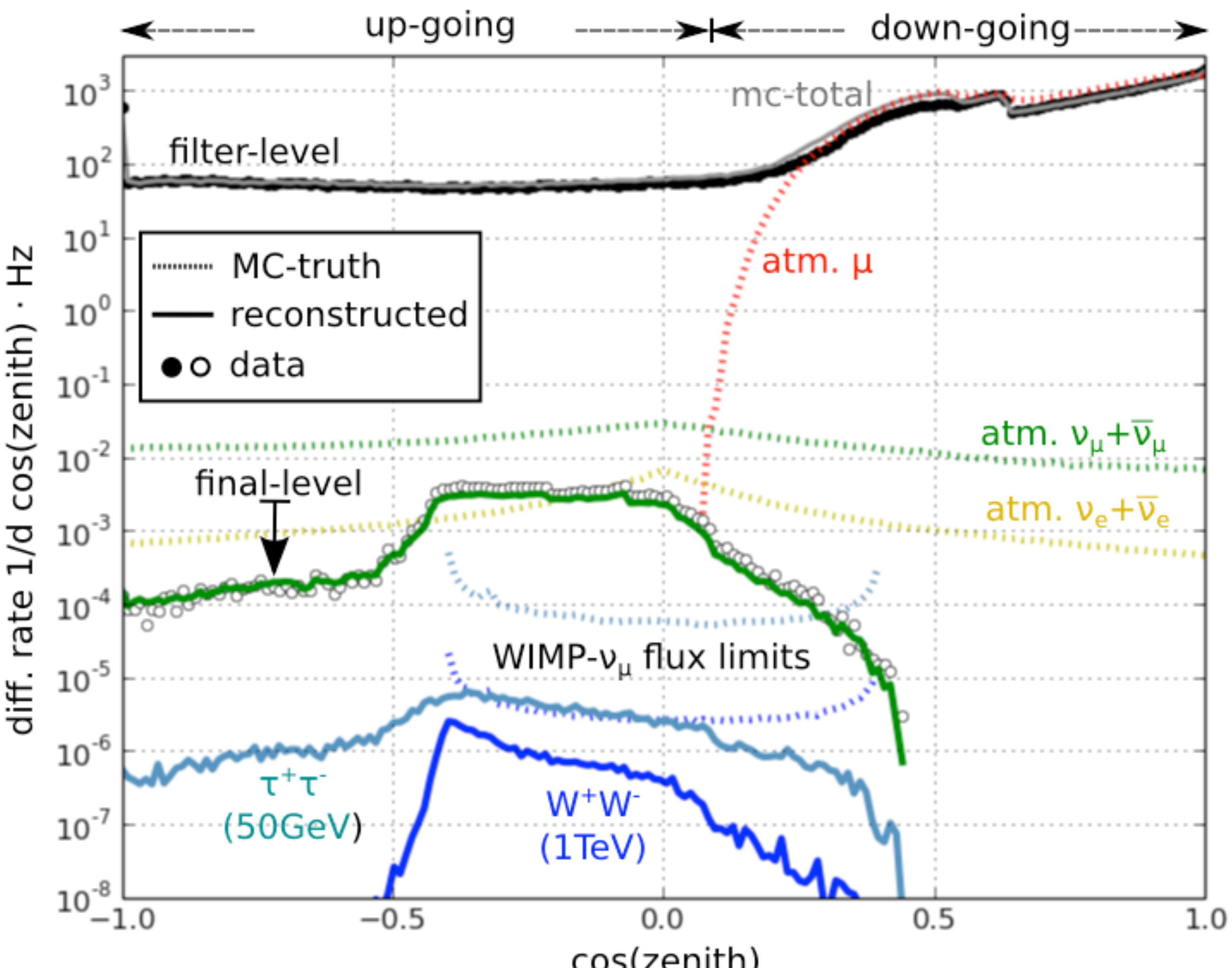

Observed events

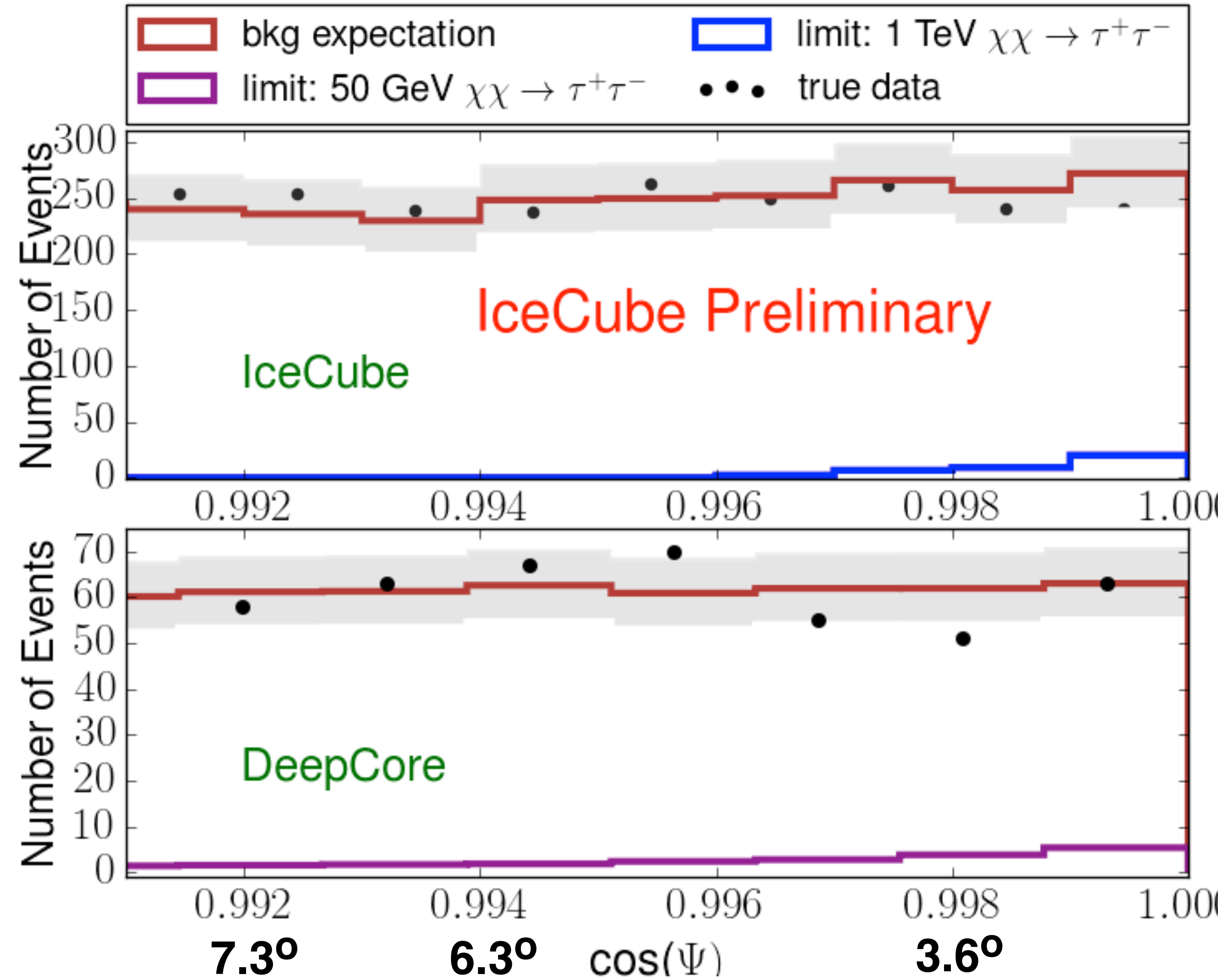

Signal pdf:

Spectral part

$$S_i(|\vec{x}_i - \vec{x}_{\rm sun}(t_i)|, E_i, m_\chi, c_{\rm ann})$$
$$= \mathscr{K}(|\vec{x}_i - \vec{x}_{\rm sun}(t_i)|, \kappa_i) \times \mathscr{E}_{m_\chi, c_{\rm ann}}(E_i)$$

Monovariate Fisher Bingham distribution from directional statistics

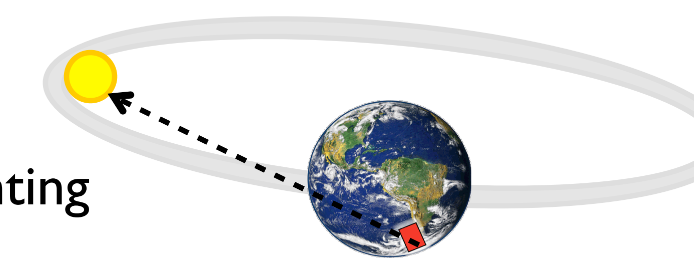

- Use track events for better pointing
- Search for an excess of events from the direction of the Sun
- Observed events consistent with background only expectations

Background pdf: $\mathscr{B}_i(tx_i, E_i) = B(\delta_i) \times P(E_i|\phi_{\rm atm})$

Likelihood: $\mathscr{L}(n_s) = \prod_N \left(\frac{n_s}{N} S_i + (1 - \frac{n_s}{N})\mathscr{B}_i\right)$

Solar WIMPs Summary

IceCubeColl., arXiv:1612.05949v1

ANTARES JCAP 1311 (2013) 032 and Phys.Lett. B759 (2016) 69-74

IceCube Phys. Rev. Lett. 110, 131302 (2013) and JCAP 04 (2016) 022

Super Kamiokande Astrophys.J. 742 (2011) 78 and Phys. Rev. Lett. 114 (2015) 141301

Baksan JCAP 1309 (2013) 019

Baikal NT200 Astropart. Phys 62 (2015) 12-20

Spin-dependent scattering

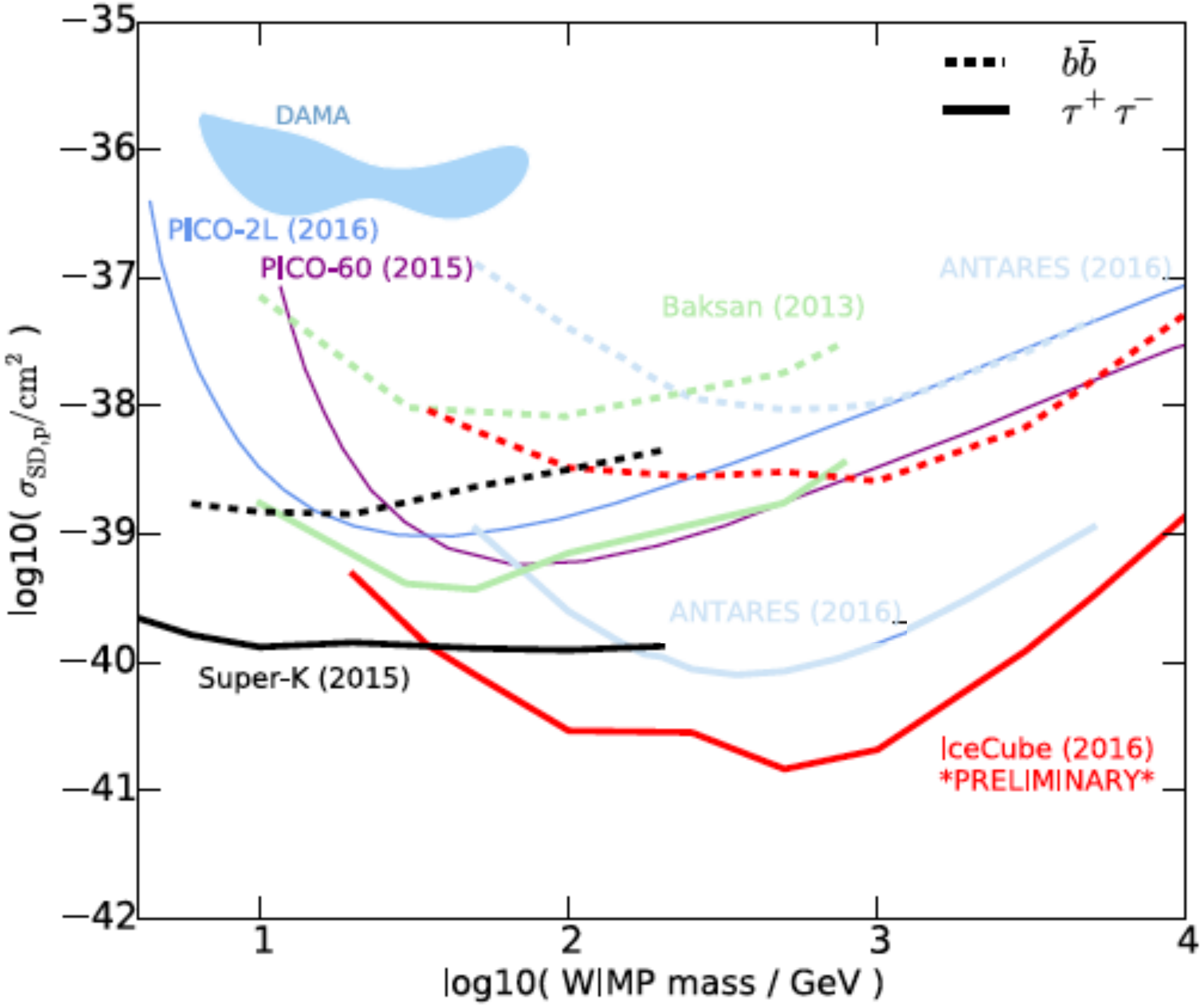

Spin-independent scattering

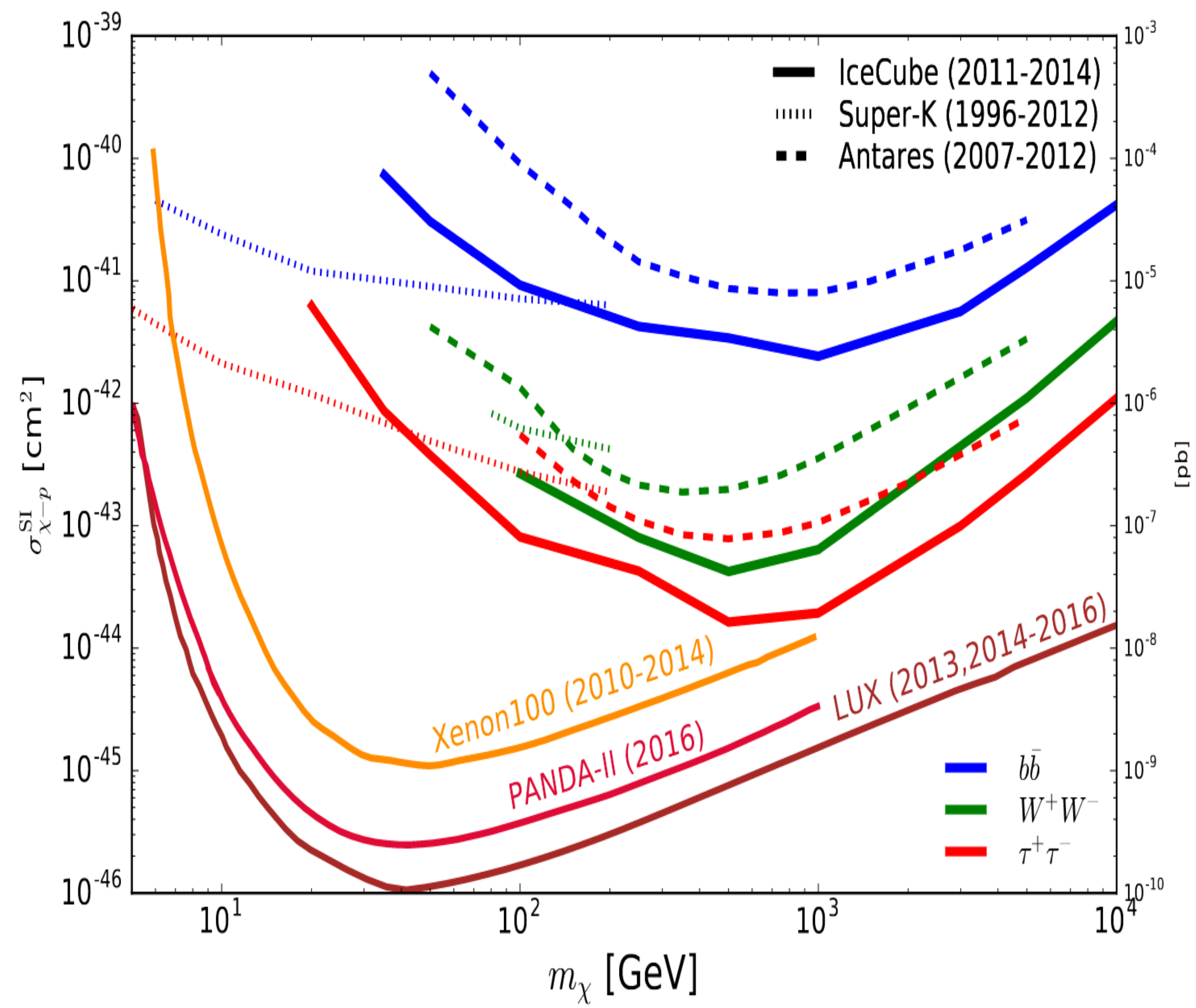

Solar WIMPs (Spin-dependent)

IceCubeColl., arXiv:1612.05949v1

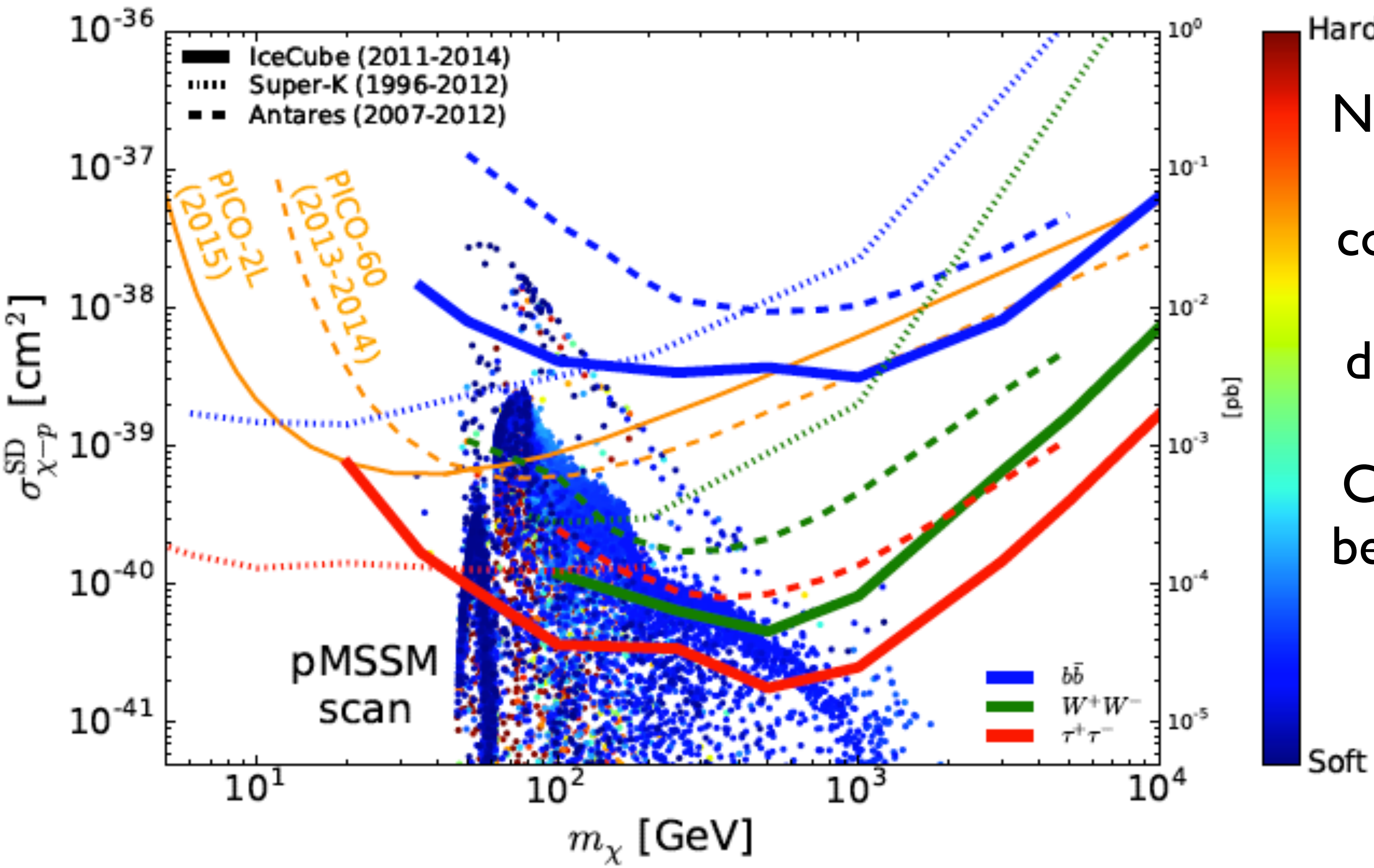

Neutrino bounds extremely competitive with Dark Matter direct detection & Can test models beyond the reach of LHC

- pMSSM model scans
  - Hard / Soft defined by fraction of hard and soft final states

No evidence for dark matter

nulike

http://nulike.hepforge.org./

JCAP 04 (2016) 022 / http://arxiv.org/pdf/1601.00653.pdf

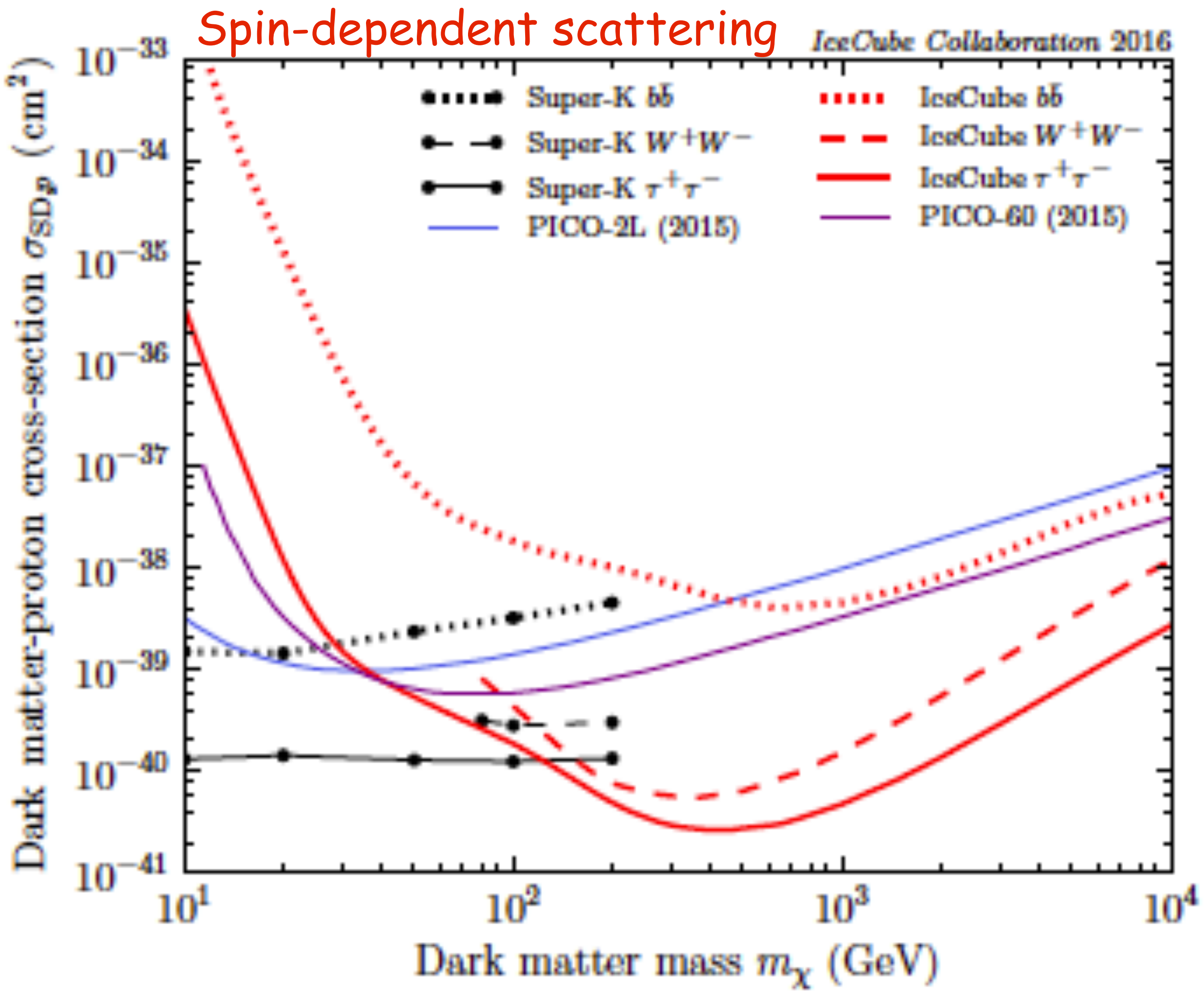

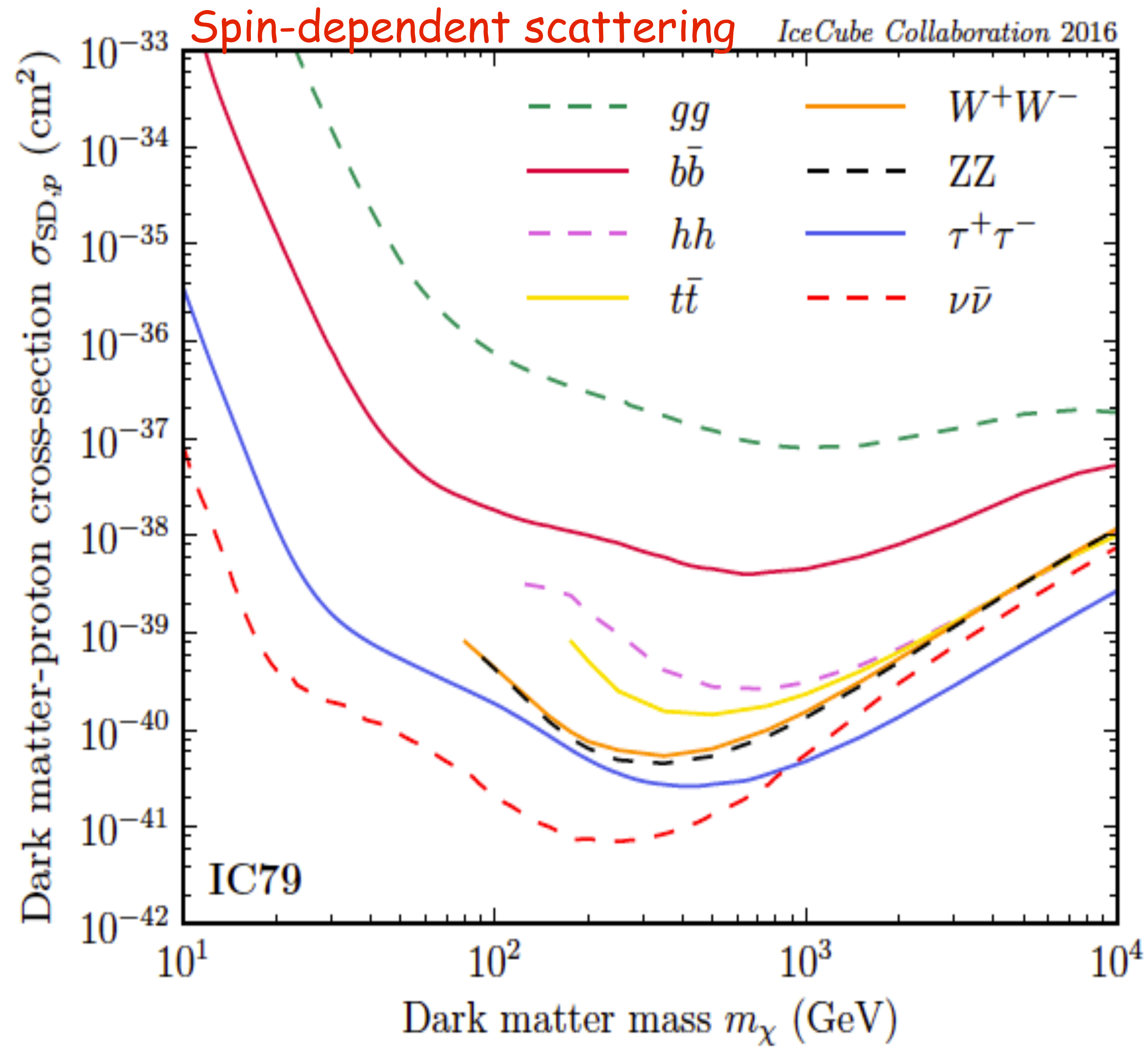

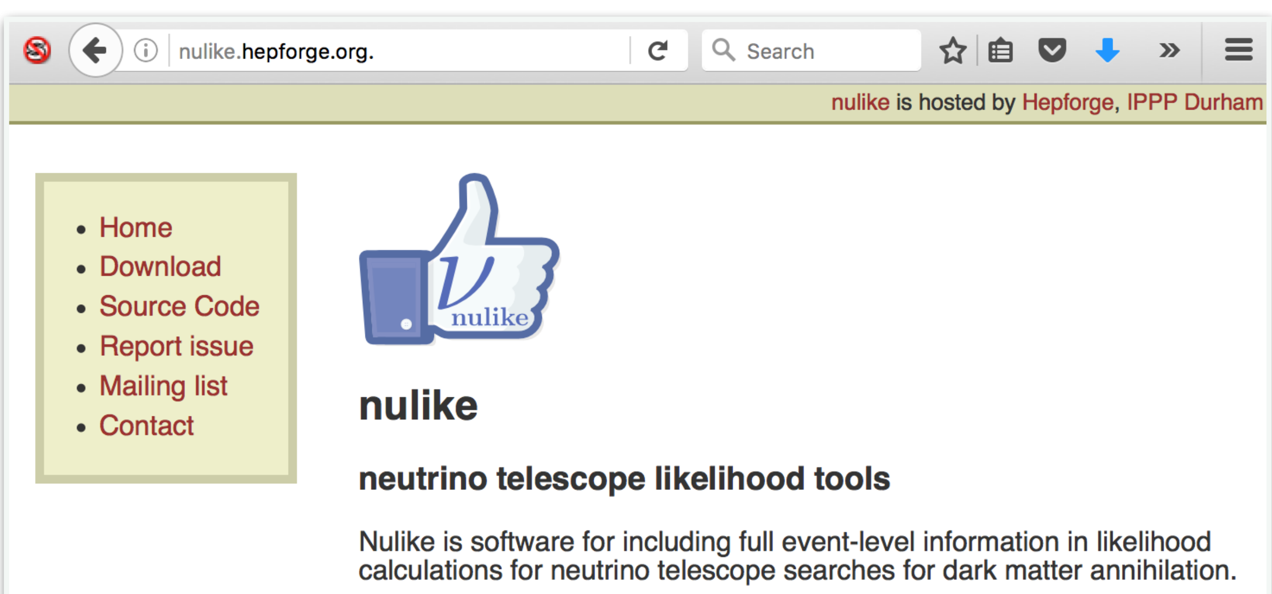

Likelihood includes:

- energy and directional information

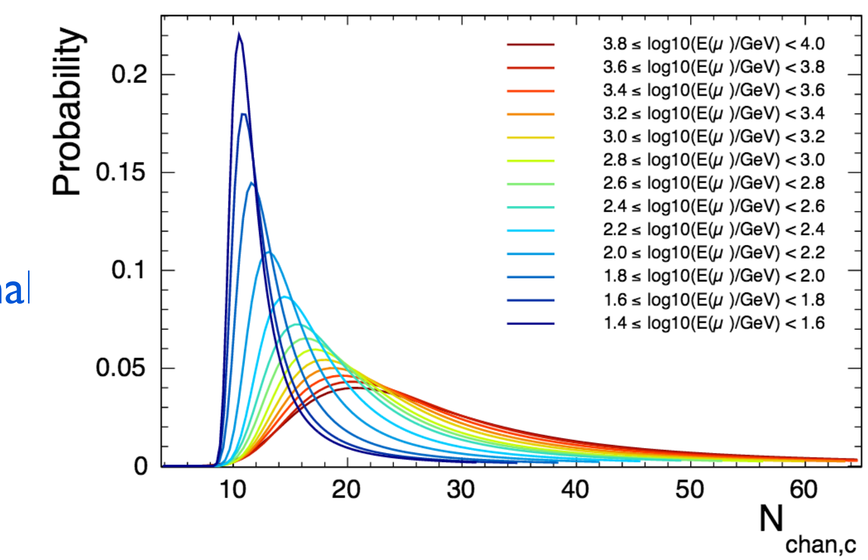

Solar WIMP Capture

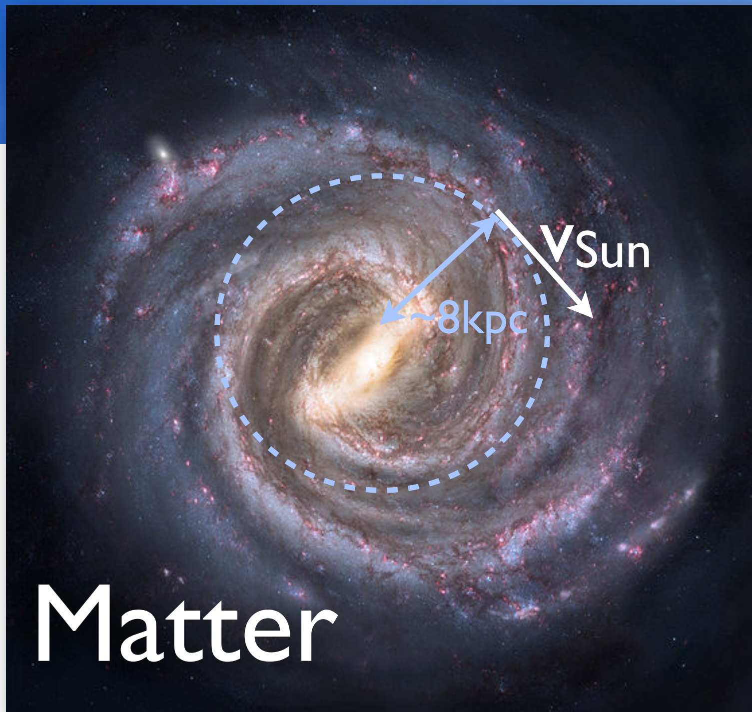

+

Standard assumption

DM isotropic with Maxwellian velocity distribution

... consequence of a density profile $\rho(r) \propto r^{-2}$ of collisionless particles

$$f(u) = \sqrt{\frac{3}{2\pi}}\frac{u}{v_\odot v_{\rm rms}}\left(\exp\left(-\frac{3(u-v_\odot)^2}{2v_{\rm rms}^2}\right) - \exp\left(-\frac{3(u+v_\odot)^2}{2v_{\rm rms}^2}\right)\right).$$

Relative velocity to the Sun

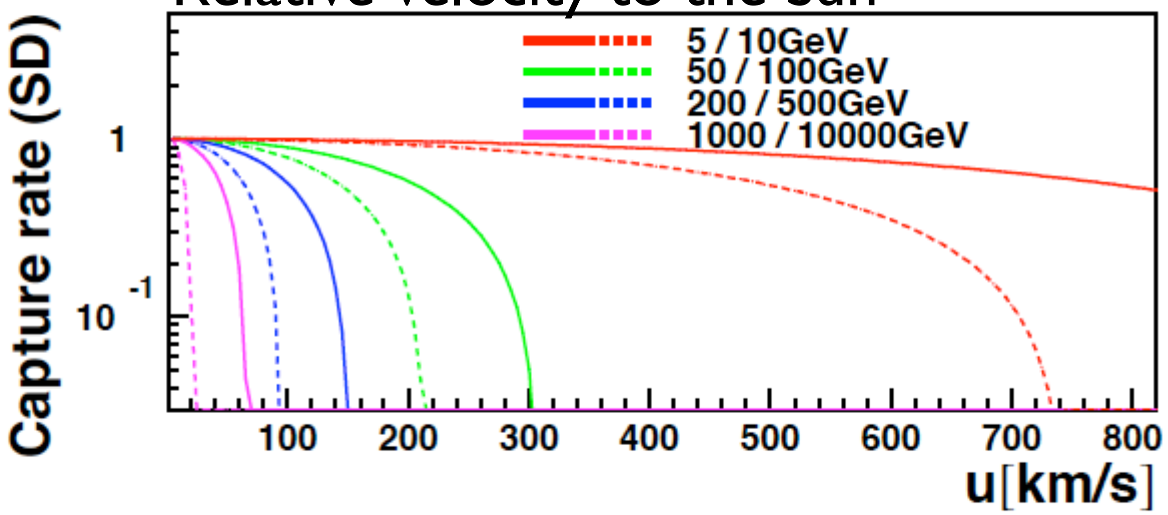

Galactic frame (assume v_{Sun}=220km/s)

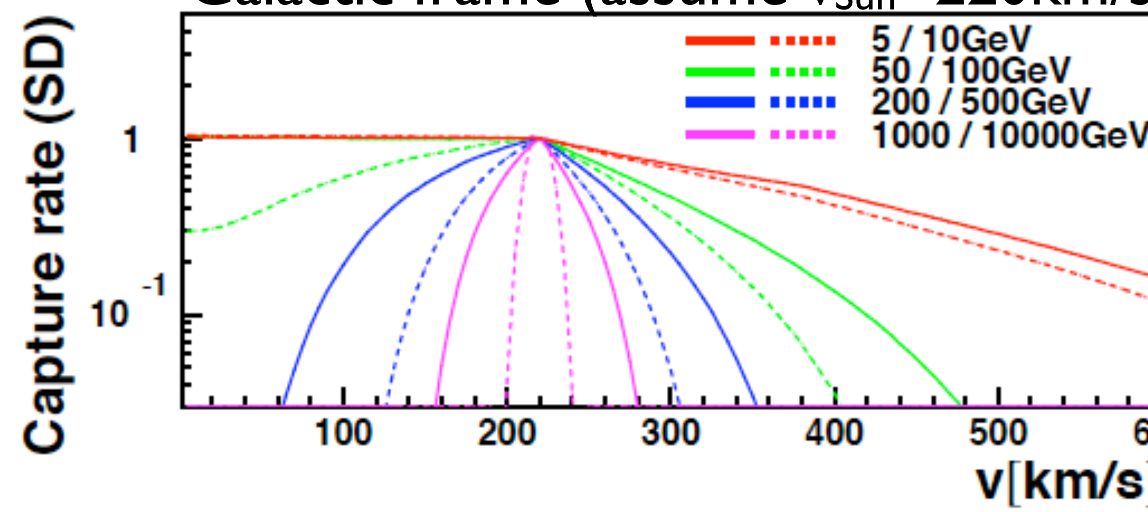

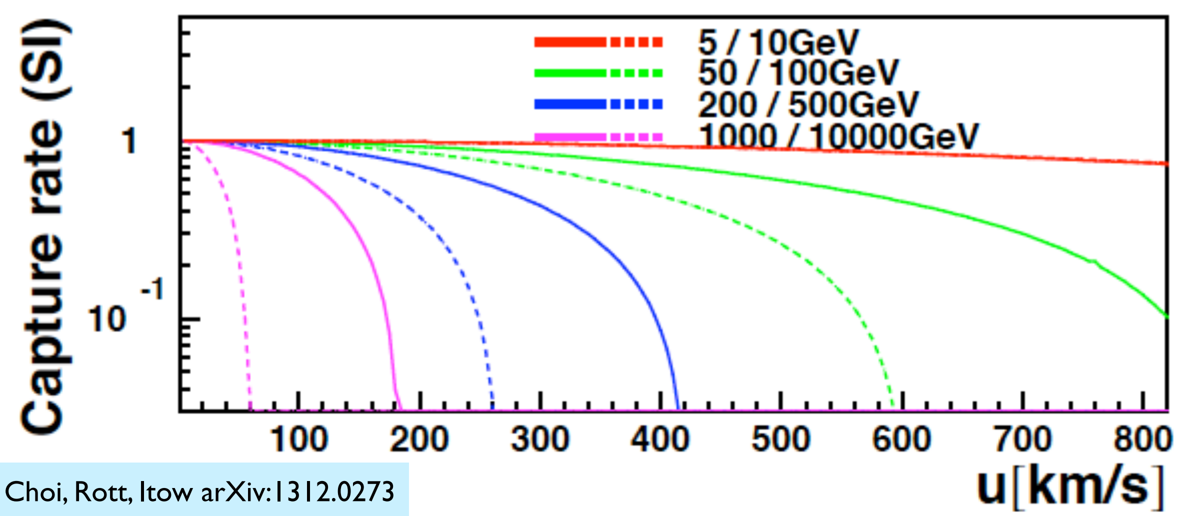

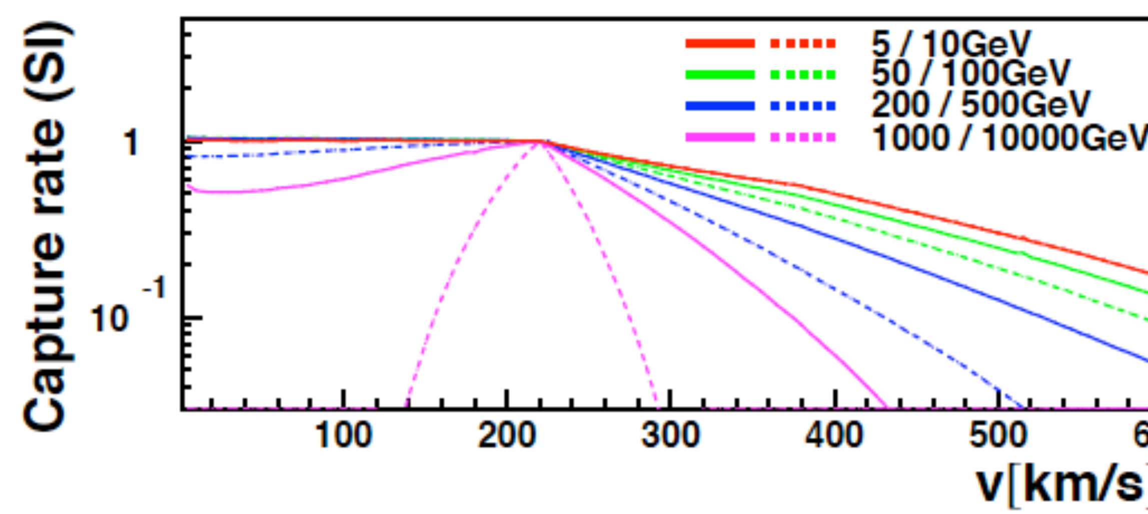

Choi, Rott, Itow arXiv:1312.0273

Impact of velocity distribution

- Explore the change in capture rate using different velocity distributions obtained from dark matter simulations

Choi, Rott, Itow JCAP 1405 (2014) 049

f(v) in Galactic frame at solar circle

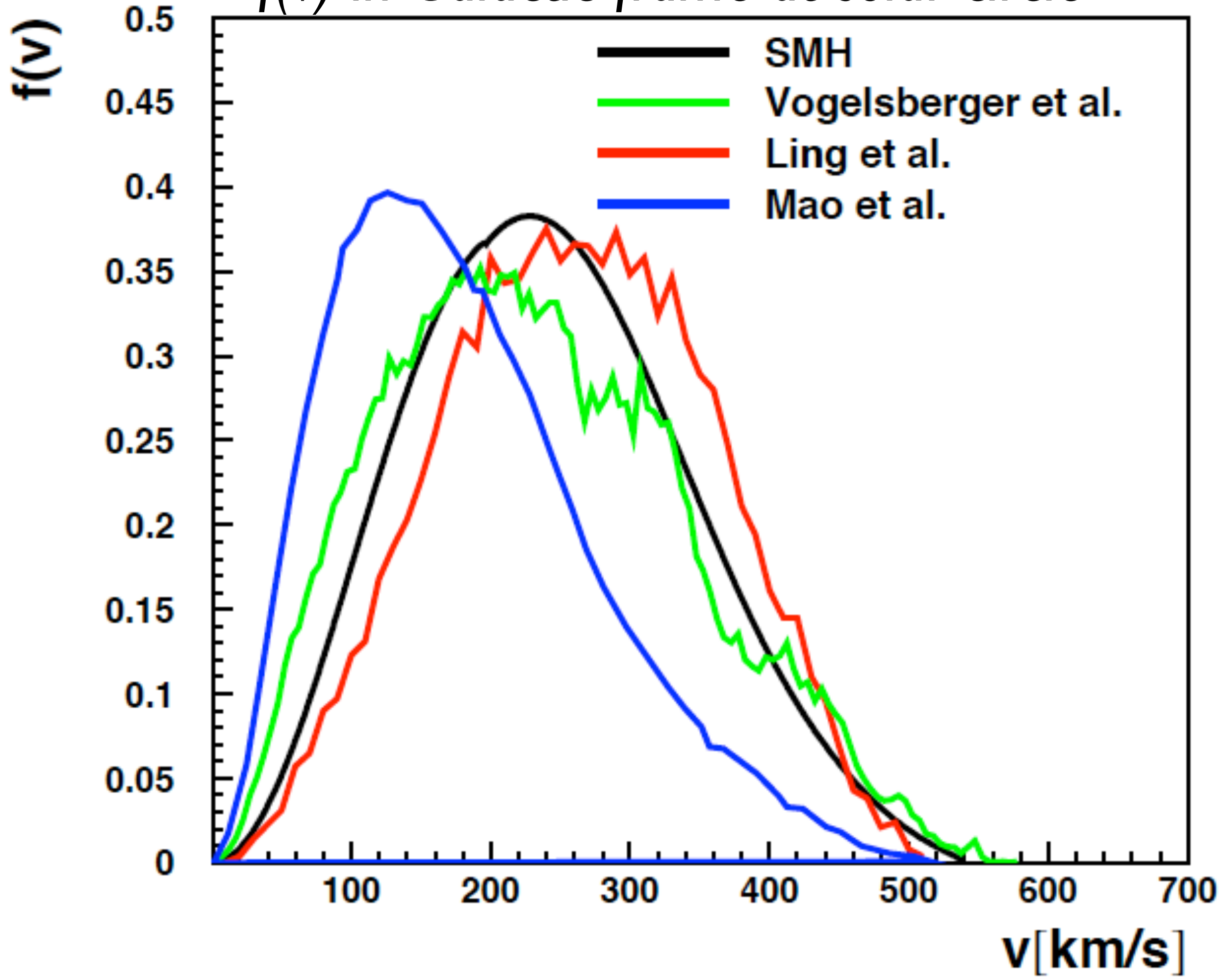

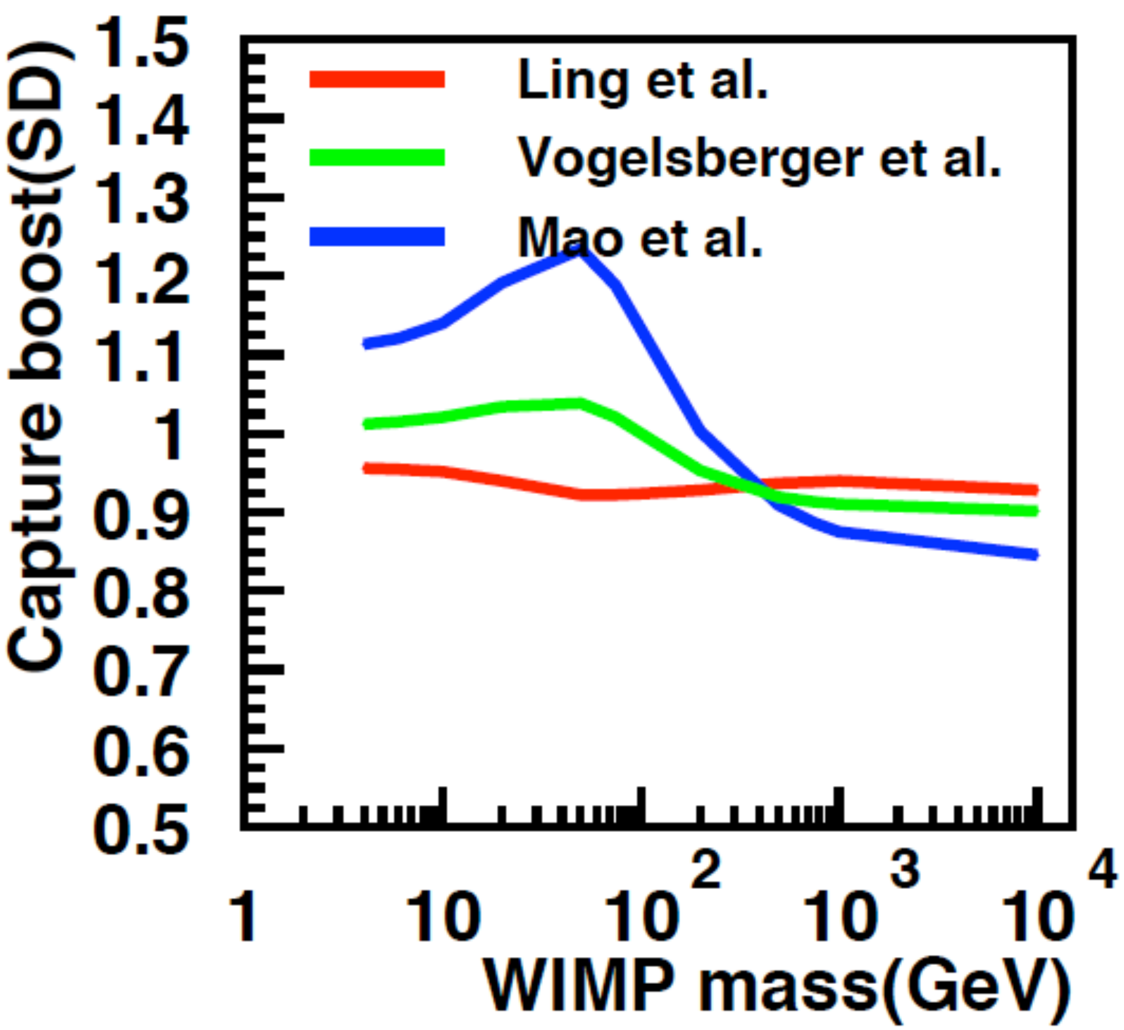

- A comparison of captures rates for different WIMP velocity distributions show that overall changes in the capture rate are smaller than 20%

Impact of astrophysical uncertainties

M. Danninger & C. Rott "Solar WIMPs Unraveled" – Physics of the Dark Universe (Nov 2014)

Interactive tool to study impact of astrophysical parameters

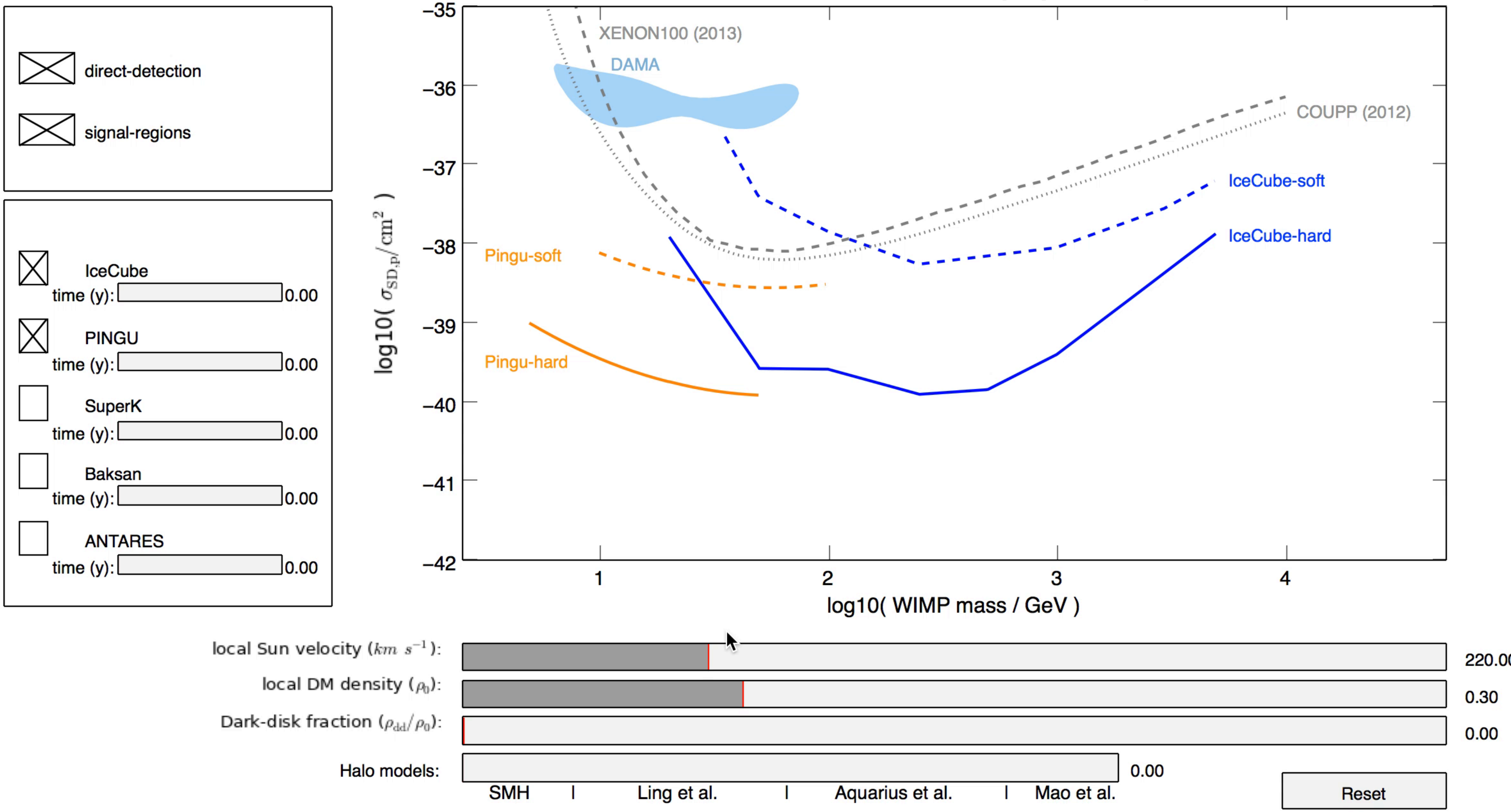

https://mdanning.web.cern.ch/mdanning/public/Interactive_figures/

Local Dark Matter Density

Particle Data Group (PDG)

110 2. Astrophysical constants

Solar angular velocity around the Galactic center	Θ_0/R_0	30.3 ± 0.9 km s^{-1} kpc^{-1}	[17]
Solar distance from Galactic center	R_0	8.4(6) kpc	[17,18]
circular velocity at R_0	v_0 or Θ_0	254(16) km s^{-1}	[17]
local disk density	$\rho_{\rm disk}$	3–12 $\times 10^{-24}$ g cm^{-3} $\approx$ 2–7 GeV/c^2 cm^{-3}	[19]
local dark matter density	ρ_χ	canonical value 0.3 GeV/c^2 cm^{-3} within factor 2–3	[20]
escape velocity from Galaxy	$v_{\rm esc}$	498 km/s $< v_{\rm esc} <$ 608 km/s	[21]

Canonical value of 0.3GeV/cm³ within a factor of 2 or 3

20. Sampling of many references:
M. Mori *et al.*, Phys. Lett. **B289**, 463 (1992);
E.I. Gates *et al.*, Astrophys. J. **449**, L133 (1995);
M. Kamionkowski and A.Kinkhabwala, Phys. Rev. **D57**, 325 (1998);
M. Weber and W. de Boer, Astron. & Astrophys. **509**, A25 (2010);
P. Salucci *et al.*, Astron. & Astrophys. **523**, A83 (2010);
R. Catena and P. Ullio, JCAP **1008**, 004 (2010) conclude $\rho_{\rm DM}^{\rm local} = 0.39 \pm 0.03$ GeV cm^{-3}.

Dark Matter Direct Detection

Direct detection community has adopted 0.3GeV/cm³

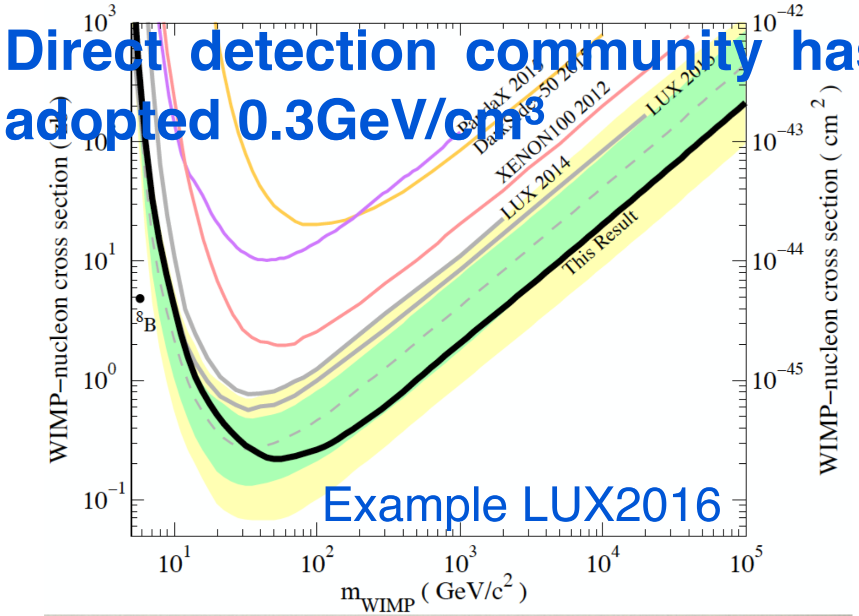

Example LUX2016

Theorists response

"Everybody is well aware of the uncertainty in the local dark matter density. Limits scale linear with local dark matter density. I believe theorists are capable of simple multiplication if they want to know a limit different from the standard local dark matter density."

Local Dark Matter Density Determinations

- R. Catena, P. Ullio, A novel determination of the local dark matter density, JCAP 1008 (2010) 004.
- P. J. McMillan, Mass models of the Milky Way, Mon.Not.Roy.Astron.Soc. 414 (2011) 2446–2457.
- P. Salucci, F. Nesti, G. Gentile, C. Martins, The dark matter density at the Sun's location, Astron.Astrophys. 523 (2010) A83.
- F. Nesti, P. Salucci, The Dark Matter halo of the Milky Way, AD 2013, JCAP 1307 (2013) 016.

Local dark matter density closer to around 0.4GeV/cm³

On the horizon: With ESA's Gaia satellite (Perryman et al. 2001) we will soon have access to proper motions and parallaxes for a billion stars.

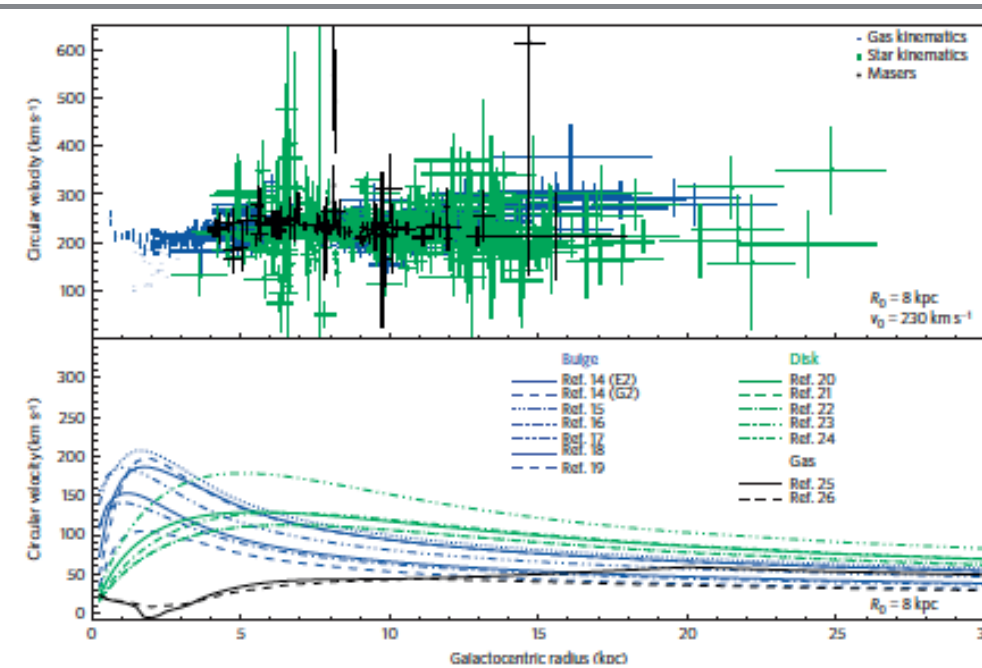

F. Iocco, M. Pato, G. Bertone, Nature Physics, DOI 10.1038

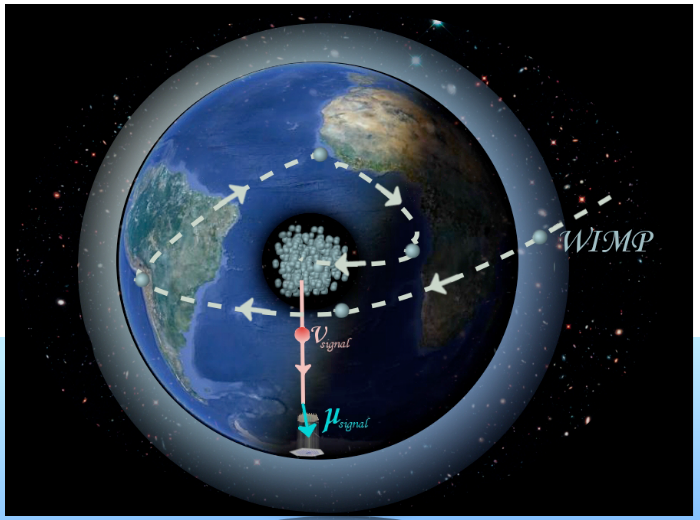

Earth WIMPs

IceCube Earth WIMPs

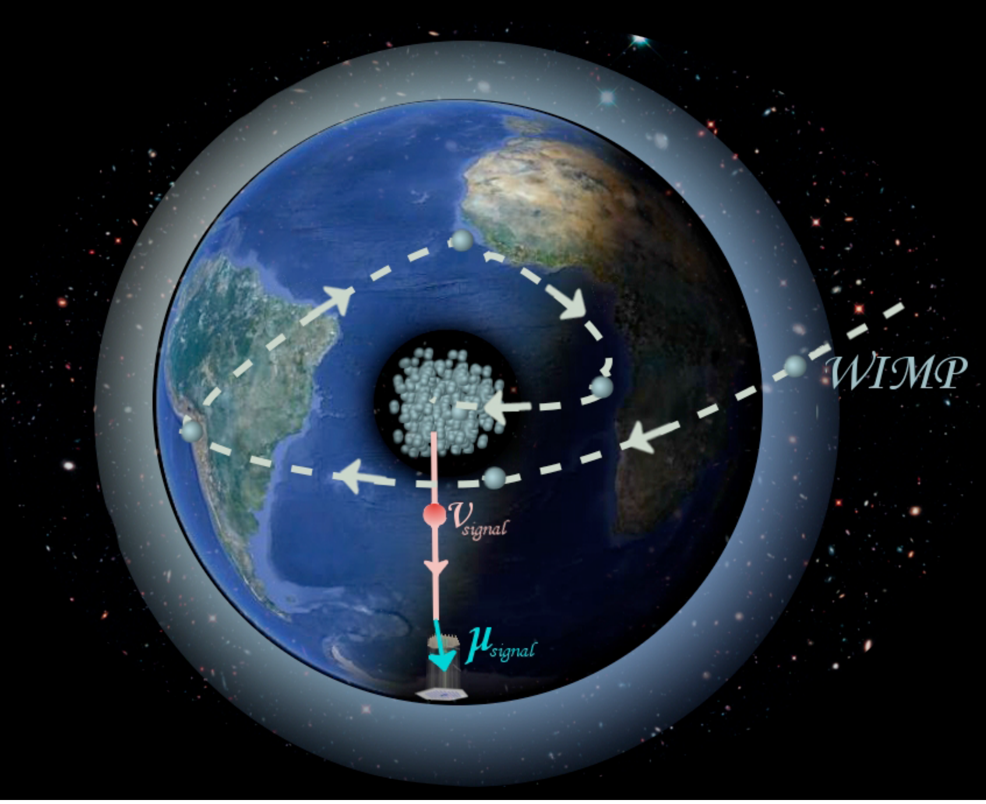

- Dark Matter could be captured in the Earth and produce a vertically up-going excess neutrino flux
- IceCube: Two statistically independent analyses
  - Low energy & High energy
  - IC86-I (327 days of livetime during 2011/12)

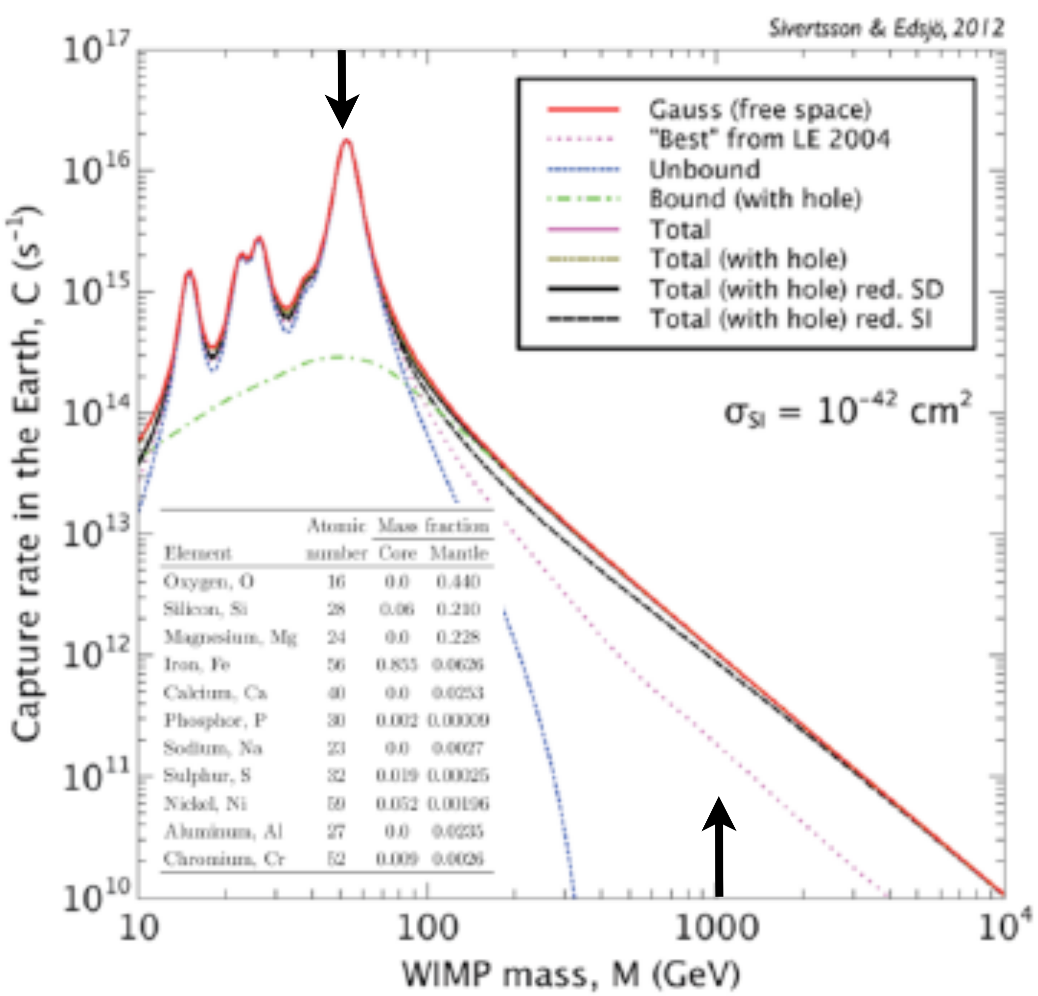

Element	Atomic number	Mass fraction Core	Mass fraction Mantle
Oxygen, O	16	0.0	0.440
Silicon, Si	28	0.06	0.210
Magnesium, Mg	24	0.0	0.228
Iron, Fe	56	0.855	0.0626
Calcium, Ca	40	0.0	0.0253
Phosphor, P	30	0.002	0.00009
Sodium, Na	23	0.0	0.0027
Sulphur, S	32	0.019	0.00025
Nickel, Ni	59	0.052	0.00196
Aluminum, Al	27	0.0	0.0235
Chromium, Cr	52	0.009	0.0026

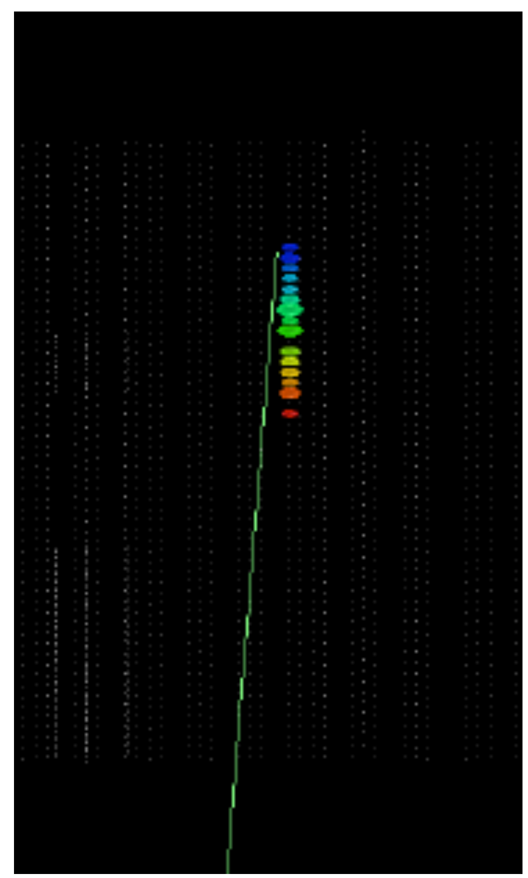

IceCube Shape analysis

$$f(\Psi|\mu) = \frac{\mu}{n_{\rm obs}} f_s(\Psi) + (1 - \frac{\mu}{n_{\rm obs}}) f_{bg}(\Psi)$$

$$\mathcal{L} = \prod_i^{n_{\rm obs}} f(\Psi_i|\mu)$$

$$\mathcal{R}(\mu) = \frac{\mathcal{L}(\mu)}{\mathcal{L}(\hat{\mu})}$$

$\hat{\mu}$ is the best fit of μ to the observation

Earth WIMPs

- Combine High-energy and low-energy analysis, based on the best sensitivity

$$\Gamma_A = \frac{C}{2}\tanh^2\left(\frac{t}{\tau}\right), \quad \tau = (CC_A)^{-1/2}$$

4.5 10⁹years

Earth typically not in equilibrium

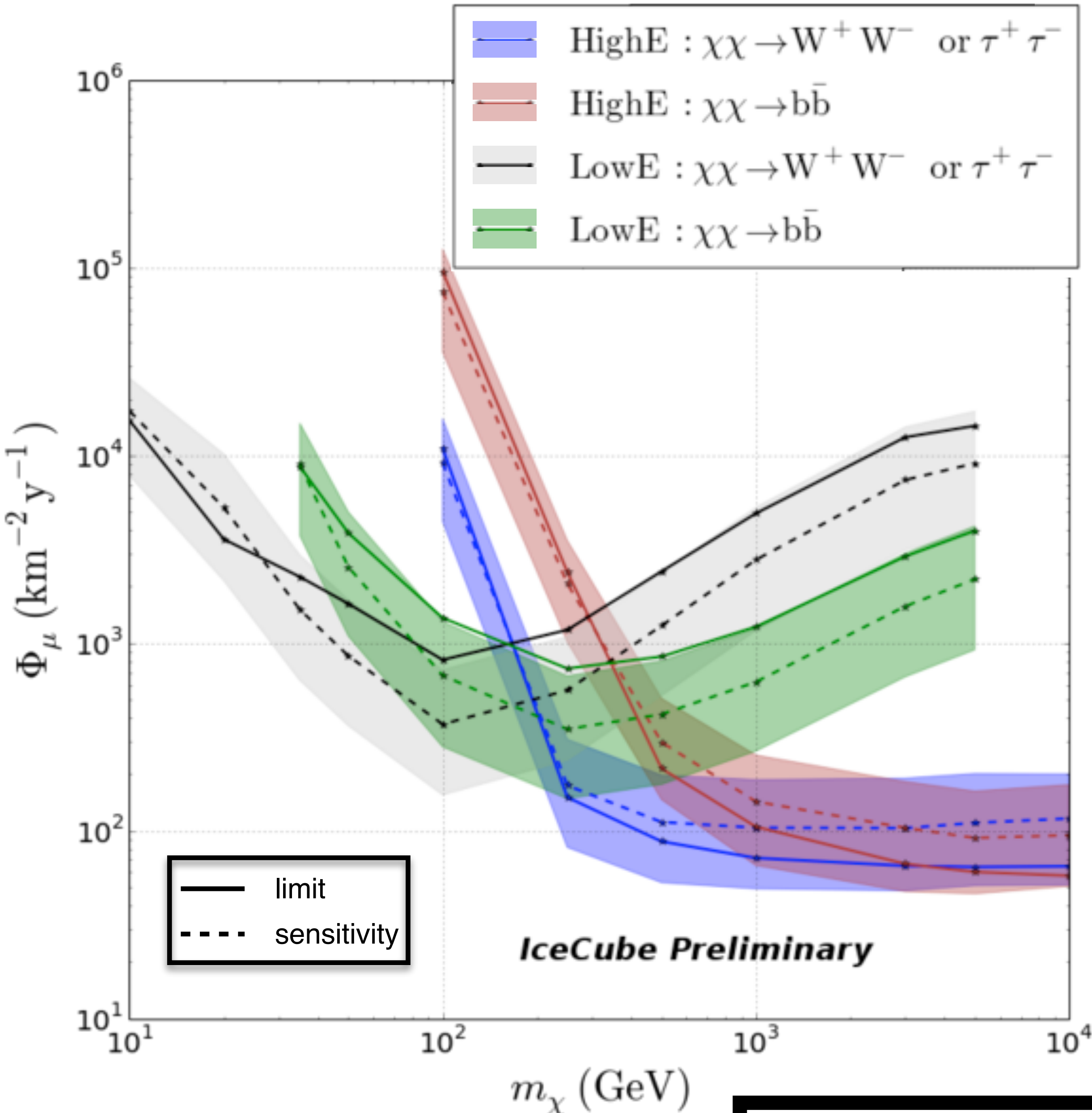

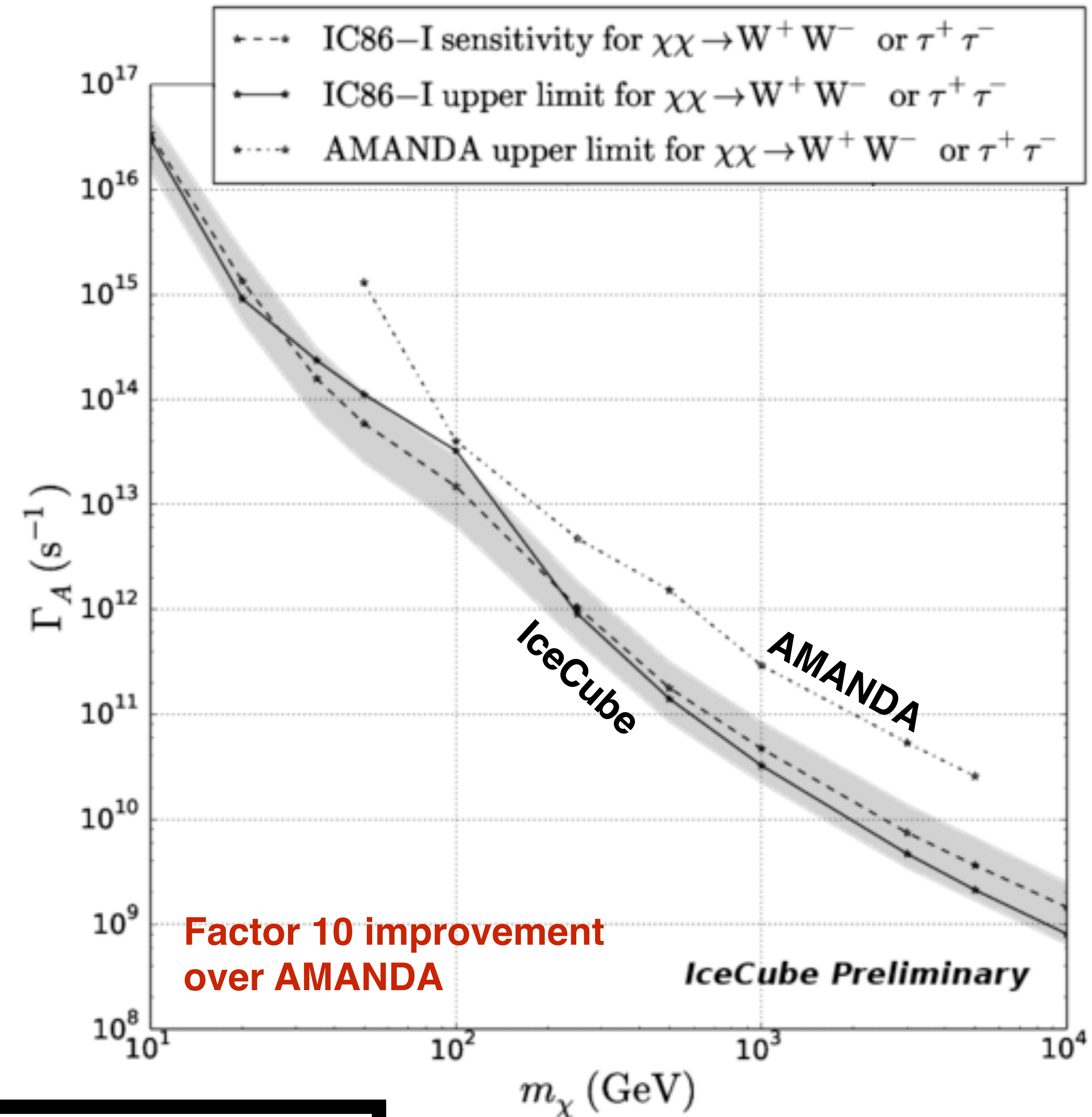

No evidence for dark matter

Publications:
- Super-K S.Desai et al (2004)
- IceCube arXiv:1609.01492
- ANTARES forthcoming

Earth WIMPs

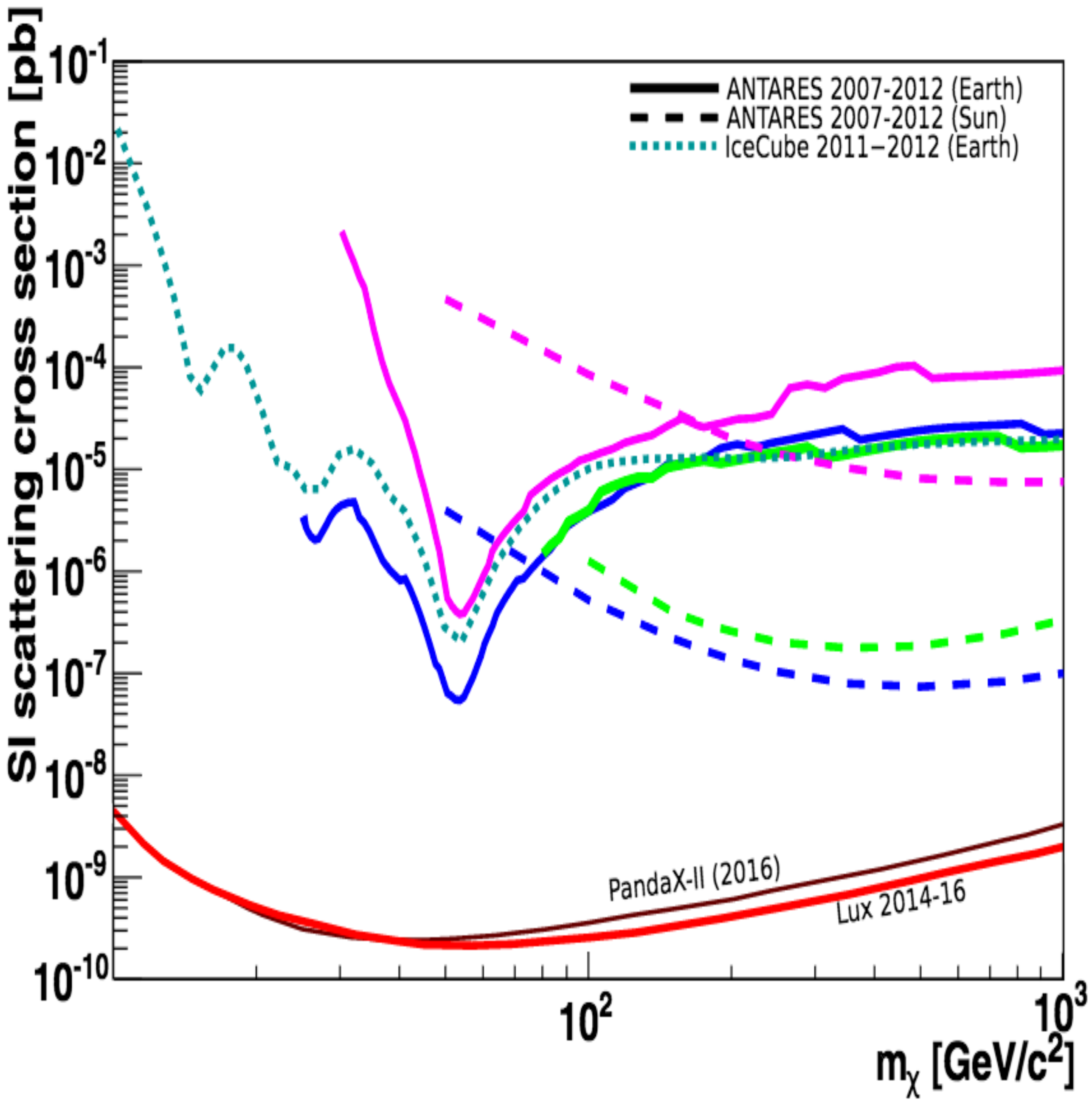

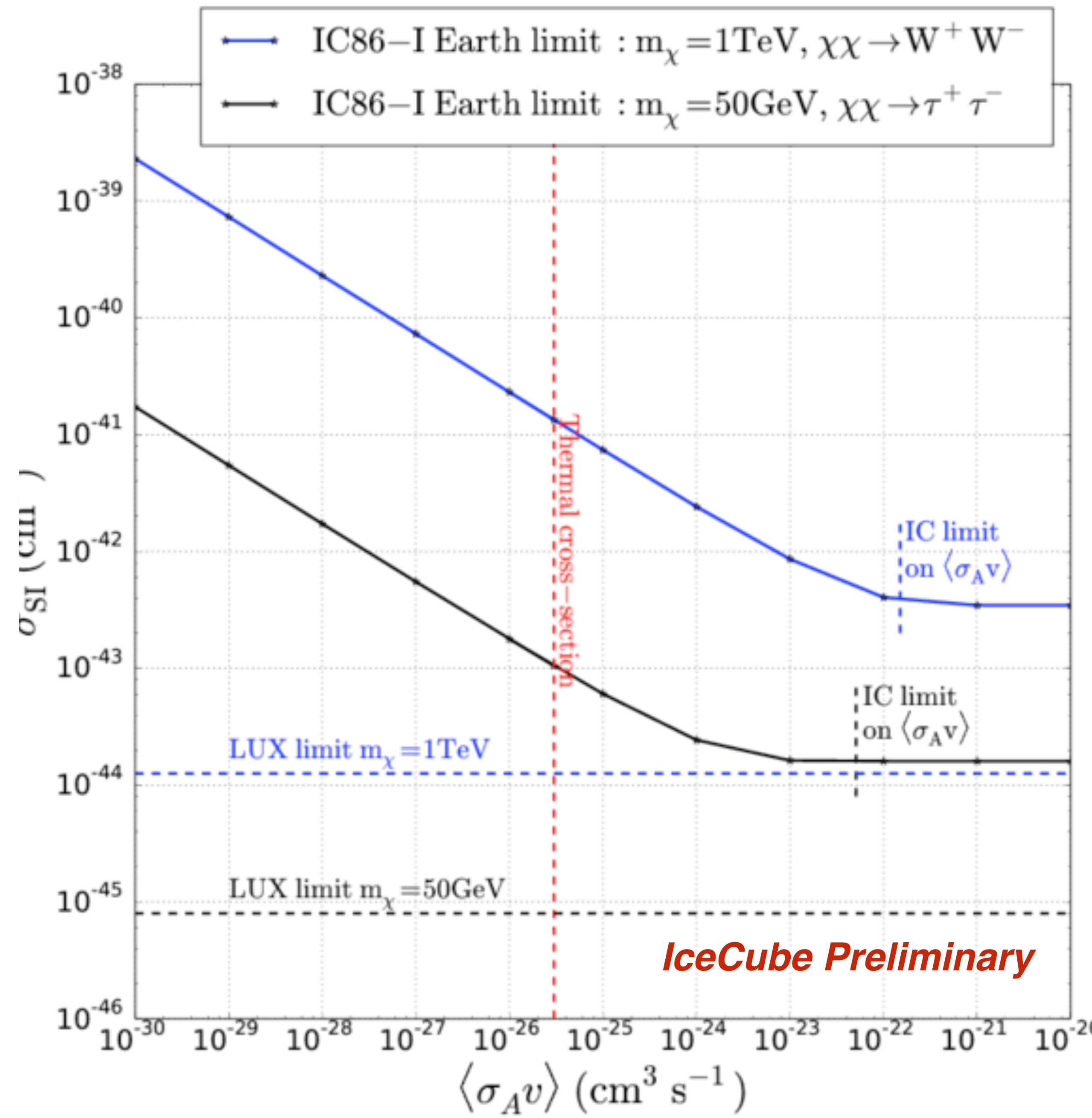

- Earth WIMP analysis more sensitivity than Solar WIMP analysis for SI scattering for m_χ close to Fe resonance
- Standard halo model was assumed. Possibility of dark disk could boost Earth WIMP bounds by two orders of magnitude

Future Plans for IceCube …

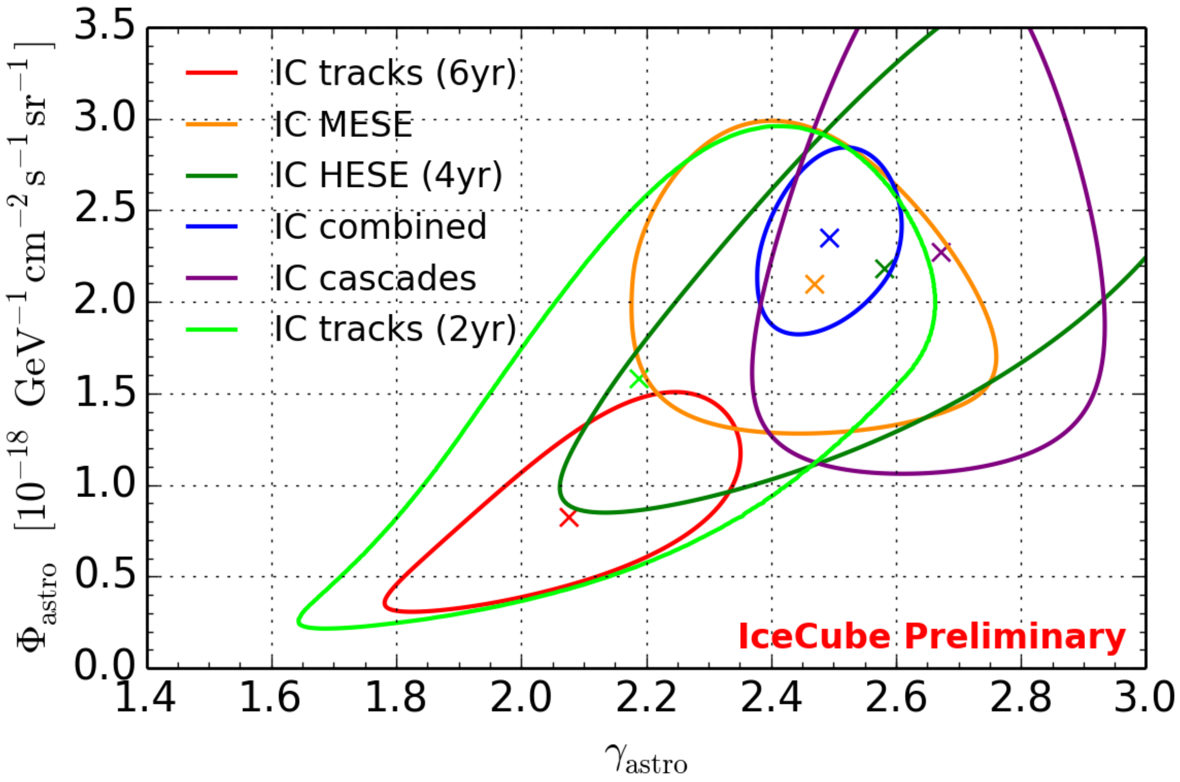

Intense interest in high-energy neutrino region

- Observations defy any simple explanation from a single generic source class
  - Multiple sources classes ?
  - Hints of new physics ?

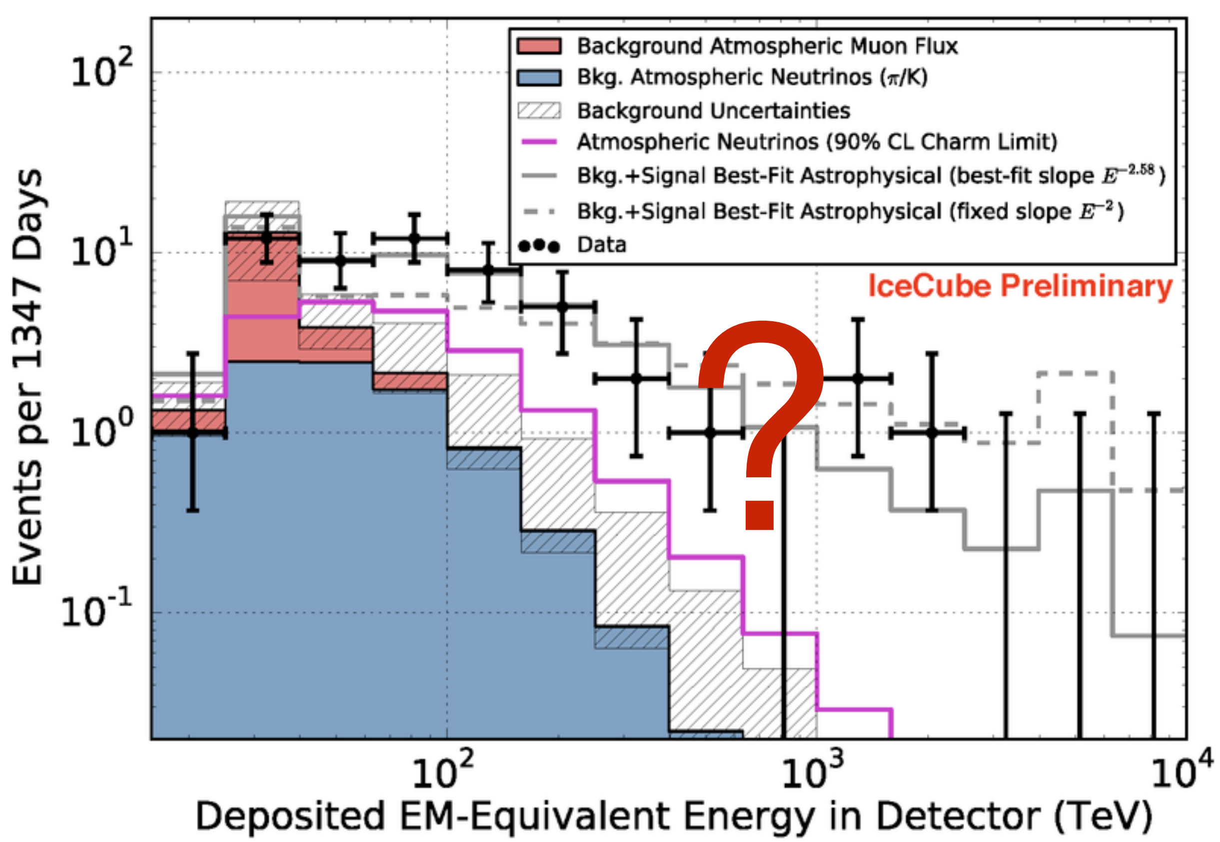

- PeV Scale Right Handed Neutrino Dark Matter
- Super Heavy Dark Matter
- Neutrino Portal Dark Matter
- Right-handed neutrino mixing via Higgs portal
- Heavy right-handed neutrino dark matter
- Leptophilic Dark Matter
- PeV Scale Supersymmetric Neutrino Sector Dark Matter
- Dark matter with two- and many-body decays
- Shadow dark matter
- Boosted Dark Matter
- …

Next generation -

IceCube Gen2 arXiv:1412.5106

- IceCube has provided an amazing sample of events, but is still limited by the small number of events
- Observed astrophysical flux is consistent with a isotropic flux of equal amounts of all neutrino flavors
  - So far non of the analyses has shown any evidence for point sources
- Where are the point sources?
- What is the flavor composition?
- What is the spectrum? Cutoff?
- Transients ?
- Multi-messenger physics?
- GZK neutrinos?
- ....

IceCube Gen2 Facility

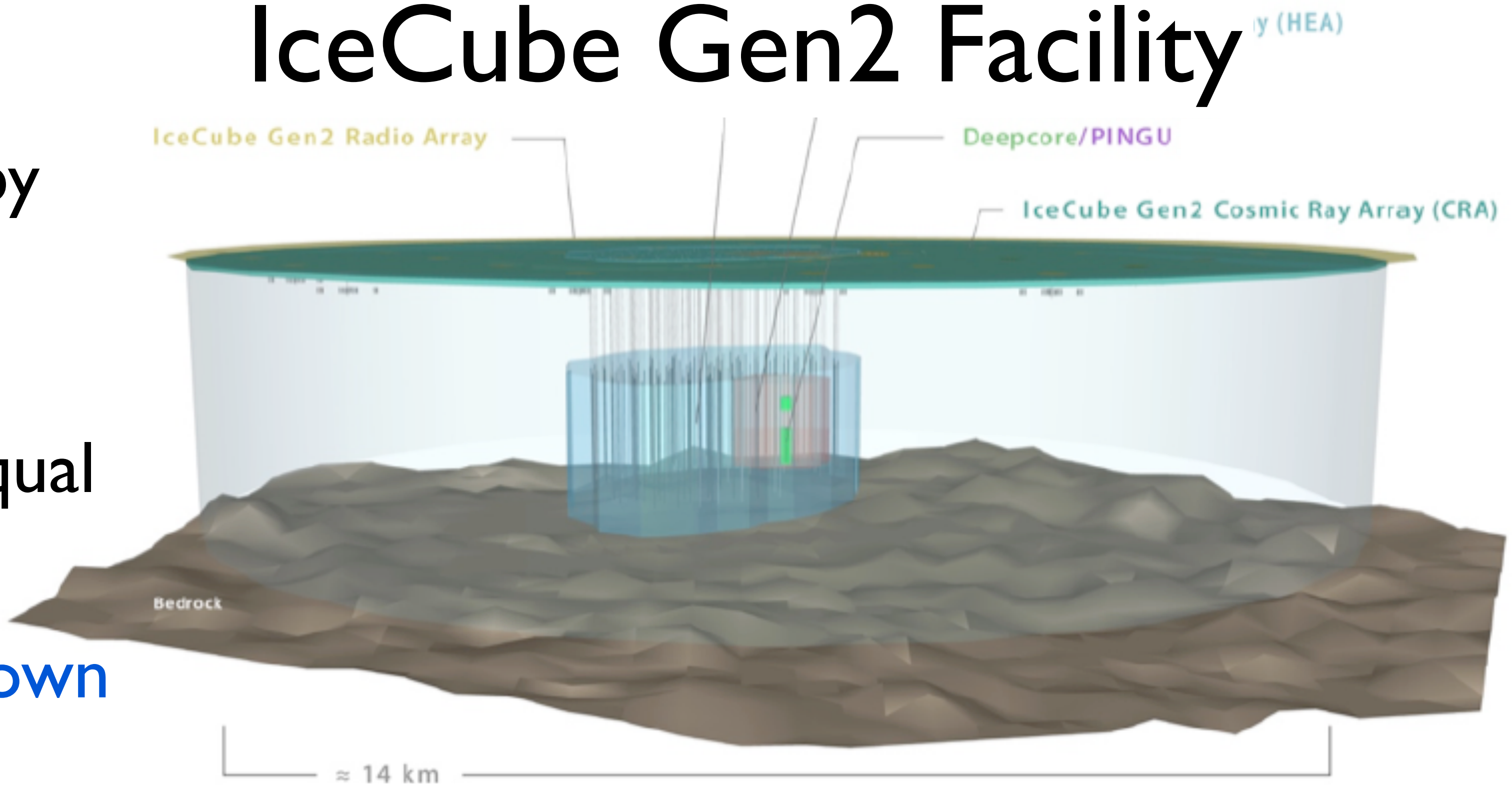

KM3NeT

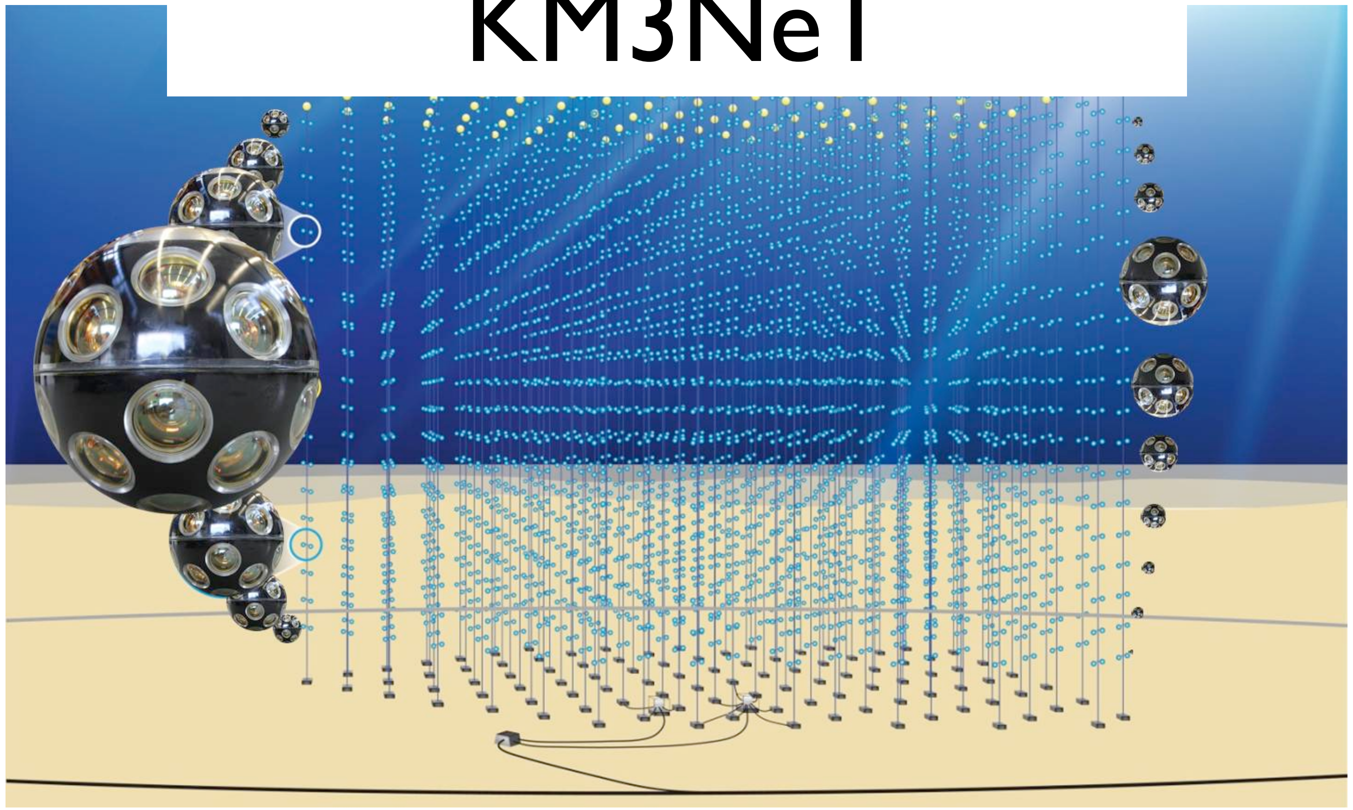

PINGU - Precision IceCube Next Generation Upgrade

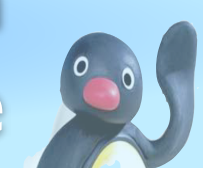

IceCube PINGU Collaboration arXiv:1401.2046

- PINGU upgrade plan
  - Instrument a volume of about 5MT with 20-26 strings
  - Rely on well established drilling technology and photo sensors
  - Create platform for calibration program and test technologies for future detectors
- Physics Goals:
  - Precision measurements of neutrino oscillations (mass hierarchy, ...)
  - Test low mass dark matter models

New PINGU Geometry

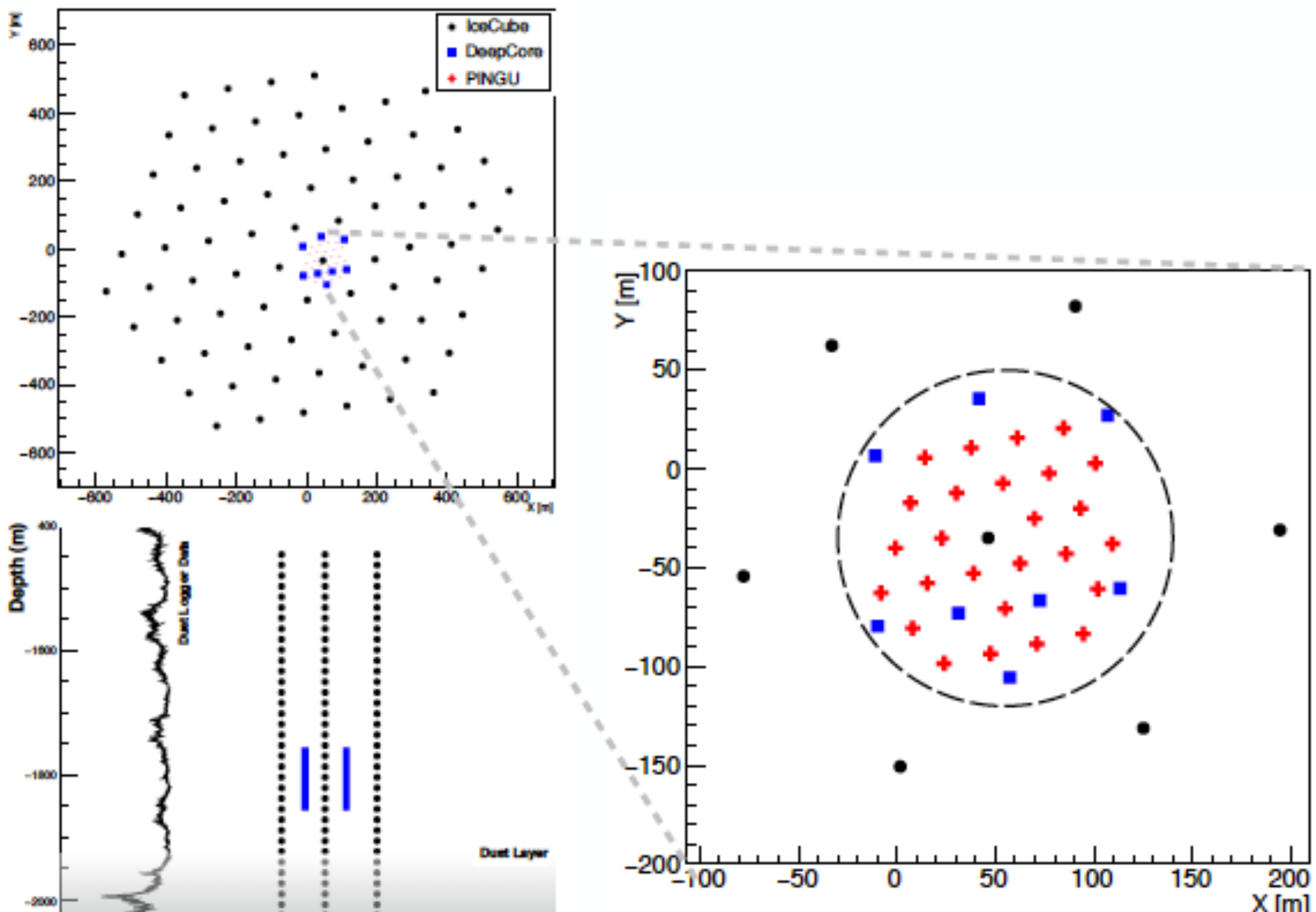

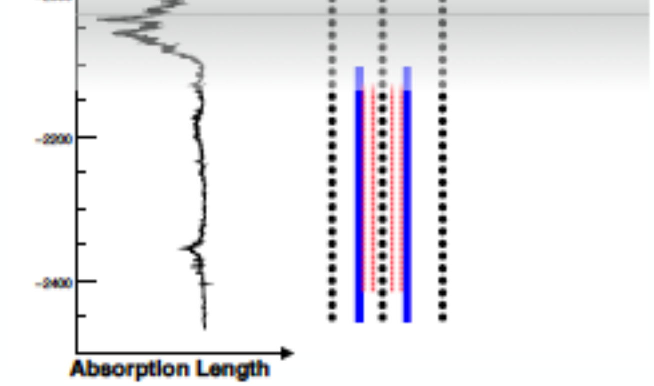

Compared to 40 string geometry
1. One less drilling/deployment season
2. Fewer holes drilled (saves fuel)
3. Fewer holes and one less season means we can refurbish drill rather than build a new one.

PINGU LOI to be updated shortly

Short version https://arxiv.org/pdf/1607.02671.pdf

Summary

- Dark Matter is one of the most exciting problem in modern physics
- There is overwhelming evidence for dark matter, but still we have no hint what it is
- Indirect searches for dark matter represent a key effort to identify dark matter
- Different search techniques are complementary
- The search goes on, many exciting experiments on the horizon